NETWORK ASCENT

TRENDS AND CHALLENGES OF THE AUTOMOTIVE INDUSTRY

PROCEEDINGS OF THE 2ND ASCENT CONFERENCE „ENGINEERING THE FUTURE“

https://net.ascent.fh-joanneum.at AscentEuProject ASCENT2020EU

Co-funded by the Erasmus+ Programme of the European Union

The European Commission support for the production of this publication does not constitute an endorsement of the contents which reflects the views only of the authors, and the Commission cannot be held responsible for any use which may be made of the information contained therein. Project number: 585796-EPP-1-2017-1-AT-EPPKA2-CBHE-JP

IMPRESSUM

Cover image Julio Caesar Lopez Martinéz
Layout Valentina Morianz

FH JOANNEUM Gesellschaft mbH Publishing
Alte Poststraße 149
A-8020 Graz
www.fh-joanneum.at

ISBN eBook: 978-3-903318-02-1

Co-funded by the Erasmus+ Programme of the European Union

The European Commission support for the production of this publication does not constitute an endorsement of the contents which reflects the views only of the authors, and the Commission cannot be held responsible for any use which may be made of the information contained therein. Project number: 585796-EPP-1-2017-1-AT-EPPKA2-CBHE-JP

CONTENTS

Co-funded by the Erasmus+ Programme of the European Union

The European Commission support for the production of this publication does not constitute an endorsement of the contents which reflects the views only of the authors, and the Commission cannot be held responsible for any use which may be made of the information contained therein. Project number: 585796-EPP-1-2017-1-AT-EPPKA2-CBHE-JP

Scientific Committee

Scientific Chair:

Horacio Ahuett and Pedro-Orta (Instituto Tecnológico y de Estudios Superiores de Monterrrey)

Pedro Urbina (TEC)
Veronica Luna (UNLP)
Santiago Maiz (UNS)
Gabriel Defranco (UNLP)
Gabriela Pesce (UNS)
Héctor Chiacchiarini (UNS)
Jorge Abel Avendaño Alcaraz (TEC)
Joel Castillo Gómez (TEC)
Karl-Heinz Reisinger (FHJ)
Fernando Pinto (UFRJ)
Claudio Martins (UNLP)
Marcelo Alves (USP)
Aleix Barrera Corominas (UAB)
Clara Horvath (AVL)
Pedro Antonio Orta-Castañon (TEC)
Horacio Ahuett (TEC)

Organizing Committee:

General Chair:

José Emiliano Martínez Ordaz (Universidad Iberoamericana)

Eva Penz (Fachhochschule JOANNEUM)
Claudia Fussenecker (Hochschule Düsseldorf)
Cecilia Inés Suárez (Universitat Autonoma de Barcelona)

Co-funded by the Erasmus+ Programme of the European Union

The European Commission support for the production of this publication does not constitute an endorsement of the contents which reflects the views only of the authors, and the Commission cannot be held responsible for any use which may be made of the information contained therein. Project number: 585796-EPP-1-2017-1-AT-EPPKA2-CBHE-JP

THURSDAY, 18TH OF MARCH 2021

08:00-08:15	**Opening of the Conference** Edgar Ortiz Loyola *Head of the Department of Engineering Studies for Innovation, IBERO*	
08:15-08:25	**Introduction of the ASCENT Project and Network** Kurt Steiner *Project Manager FHJ ASCENT*	**FH JOANNEUM** Institute of Automotive Engineering
08:30 – 09:30 (incl. Q&A)	**Key- Note:** **Introduction of Connected and Autonomous Vehicle Research and Development in Thailand** Dr. Witaya, Dr. Nuksit *Robotics Society & Chulalongkorn University, Thailand*	
9:40 – 10:40 (incl. Q&A)	**Key-Note:** **Evolution and Future Human Mobility** Dr. Hermann Knoflacher *University of Technology, Vienna*	
10:40-11:00	**Virtual Coffee Break**	
Parallel Sessions Paper Presentations	**FUTURE MOBILITY** **Chair:** Universidad Iberoamericana (IBERO)	**ENGINEERING EDUCATION** **Chair:** Tecnologico de Monterrey (ITESM)
11:00-11:30 (30min incl. Q&A)	**Session 1:** **An autonomously driving model vehicle** Florian Diernberger, Fritz Patrick *Institute of Automotive Engineering, University of Applied Sciences JOANNEUM (FHJ)*	**Session A:** **Educating Future Engineers-Challenges in University-Education** Jörg Niemann, Claudia Fussenecker, Martin Schlösser, Marius Schöning, Alexander Paul *Hochschule Düsseldorf (HSD)*
11:30-12:00	**Session 2:** **Urban mobility: emerging costs in transport selection** María de la Paz Moral, Gabriela Pesce *Dpto. de Ciencias de la Administración, Universidad Nacional del Sur (UNS)*	**Session B:** **Education and training of service engineers – A toolbox of methods for the digital business transformation** Jörg Niemann, Claudia Fussenecker, Martin Schlösser, *Hochschule Düsseldorf (HSD)*
12:00-12:30	**Session 3:** **Electric Powertrain System Design for Low Weight Urban Motorcycle Prototype** Bernardo Lessa Guerra, Fernando A.de Noronha C.P., *Mechanical Engineering Department, Polytechnic S., Federal University of Rio de Janeiro (UFRJ)*	**Session C:** **Introduction to knowledge and design of car mechanical parts in the early stages of a mechanical engineering degree** Fuertes Laural, Gavino Sergio, Lopresti Laura, Speroni Lucas, Defranco Gabriel *Universidad de La Plata (UNLP)*

Co-funded by the Erasmus+ Programme of the European Union

The European Commission support for the production of this publication does not constitute an endorsement of the contents which reflects the views only of the authors, and the Commission cannot be held responsible for any use which may be made of the information contained therein. Project number: 585796-EPP-1-2017-1-AT-EPPKA2-CBHE-JP

12:30-13:00	**Session 4:** **Sliding Mode Control of a Hybrid Battery-Super capacitor Energy Management System** Ezequiel Orozco, Héctor Chiacchiarini *Dpto. de Ing. Eléctrica y de Computadoras,* *Universidad Nacional del Sur (UNS)*	**Session D:** **Students motivation using extracurricular activities** Marcelo Augusto L. Alves, *Escola Politécnica da USP, Brazil (USP)*
13:00 – 13:15	**Feedback to the 1st Conference day**	

FRIDAY, 19TH OF MARCH 2021

08:50	**Opening of the Conference** Edgar Ortiz Loyola *Head of the Department of Engineering Studies for Innovation, IBERO*	
09:00 – 09:45	**Key- Note:** **Climate-friendly lifestyles & mobility** Dr. Gerfried Jungmeier *Joanneum Research, Austria*	
09:45 – 10:30	**Key- Note:** **Urban Living Labs – New Mobility Concepts** Oliver Lah *Urban Electric Mobility Initiatives, Germany*	
10:40-11:00	**Virtual Coffee Break**	
Parallel Sessions Paper Presentations	**FUTURE MOBILITY** **Chair:** Universidade de Sao Paulo (USP)	**ENGINEERING EDUCATION** **Chair:** Universidad Nacional del Sur
10:45-11:15	**Session 1:** **Comparison of Electric Drive and Combustion Engine under Consideration of Product Lifecycle Management** Ilias El Hajjami *University of Applied Sciences Düsseldorf, Germany (HSD)*	**Session A:** **Design, Fabrication and Project Workflow of LowCost Impact Attenuator for Formula SAE Cars** João Victor da Cruz Almeida, Clara Roussenq Daibert, Matheus Belo de Lima, Marcus Vinicius F. Silva, Fernando A. de N.C.Pinto, *Mechanical Engineering Department, Polytechnic School, Federal University of Rio de Janeiro (UFRJ)*

Co-funded by the Erasmus+ Programme of the European Union

11:15-11:45	**Session 2:** **Calculation of splashing Losses in an Spur Gearbox with SPH-Method** Ermin Hujdur *University of Applied Sciences JOANNEUM, Austria (FHJ)*	**Session B:** **Analytical sizing of a heat exchanger for a FSAE combustion car** João Gabriel Barcelo dos Santos, Fernando A. de N.C.Pinto, *Mechanical Engineering Department, Polytechnic School* *Federal University of Rio de Janeiro (UFRJ)*
11:45-12:15	**Session 3:** **Method for Reducing Uncertainty in Obstacle Detection applied to Autonomous Vision-Based Navigation** Rogerio Barbosa dos Reis, *Mechanical Engineering Department, Polytechnic School, Federal University of Rio de Janeiro (UFRJ)*	**Session C:** **A proof of concept system for the implementation of optimization path planning strategies in additive manufacturing** Sergio Alejandro Salinas-Saenz, Pedro Orta-Castañón, Horacio Ahuett-Garza *Tecnologico de Monterrey, Escuela de Ingeneria y Ciencias (ITESM)*
12:15 -12.30	**Virtual Coffee Break**	
12:30 – 13:15	**Key- Note:** **Virtual reality and augmented reality techniques** **Javier Posselt,** *Groupe Renault, France*	
13:15: 14:00	**Session 2:** **Status of Automotive industry in Mexico and its relationship with Industry 4.0** Jose Zozaya, *President of AMIA (Mexican Association of the Automotive Industry) Mexico* Clelia Hernandez, *Director of Nuevo León 4.0 Initiative, Mexico*	
14:00– 14:15	**Video:** **The 6 ASCENT Competence Centers**	
14:15– 14:30	**Feedback to the 2nd Conference day**	
14:30-14:45	**Closing Ceremony of the 2nd ASCENT Conference**	

Co-funded by the Erasmus+ Programme of the European Union

The European Commission support for the production of this publication does not constitute an endorsement of the contents which reflects the views only of the authors, and the Commission cannot be held responsible for any use which may be made of the information contained therein. Project number: 585796-EPP-1-2017-1-AT-EPPKA2-CBHE-JP

About the ASCENT Project, the ASCENT Network and the 2nd ASCENT Cross-Border Conference "Engineering the Future" on 18th and 19th of March 2021

The ASCENT Project

ASCENT - Competence Centres for Automative Engineering to increase the positive impact on regional economic development in Argentina, Brazil and Mexico

- Erasmus+ Capacity Building in Higher Education Joint Project
- Coordinating Institution: FH JOANNEUM Gesellschaft mbH (Austria)
- Project Duration: 15.10.2017-14.04.2021 – 42 months
- Target countries: Argentina, Brazil and Mexico

All ASCENT partners are globally seen very strong and important markets of the automotive industry. Their participation and development in this sector does therefore influence regional economic stability.

As of 2016, a potential lack of engineers focusing on automotive engineering as well as few cooperation between universities and businesses was detected and is addressed in the frame of ASCENT. The ASCENT project aims to improve the current situation at the participating higher education institutions in Argentina,
Brazil and Mexico and its regional industries that are connected.

Through capacity building trainings, local academic staff, students and companies will receive upgraded knowledge on automotive engineering and sales management for engineers to reach the following aims:

- To spread knowledge by the implementation of workshops, counselling and training sessions offered
  by the competence centres at each LA partner institution
- To increase the number of projects in Automotive Engineering
- To enlarge university-business cooperation To increase employability of engineering graduates

MAIN OUTPUTS

CAPACITY BUILDING

ASCENT builds up capacity on automotive engineering sales management strategies and soft skills for engineers at higher education institutions in Argentina, Brazil and Mexico through international expert training to create awareness and spread the idea of these topics on academic but also industry level to ensure future growth of university-business cooperation.

COMPETENCE CENTRES

ASCENT implements six competence centres focusing on automotive engineering, sales management strategies and soft skills for engineers at partner higher education institutions to establish a knowledge hub for the core topics.

NETWORK

NETWORK ASCENT builds up a network and a knowledge exchange platform for international exchange on automotive engineering and sales management for engineers.

Co-funded by the Erasmus+ Programme of the European Union

Main Target Groups of the ASCENT Project

The main target groups within the ASCENT project are as following:

- HEIs leaders and managers of the areas of automotive engineering and sales management for engineers
- Academic staff focusing automotive engineering and sales management for engineers
- Students and student associations studying automotive or mechanical degree programmes who aiming to improve the automotive industry in the participating countries
- Companies operating in the automotive industry
- Automotive associations and political partners

The ASCENT Network

The ASCENT network aims for international exchange on the topics of automotive engineering and soft skills for engineers among all target groups of the project. The integrated blog is used as a knowledge transfer platform and its aim is to share knowledge among the members of the network on the project´s core topics and to spread the existence of the competence centres as expertise hubs.

The vision of the ASCENT Network is to become a sustainable reference for education and training to overcome challenges of the automotive industry in the Latin American Region through collaborating with the industry.

The ASCENT Network aims to become a strategic partner of the automotive industry in order to be able to fulfill market needs by equipping future engineers with the right skills and competences, and supporting their development. All partners and network members will also benefit from increasing international collaboration. An impact on all other target groups such as associations related to the automotive industry and/or universities and students will be reached through the network activities.

The ASCENT Conferences

This 2nd cross-border conference has the objective to unite the international engineering community to directly help and shape the future of our societies. In the frame of the ASCENT project we try to connect engineers, students, academics and companies while discussing and reviewing relevant engineering topics. Bringing these target groups together allows us to enrich the international ASCENT Network.

The 1st ASCENT Cross-Border Conference was held in Sao Paulo, Brazil in 2020 and inaugurated the ASCENT Network. This is the announcement of the 2nd ASCENT Conference, which is organized by our partner university IBEROAMERICANA (IBERO) in Mexico City. The main aim of this conference is to unite international experts, students and companies, acting in the automotive industry. The conference is part of the ASCENT project "Competence centres for automotive engineering to increase the positive impact on regional development in Argentina, Brazil and Mexico", co-funded by the European Commission through the Erasmus+ programme.

Co-funded by the Erasmus+ Programme of the European Union
The European Commission support for the production of this publication does not constitute an endorsement of the contents which reflects the views only of the authors, and the Commission cannot be held responsible for any use which may be made of the information contained therein. Project number: 585796-EPP-1-2017-1-AT-EPPKA2-CBHE-JP

The 2nd conference took place on 18th and 19th of March 2021 in a lively and informal virtual venue. A variety of trends & challenges regarding automotive engineering have been presented and discussed in an interdisciplinary and creative environment. The focus was laid on the current trends such as lightweight design, industry 4.0, connectivity as well as practices experienced in different contexts implying the role of mechanics in contributing to the development in social, economic, and environmental perspectives in the field of automotive engineering.

Numerous papers that will make a contribution to a better future through efficient and environmental friendly mobility concepts and designs have been presented and are published in this proceedings.

In particular, the contributions focused on how trends in automotive engineering can be harnessed in order to enhance energy efficiency, lightweight design and connectivity while taking collaboration and educational aspects into account.

Conference Topics

Mobility Trends
electric vehicles (battery, powertrain)
autonomous vehicles
new mobility concepts
ultra-light vehicles
vehicle systems design (powertrain, suspension, safety)

Industry 4.0 in Automotive Engineering
internet of things/connected vehicles
virtual and augmented reality
collaborative robotics
digital manufacturing
big data
cost models for industry 4.0

Engineering Education
emerging technologies in education
industry-academia collaboration for engineering education
project management
soft skills for engineers

Co-funded by the Erasmus+ Programme of the European Union
The European Commission support for the production of this publication does not constitute an endorsement of the contents which reflects the views only of the authors, and the Commission cannot be held responsible for any use which may be made of the information contained therein. Project number: 585796-EPP-1-2017-1-AT-EPPKA2-CBHE-JP

Co-funded by the Erasmus+ Programme of the European Union
The European Commission support for the production of this publication does not constitute an endorsement of the contents which reflects the views only of the authors, and the Commission cannot be held responsible for any use which may be made of the information contained therein. Project number: 585796-EPP-1-2017-1-AT-EPPKA2-CBHE-JP

AUTONOMOUSLY DRIVING MODEL VEHICLE

Florian Diernberger, Patrick Ayrton Fritz

FH Joanneum, Institute of Automotive Engineering
florian.diernberger@edu.fh-joanneum.at, patrick.fritz@edu.fh-joanneum.at

ABSTRACT

The aim of this work was to develop a computer program with which a model car will be enabled to drive autonomously. For this purpose, a commercially available model car equipped with a camera and a Raspberry Pi microcomputer was employed. The images taken by the camera served as the only input to the software. In a first step, the computer vision library OpenCV was used for the lane detection and calculation of the steering angles. In a subsequent step, an artificial neural network was used to turn the model car into a deep-learning, self-driving vehicle that is not only able to detect and follow lanes, but also to recognize and respond to traffic signs and people on the road. The Deep Pi Car series by David Tian (Tian, 2019) has been used for orientation throughout the entire work.

Keywords: Autonomous model vehicle, machine learning, deep learning, artificial neural networks

INTRODUCTION

More and more vehicles are equipped with assistance systems that help the driver with specific tasks, for example, a lane-keeping assistant. In the future these systems will reach a maturity level that allows them to undertake driving tasks without the need of a person monitoring them. The concept of machine learning is used in the development of such vehicles. For that purpose, artificial neural networks (ANNs) are trained to perform specific tasks and are then implemented in the control software. The big benefit of machine learning is that complex coherences do not have to be programmed by hand. Neural networks learn these coherences by many examples in form of an input and desired output.
The aim of our work was to develop software with which a model car could drive autonomously. With that software the car should be able to follow lanes and detect objects on a road. The work of David Tian (Tian, 2019) provided useful orientation. The model car in use is equipped with a camera in the front and a Raspberry Pi microcomputer that runs the software. The images taken by the camera serve as the input of the software. The image is then analyzed by the ANNs and the result is used to control the model car.
The work was accomplished by the authors within an undergraduate research project in their third year of study (Diernberger & Fritz, 2020).

OBJECTIVES

In the first step, a program should be created with the coding language Python and the computer vision library OpenCV (OpenCV Team, 2020). With the help of this program, the model vehicle should be able to follow a lane. To start with, the detection of the lanes and the computation of the corresponding steering angle should be accomplished without machine learning. For that, various algorithms are used which analyze and process the image and calculate an appropriate steering angle. Next, the lane-following software should be adapted to incorporate machine learning. Therefore, a model of an ANN has to be trained with images from the onboard camera with the correct steering

Co-funded by the Erasmus+ Programme of the European Union

The European Commission support for the production of this publication does not constitute an endorsement of the contents which reflects the views only of the authors, and the Commission cannot be held responsible for any use which may be made of the information contained therein. Project number: 585796-EPP-1-2017-1-AT-EPPKA2-CBHE-JP

angle given. With this neural network the vehicle should be able to follow a lane based on the incoming pictures of the camera. The architecture of this ANN is based on the convolutional neural network (CNN) developed by NVIDIA (Bojarsk, et al., 2016). To create and execute ANNs, the TensorFlow-framework (TensorFlow, n.d.) and Keras-library (Keras, n.d.) are used. The training of ANNs requires a lot of computational power. As a consequence, this training would be a time-consuming process on a personal computer. Hence, Google Colab (Google Colab, n.d.) is used, which offers a programming environment where all the calculations are executed on their servers.

In the last step, the software should be extended by an object detection feature. For this case, another model has to be trained, whose purpose is to detect objects within an image. After the detection, the vehicle should initiate the appropriate action for the detected object, for example, to halt the vehicle at a stop sign. The software should be able to perceive objects that are common on a road, like various traffic signs, traffic lights and pedestrians. These different objects are then used to train the model.

METHODOLOGY

3.1. Preparation

Before the software development started, the model vehicle was assembled and the remote access to the Raspberry Pi was established. Furthermore, a circuit to test, validate, and improve the self-driving systems was installed.
The model vehicle used was the Smart Video Car Kit V2.0 from SunFounder (SunFounder, 2020), as depicted in Figure 1. This vehicle is equipped with a camera which will be the only sensor of the autonomous driving-system. The Raspberry Pi Model 4 is used as the onboard computer. This single-board computer handles all the calculations and is also responsible for actuating the motors of the model car. To do so, the Raspberry Pi is connected with the so-called Robot HATS board, which serves as an interface for controlling the hardware of the vehicle. This board is then connected to other components, such as the PWM-controller, which controls all the actuators. The kit has, in total, five electromotors: two at the rear for propulsion, one for steering, and two to tilt and pan the camera unit. For the machine learning part, a Coral USB Accelerator (Google, 2020) was added to the vehicle as well. This unit provides additional computation power for processing machine learning-models. This accelerator is directly plugged into the Raspberry Pi via an USB 3-cable. The electrical energy, that is necessary to operate the model car, is obtained from two batteries, which are mounted at the underbody.

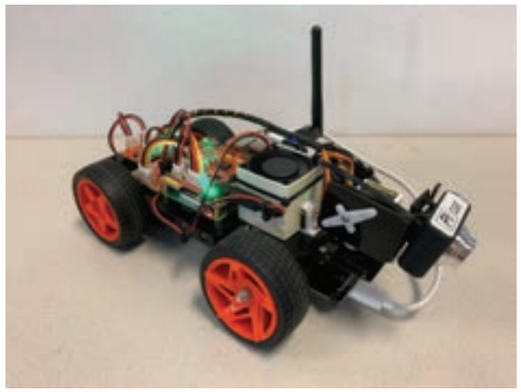

Figure 1: Model vehicle

Co-funded by the Erasmus+ Programme of the European Union

The European Commission support for the production of this publication does not constitute an endorsement of the contents which reflects the views only of the authors, and the Commission cannot be held responsible for any use which may be made of the information contained therein. Project number: 585796-EPP-1-2017-1-AT-EPPKA2-CBHE-JP

For the launch or termination of the self-driving software on the car, a computer was remotely connected with the Raspberry Pi. In the following text, this remote computer is referred to as PC. With the help of the PC, the Raspberry Pi was operated entirely remotely. As a result, no cables had to be attached to the car which is a necessary requirement for independent driving. To accomplish that, the Raspberry Pi and the PC were connected to the same VPN that offers static IP-addresses. This property plays an important role, since the IP-address is used to establish the connection between the two machines. In order to operate the Raspberry Pi on the PC, a Virtual Network Computing (VNC) software was used. With that, the screen content of the Raspberry Pi could be displayed on the PC.

In order to run and program the self-driving software, various software packages were needed and had to be installed beforehand. First, Python 3 was needed, since the autopilot-software is written in that language. For additional functionality, the libraries OpenCV, TensorFlow, and Keras had to be installed too. OpenCV offers computer vision related functions and is used for image processing (OpenCV Team, 2020). TensorFlow and Keras are required for the machine learning part. These packages allow to create and run models in Python (TensorFlow, n.d.).

In the development process, testing played an important role as it was used to find problems and to improve the product. In our case, a test track was created where the lane-following and the object detection capabilities were examined. The lanes of the circuit were replicated by red tape which was stuck on the floor. The circuit provides straight segments, sharp corners as well as S-bends. Due to that versatile track layout, the autonomous steering system could be precisely calibrated. For the object detection, different traffic signs were placed all over the track.

Lane navigation via OpenCV

For the lane navigation, two main steps were needed. The first step was the processing of the image and the detection of the lanes. Next, based on the detected lanes, a steering angle was calculated. In order to improve the steering behavior of the car, the calculated steering angle was corrected subsequently.

First, a picture with the board camera was taken (Figure 2). This image covers the area in front of the vehicle. The target was to detect the lanes inside this image. To do so, the image was converted from the RGB- to the HSV-color space, since our algorithm detects the lanes by their color – in our case red. If this detection were done in the RGB-color space, it would be quite difficult to determine the red pixels. As lighting, shadows and reflections change the appearance of the lanes in the image, also darker and brighter shades of red must be taken into account. In the HSV-color space, instead, the color itself is described by the value hue, the two other values define the saturation and brightness (Häßler, 2017). Thus, all red pixels, independent of their saturation and brightness, were found and marked in the image. The so-called color mask is shown in Figure 3. The white areas, which do not belong to the lanes, were removed in a subsequent step.

Figure 2: Image taken with board camera

Figure 3: Color mask

Co-funded by the Erasmus+ Programme of the European Union

The European Commission support for the production of this publication does not constitute an endorsement of the contents which reflects the views only of the authors, and the Commission cannot be held responsible for any use which may be made of the information contained therein. Project number: 585796-EPP-1-2017-1-AT-EPPKA2-CBHE-JP

Afterwards, the processed image is passed to the edge-detection. For that, the Canny algorithm is used. This algorithm is part of the OpenCV library and can be called with a single command. This function analyzes the color mask image and draws a line around all white areas (Mordvintsev & K., 2013a). Then the line fragments, which are not part of the lanes, are removed. Since the lanes are found on the lower half of the image, and these disturbances only happen in the upper area of the picture, the problem was resolved by simply drawing a black rectangle over the upper half of the image. The result can be seen in Figure 4.

Figure 4: Edge detection

This picture was used to detect lines by making use of the Hough Line Transformation. This function tries to lay straight line segments along the white edges (Mordvintsev & K., 2013b). If the edge is curved, multiple shorter lines are returned from this function. The detected lines are shown in Figure 5. Afterwards, all the coordinates from these lines are processed and are merged into lanes. To do so, the position and the slope of the line segments were used to determine if the segments are part of the left or right lane. Once they are assigned to a lane, a regression line is calculated with the coordinates of the segments. The result is one line per lane marking that can be used to calculate the steering angle, see Figure 6

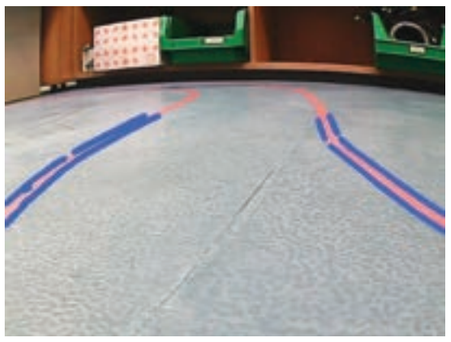

Figure 5: Hough Line Transformation

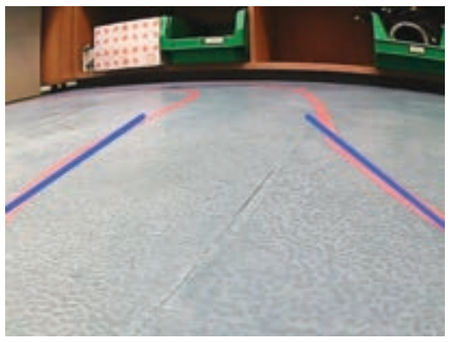

Figure 6: Merge lines to two lanes

Co-funded by the Erasmus+ Programme of the European Union

The European Commission support for the production of this publication does not constitute an endorsement of the contents which reflects the views only of the authors, and the Commission cannot be held responsible for any use which may be made of the information contained therein. Project number: 585796-EPP-1-2017-1-AT-EPPKA2-CBHE-JP

The steering angle is calculated by means of the upper coordinates of the two lines, as they are highlighted in Figure 7 with green dots. The centered, vertical line represents the current heading of the vehicle. However, if the car is driving into a curve, this heading would lead the car to leave the lane. To prevent this, the center between the two green dots is calculated in order to receive the orthogonal distance to the vertical line (blue dot). When a line is drawn between this point and the point at the bottom center of the image (blue line), the desired steering angle can be found. It is the angle between the blue line, and the vertical line. In case that only one lane marking is detected, for example in curves, the steering angle equals the angle of the single detected line.

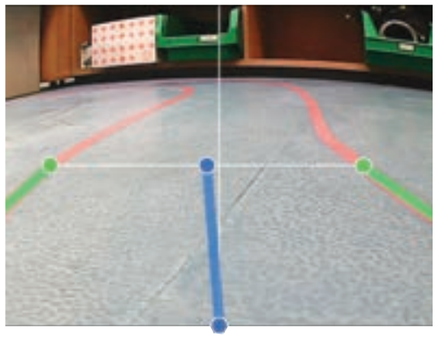

Figure 7: Steering angle calculation

However, these calculated steering angles cannot directly be used for steering, as the result would not be sufficient. To eradicate the problems and improve the steering behavior of the model vehicle, the angle needs to be corrected. The respective algorithm has to be able to increase or decrease the angle, depending on the current situation. For example, the steering angle is decreased when driving into a curve, in order to prevent the car from cutting inside turns.

Lane navigation machine learning

The lane navigation via machine learning should also work with images from the board camera as input. For this purpose, an ANN predicts a steering angle based on the input image. To this end, the ANN has to be trained for that specific task.
Since our OpenCV based lane navigation software performs quite well on the test track, it was used to train the ANN. With that, the training data was generated while the vehicle was driving on its own on the test track. During this process, every camera frame was stored on the Raspberry Pi's memory card; the corresponding steering angle of the car is part of the file name. Since the lanes on these images are only located on the bottom half of the picture, the upper area has been cut away. Additionally, all images were scaled to a resolution of 200 x 66 px, as this was demanded by the ANN in use. An example of such a training image is shown in Figure 8.

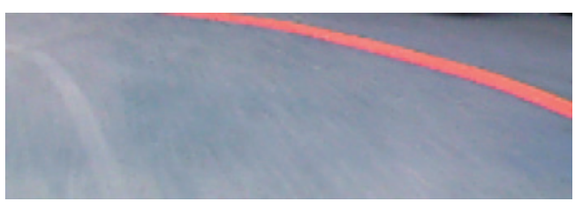

Figure 8: Example for training image; the steering angle in this case is −10°

Co-funded by the Erasmus+ Programme of the European Union

The model for the ANN is based on the convolutional neural network (CNN) model created by NVIDIA. This type of an ANN is often used in image processing applications. The NVIDIA model was already used in research vehicles participating in real traffic. (Bojarsk, et al., 2016)
The creation of the model and its training were both accomplished with the help of a Google Colab Notebook. Colab is a web application that offers a programming environment where all the processing is done on a Google server (Google Colab, n.d.). Thus, the training duration of the model is reduced significantly since this service is executed on powerful servers. First, the model was created using the Keras-library. Then, the model was trained with the prepared images. Some of these images were also randomly augmented, in order to make the model more solid. For example, the brightness of the image could be modified, it could be blurred or horizontally flipped. After the training, the functionality of the model was validated with some test images. When the model predicted a reasonable steering angle, it was downloaded from Google Drive and was then integrated in the self-driving software.
In this case, no steering angle had to be calculated, since all necessary steps were done by the model. For that, the current camera frame was passed to the model at runtime, which then predicted a matching steering angle based on the image. Again, the picture had to be be cropped and scaled to the required resolution of 200 x 66 px beforehand. The returned steering angle was then directly used to set the steering actuator.

Object detection

With the lane navigation software, the car can steer autonomously and thus follow the course of the road. However, the software does yet not recognize obstacles, pedestrians, or traffic signs. With the implementation of object detection, the car is able to react to specific situations, like, for example, braking in the case of an obstacle, or changing the speed at a speed limit sign.
For the training, many images of the objects, which the car should detect were taken. In our case 150 training images plus 32 augmented ones, and 16 testing images were used. These pictures contain all the objects at different viewing angles, different sizes, and different light conditions. Two of these training images can be seen in Figure 9.

Figure 9: Training data

After all the pictures were taken, every single object inside these pictures were labelled by hand. This was done by dragging a bounding box around the object in the image and allocating this box to the corresponding object, as depicted in Figure 10. This process was carried out with the program labelImg, which saves the bounding box and label data in a separate XML-file for every image (Tzuta, 2019). Afterwards, all these images and XML-files were uploaded to Google Drive for the training of the model.

Co-funded by the Erasmus+ Programme of the European Union

Figure 10: Object labelling

In our case, the model which is trained is not built from scratch, since the training of a completely new object detection model is very time consuming. To bypass this, a pretrained model was chosen. Nevertheless, it is still possible to train a model which is able to detect any object. In this work, a model that had been pretrained with the COCO dataset (common objects in context) was used. The training process was also carried out on Google Colab and took around 5 hours 30 minutes. Afterwards, the model was validated with some images that showed various traffic signs, toy figures, or no objects at all. If the bounding boxes are drawn correctly by the model, and the object type is detected properly, the training goal is reached. For that, the trained model and a file with all the object labels were then downloaded from the cloud and saved in our software directory.
At this point, the model car is able to detect objects, but still could not take any measures when an object was detected. For that purpose, an action function for every detectable object had to be created, which was responsible for a certain reaction. For example, the action function for a red traffic light halts the car.

However, there may be situations where multiple objects at the same time appear in one image. In this case, all the detected objects are processed, prioritized, and only the important ones call an action function. A demonstration of this functionality can be seen in Figure 11. If there are multiple objects of the same category (e.g.: stop signs, traffic lights, speed limit signs, etc.), only the nearest one to the vehicle can call an action function. In this case, two stop signs were detected. However, only the nearer one, which is marked by a red bounding box, can call the action function to stop the vehicle. The other stop sign is ignored at the moment, which is shown by the gray bounding box. The traffic light to the left is not grayed out, since this object belongs to another category than the stop signs.

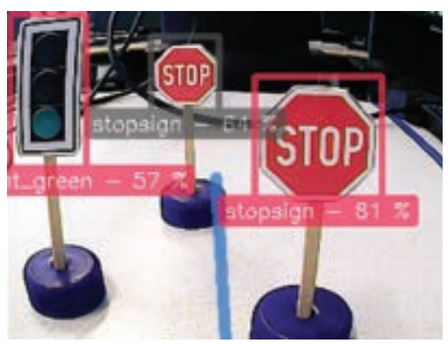

Figure 11: Demonstration of object processor

Co-funded by the Erasmus+ Programme of the European Union

The European Commission support for the production of this publication does not constitute an endorsement of the contents which reflects the views only of the authors, and the Commission cannot be held responsible for any use which may be made of the information contained therein. Project number: 585796-EPP-1-2017-1-AT-EPPKA2-CBHE-JP

All objects which are marked red are then passed to another algorithm which observes the distance of the objects to the car. This is an important step, since otherwise the software would immediately call an action function as soon as an object is detected. In case of a red traffic light, for example, the car would stop way before it. This behavior is fixed by not calling the action function until the object is near enough. If a red traffic light were detected with this function implemented, the car would drive to the traffic light and break in front of it.

RESULTS

The software is now able to follow lanes and react to specific objects on the road fully autonomously. The lane navigation system is responsible for steering and thus guiding the vehicle along a road. The object detection part can halt the car, or change its speed, if a speed limit sign demands that.

The lane navigation via OpenCV works properly with any lane color, as it can be defined in a configuration file, although, the machine learning solution was solely trained with red lanes on a blue surface. As a result, the system only works with red lanes in this case and struggles under other conditions. When comparing both of the two lane navigation solutions on our test track, the machine learning mode showed better results. It is less prone to difficult lighting conditions and thus works more reliably. The hand coded algorithm using OpenCV has some difficulties with reflections on the floor and with dim areas on the track. At such spots, the car often swings off the road since the lanes could not be properly detected.

The object detection shows good results when the objects are near to the camera. However, on the test track the car has some difficulties recognizing the objects. It has problems to detect objects which are further away and it often cannot distinguish between the different speed limit signs, as their appearance is very similar. However, if the objects are closer to the camera and the car is driving at low speeds, the model is able to detect the trained objects correctly in most cases, as seen in Figure 12.

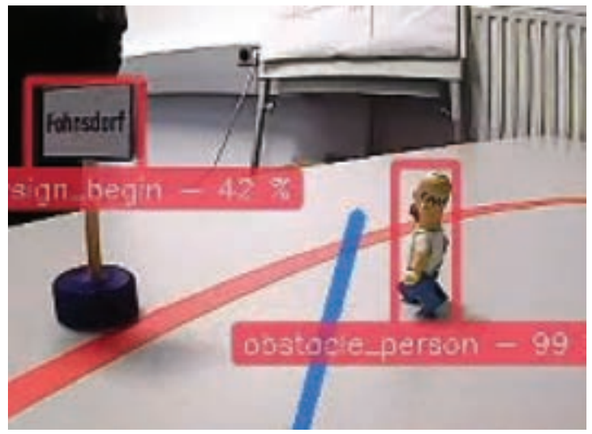

Figure 12: Object detection while driving, the blue line visualizes the current steering angle

Co-funded by the Erasmus+ Programme of the European Union

The European Commission support for the production of this publication does not constitute an endorsement of the contents which reflects the views only of the authors, and the Commission cannot be held responsible for any use which may be made of the information contained therein. Project number: 585796-EPP-1-2017-1-AT-EPPKA2-CBHE-JP

Wrongly detected boundary signs pose a further problem. Different rectangular shapes in an image are classified as boundary signs. In addition, the red lane of the test track is often interpreted as a crossed-out boundary sign, see Figure 13. This problem occurs due to the way boundary signs were trained to the model. In order to make the model recognize any boundary sign, no matter what toponym is written on it, blank signs were part of the training data. Still, these blank signs were also mixed with regular boundary signs for training, as it can be seen in Figure 14

Figure 13: Mistakenly detected boundary sign

Figure 14: Training data for boundary signs

CONCLUSION

The software has a lot of potential for improvement, which is work in progress. The lane navigation via machine learning could be improved by expanding the training data with more lane and floor colors. With that, the model should be able to work properly under any conditions. And, in addition, more training should be done with images taken under unfavorable lighting conditions, such as dim and very brightly lit ones.

Furthermore, the performance and reliability of the object detection can be improved with more training data. Many more pictures are needed to ensure a decent detection of all objects. Especially pictures where the objects are further away from the camera should improve the ability to recognize objects earlier. The distinction of the different speed limit signs can also be improved with a much larger pool of training data. Finally, the training of the boundary signs shall only be done with signs containing different town names. Our approach to use these signs without any toponyms turned out to be a wrong decision, since any rectangular geometry in an image is now recognized and highlighted as a boundary sign.

Co-funded by the Erasmus+ Programme of the European Union

The European Commission support for the production of this publication does not constitute an endorsement of the contents which reflects the views only of the authors, and the Commission cannot be held responsible for any use which may be made of the information contained therein. Project number: 585796-EPP-1-2017-1-AT-EPPKA2-CBHE-JP

REFERENCES

Bojarsk, M., Del Testa, D., Dworakowski, D., et al. (2016). *End to End Learning for Self-Driving Cars. Retrieved July 17, 2020, from https://arxiv.org/pdf/1604.07316.pdf*

Diernberger, F., & Fritz, P. A. (2020). *Autonom fahrendes Modellfahrzeug*. Bachelor's Thesis. Institute of Automotive Engineering, Joanneum University of Applied Sciences, Graz

Google. (2020). *USB Accelerator.* Retrieved June 26, 2020, from https://coral.ai/products/accelerator/

Google Colab. (n.d.). *What is Colaboratory?* Retrieved July 2, 2020, from https://colab.research.google.com/notebooks/welcome.ipynb?hl=en

Häßler, U. (2017, July). *HSB/HSV und HSL-Farbmodell*. Retrieved March 26, 2020, from https://wisotop.de/hsv-und-hsl-farbmodell.php

Keras. (n.d.). *About Keras*. Retrieved July 2, 2020, from https://keras.io/about/

Mordvintsev, A., & K., A. (2013a). *Canny Edge Detection*. Retrieved April 16, 2020, from https://opencv-python-tutroals.readthedocs.io/en/latest/py_tutorials/py_imgproc/py_canny/py_canny.html

Mordvintsev, A., & K., A. (2013b). *Hough Line Transform*. Retrieved April 20, 2020, from https://opencv-python-tutroals.readthedocs.io/en/latest/py_tutorials/py_imgproc/py_houghlines/py_houghlines.html

OpenCV Team. (2020). *About.* Retrieved March 17, 2020, from https://opencv.org/about/

SunFounder. (2020). *SunFounder PiCar-V Kit V2.0 for Raspberry Pi*. Retrieved March 2, 2020, from https://www.sunfounder.com/smart-video-car-kit-v2-0.html

TensorFlow. (n.d.). *Why TensorFlow.* Retrieved July 1, 2020, from https://www.tensorflow.org/about?hl=en

Tian, D. (2019, April 19). *DeepPiCar — Part 1: How to Build a Deep Learning, Self Driving Robotic Car on a Shoestring Budget.* Retrieved March 3, 2020, from https://towardsdatascience.com/deeppicar-part-1-102e03c83f2c

Tzuta, L. (2019, May 26). *labelImg 1.8.4.* Retrieved August 4, 2020, from https://pypi.org/project/labelImg/

Co-funded by the Erasmus+ Programme of the European Union

The European Commission support for the production of this publication does not constitute an endorsement of the contents which reflects the views only of the authors, and the Commission cannot be held responsible for any use which may be made of the information contained therein. Project number: 585796-EPP-1-2017-1-AT-EPPKA2-CBHE-JP

URBAN MOBILITY: EMERGING COSTS IN TRANSPORT SELECTION

María de la Paz Moral[1], Gabriela Pesce[2]

[1] *Departamento de Ciencias de la Administración, Universidad Nacional del Sur, paz.moral@uns.edu.ar*
[2] *Departamento de Ciencias de la Administración, Universidad Nacional del Sur, gabriela.pesce@uns.edu.ar*

ABSTRACT

Urban mobility decisions involve multidimensional aspects such as time, money as well as the potential impact on the environment and society. These dimensions do not lead to a prevalent transportation mode that could satisfy the mentioned criteria altogether. In modern cities, roads promote private transport and the particular car is the central instrument of the mobility system. This scenario causes environmental, social and economic issues (Aliano, Blanco, Díaz Almassio, Keesler, & Sosa, 2019). Smart and sustainable mobility emerges as a solution by offering efficient, clean and equitable transportation for people, goods and data (Prada, Romera, Añez, & Sánchez, 2015). In this context, a comprehensive analysis of urban mobility becomes necessary.
In this work, we carry out a comparative economic analysis of personal urban mobility, considering the following mobility alternatives: a) on foot, b) pedal bicycle, c) electric skateboard, d) motorcycle, e) fuel car, f) electric car. This paper presents a quali-quantitative approach of exploratory scope based on a case study, where we analyze a typical person who lives in the city of Bahía Blanca (Argentina) and does not use shared mobility. The primary sources of data are participant observation and interviews with a mobility entrepreneur. As secondary sources, we included technical information from transportation companies.
The economic analysis developed in this work is based on the marginal cost model. It includes explicit costs, generally considered in the mobility decision, and implicit costs, such as those associated with travel time. In terms of costs, our results show that for a journey of 10 km per day the preferred transport mode is fuel motorcycle. However, there is a trend towards more sustainable mobility modes, such as smaller and electric vehicles, so we also included a preliminary qualitative assessment of environmental impact.

Keywords: sustainable vehicles, urban mobility costs.

1. INTRODUCTION

In today's society, there is a greater concern for the environment and, especially in the last decade, it has become an important subject in the institutional and political agenda of most countries. According to a survey carried out by IPSOS Consulting among consumers in 28 countries, people indicate a growing concern about global warming, air pollution and waste management.

In the context of environmental concerns, together with transit problems in large cities, new trends in urban mobility are emerging (Figure 1). Among them, electric vehicles stand out for reducing noise pollution significantly. They are also more sustainable, as they use electricity from potentially renewable sources and do not emit greenhouse gases. The main drawback of this technology is the

Co-funded by the Erasmus+ Programme of the European Union

required infrastructure, as the installation of recharging stations. The use of smaller vehicles, such as motorcycles, bicycles and skateboards, in urban areas also increased dramatically. An advantage of these vehicles is the mobility speed up, which also alleviates traffic jams.

In addition to electric vehicles, shared mobility systems have also been developed. In these systems, vehicles improve transport efficiency by increasing the use/capacity ratio, which results in better urban traffic flows, less pollution and parking demand reduction. This type of system must be coordinated and regulated, and its success depends on a cultural change where the transport service quality prevails over private property. It is worth mentioning that shared electric bicycles are another solution adopted by many cities around the world.

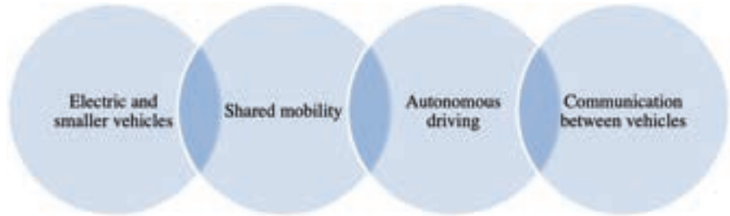

Figure 1: Urban mobility trends. Source: own elaboration.

More sophisticated advances, from a technical point of view, tend towards the production of driving vehicles with higher degrees of autonomy and communication between vehicles. It is expected that this will lead to smarter traffic, fewer accidents and traffic jams, parking efficiency, and less infrastructure. Autonomous drones for people transportation are an example of intelligent vehicles, and it represents a highly evolved solution for developed cities and short distance mobility.

Although several shared mobility systems and public transport, including metro, bus or trains, have been evaluated in terms of their convenience at the aggregate level (Buehler, Pucher, Gerike, & Götschi, 2016; Camagni, Gibelli, & Rigamonti, 2002), the emergence and increase in the use of these means of transport should also be evaluated from the perspective of the individual making the urban mobility decision. This kind of decision involves multidimensional aspects such as time, money as well as the potential impact on the environment and society. These dimensions do not lead to the existence of a prevalent transportation mode that could satisfy the mentioned criteria altogether. In modern cities, roads foment private transport, where the particular car is the central instrument of the mobility system. This scenario causes environmental, social and economic issues (Aliano et al., 2019). Smart and sustainable mobility emerges as a solution by offering efficient, clean and equitable transportation for people, goods and data (Prada et al., 2015).

2. OBJECTIVES

The main objective of this paper is to carry out a comparative economic analysis of personal urban mobility for a typical individual who lives in the city of Bahía Blanca (Argentina), considering the following alternatives:

a) by foot,
b) pedal bicycle,
c) electric skateboard,
d) motorcycle,
e) fuel car,
f) electric car.

Co-funded by the Erasmus+ Programme of the European Union

The European Commission support for the production of this publication does not constitute an endorsement of the contents which reflects the views only of the authors, and the Commission cannot be held responsible for any use which may be made of the information contained therein. Project number: 585796-EPP-1-2017-1-AT-EPPKA2-CBHE-JP

The main goal of this work was accomplished through the following specific objectives:

- Define convenient means of transport for urban mobility of a typical individual who lives in a middle sized city in Argentina.
- Determine indifference points by calculating equal-cost distances for which it would be convenient to move by using one vehicle or another.
- Qualitatively evaluate current environmental impacts of the means of transport under study.

Due to the urban mobility characteristics of the city evaluated in this work, neither shared mobility nor train systems are considered due to the lack of these services at the intra-city level.

The results from this study are potentially useful for decision-making by individuals who consider the total efforts of urban mobility, and not just economic expenses.

3. LITERATURE REVIEW

3.1. Trends in mobility

Car use and ownership have increased over the past decades in most countries around the world (Buehler et al., 2016). Likewise, greenhouse gas emissions have continued to grow, with transport being one of the largest contributors. This is a major reason why it is crucial to introduce more sustainable alternatives (Reddy & Balachandra, 2012).

According to Bertolini & le Clercq (2003), there are no mobility alternatives that satisfy both the accessibility quality provided by private motorized transport and sustainability. As a result, private motorized transport prevails compelling cities to implement policies to reduce traffic congestion. As described by Gakenheimer (1999), such policies include driving restrictions, highway privatization, pricing on assertive congestion and ownership, new technologies, car sharing, and land use planning. These are approaches more common in the developing world. Europe, on the other hand, has already implemented incentives for low-emission vehicles with the goal of reducing traffic jams and pollution. There are also modal shift policies to encourage active travel (cyclists and pedestrians), public transport and/or joint mobility promoting the use of bikes, car-sharing and car-pooling (Pinna, Masala, & Garau, 2017).

In metropolitan regions, sharing goods and items is emerging as a new trend, giving rise to the so-called Shared-Economy. In addition, there is a growing promotion of cycling, as an innovative, environmentally friendly and energy efficient form of mobility (Paul & Bogenberger, 2014). Jakovcevic, Caballero & Ledesma (2015) considers sustainable mobility as a component of smart mobility. The main aspect of smart mobility is connectivity because users can transmit traffic information in real time enabling public administrators to simultaneously conduct dynamic management. Also, cities share their data so that best practices can be identified and applied in other urban contexts.

Jakovcevic et al. (2015) delved into the shared bicycle system and found that it satisfies to a great extent three of the most valuable aspects when it comes to choosing a means of transport: speed, arrival time control and economic savings (instrumental aspects). Satisfying these aspects is essential to initiate a behavioral change in mobility. Entertainment and comfort (affective aspects), perceived as less positive, were classified as secondary aspects. However, if the bicycle choice is based only on instrumental motivations, it may not be maintained over time. As pointed out by Jakovcevic et al. (2015), environmental psychology studies indicate that only those people with pro-environmental

Co-funded by the Erasmus+ Programme of the European Union

behavior tend to sustain the bike use over time.

Despite the advantages of shared bicycle systems, users reported two main frustrations: difficulties to find available bikes and the impossibility to return the bike because of either lacking stations nearby the user's destination or full stations (Kaltenbrunner, Meza, Grivolla, Codina, & Banchs, 2010). Jakovcevic et al. (2015) suggest that increasing the number of stations, thus improving accessibility, would be the most efficient policy to make shared bicycles more popular. This measure would have a clear impact on speed, which is the most valuable aspect from the user perspective. Another important measure would be bicycle maintenance, which should also improve availability. Finally, user evaluations on travel safety can still be improved by enhancing bicycle lanes conditions or by creating new routes that would isolate users more from motor traffic.

Several studies show an increase in bicycle use as a transport mode: Buehler et al. (2016) show that in cities like Singapore, Hong Kong, Seoul, London, Paris, Copenhagen, and Stockholm there has been a decrease in car use and an increase in walking, bicycling, and public transport modes over the past two decades. Bertolini & le Clercq (2003) reveal a growing proportion of bicycle travel and a decline in both car use and public transport proportions in total journeys in Amsterdam.

In contrast to the aforementioned studies, Schrank, Eisele & Lomax (2012) project that the growth in alternative transport modes (biking, walking) will continue at the same rate.

3.2. Empirical evidence of costs in means of transport

The current level of fuel-based vehicles use should decrease not only because of the associated environmental damage, but also because fossil fuel reserves are finite and will be expensive as it becomes scarce. On the other hand, alternative fuels are already expensive and technological innovations will likely raise costs. Still, it would be beneficial to encourage shifts in mobility preferences. This is expected to increase the importance in the market of electric-based transport modes (Wegener, 2012). Regarding urban passenger transport, Regoli Roa, Bobbio & Brondino (2013) point out that the set of opportunities is defined as the different alternative modes of transport available from which an individual can select considering his/her restrictions and costs. These aspects were considered in the current work.

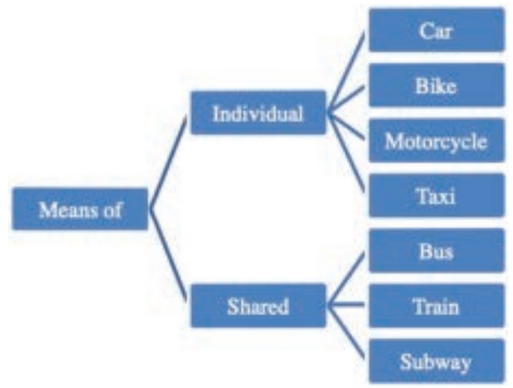

Figure 2: Means of transport. Source: own elaboration based on Regoli Roa et al. (2013).

The cost analysis of both individual and shared means of transport in the city of Santa Fe reveals that a modal balance is required in order to reduce costs. The analysis should be carried out by comparing intervention and decentralization scenarios, considering various cost categories, namely operational, time, and air and noise pollution.

Co-funded by the Erasmus+ Programme of the European Union

Cost categories	Description
Operating costs	Costs generated by each transport mode considering productive efficiency.
Time costs	Travel time cost considering congestion and time costs in general.
Air pollution costs	Environmental externalities valuation by estimating the cost of air improvement. The cost estimation includes health costs as an avoidable cost given that reducing pollution is expected to reduce health expenses.
Noise pollution costs	Cost is estimated by the avoided costs method. It estimates the monetary value that society saves as a result of noise level reduction. This method assesses the effect of noise according to its impact on property depreciation of certain neighborhoods.

Table 1: Description of cost categories and cost estimation method
Source: own elaboration based on Regoli Roa et al. (2013).

Despite high costs, efficiency and equity are also crucial factors that would be greatly benefited by policies that promote the development of attractive shared transport systems (Regoli Roa et al., 2013).

Finally, Jurdak (2013) argues that dynamic costing structures or incentive schemes are suitable for charging public bicycle systems because they use sensitivity analysis around pricing boundaries in usage patterns. Therefore, dynamic costing and incentives have to find the right balance between equity in bicycle access penalizing longer trips with higher costs, and demand optimization in target locations, by reducing the cost at some locations.

4. METHODOLOGY

4.1. Methodological details

This paper presents a quali-quantitative approach of exploratory scope based on a case study (Yin, 1994), where we analyze a typical individual who lives in the city of Bahía Blanca (Argentina) and does not use shared mobility systems. In this work, the primary sources of data are participant observation and interviews with a sustainable mobility entrepreneur, mechanics and engineers. As secondary sources, we included technical information from transportation companies. More details are presented in Table 2.

Co-funded by the Erasmus+ Programme of the European Union

Methodological approach		Details
Scope	Exploratory	Studies on individual transportation costs in Bahía Blanca, Argentina are lacking
Time costs	Case study	Not generalizable and adjusted to the particular characteristics of the geographical area under study
Object of study	Personal urban means of transport of a typical individual who lives in Bahía Blanca (Argentina)	The individual is in good health conditions to move in any means of transport. He/she daily commutes 10 kms to work, a usual distance for citizens of the neighborhoods with the highest population density who travel to the city center, considering its dimension. This distance assumption is sensitized in section 5.2 of the article.
	About the city	The city is located in the southwest of Buenos Aires state, Argentina. It is a medium-sized city with an urban cluster area of 2,247 km2 and a population of 301,572. In the city, there is no train transport and no formal pooling mobility systems, except for the bus.
Data sources	Primary	Participant observation (time measurement) 2. Semi structured interview with a sustainable mobility company entrepreneur (see interview scripts in Appendix) 3. Specific queries with mechanics and engineers.
	Secondary	1. Manuals 2. Technical information of companies that provide means of transport. 3. Official websites of companies in the mobility industry.

Table 2: Description of methods used in this work
Source: own elaboration.

A recent study of characterization and flow of the vehicular fleet of Bahía Blanca, carried out by Grassi, Brignole & Díaz (2020), shows that private sedan cars account for 60 to 75% of the vehicles that transit, while motorcycles represent 10 to 15% of the vehicles that circulate in the downtown area. Trucks and light-duty vehicles follow in importance. It should be noted that the cited study does not analyze small vehicles (bicycles, scooters, etc.) traffic. Information about this was found in a report published by the Secretary of Urban Mobility and Public Spaces of Bahía Blanca (2020), which reveals an increase in the circulation of bicycles (from 5.65% to 15.43% in 46 days) and micromobility vehicles, mainly electric skateboards, in the macro-center area of Bahía Blanca.

The importance of alternative transport availability can be crucial in a public health emergency scenario, such as the current COVID-19 pandemic, where non-shared mobility systems seem to have additional advantages and are safer alternatives according to public policy recommendations.

Co-funded by the Erasmus+ Programme of the European Union

In this paper, we analyze small and medium-sized means of transport, highlighting that the choice includes traditional ones, such as pedal bicycles, fuel motorcycles, fuel cars, as well as modern means, such as electric skateboards and electric cars. Technical specifications of the analyzed mobility systems are defined in Table 3, excluding transport by foot as it does not require additional details.

Means of transport	Technical specifications
Pedal bicycle	Urban Aluminum Folding Bike - Adjustable handlebar Imported 24 inches 8 speeds Weight: 13 kg
Electric skateboard	Motor: 36V / 300W National Production Autonomy of 30 km. Charging time: 4 hours. 1000 charge cycles (lithium battery) Solid 8” tire Maximum charger 2 amp at 220V
Fuel motorcycle	Urban fuel motorcycle Displacement: 110 CC Maximum load: 150 kg Fuel tank: 4,5 L Maximum speed: 80 km/h
Fuel car	Sedan Mid-range - segment B 5 doors 1.6L engine Fuel tank: 47 to 55 L Maximum speed: 173 to 217 km/h Consumption: combined 7.5 l/100 km (city 10, route 5.9)
Electric car	Two-seater electric urban sedan Category L7 in Argentina – National Production 8kW and 180 Nm motor Lithium battery that can be charged up to 220V (10A) in 6 hours of 3000 charge cycles Autonomy of up to 150 km Maximum speed limited to 105 km/h Trunk with capacity for 300 liters

Table 3: Technical specifications of the chosen means of mobility
Source: own elaboration.

Co-funded by the Erasmus+ Programme of the European Union

4.2. Economic data

For the economic analysis, the marginal costing method is applied. Kilometers traveled by each means of transport is used as the cost unit measure. This method distinguishes fixed costs, which do not change with the level of activity or traveled distance, from variable costs, which do depend on traveled units. Among the fixed and semi-fixed costs, which are expressed in monetary units per year, the following costs are independently assessed: maintenance and repair costs, opportunity cost of invested capital, insurance and taxes and expenses of parking and personal protective equipment (where applicable). As variable costs, expressed in monetary units per kilometer, we identify the cost of fuel or electrical energy, lubricants, and the opportunity cost for mobility time. Asset depreciation behavior requires a particular analysis in order to determine whether it should be computed as fixed or variable. In this work this is done by analyzing whether the loss in value is higher due to use (variable) or to obsolescence (fixed). For this purpose, the aging level is calculated as the ratio of kilometers of
useful life by years of useful life and it is compared against the level of use. For each vehicle, fixed depreciation is considered when the kilometers traveled is less than the aging level, which indicates obsolescence. Variable depreciation applies when value is lost mostly through use. For all the cases analyzed, and assuming that the vehicle is used 312 days per year to travel 10 km daily, depreciations classified as fixed.

Costs are specified in American dollars (US$) based on estimated prices in Argentine pesos (AR$), which is the legal currency. Costs are updated to December 2020 so as to consider local inflation. Currency conversion into dollars is carried out using the official retail exchange rate published by the Central Bank of Argentina on December 17, 2020, which corresponds to AR$ 88.18/US$.

The travel time for a 10 kilometers journey per day, shown in Table 4, is computed as an opportunity cost. It represents what an individual loses by investing that time in mobility for each means of transport. An example of a loss could be working time, which is quantified by the loss of professional fees after taxes.

Means of transport	By foot	Pedal bicycle	Electric skateboard	Motorcycle	Fuel car	Electric car
Pedal bicycle	2.00	0.83	0.92	0.40	0.33	0.33
Electric skateboard	0.20	0.08	0.09	0.04	0.03	0.03

Table 4: Travel time according to means of transport
Source: own elaboration.

Maintenance and repair costs are calculated on an annual average base according to maintenance plans for each vehicle. It includes technical verification cost, where applicable. This excludes smaller vehicles.

Investment values for all vehicles are evaluated based on purchase prices, so the market and acquisition values coincide. A risk-free rate is considered for calculating the opportunity cost of invested capital of 2.88% per year in US dollars, equivalent to the average yield of American t-bonds of the last 5 years (Damodaran, 2020).
Vehicle insurance considered in this work covers theft and total destruction as well as third party liability. The automotive state tax is an aliquot on the value of the good and it applies only to fuel vehicles.

Co-funded by the Erasmus+ Programme of the European Union

5. RESULTS AND DISCUSSION

5.1. Costs matrix

Table 5 shows the results of the estimated costs for each means of transport, specifying both variable and fixed costs.

Costs	by foot	Pedal bicycle	Electric skate-board	Motor-cycle	Fuel car	Electric car
Variable costs (US$/km)						
Fuel/ Electrical energy	-	-	0.005	0.022	0.100	0.012
Lubricants	-	0.002	-	0.002	0.001	0.001
Opportunity cost for mobility time	1.588	0.661	0.730	0.318	0.262	0.262
Depreciation (depends)	-	-	-	-	-	-
Subtotal ($ per kilometer)	**1.588**	**0.663**	**0.735**	**0.341**	**0.363**	**0.275**
Fixed costs (US$/year)						
Maintenance and repair costs	-	13.61	9.53	54.89	371.23	199.14
Depreciation (depends)	-	136.09	226.81	97.30	1.731.69	2.000.00
Opportunity cost of invested capital	-	19.60	26.13	28.02	498.73	576.00
Insurance and taxes	-	141.49	141.49	184.89	637.56	402.81
Expenses of parking	-	68.04	-	272.17	489.91	489.91
Personal protective equipment	-	8.82	8.82	8.22	-	-
Subtotal ($ annual)	**0.00**	**387.64**	**412.77**	**645.50**	**3.729.11**	**3.667.86**
Annual total cost assuming 10 km daily (US$/year)	**4953.50**	**2456.09**	**2706.39**	**1710.43**	**4861.62**	**4526.83**

Table 5: Costs in transport selection **Source:** own elaboration.

As it can be observed in Table 5 and Figure 3, the ranking of the means of transport from the cheapest to most expensive is the following: 1. fuel motorcycle; 2. pedal bicycle; 3. electric skateboard; 4. electric car; 5. fuel car; 6. on foot.

Co-funded by the Erasmus+ Programme of the European Union

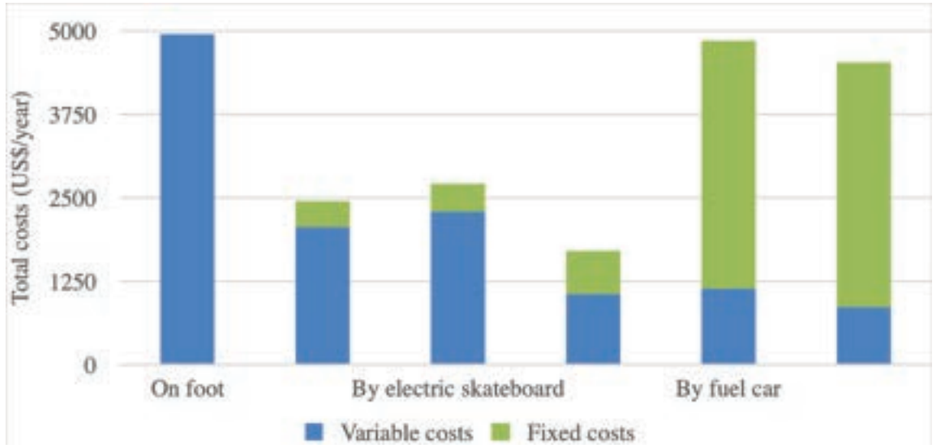

Figure 3: Total annual cost by means of transport. **Source:** own elaboration.

In smaller vehicles and on foot, variable costs constitute the most important component of the total cost. In particular, the main source of variable costs is the opportunity cost of the time invested in mobility. In contrast, for large vehicles, such as fuel and electric cars, fixed costs represent more than 75% of the total, as shown in Figure 4.

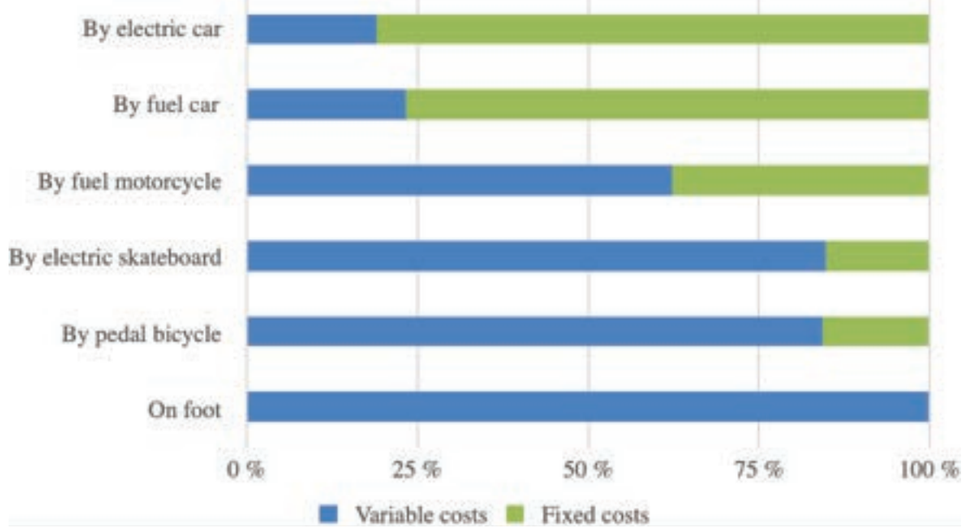

Figure 4: Share of fixed and variable costs. **Source:** own elaboration.

As summarized in the third column of Table 6, the highest cost for all means of transport is of implicit nature, which means that it does not involve a monetary expense. When analyzing payable or cash costs, specified in the fifth column of Table 6, one can note that energy never represents the most important cost.

Co-funded by the Erasmus+ Programme of the European Union

Means of transport	Maximum cost		Maximum payable cost	
	Concept	% over total costs	Concept	% over total costs
By foot	Opportunity cost for mobility time	100.00%	None	0.00%
Pedal bicycle	Opportunity cost for mobility time	84.00%	Insurance	5.76%
Electric skateboard	Opportunity cost for mobility time	84.19%	Insurance	5.23%
Fuel motorcycle	Opportunity cost for mobility time	57.92%	Expenses of parking	15.91%
Fuel car	Depreciation	35.62%	Insurance and taxes	13.11%
Electric car	Depreciation	44.18%	Expenses of parking	10.82%

Table 6: Maximum costs in transport selection **Source:** own elaboration.

5.2. Sensitivity analysis and indifference distances

Using the difference between variable and fixed costs, indifference distance is calculated as the point where the total cost of two means of transport coincide. This distance allows to determine convenience ranges in daily distances for each means of transport. The annual indifference distance is defined as follows:

$$ID = \frac{FC_i - FC_j}{VC_j - VC_i}$$ **Equation 1**

In Equation 1, ID is the annual indifference distances for transport means i and j, FC_i is the annual fixed cost for transport system i and VC_i corresponds to the total variable cost per kilometer for i.

Table 7 presents the results of the sensitivity analysis for distances, which are expressed in kilometers/day. In addition, convenience ranges, shown in Table 8, were obtained by analyzing the results of Table 7.

	By foot	Pedal bicycle	Electric skateboard	Fuel motorcycle	Fuel car	Electric car
By foot		1.34	1.55	1.66	9.76	8.96
Pedal bicycle	1.34		always bike	2.57	35.70	27.12
Electric skateboard	1.55	always bike		1.89	28.56	22.69
Fuel motorcycle	1.66	2.57	1.89		always motorcycle	146.75
Fuel car	9.76	35.70	28.56	always motorcycle		always electric car
Electric car	8.96	27.12	22.69	146.75	always electric car	

Table 7: Sensitivity analysis and indifference distances **Source:** own elaboration.

Co-funded by the Erasmus+ Programme of the European Union
The European Commission support for the production of this publication does not constitute an endorsement of the contents which reflects the views only of the authors, and the Commission cannot be held responsible for any use which may be made of the information contained therein. Project number: 585796-EPP-1-2017-1-AT-EPPKA2-CBHE-JP

If means of transport preference is analyzed in terms of costs, pedal bicycle is preferred over electric skateboard, as this system has higher annual fixed and variable costs per kilometer. Fuel car is defeated by fuel motorcycle and electric car, since these have lower variable and fixed costs. In the case of electric car, despite having higher depreciation and opportunity cost of invested capital, fixed costs are compensated by lower maintenance expenses and taxes.

Daily distance interval (km/day)	Most convenient means of transport
[0; 1.34)	By foot
[1.34; 2.57)	Pedal bicycle
[2.57; 146.75)	Fuel motorcycle
[146.75; +infinity)	Electric car

Table 8: Distances to establish the convenience for each means of transport **Source:** own elaboration.

Finally, we carried out a univariate sensitivity analysis on the opportunity cost of the time invested in the trip. Table 9 shows the preferred transport system for a travel distance of 10 km/day as a function of professional fees ranges. People with low pay or fees move on foot and the preference shifts to bicycle when they earn more. This is followed by fuel motorcycle and the better paid individuals choose electric car. This explains why for the range of professional salaries currently paid in Argentina, the motorcycle corresponds to the most economical means of transport.

Professional fees interval (US$/hour)	Most convenient means of transport
[0.00; 1.48)	By foot
[1.48; 2.42)	Pedal bicycle
[2.42; 136.89)	Fuel motorcycle
[136.89; +infinity)	Electric car

Table 9: Ranges of fees/wages to establish the convenience of each means of transport **Source:** own elaboration.

5.3. Qualitative impacts of transport systems on the environment

In addition to economic factors, there are subjective factors that potentially influence the selection of a means of transport. According to the interviewed entrepreneur, one of the reasons that customers usually mention when buying electric vehicles is related to a reduction of negative effects on the environment.

The most relevant environmental impacts are carbon dioxide emissions and battery disposal, as well as noise pollution and the energy type used by a vehicle. Table 10 shows a gradient of environmental impacts for each means of transport where the number of “x” increases with the environmental damage associated with a given means of transport. As an example, moving on foot or by pedal bike are the most environmentally friendly forms of transportation and this is why they have the minimal number of “x”.

Co-funded by the Erasmus+ Programme of the European Union
The European Commission support for the production of this publication does not constitute an endorsement of the contents which reflects the views only of the authors, and the Commission cannot be held responsible for any use which may be made of the information contained therein. Project number: 585796-EPP-1-2017-1-AT-EPPKA2-CBHE-JP

Environmental impacts	by foot	Pedal bicycle	Electric skate-board	Fuel Motor-cycle	Fuel car	Electric car
Carbon dioxide emissions	x	xx	xx	xxxx	xxxxx	xx
Battery disposal	x	x	xxxx	xx	xx	xxxxx
Noise pollution	x	xx	xx	xxxxx	xxxx	xx
Use of non-renewable energy sources	x	x	x	xxxx	xxxxx	x

Table 10: Environmental impacts **Source:** own elaboration.

Based on carbon dioxide (CO2) emissions, we differentiate the urban transport systems as follows (Revista Turbo, 2018):

Walking is the form of urban mobility that generates the minimal carbon footprint, since it is a natural act and does not require extra energy.

Riding a bicycle does require more effort than walking and some calculations suggest that 16 grams of carbon are released per kilometer traveled. Also, manufacturing can contribute with extra 5 grams/km of carbon, thus reaching 21 grams of total emissions.

Fuel cars emit 271 grams of CO2 per passenger per kilometer.

Although the lithium-ion batteries in electric vehicles are manufactured with non-renewable materials, according to EcoInventos (2020) most of these materials can be reused. In particular, nickel, cobalt, manganese, and lithium can be recovered and reused as raw materials. There are some companies that are already showing significant progress in this respect. For example, the Finnish company Fortum has very high standards and is able to recycle 80% of lithium-ion battery components. This is a significant improvement over the 50% required by the European Union. Finally, China, where electric cars and buses are already quite popular, is developing electric car battery recycling programs in order to benefit from batteries that reach their useful life.

6. CONCLUSION

The economic analysis developed, based on the marginal cost model, includes not only explicit costs that are generally considered in the mobility decision, but also implicit costs such as those associated with travel time, whose importance became evident in this work.

The results of this research show the following ranking of the means of transport from the cheapest to the most expensive: 1. Fuel motorcycle; 2. bicycle pedal; 3. electric skateboard; 4. electric car; 5. fuel car; 6. on foot. In particular, for a journey of 10 km per day and over a wide range of distances (from 2.57 to 146.75 daily km), the more economical mode of transport is the fuel motorcycle. For shorter distances, the use of a pedal bike prevails. However, in Bahía Blanca there is a trend towards more sustainable means of mobility with a consistent growth in the use of small and electric vehicles. This is the main reason why the results of this research are complemented with a preliminary qualitative evaluation of environmental impacts.

Among the limitations of the paper, it stands out that it is a case study so the results are not generalizable for other vehicle models neither for future times or places in the world.

Co-funded by the Erasmus+ Programme of the European Union

Finally, ideas for future work include the quantification of environmental effects described in the previous section, the evaluation of the effects on health of the different transport systems, as well as mobility habits of citizens and the analysis of other alternative means of transport, such as the electric motorcycle.

REFERENCES

Aliano, S., Blanco, G., Díaz Almassio, N., Keesler, D., & Sosa, B. (2019). *Movilidad sustentable: desafíos para la Argentina.* Centro de Tecnologías Ambientales y Energía de la Universidad Nacional del Centro de la Provincia de Buenos Aires (UNICEN) para la Fundación Ambiente y Recursos Naturales (FARN), socio Climate Transparency.

Bertolini, L., & le Clercq, F. (2003). Urban Development without more Mobility by Car? Lessons from Amsterdam, a Multimodal Urban Region. *Environment and Planning A: Economy and Space*, 35(4), 575–589.

Buehler, R., Pucher, J., Gerike, R., & Götschi, T. (2016). Reducing car dependence in the heart of Europe: Lessons from Germany, Austria, and Switzerland. *Transport Reviews*, 36(1), 1-25.

Camagni, R., Gibelli, M. C., & Rigamonti, P. (2002). Urban mobility and urban form: the social and environmental costs of different patterns of urban expansion. *Ecological economics*, 40(2), 199-216.

Damodaran, A. (2020). Annual returns on investments form 1928 up to 2019. Available in: http://pages.stern.nyu.edu/~adamodar/New_Home_Page/datafile/histretSP.html

EcoInventos (2020). Nueva solución de reciclaje de baterías de iones de litio, se recuperan hasta el 80% de los materiales. Available in: https://ecoinventos.com/solucion-de-reciclaje-de-baterias-de-iones-de-litio/#:~:text=%C2%BFC%C3%B3mo%20se%20reciclan%20las%20bater%C3%ADas,un%20proceso%20de%20precipitaci%C3%B3n%20qu%C3%ADmica.

Gakenheimer, R. (1999). Urban mobility in the developing world. Transportation Research Part A: Policy and Practice, 33(7-8), 671-689.

Grassi, Y. S., Brignole, N. B. & Díaz, M. F. (2020). *Hacia el desarrollo de una movilidad inteligente para la ciudad de Bahía Blanca: Primer enfoque sobre la caracterización de la flota vehicular del microcentro.* Paper presented in the International Conference of Production Research - Americas 2020.

Jakovcevic, A., Franco, P., Caballero, R., & Ledesma, R. (2015). Determinantes psicológicos de las conductas de movilidad: Un estudio de revisión. *Revista Argentina de Ciencias del Comportamiento,* 7(2), 59-77.

Jurdak, R. (2013). The impact of cost and network topology on urban mobility: A study of public bicycle usage in 2 US cities. PloS one, 8(11), e79396.

Kaltenbrunner, A., Meza, R., Grivolla, J., Codina, J., & Banchs, R. (2010). Urban cycles and mobility patterns: Exploring and predicting trends in a bicycle-based public transport system. *Pervasive and Mobile Computing,* 6(4), 455-466.

Paul, F., & Bogenberger, K. (2014). Evaluation-method for a station based urban-pedelec sharing system. *Transportation Research Procedia*, 4, 482-493.

Pinna, F., Masala, F., & Garau, C. (2017). Urban policies and mobility trends in Italian smart cities. *Sustainability,* 9(4), 494.

Prada, F. P., Romera, G. V., Añez, V. F., & Sánchez, J. D. (2015). Movilidad inteligente. *Economía industrial,* (395), 111-121.

Reddy, B. S., & Balachandra, P. (2012). Urban mobility: A comparative analysis of megacities of India. *Transport Policy,* 21, 152-164.

Regoli Roa, S., Bobbio, H., & Brondino, L. (2013). Investigación científica: Costos sociales y regulación de la movilidad urbana. *Ciencias Económicas,* 10(1), 47-62.

Revista Turbo (2018). ¿Cuánto carbono producen los distintos tipos de vehículo?. Available in: http://www.revistaturbo.com/noticias/cuanto-carbono-producen-los-distintos-tipos-de-vehiculo-1197

Secretary of Urban Mobility and Public Spaces of Bahía Blanca (2020). Available in: https://noticias.bahia.gob.ar/2020/10/27/informe-de-circulacion-vehicular-en-calle-19-de-mayo-marca-un-incremento-en-el-uso-de-bicicletas/.

Wegener, M. (2013). The future of mobility in cities: Challenges for urban modelling. Transport Policy, 29, 275-282.

Yin, R. K. (1994). Case Study Research: *Design and Methods, Applied Social Research Methods.* Newbury Park: Sage.

Co-funded by the Erasmus+ Programme of the European Union

APPENDIX

Script of the interview with a mobility entrepreneur

1. How was your sales trend this year and what is the relative importance of each product line (motorcycles, bicycles, skateboards)?
2. Why do your customers buy means of electric mobility? What are the most mentioned arguments or reasons?
3. Forecasts of the mobility market.
4. Do you think it is feasible to develop the electric car market in Bahía Blanca?
5. Recommended maintenance service for each means of transport.
6. Kilometers and years of useful life for each means of transport.

Co-funded by the Erasmus+ Programme of the European Union

18.3 ELECTRIC POWERTRAIN SYSTEM DESIGN FOR LOW WEIGHT URBAN MOTORCYCLE PROTOTYPE

Bernardo Lessa Guerra [1], Prof. Dr.-Ing. Fernando Augusto de Noronha Castro Pinto [2]

[1] Student, Mechanical Engineering, Polytechnic School, Federal University of Rio de Janeiro, bernardo.guerra@poli.ufrj.br
[2] Professor, Mechanical Engineering Department, Polytechnic School, Federal University of Rio de Janeiro, fcpinto@poli.ufrj.br

ABSTRACT

Advances in Electric Vehicle Technology have increased their implementation capabilities. However, there is still a lot of development to be done in terms of lightweight small port EVs for common city use. In this article, a powertrain system design is developed aimed at high autonomy utilizing city track mapping and energy consumption simulations for a low weight motorcycle prototype for delivery services. A digital methodology is used for stipulating energy consumption and power through track mapping utilizing satellite data and motorcycle data for sizing all components and structure of the prototype's powertrain. This result is then compared to a comparative methodology and the energy demand is established.
Furthermore, with energy consumption and overall power needed, the system was designed to ensure ease of maintenance for common everyday use and accessibility utilizing CAD software and FEA to determine the best ratio between accessibility, cost, and mass.

Keywords: Motorcycle, Electric Powertrain, Solidworks, Optimum Lap, Battery Cooling.

1. INTRODUCTION

Motorcycles represent an efficient and reliable transport for urban use. They have become common in cities and the main tool of work for many services, especially for delivery. Their utilization has increased over the last decade in Brazil (Caldeira, A. (2020)) and the high number of motorcycles present today represent a big opportunity for the development of an electric counterpart to the common internal combustion models in the market in an effort to reduce pollution (particle and noise) and provide a safer and more reliable transport.

However, urban-use vehicles also present some challenges. Contrary to many prototypes aimed at racing, such as those developed for student competitions and professional motorsport, these types of prototypes face more challenges in terms of autonomy instead of power and time. This results in a need for a balance between autonomy and cost to not create either an expensive vehicle compared to combustion engine models nor a heavy and impractical transport.

For this, the present work compared methodologies for estimating power, designed the tractive requirements and charging implementations, the accumulator, cooling method, internal safety systems, and cost for development and for charging the prototype.

Co-funded by the Erasmus+ Programme of the European Union

2. OBJECTIVES

To define the objectives of the prototype, a survey was done to identify the necessities of delivery workers for a typical workday. The survey aimed at identifying key components in determining autonomy, hours of work, typical distances from distribution center to residence, average speed, weekly cost with refueling, access to charging during work hours, and most common motorcycle models utilized.

From the responses, non-motorcycle responses were filtered and some directions were defined. Firstly, instead of constructing an entirely new motorcycle structure and components, it was decided to utilize a mass-market produced model as a base for the prototype. From the results, 62% of those interviewed reported utilizing a 150-160CC Engine Motorcycle while 19% said they used a 250CC model and only one answered using a 300CC model. Due to the responses and lower-costs than available 2021 models for 250 and 300CC, a 160CC base motorcycle was chosen for the prototype.

For determining range, it was observed that on average, the interviewed mentioned an average of 9.63km per journey and 14-15 journeys daily for an estimate of 140-150km. However, due to cost restrictions to build the full prototype, the total autonomy was reduced to 100km. Related to the speed, most answers reported driving between 60 to 90km/h on average, thus an average speed of 75km/h in the planned route was set as the objective. Although this value may seem high for urban environments.

Another objective established previously was to limit project cost at R$40,000.00. This was done due to resource availability and as a goal to construct a prototype that could be expanded into the market at lower and more competitive prices.

3. LITERATURE REVIEW

Country policies and lack of incentive to create EV infrastructure are one of the burdens to shifting from Internal Combustion Engines (ICE) to hybrid or electric vehicles. Although Brazil has bills for reducing taxes on import of electric vehicles, incentives are still lacking for charging infrastructure for public use. In Li, Y. (2016) a study into practices for deployment of infrastructure is conducted comparing China and Brazil. In his work, it is presented that although both countries are major emerging markets for EVs, China's incentives to replace its public transportation fleet to electric and construction of charging stations have played a significant role in promoting the shift while these incentives in Brazil have been limited. However, it is also presented that another obstacle is commercial cost, with total cost reduction in most models balancing combustion counterparts for a minimum of 3000km driven per month.

Research on available battery cells explained more thoroughly in Section 6, showed that for developing the prototype, the biggest costs would be associated with batteries, motors, and controllers and thus, indicated that accumulator capacity and energy density would be the biggest financial impactor. A Cost-Report presented in Lasciato, L (2019) and a study into the cost of an electric conversion done in Kaleg et. al (2015) also corroborated this hypothesis. For the Motostudent team, the Batteries and Competition Fee (which included the Electric Motor) represented roughly 60% of the costs and for the electric conversion the batteries represented 34% of the total cost.

Co-funded by the Erasmus+ Programme of the European Union

Considering also that import taxes on batteries to Brazil would represent an additional cost, a more affordable option is needed for the transition from combustion to electric, since 160cc base models cost roughly 1700 to 3000 USD locally.
This article proposes a design aimed at solving this problem through the creation of the electric powertrain utilizing mainly Brazilian suppliers and self-development of most components and connections while being in accordance to the necessities and common use of combustion motorcycles from delivery services and delivery workers.

4. ENERGY ESTIMATION

For the urban motorcycle project, a key factor was determining energy consumption during a full day's work. To do this, two methodologies were used. The first relied solely on free software and physically estimated motorcycle data. The second was through a comparative methodology with the combustion counterpart. These results were then compared to determine if a fully digital methodology utilizing free software would suffice for sizing the accumulator and the result with the highest energy consumption was used for safety.

4.1. Numeric Methodology

The first methodology involved creating a 30km route that would require different speeds, turns, and city scenarios. To do this, the route was planned on google maps ensuring that it would include all regions of Rio de Janeiro (see Fig. 1). This route was then mapped utilizing the free Open Source software ImageJ for determining distances and radius of curvatures. The information was input into OptimumLap by creating a track with the measured data, creating a motorcycle model, and inputting motor RPM x Torque data. OptimumLap simulates lap times, energy consumption, speed, torque, and other parameters utilizing a point-mass simulation.

Figure 1: Route Map made on Google Maps

Co-funded by the Erasmus+ Programme of the European Union

4.2. Comparative Methodology

Due to the pandemic, the evaluation through field data was not possible, thus another method was utilized for comparison against the numeric method. Saraiva, I. B. (2016) proposed in his thesis a motorcycle prototype based on a 250CC motorcycle. For estimating energy consumption, he compared the combustion engine yield efficiency in the wheel and used this result to extract how much energy would be needed for the motorcycle to have the desired autonomy. To apply this methodology to the 160CC base model, estimated fuel consumption and tank capacity from the manual were utilized (see Table 1).

Model	160CC Motorcycle
Fuel tank capacity	14-15 liters
Estimated efficiency	40-41km/l
Autonomy per full fuel tank	580-600km

Table 1: Fuel and Autonomy of 160CC Motorcycle

Assuming that the energy density of gasoline is 8.89kWh/liter (Government of Canada. (n.d.)) and that, according to Bottiglione, F. et al (2007), a motorcycle combustion engine has an efficiency of 15% on average, we can infer that the energy consumption for 41km on the ICE motorcycle:

$$E_{final} = E_{gasoline}\eta_{combustion\ engine} = 8.89 \times 0.15 = 1.3335 kWh/l$$

And the energy consumption per kilometer for the reference motorcycle:

$$A_{energy} = \frac{E_{final}}{D_{CG160}} = \frac{1.3335}{41} = 0.0325 kWh/km$$

With this information, an estimative can be drawn utilizing the data from the motor used as a base in the previous methodology and the transmission efficiency, using as reference the university's Formula SAE Electric Chain and Gear Transmission, the energy needed in the battery pack is calculated as:

$$E_{prototype} = \frac{Desired\ Autonomy\ per\ Charge}{A_{energy}\eta_{motor}\eta_{transmission}} = \frac{100}{0.0325 \times 0.815 \times 0.8914} = 4022.12\text{-}4220.74 kWh \text{ depending on load}$$

Co-funded by the Erasmus+ Programme of the European Union

5. MOTOR, CONTROLLER AND GEAR RATIO DECISION

With the methodology proposed, different motors were compared against each other. The main options evaluated were locally produced or commercialized models. Apart from that, a 6kW, 13Nm induction motor and respective inverter were available in the laboratory and so, were used as a base for initial simulation and to assess if the motor would be fit for the prototype, for which two simulations were made. The first to determine the most efficient final gear ratio that would satisfy the maximum and average speed. This simulation returned that the best gear ratio, considering a motorcycle without changing gears, would be of 4.8 with the closest values to the initial objectives (see Figure 2). With the results of the gear ratio, a final simulation reported that the motor was sufficient for the defined objectives, although the calculation discarded the speed limits of each route. This can be seen in Figure 2(d), where the track map graph reports a maximum velocity of 88.43km/h, an average speed of 79.33km/h, and energy consumption of approximately 1.25kWh for the simulation and 4.5kWh for 100km autonomy.

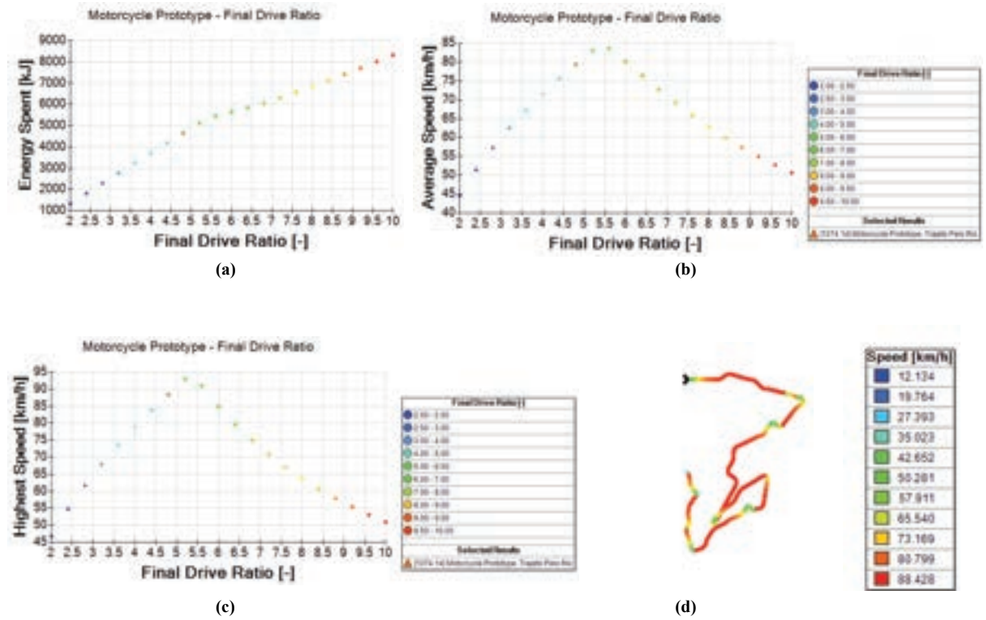

Figure 2 a) Energy consumption x Drive Ratio, b) Average Speed x Drive Ratio, c) Top Speed x Drive Ratio, d) Speed during the path

The results were similar to the methodology proposed in the previous section, although utilizing more data. The result from this method was chosen, as it requires more energy than the comparative method and thus, would result in a safety margin that could be further evaluated with physical testing when the prototype is constructed and when access to the laboratory is possible. It was decided to proceed with the mentioned motor.

Co-funded by the Erasmus+ Programme of the European Union

6. BATTERY CONFIGURATION DECISION

Since the chosen motor operates at a voltage of 72V, utilizing the total energy needed from the simulations, a battery capacity of approximately 62.5Ah was calculated. From this, extensive research into available models was conducted to select the best setup in terms of volume, weight, and price. For chemistry, only Lithium-ion cells were considered due to energy density and cost when compared to other chemistries. For format, cylindrical cells were chosen due to packaging, cooling, and physical limitations compared to other constructions. The cylindrical models found also tended to weigh less (for a complete battery pack) than prismatic and pouch counterparts of similar price ranges.

Brand - Model	Capacity (mAh)	Voltage (V)	Total Weight (kg)	Max. Continuous Discharge Current (A)	Number of Cells
Samsung INR18650-25R	2500	3.6	24.57	20	546
Samsung INR18650-35E	3500	3.6	18	8	360
Samsung ICR18650-22P	2200	3.6	27.4	10	609
Panasonic NCR18650GA	3500	3.6	16.2	10	360
Energus Li2x-10pGA	66000	3.6	22.05	200-325	21

Table 2: Main Battery Cell options analyzed

Apart from this, after filtering solutions and comparing only cells available in Brazil to reduce associated cost, the Samsung INR18650-35E was chosen due to large availability, highest Wh/Reais out of the cells analyzed, lowest total weight, and closest fit for the current demand for starting and nominal operation (see table 3). These cells were then arranged into a 20s27p configuration.

Cell Manufacturer and Model	Samsung INR18650-35E
Nominal Capacity	3500mAh
Maximum Voltage	4.2V
Nominal Voltage	3.6V
Maximum Discharge Rating (Continuous)	8A
Maximum Discharge Rating (Not for continuous)	13A
Charging Current	1.7A
Maximum Charging Current	2A
Cell Chemistry	$LiNiCoAlO_2$

Table 2: Main Battery Cell options analyzed

Co-funded by the Erasmus+ Programme of the European Union

7. MECHANICAL DESIGN OF BATTERY PACK

The battery configuration was separated into smaller submodules. This was done to adapt the battery pack for easy maintenance, construction and to be adaptable to other configurations for other prototypes. For this, the configuration was divided into smaller 20s3p submodules (see Figure 3). To create these submodules, a holder structure for the cells was designed to be 3D printed in thermal-resistant and insulating material. With cost restrictions, the ABS High-Temperature filament was chosen due to thermal and insulation properties in comparison to other filaments in the same price range. Nonetheless, with the cooling system presented in section 7.4, these holders would not exceed melting temperature.

Figure 3: Proposed Battery Module Design

7.1. Battery connectors and fuss

With thermal-runway and limitations imposed by cell chemistry and design, lithium-ion cells require temperature, charge balance, and current monitoring as well as fail-safe systems to ensure no cascade effects from malfunction to the accumulator system. One method for this is constructing the battery connections to act as safety measures for separating defective cells without compromising battery pack operation. Thus, for a city-oriented design, these were projected to act as fuse-connections. These systems can be created with wires or plates. However, due to availability, feasibility for soldering (point weld), and design capability, plates were chosen for the fuse-connectors.

For the batteries selected in the previous section, connections were set to operate in the range of 8 to 13A with melting and consequent disconnection at currents above those limits and for long operation at the upper limit.

Selection of material for the fuse-connectors was done based on cost, fabrication capabilities, electrical properties, and ease of installation. Common conductive materials utilized presently include copper, nickel, and aluminum alloys. An advantage of constructing the fuses out of these materials is reducing cost from wide distribution. However, although a poorer electrical conductor, nickel plates have the advantage of lower cost for 0.2 to 0.5mm thickness strips, which can be easily cut and bent into design format, and ease of connection through point welding.

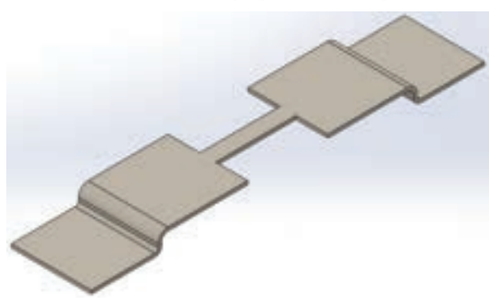

Figure 4: Cell to cell fuse-connector design

Co-funded by the Erasmus+ Programme of the European Union

Nickel plates were then designed utilizing a 0.2mm thick nickel plate seen in Figure 4, with two central cuts to create a region aimed at operation with the aforementioned requirements, and bends for the residue to be collected by polycarbonate sheets located between the cells and holders so as to not damage the battery body. As can be seen in Figure 5, the thermal-electric simulation conducted on these utilizing Ansys showed that the fuse plate with a 1mm wide central piece could operate at a maximum temperature of 889.18C for 8A during continuous discharge and 1335.5C for 13A discharge, and 1452.5C for 14.5A.

(a)

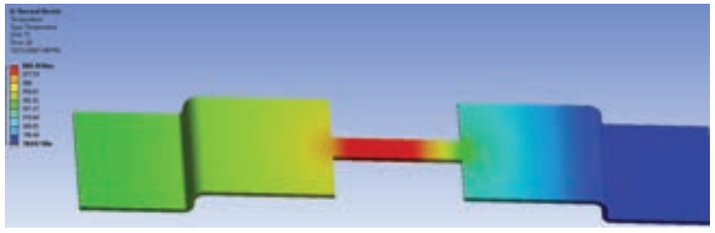

(b)

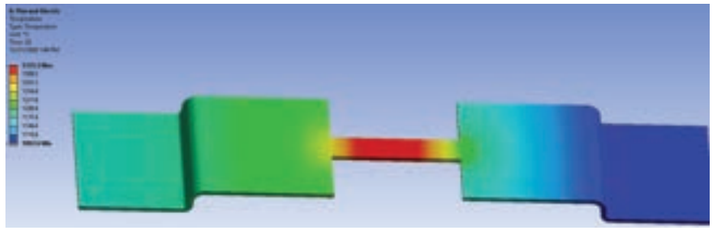

(c)

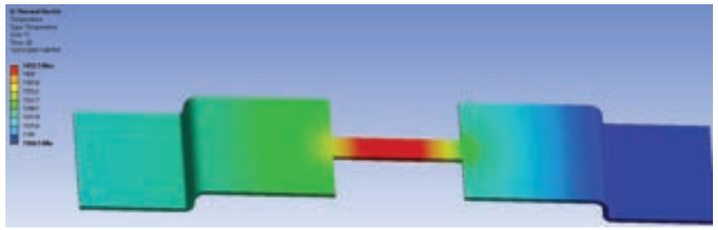

Figure 5. Nickel Plate under a) 8A current, b) 13A current and c) 14.5A current.

The fuse-connectors connected to the first and final cells of each row of series connections were connected to inter-module parallel connections. However, with accessibility stated as a priority for design, it would be necessary to disconnect and reconnect the modules in another setting without damages, no necessity for removing solderings, and be done with widely available materials. With the design aimed at continuous operation, safety systems provided by the electronics and the Nickel fuse-connectors present, from the 3 most widely available materials, copper had the highest conductivity, the lowest resistivity, and similar cost to both. Thus, it was decided to implement copper pieces at the end of each module. These pieces were designed with a wide piece at the bottom, constructed from a copper plate and bolt fixture pieces made with copper square bars. The Nickel pieces are soldered to the copper pieces and separate copper plates were implemented for connecting the modules as can be seen from the connection arrangement of the modules in Figure 6. To ensure no rotation from the bolts during operation, tab washers are also installed and bent.

Co-funded by the Erasmus+ Programme of the European Union

The European Commission support for the production of this publication does not constitute an endorsement of the contents which reflects the views only of the authors, and the Commission cannot be held responsible for any use which may be made of the information contained therein. Project number: 585796-EPP-1-2017-1-AT-EPPKA2-CBHE-JP

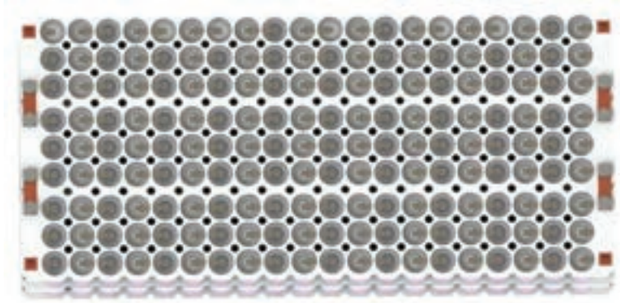

Figure 6: Assembly of Modules with Copper Plate and Bolt Connections

7.2. Connections from accumulator to tractive system

For connecting the accumulator to the tractive system, due to the nature of the prototype, a 3-step verification and fuse protection system was implemented. The 3-step safety measure is done utilizing accumulator isolation relays (AIRs) which are responsible for connecting/disconnecting the traction system depending on signals from the safety circuits, such as the Shutdown and Pre-Charge circuits. For the cabling connecting the tractive system, the motor has a nominal current of 120A and a maximum current of 228A. However, with the battery chosen, the maximum current output from the battery pack would be 234A for non-continuous discharge. Due to this, the cable was chosen to be able to withstand a current of at least 240A and which had electromagnetic shielding to prevent electromagnetic interference. The cable chosen was a Coroplast 25mm shielded by braided wire and metal foil which is described in Table 4.

Wire type	Coroplast, silicone-insulated single-core high voltage automotive cable
Cross-sectional area	25mm²
Maximum operating voltage	600V AC / 1000V DC
Current Rating	Ambient temperature +20 °C = 274 A, +85 °C = 216 A,+105 °C = 192 A, +125 °C = 164 A
Shielding	Tinned copper braiding and ALU-PET foil
Connections	Accumulator to HVD and Controller, Controller to Motor

Table. 4: Shielded Coroplast HV Cable

To guarantee that all parts of the tractive system are fully operational, a series of safety circuits inspect if the accumulator and control systems are functioning before permitting current flow through the controller. Thus, Normally Open relays were chosen for the design. Two relays are placed to connect the negative terminal of the inverter to the battery pack and a third is connected associated with the Pre-Charge system to connect the positive terminal as can be seen in Figure 8. Since it was previously determined by the Electronics team that a 12 VDC lead-acid battery would be used for all control electronics and the motor operates at currents from 120 to 230A, the chosen AIRs were two Gigavac GV200s and one GX14 (see Figure 7). This setup was chosen due to one of each of the AIRs being available currently from previous projects and the physical layout of the GV200 having a smaller base area.

Co-funded by the Erasmus+ Programme of the European Union

The European Commission support for the production of this publication does not constitute an endorsement of the contents which reflects the views only of the authors, and the Commission cannot be held responsible for any use which may be made of the information contained therein. Project number: 585796-EPP-1-2017-1-AT-EPPKA2-CBHE-JP

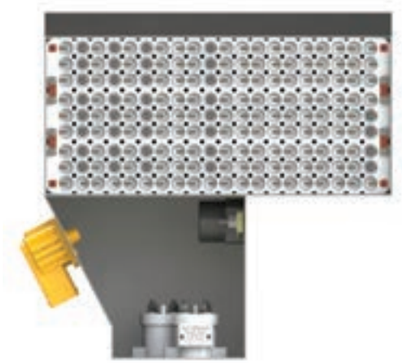

Figure 7: Assembly of HV Connectors and AIRs

AIR	Gigavac GX14 and GV200 - Coil Designation B
Contact Config	SPST-NO
Continuous DC rating	350A
Nominal Coil Voltage	12VDC
Maximum Coil Voltage	16VDC
Maximum Operation Voltage	800VDC
Temperature Rating	-55 to +85C

Table. 5: Gigavac GX14 and GV200

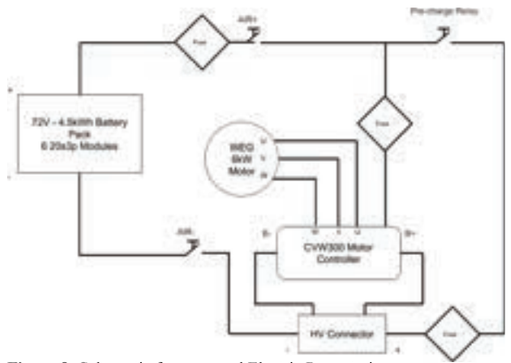

Figure 8: Schematic for proposed Electric Powertrain

Finally, to prevent damage to components, high current fuses were placed between all connections from the accumulator to the HV Connector and inverter (See Fig. 8). The fuses protect the cables while other security systems monitor the electrical components.

Since the system operates at a voltage of 72V and a nominal and peak current of 120 and 234A, respectively, a Fast Action 250A 80VDC fuse was chosen as this was the closest to the project

Co-funded by the Erasmus+ Programme of the European Union

The European Commission support for the production of this publication does not constitute an endorsement of the contents which reflects the views only of the authors, and the Commission cannot be held responsible for any use which may be made of the information contained therein. Project number: 585796-EPP-1-2017-1-AT-EPPKA2-CBHE-JP

specifications. Although different options are available, spare LittelFuse fuses of the same current rating were available from the Formula SAE Electric team and, thus, were implemented into the design. It was observed that, when comparing the nominal to the maximum current, the motor would have a nominal operation with 52.6% of the peak current, below the recommended operation of a maximum of 75% of the fuse current rating by LittelFuse.

7.3. Charging

For charging the accumulator, an Elcon PFC 2500 charger was available, and so, the charging system was adapted to work with the model and reduce prototyping costs. Charging is done by connecting the terminals of the PFC 2500 to the positive and negative HV Connectors positioned at the top of the battery pack and fit in the same position as the port for refueling in the base motorcycle.

7.4. Accumulator Cooling

Lithium-ion cells, though one of the most widely used types of batteries for electric vehicles, also have some setbacks. In terms of cooling, these cells tend to lose capacity and can create safety concerns when operating at high temperatures and poorer performance when at very low temperatures. Since this prototype is currently being developed with a city scenario in Rio de Janeiro, low temperatures were not a concern. However, high temperatures need to be accounted for and controlled. The heating from a battery cell occurs due to many aspects, such as internal resistive heating, enthalpy and electrochemical changes during charge and discharge (Katoch, S. S., & Eswaramoorthy, M. (2020)). When overheating, a battery cell may charge and discharge unevenly and thermal runaway may result in explosions, fire and other safety hazards.

Thus, a cooling structure is needed. To first understand how much cooling the battery pack would need, a maximum temperature for the operation was defined. The maximum operating temperature at the cell surface was 60 °C for discharge and 50 °C for recharge. Thus, to ensure the battery pack would not operate close to its upper limit and to permit regeneration from braking, a maximum temperature of 50°C was adopted as the limit for operation.

With the restrictions due to the pandemic, a physical testing method had to be discarded. Since the cooling system was aimed at keeping an overall temperature stable, simplifications were made to consider some parameters for the cells that were missing from datasheets and had to be estimated based on literature and studies with similar cells. For this, Table 6 was defined for the analysis.

Parameter	Value	Unit
Mass	0.05	kg
Diameter	0.06525	m
Length	0.01855	m
Density	2835.4	kg/m^3
Specific Heat	830	$Jkg^{-1}K^{-1}$
Internal Impedance	0.035	Ω
External Area	0.0038	m^2
Thermal Conductivity	8	$Wm-2K^{-1}$

Table. 6: Parameters for analyzing thermal behavior of Battery Cell

Co-funded by the Erasmus+ Programme of the European Union

The European Commission support for the production of this publication does not constitute an endorsement of the contents which reflects the views only of the authors, and the Commission cannot be held responsible for any use which may be made of the information contained therein. Project number: 585796-EPP-1-2017-1-AT-EPPKA2-CBHE-JP

With these assumptions, the heat generation rate of a single lithium-ion battery was assumed as the internal resistance Joule Heating, without considering Chemical Balance and Entropy changes (Magnusson, A. E. (2016)) which would require more data. From this, it was calculated that the battery proposed would have a dissipated power of 2.24 W.

Figure 9: Fan Inlet Design cut through the symmetry plane

For designing the cooling system, a fan-forced convection method was implemented. As can be seen in Figure 9, a series of slits were cut at the frontal and backward-facing faces of the accumulator structure to conduct the air through the bodies of the cylindrical cells inside the battery pack. In this design, a Push fan configuration was created, with the cells fixed into the holder structures and an external polycarbonate compartment, also cut through at the slits, separating the two sets of battery modules and isolating the inter-module connections and bolts from the external steel structure.

To evaluate the performance of this design, a Conjugate Heat Transfer (CHT) K-Omega SST Turbulence Model Simulation was created in SimScale to simulate the thermal management of the battery pack at different air inlet velocities. As seen in Figure 10, any load with an air intake velocity above 6 m/s at a 27 °C ambient temperature is able to maintain the batteries at the safe operation range with a maximum temperature of 48.13 °C located at cells near the middle of the lower module. This pattern of temperature distribution with the highest temperature located at near-center lower-module cells can be seen in the temperature distributions for 20m/s and 8m/s intake air velocity as well.

Co-funded by the Erasmus+ Programme of the European Union

The European Commission support for the production of this publication does not constitute an endorsement of the contents which reflects the views only of the authors, and the Commission cannot be held responsible for any use which may be made of the information contained therein. Project number: 585796-EPP-1-2017-1-AT-EPPKA2-CBHE-JP

(a)

(b)

(c)

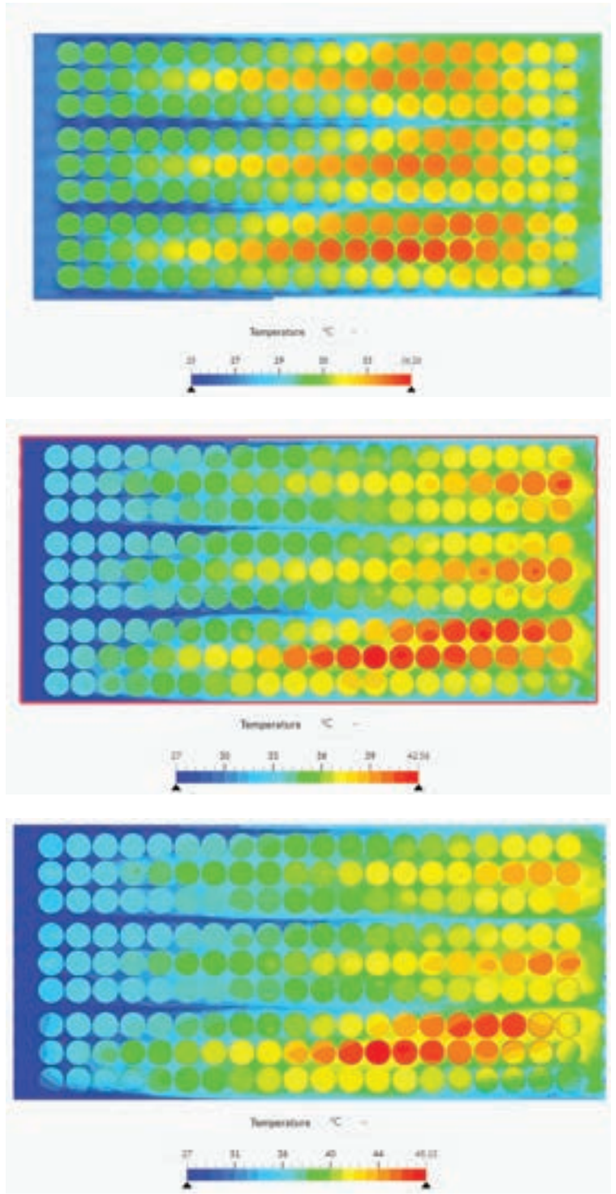

Figure 10: a) Heat Distribution with 20m/s air inlet velocity, b) 8m/s air inlet velocity and c) 6m/s for Push Configuration

However, with the air intakes into the internal space of the accumulator, water and dust particles represented a risk to the safe operation of the accumulator. To safeguard against this, a filter is to be implemented at the inlets and outlets which will be tested and evaluated against different testing scenarios in the laboratory to finalize the decision between filter materials and fans available for the airflow requirements.

Co-funded by the Erasmus+ Programme of the European Union

The European Commission support for the production of this publication does not constitute an endorsement of the contents which reflects the views only of the authors, and the Commission cannot be held responsible for any use which may be made of the information contained therein. Project number: 585796-EPP-1-2017-1-AT-EPPKA2-CBHE-JP

8. COST OF USE

When studying the market implementation and the target audience exposed in this work, even with increased autonomy and efficiency, one main objective must be achieved: The electric motorcycle must result in lower operating costs compared to the combustion counterparts.
With the proposed design and expected energy consumption, an estimate for cost per kilometer can be extracted from the combustion and electric designs. Using the current average price for normal gasoline (G1. (2020)) and Rio de Janeiro's base cost per kWh (Brêtas, P. (2020)), the cost per kilometer when running on gasoline is estimated to be 0.107 Brazilian Reais per kilometer, where P represents Price of fuel or energy source and D represents Autonomy per Liter (Gasoline) or kWh (Electric). The electric design proposed, has a cost per kilometer of Brazilian Reais, roughly 28.9% of the cost for the combustion counterpart. With the proposed cost of the prototype, the difference to the ICE counterpart would be recovered after 400.000km, not taking maintenance into consideration.

$$C_{gas} = P_{liter\ of\ gasoline} / D_{combustion\ engine} = R\$4.368 / 41\ km = R\$0.107\ per\ Km$$

$$C_{electric} = P_{kWh} / D_{electric\ motor} = R\$0.683 / 22.22\ km = R\$0.031\ per\ Km$$

8. CONCLUSION

This article proposed a design concept that could be implemented for common use of an electric motorcycle, seeking to contribute to the development of more sustainable and efficient transportation. Due to cost restrictions, the research goal for autonomy could not be achieved. However, prototype material costs and overall development aimed at maximizing the use of cheaper materials which, in large-scale production, could prove capable of increasing autonomy and efficiency with cost reductions. Current prototype material cost estimates are presented in Table 7 including the value of already available components. As can be seen, the project is estimated to be built under the cost limitation described in the Objectives section. As mentioned in Section 8, this cost would be recovered in 400.000km, which is very high for a commercial application. However, since this is a prototype cost and not a final unit cost, this value can be lowered through mass production, monetary change and national battery production.

Component	**Price (R$)**
Base Motorcycle	+9700.00
Motor and Inverter	+11000.00
Accumulator	+21275.00
Electronics	+1220.00
Chassis	+1100.00
Sale of Combustion Engine	-4500.00
Total	**39795.00**

Table 7: Estimated Material Costs for Construction of Proposed Design

Co-funded by the Erasmus+ Programme of the European Union

The European Commission support for the production of this publication does not constitute an endorsement of the contents which reflects the views only of the authors, and the Commission cannot be held responsible for any use which may be made of the information contained therein. Project number: 585796-EPP-1-2017-1-AT-EPPKA2-CBHE-JP

Next stages in development, other steps of design that were outside the scope of this work are to be implemented. These include field testing for ensuring simulation reliability, implementation of regenerative braking into controller programming for increasing autonomy, construction of a new chassis for housing new electrical components, motor thermal-electromagnetic characterization for a more in-depth study of the prototype's efficiency, and a manufacturing implementation plan for studying mass-market prices for a final version of the vehicle.

REFERENCES

Ashish, U., Raj, B., & Kumar, A. (2016). DESIGN AND FABRICATION OF AN ACCUMULATOR CONTAINER OR BATTERY PACK FOR A FORMULA STUDENT VEHICLE. *International Journal of Research in Engineering and Technology,* 05(15), 20–29. https://doi.org/10.15623/ijret.2016.0515006

Bottiglione, F., Contursi, T., Gentile, A., & Mantriota, G. (2014). The Fuel Economy of Hybrid Buses: The Role of Ancillaries in Real Urban Driving. Energies, 7(7), 4202–4220. https://doi.org/10.3390/en7074202

Brêtas, P. (2020, December 17). Conta de luz sobe com variação de ICMS no Rio; veja simulação. O Globo. https://oglobo.globo.com/economia/conta-de-luz-sobe-com-variacao-de-icms-no-rio-veja-simulacao-24800640

Caldeira, A. (2020, September 13). Motociclistas crescem 54% em dez anos no Brasil; veja o perfil de quem roda. 13/09/2020 - UOL Carros. https://www.uol.com.br/carros/colunas/infomoto/2020/09/13/motociclistas-crescem-54-em-dez-anos-no-brasil-veja-o-perfil-de-quem-roda.htm

Drummond, E., Condro, P., Cotton, B., Cox, C., Pinegar, A., Vickery, K., & Prins, R. (2019). Design and Construction of an Electric Motorcycle. *2019 Systems and Information Engineering Design Symposium (SIEDS)*, 0. https://doi.org/10.1109/sieds.2019.8735634

Government of Canada. (n.d.). *Understanding the tables.* https://www.nrcan.gc.ca/energy-efficiency/energy-efficiency-transportation-alternative-fuels/personal-vehicles/choosing-right-vehicle/buying-electric-vehicle/understanding-the-tables/21383

G1. (2020, November 13). Preço da gasolina sobe nos postos na semana, mostra ANP. G1.https://g1.globo.com/economia/noticia/2020/11/13/preco-da-gasolina-sobe-nos-postos-na-semana-mostra-anp.ghtml

Kaleg, S., Hapid, A., & Kurnia, M. R. (2015). Electric Vehicle Conversion Based on Distance, Speed and Cost Requirements. Energy Procedia, 68, 446–454. https://doi.org/10.1016/j.egypro.2015.03.276

Katoch, S. S., & Eswaramoorthy, M. (2020). A Detailed Review on Electric Vehicles Battery Thermal Management System. *IOP Conference Series: Materials Science and Engineering,* 912, 042005. https://doi.org/10.1088/1757-899x/912/4/042005

Lasciato, L., Peroni, L. (2019). *Feasibility study of an Electric Racing Motorcycle for the Motostudent Competition* [Master Thesis]. Politecnico di Torino.

Li, Y. (2016). Infrastructure to Facilitate Usage of Electric Vehicles and its Impact. Transportation Research Procedia, 14, 2537–2543. https://doi.org/10.1016/j.trpro.2016.05.337

Magnusson, A. E. (2016). *Modelling of battery cooling for Formula Student application - 3D Simulation of air cooled lithium-ion battery with COMSOL Multiphysics®, applied on 2016 years KTH Formula Student car "EV12e"*. [Bachelor's thesis]. KTH School of Industrial Engineering and Management.

Mao, Z., & Yan, S. (2016). Research on the Heat Dissipation Characteristics of Lithium Battery Spatial Layout in an AUV. *Discrete Dynamics in Nature and Society, 2016,* 1–15. https://doi.org/10.1155/2016/6269539

Peter Valdes-Dapena, CNN Business. (2019, December 31). Going electric could help revive the motorcycle industry. CNN. https://edition.cnn.com/2019/12/31/cars/electric-motorcycles/index.html

Rad, M. S., Danilov, D. L., Baghalha, M., Kazemeini, M., & Notten, P. H. L. (2013). Thermal Modeling of Cylindrical LiFePO4 Batteries. Journal of Modern Physics, 04(07), 1–7. https://doi.org/10.4236/jmp.2013.47a2001

Saraiva, I. B. (2016). *Estudo de Projeto de Motocicleta Elétrica* [Unpublished bachelor's thesis]. Universidade Federal do Rio de Janeiro.

Xu, M., Zhang, Z., Wang, X., Jia, L., & Yang, L. (2014). Two-dimensional electrochemical–thermal coupled modeling of cylindrical LiFePO4 batteries. *Journal of Power Sources*, 256, 233–243. https://doi.org/10.1016/j.jpowsour.2014.01.070

Youngki Kim, Mohan, S., Siegel, J. B., Stefanopoulou, A. G., & Yi Ding. (2014). The Estimation of Temperature Distribution in Cylindrical Battery Cells Under Unknown Cooling Conditions. *IEEE Transactions on Control Systems Technology,* 22(6), 2277–2286. https://doi.org/10.1109/tcst.2014.2309492

Co-funded by the Erasmus+ Programme of the European Union

The European Commission support for the production of this publication does not constitute an endorsement of the contents which reflects the views only of the authors, and the Commission cannot be held responsible for any use which may be made of the information contained therein. Project number: 585796-EPP-1-2017-1-AT-EPPKA2-CBHE-JP

SLIDING MODE CONTROL OF A HYBRID BATTERY-SUPERCAPACITOR ENERGY MANAGEMENT SYSTEM

Ezequiel Orozco1, Héctor Chiacchiarini[2]

Dpto. de Ing. Eléctrica y de Computadoras,
Universidad Nacional del Sur (UNS),
Bahía Blanca, Argentina.

[1]*E-mail: ezequieloro9@gmail.com*

[2] *Instituto de Inv. en Ing. Eléctrica "Alfredo Desages" (IIIE),*
Universidad Nacional del Sur (UNS) - CONICET, Bahía Blanca, Argentina.
E-mail: hgch@uns.edu.ar

ABSTRACT

This work presents an Energy Management System (EMS) for a Hybrid Energy Storage system (HESS) composed by battery and supercapacitor (SC) which splits the power demand over the two storage devices, preventing the battery to be stressed by fast changing current demands. High frequency current components are mainly derived to the SC who has to respond to the fast changing power demand, while the battery is reserved to smoothly recharge the SC when necessary. Sliding mode control (SMC) is used, and simulation results are included, showing an adequate performance.

Keywords: Energy management, Energy storage, sliding mode control.

INTRODUCTION

The market share of electric vehicles (EVs) and hybrid electric vehicles (HEVs) is gradually increasing, pushing a fast development of the associated technologies in response to the actual demands and challenges about sustainable economy.

Lithium-Ion (Li-ion) batteries have many comparative advantages respect to other storage technologies and nowadays are mainly selected for electric transportation (Emadi, 2015, Opitza et al., 2017). Actually, battery technologies offer high performance devices with increasing energy density but still being costly devices suffering from degradation problems due to normal usage (Wang et al., 2020). Those problems have to be properly addressed following adequate usage rules (Waldman et al., 2014, Xie et al., 2014) to preserve their health (Kabir & Demirocak, 2017, Xu et al., 2018, Jafari et al., 2018, Chiacchiarini et al., 2020).

Batteries can be combined with other storage devices (e.g Battery, Fuel Cell and SC, or battery and SC) creating HESS where the technological advantages of each device can be exploited in a proper way (Amaya et al., 2020). In such HESS, an EMS is needed to coordinate the proper usage of each device while preserving its health (Yue et al., 2019, Biswas & Emadi, 2019, Fu et al., 2020). The battery health depends on the current demand, cycling, temperatures, and other factors which produce

Co-funded by the Erasmus+ Programme of the European Union

degradation of the internal components, impacting mainly on the output impedance, on the storage capacity and finally on the lifespan.

The electrical factors to consider for battery preservation are: state of charge (SoC), current demand, current variations and cycling. Thus, an adequate EMS should implement adequate preservation rules (Chiacchiarini et al., 2020) by distributing the current demand between the battery and the other storage devices, to reduce the stress on the battery and preserve its health and lifespan.

OBJECTIVES

This work presents a EMS for an hybrid combination of battery+SC which splits the power demand over the two storage devices, preventing the battery to be stressed by fast-changing current demands. The demand of high frequency current components is mainly derived to the SC who has to respond to the fast changing power requests, while the battery is reserved to smoothly recharge the SC when necessary. The control strategy is based on sliding modes (Utkin, 1992). The sliding dynamics is designed such that the SC can react to fast current changes, and the battery can provide the average power demand, needed to restore the SC SoC. The system is an active parallel architecture as shown in Fig. 1. Sliding controllers are designed to command each dc-dc converter in order to implement the strategy. Simulation results are included to illustrate the basic idea and the system performance. The objective of this work is to evaluate the feasibility and complexity of this control strategy, explore the advantages and detect possible disadvantages related to the effective use of this EMS for HESS like the one or for more complex configurations.

LITERATURE REVIEW

A common HESS incorporates a supercapacitor as a secondary storage device, which has the capacity of providing high power peaks on demand. The primary device generally is a battery, or a Fuel cell, which usually provides the average power. This combination has shown to be useful, requiring a properly designed EMS strategy (see Kouchachvili et al. 2018, Vukajlović et al., 2020 and references therein).

A well know and simple topology for EMS is included in (Emadi, 2015). The objective is to regulate the dc-link voltage by properly adjusting the currents flowing through the battery and SC subsystems. The strategy proposed in (Emadi, 2015) splits the current demand into high-frequency and low frequency components. The high-frequency components are demanded to the SC and the low frequency components are demanded to the battery. Therefore, the battery is not stressed with step-like changes of current, somehow preserving its health.

But also the EMS should command each device according to specific rules with the objective of attending the energy demand while simultaneously applying specific restrictions on the operation of each device (Yue et al., 2019, Biswas & Emadi, 2019, Fu et al., 2019). For the EMS to deal with, and manage, the state of charge of the devices, it is necessary to incorporate more sophisticated internal control loops, including also state monitors as presented in (Amaya et al., 2016, Amaya et al., 2017, Amaya et al., 2020). A comparison between a proposal with state monitors and a classical scheme using voltage controllers is presented in (Amaya et al., 2016) where the state monitors allow to handle smoother transitions between the currents demanded to the battery and to the SC, keeping a better regulation on the SC voltage while reducing the stress of the battery. In (Cabrane et al., 2020) it is presented the conventional frequency-splitting strategy for a solar vehicle where batteries and SC configure the HESS.

Co-funded by the Erasmus+ Programme of the European Union

The European Commission support for the production of this publication does not constitute an endorsement of the contents which reflects the views only of the authors, and the Commission cannot be held responsible for any use which may be made of the information contained therein. Project number: 585796-EPP-1-2017-1-AT-EPPKA2-CBHE-JP

Power splitting EMS algorithms are mainly based on two concepts: ruled based algorithms, and optimization algorithms. The first ones usually do not need predictions of future driving situations, neither rely on sophisticated dynamic models to command the power drivers. The second ones certainly need the use of predictions and models. The first ones are usually designed based on engineering experience, and specified behaviour, and the optimization algorithms produce automatic results which are dependent on the quality of the performed predictions. Ruled-based algorithms could also be complemented by adequate optimization algorithms. In (Zhai et al., 2020 and references therein) it is done a review of different ruled-based, and optimization algorithms. It is proposed there an optimization procedure to split the power demand between battery and SC, although relying on predictions of the vehicle velocity.

The work of (Hussain et al., 2019) includes an algorithm to create an EMS for a semi-active battery-SC HESS creating the power splitting from fuzzy logic rules and a low pass filter, combined with adaptive PI controllers. The work of (Yang et al., 2020) presents a robust fractional-order sliding-mode control of a fully active battery/supercapacitor hybrid energy storage system used in electric vehicles, which produces a power splitting strategy using a ruled-based algorithm.
Sliding modes are particular dynamic responses obtained on systems with variable structure (Utkin, 1995), or where nonlinear discontinuous controllers are used. A well-known property of SMC is the capacity of sustain a closed loop dynamics invariant against certain kind of parametric perturbations. Also, the design and implementation simplicity are appreciated advantages.

A SMC strategy for the EMS of a HESS is presented by (Song et al., 2017) using classical linear sliding surface to control the battery and SC currents to their reference values. Also a SMC is developed by (Wang et al., 2017) to drive the SC and battery currents to their reference values using also estimators to obtain the load current and external voltages. Again, a classical linear sliding surface is used.
Boost converters in particular are suitable to be controlled by classic output feedback linearization techniques (Marino & Tomei, 1996) by properly selecting an adequate output function, which is also suitable for designing a sliding surface for SMC.

METHODOLOGY

Although many authors have developed and used SMC for different applications during the last 90 years, important advances appeared during the last decades thus increasing the application areas. In particular, some authors have focused on the design of EMS for HESS using SMC but there are not many cases where nonlinear sliding surfaces are used. This work in particular explores the use of a nonlinear sliding surface, seeking for dynamic decoupling between the current waveform provided by the SC and the current waveform provided by the battery, while at the same time regulating the SC SoC, and the dc-link voltage. The proposed control structure is composed by two independent sliding controllers. One designed to command the SC current to satisfy the load demand while regulating the dc-link voltage, and the other one oriented to regulate the SC SoC.

The rest of the work is organized as follows: The system architecture and SMC strategy are presented below, followed by simulation results. Finally the main conclusions and recommendations about perspectives for future work are described in the last sections.

Co-funded by the Erasmus+ Programme of the European Union

System Architecture

The HESS is composed by a battery and a SC, both connected to a capacitive dc bus by bidirectional boost-Buck converters, and where the traction motor is driven by a bidirectional full bridge converter feeded from the dc bus (Fig. 1). The load current, and the currents provided by the storage devices are driven by switched converters under PWM operated at high frequency and in general will have discontinuous pulsed behaviour. This produces a high frequency ripple on the voltage of the dc-link capacitor and on the inductance currents, which usually cannot be compensated by the control loop. Then, for control purposes, it is adequate to get rid of this ripple effect. For that, the averaged variations of the dc-link voltage and inductance currents are evaluated using the input-output power balance equations on the converters, and the measurements are low-pass filtered.

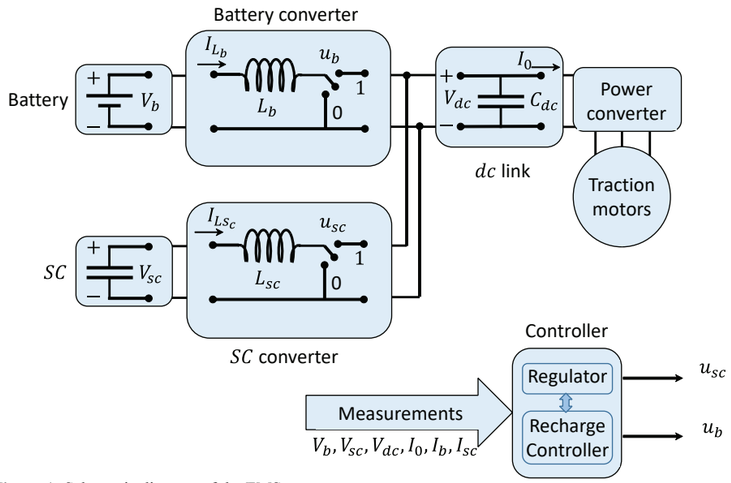

Figure 1: Schematic diagram of the EMS.

So, the high-frequency switching effect can be neglected for control purposes, considering an averaged dynamic model as:

$$C_{dc}\dot{V}_{dc} = u_b I_{L_b} + u_{sc} I_{L_{sc}} - I_0, \quad (1)$$

$$L_b \dot{I}_{L_b} = V_b - V_{dc} u_b, \quad (2)$$

$$L_{sc} \dot{I}_{L_{sc}} = V_{sc} - V_{dc} u_{sc}, \quad (3)$$

$$\dot{V}_b = f I_{L_b}, \quad (4)$$

$$C_{sc} \dot{V}_{sc} = -I_{L_{sc}}, \quad (5)$$

where the electric variables represent the average behaviour of the instantaneous voltages and currents, and the control signals are the duty cycles of the PWM drivers. Function in (4) has to be adjusted according to the battery chemistry and configuration. As a first approximation, for control purposes it can be approximated by a capacitive behaviour similar to (5), considering an equivalent capacitance that creates a voltage variation of similar magnitude as the battery voltage variation when its charge changes from $SoC = 0$ to $SoC = 100\%$.

Co-funded by the Erasmus+ Programme of the European Union

SMC Strategy

The objective is to indirectly regulate the dc-link voltage at a specific set point, by using the energy stored in the SC. For that, an adaptation of a standard procedure for the boost converter control in sliding mode is used, as will be explained below. Simultaneously the SC energy is restored from the battery using other sliding controller to regulate the battery current according to a slowly varying reference signal.

a) Regulator design

The first control loop will include the SC and the dc-link. The total averaged energy stored in the dc-link and the inductances of the SC and battery converters is

$$E_0 = \frac{1}{2}C_{dc}V_{dc}^2 + \frac{1}{2}L_{sc}I_{L_{sc}}^2 + \frac{1}{2}L_bI_{L_b}^2 \tag{6}$$

Under steady state operation the SC current should be null, the battery should be providing the load current, and the dc-link should have constant voltage $\bar{V}_{dc}$. So the steady state energy should be

$$\dot{E}_0^* = \frac{1}{2}C_{dc}\bar{V}_{dc}^2 + \frac{1}{2}L_b\frac{\bar{V}_{dc}}{Vb}^2 I_0^2$$

for constant I_0. But as I_0 is usually varying due to the load demand, and the battery current is not allowed to have fast variations, the reference energy has to include the SC current, so defining the reference energy as

$$\dot{E}_0^*t := \frac{1}{2}C_{dc}\bar{V}_{dc}^2 + \frac{1}{2}L_b\bar{I}_b^2 + \frac{1}{2}L_{sc}\frac{\bar{V}_{dc}}{V_{sc}}I_0 - \frac{V_b}{V_{sc}}\bar{I}_b^{\,2}, \tag{7}$$

where $\bar{I}_b$ is created by the SC voltage controller, and $\dot{E}_0^* = \lim_{\bar{I}_b \to \frac{\bar{V}_{dc}}{V_b}I_0} \dot{E}_0^*$

That allows the definition of the energy error output $e = E_0 - \dot{E}_0^*t$ which has to be driven to zero by the closed loop controller. The error output e has relative degree 2, since using (6)

$$e = E_0 - \dot{E}_0^*t \tag{8}$$

$$\dot{e} = C_{dc}V_{dc}\dot{V}_{dc} + L_{sc}I_{L_{sc}}\dot{I}_{L_{sc}} + L_bI_{L_b}\dot{I}_{L_b} - \dot{E}_0^*t, \tag{9}$$

And using (1),… (3):

$$\dot{e} = V_{dc}u_bI_{Lb} + u_{sc}I_{Lsc} - I_0 + I_{L_{sc}}V_{sc} - V_{dc}u_{sc} + I_{L_b}V_b - V_{dc}u_b - \dot{E}_0^*t, \tag{10}$$

$$\dot{e} = I_{L_{sc}}V_{sc} + I_{L_b}V_b - V_{dc}I_0 - \dot{E}_0^*t, \tag{11}$$

where, after considering negligible the effects of $\dot{\bar{V}}_{dc}$, $\dot{\bar{V}}_b$ and $\dot{\bar{V}}_{sc}$,

$$\dot{E}_0^*t = L_b\bar{I}_b\dot{\bar{I}}_b + L_{sc}\frac{\bar{V}_{dc}}{V_{sc}}I_0 - \frac{V_b}{V_{sc}}\bar{I}_b\frac{\bar{V}_{dc}}{V_{sc}}I_0 - \frac{V_b}{V_{sc}}\dot{\bar{I}}_b. \tag{12}$$

This shows that the derivative of the energy error is dependent on the instantaneous input-output power balance, and does not depend on the control inputs, thus the relative degree is higher than one.

Co-funded by the Erasmus+ Programme of the European Union

The European Commission support for the production of this publication does not constitute an endorsement of the contents which reflects the views only of the authors, and the Commission cannot be held responsible for any use which may be made of the information contained therein. Project number: 585796-EPP-1-2017-1-AT-EPPKA2-CBHE-JP

Evaluating now

$$\dot{e} = \dot{I}_{L_{sc}}V_{sc} + \dot{I}_{L_b}V_b - \dot{V}_{dc}I_0 + I_{L_{sc}}\dot{V}_{sc} + I_{L_b}\dot{V}_b - V_{dc}\dot{I}_0 - \dot{E}_0^*t, \tag{13}$$

and using also (4), (5)

$$\dot{e} = \frac{V_{sc}^2}{L_{sc}} + \frac{V_b^2}{L_b} - \frac{I_{Lsc}^2}{C_{sc}} + I_{L_b}fI_{L_b} + \frac{I_0^2}{C_{dc}} - V_{dc}\dot{I}_0 - \dot{E}_0^*t - u_b\frac{V_bV_{dc}}{L_b} + \frac{I_{Lb}I_0}{C_{dc}} - u_{sc}\frac{V_{sc}V_{dc}}{L_{sc}} + \frac{I_{Lsc}I_0}{C_{dc}}, \tag{14}$$

where, after again considering negligible the effects of $\dot{\bar{V}}_{dc}$, $\dot{\bar{V}}_b$ and $\dot{\bar{V}}_{sc}$,

$$\dot{E}_0^*t = L_b\dot{\bar{I}}_b^{\,2} + L_b\bar{I}_b\dot{\bar{I}}_b + L_{sc}\frac{\bar{V}_{dc}}{V_{sc}}I_0 - \frac{V_b}{V_{sc}}\dot{\bar{I}}_b^{\,2} + L_{sc}\frac{\bar{V}_{dc}}{V_{sc}}I_0 - \frac{V_b}{V_{sc}}\bar{I}_b\frac{\bar{V}_{dc}}{V_{sc}}I_0 - \frac{V_b}{V_{sc}}\dot{\bar{I}}_b. \tag{15}$$

It is verified that $\dot{e}$ is linearly dependent on the control signals u_b, u_{sc} if

$$\frac{V_bV_{dc}}{L_b} + \frac{I_{Lb}I_0}{C_{dc}} \neq 0, \tag{16}$$

$$\frac{V_{sc}V_{dc}}{L_{sc}} + \frac{I_{Lsc}I_0}{C_{dc}} \neq 0, \tag{17}$$

respectively, leading to e to have relative degree 2 respect to each input signals whenever those conditions are satisfied. The particular possible situation of losing the relative degree condition will be addressed later.

The main objective is to regulate the voltage V_{dc} which is affected by the load current I_0, commanded by the traction driver. By design, the system must guarantee that the SC current I_{Lsc} can react fast enough to compensate the effects of the variations of I_0.

To drive the energy error $e \to 0$, it is proposed to force the following reduced order dynamics

$$\dot{e} = -ke, \tag{18}$$

where $k > 0$ is selected according to the desired convergence speed. For that, a SMC is proposed to drive the signal $\sigma_0 := ke + \dot{e} \to 0$ in finite time by manipulating u_{sc}, while considering that u_b is a known perturbation which is manipulated by other controller designed to regulate the SC voltage.

Output σ_0 has relative degree 1 respect to u_{sc} if condition (17) is satisfied.
The special case $\frac{V_{sc}V_{dc}}{L_{sc}} + \frac{I_{Lsc}I_0}{C_{dc}} = 0$ where the relative degree condition is lost would prevent the sliding regulator to perform adequately. Nevertheless, this condition barely happens, as shown now. As the involved voltages are positive, the only possibility of losing the property of relative degree 2 occurs when $\frac{V_{sc}V_{dc}}{L_{sc}} = -\frac{I_{Lsc}I_0}{C_{dc}}$ which only happens if the involved currents are of opposite sign, but also the SC current has to be very high, usually out of the allowed bounds.

Co-funded by the Erasmus+ Programme of the European Union

The European Commission support for the production of this publication does not constitute an endorsement of the contents which reflects the views only of the authors, and the Commission cannot be held responsible for any use which may be made of the information contained therein. Project number: 585796-EPP-1-2017-1-AT-EPPKA2-CBHE-JP

For example,

for $V_{sc} = 10V$ on a minimum charge condition, with $V_{dc} = 75V$, $C_{dc} = 2400\ \mu F$, $L_{sc} = 800\ \mu Hy$,

and a maximum output current of $I_0 = 20A$, $I_{Lsc} = -\frac{C_{dc}V_{sc}V_{dc}}{I_0 L_{sc}} = -112{,}5A$.

Therefore, the possibility of losing the relative degree condition can be discarded without risk.

So, the relative degree condition proves that the time derivative $\dot{\sigma}_0$ is dependent on the control variables as shown below:

$$\dot{\sigma}_0 = k\dot{e} + \ddot{e} \tag{19}$$

$$\dot{\sigma}_0 = kI_{L_{sc}}V_{sc} + I_{L_b}V_b - V_{dc}I_0 - \dot{E}_0^{\cdot}t + \frac{V_{sc}^2}{L_{sc}} + \frac{V_b^2}{L_b} - \frac{I_{sc}^2}{C_{sc}} + I_{L_b}fI_{L_b} + \frac{I_0^2}{C_{dc}} - V_{dc}\dot{I}_0 - \dot{E}_0^{\cdot}t - u_b\frac{V_bV_{dc}}{L_b} + \frac{I_{Lb}I_0}{C_{dc}} - u_{sc}\frac{V_{sc}V_{dc}}{L_{sc}} + \frac{I_{Lsc}I_0}{C_{dc}}. \tag{20}$$

Let $$\phi = kI_{L_{sc}}V_{sc} + I_{L_b}V_b - V_{dc}I_0 - \dot{E}_0^{\cdot}t + \frac{V_{sc}^2}{L_{sc}} + \frac{V_b^2}{L_b} - \frac{I_{Lsc}^2}{C_{sc}} + I_{L_b}fI_{L_b} + \frac{I_0^2}{C_{dc}} - V_{dc}\dot{I}_0 - \dot{E}_0^{\cdot}t$$

then

$$\dot{\sigma}_0 = \phi - \frac{V_bV_{dc}}{L_b} + \frac{I_{Lb}I_0}{C_{dc}}u_b - \frac{V_{sc}V_{dc}}{L_{sc}} + \frac{I_{Lsc}I_0}{C_{dc}}u_{sc}. \tag{21}$$

The sliding mode will be set by commanding the control variable u_{sc}, while the signal u_b is commanded by an auxiliary control loop to be described later. So u_b will be considered now as an exogenous known perturbation.

The sliding mode will be set by commanding the control variable u_{sc}, while the signal u_b is commanded by an auxiliary control loop to be described later. So u_b will be considered now as an exogenous known perturbation.

Defining $\alpha = \phi - \frac{V_bV_{dc}}{L_b} + \frac{I_{Lb}I_0}{C_{dc}}u_b$ and $\beta = \frac{V_{sc}V_{dc}}{L_{sc}} + \frac{I_{Lsc}I_0}{C_{dc}}$:

$$\dot{\sigma}_0 = \alpha - \beta u_{sc}. \tag{22}$$

The equivalent control $u_{sc_{eq}}$(Utkin, 1992) is obtained by solving $\dot{\sigma}_0 = 0$ as $u_{sc_{eq}} := \alpha/\beta$ and the sliding mode will be possible if and only if $0 \le u_{sc_{eq}} \le 1$
The reaching condition is defined as

$$\sigma_0\dot{\sigma}_0 \le -\eta|\sigma_0|,\ \eta > 0, \tag{23}$$

or

$$\frac{\sigma_0}{|\sigma_0|}\dot{\sigma}_0 \le -\eta. \tag{24}$$

Co-funded by the Erasmus+ Programme of the European Union

Using (22) and considering the equality in (24), the duty cycle of the SC converter is obtained as

$$u_{sc} = \mathrm{Sat}_0^1\frac{\alpha}{\beta} + \frac{\eta}{\beta}\mathrm{Sign}\sigma_0, \tag{25}$$

where

$$\mathrm{Sat}_a^b x = \begin{cases} b \text{ if } x \ge b, \\ x \text{ if } a \le x \le b, \\ a \text{ if } x \le a. \end{cases} \tag{26}$$

Signal u_b was considered as an exogenous variable which is commanded by a secondary control loop designed to recharge the SC. The following section describes the control strategy to command u_b.

a) Recharge Controller design

The objective is use the battery to slowly regulate the energy stored in the SC. The strategy is to create a current from the battery converter to modify the balance at the dc-link node so to make the main controller to react trying to stabilize again the dc link voltage manipulating the duty cycle of the SC converter.

Due to the faster reaction of the SC controller, the average power injected by the battery converter to the dc link will be compensated by an equivalent and opposite value of power extracted from there by the SC converter, thus forcing a recharge current into the SC.

The battery converter current is evaluated from the SC voltage difference respect to a certain reference. The restoration dynamics is designed to be slow with respect to the dc link closed loop dynamics, and compatible with the battery best usage practices.

The control strategy creates a reference current $\bar{I}_b$ which is fed to the battery converter controller to set I_{Lb}. The signal $\bar{I}_b$ is created as a function of the averaged SC voltage $V_{sc_{av}}$ and averaged SC current $I_{Lsc_{Av}}$, with the purpose of restoring the state of charge of the SC. It is defined as:

$$\bar{I}_b := \mathrm{Sat}_{-I_{b_{ch}}}^{+I_{b_{dis}}}\frac{V_{sc_{av}}}{V_{b_{av}}}\gamma\bar{V}_{sc} - V_{sc_{av}} + I_{Lsc_{av}}. \tag{27}$$

This reference $\bar{I}_b$ represents the current that should be drained from the battery to compensate the average current drained from the SC and to recharge it up to the desired voltage $\bar{V}_{sc}$. It is limited up to the allowable charge ($I_{b_{ch}}$) and discharge ($I_{b_{dis}}$) currents that the battery can sustain according to its actual state of charge. The averaged quantities are obtained by low-pass filtering the measured values. The filters bandwidth is set to filter out the undesired high-frequency components, so creating a slow-changing signal for $\bar{I}_b$.

Co-funded by the Erasmus+ Programme of the European Union
The European Commission support for the production of this publication does not constitute an endorsement of the contents which reflects the views only of the authors, and the Commission cannot be held responsible for any use which may be made of the information contained therein. Project number: 585796-EPP-1-2017-1-AT-EPPKA2-CBHE-JP

Many other possible definitions may be used instead of (27). Some simple options for example are:

- To add a dead zone for the SC voltage where no recharging action could be necessary;
- To use some nonlinear smooth behaviour instead of applying saturations;
- To include some expression which could depend on other specific parameters such as temperature, battery health, vehicle speed (for example, to set a high SoC if the vehicle speed is low since the probability of acceleration is higher than the probability of deceleration, and vice versa);
- Etc.

The local controller for this battery converter has to force $e_b = I_{Lb} - \bar{I}_b \to 0$. Again, a simple SMC is designed as follows:

Let $\sigma_b = e_b$ be the desired sliding output. It is verified that $\dot{\sigma}_b$ has relative degree 1 since using (2) $\dot{e}_b = \dot{I}_{Lb} - \dot{\bar{I}}_b = \frac{V_b - V_{dc}u_b}{L_b} - \dot{\bar{I}}_b$, which is linearly dependent on .

The reaching condition is defined as

$$\sigma_b\dot{\sigma}_b \le -\eta_b|\sigma_b|,\ \eta_b > 0, \tag{28}$$

or

$$\frac{\sigma_b}{|\sigma_b|}\dot{\sigma}_b \le -\eta_b. \tag{29}$$

Now, replacing $\dot{\sigma}_b$

$$\frac{\sigma_b}{|\sigma_b|}\frac{V_b}{L_b} - \dot{\bar{I}}_b - \frac{V_{dc}u_b}{L_b} \le -\eta_b, \tag{30}$$

$$Sign\sigma_b\frac{V_b}{L_b} - \dot{\bar{I}}_b - \frac{V_{dc}u_b}{L_b} + \eta_b \le 0. \tag{31}$$

Considering the equality, the condition leads to the duty cycle of the battery converter defined

$$u_b = Sat_0^1\frac{V_b}{V_{dc}} - \frac{L_b}{V_{dc}}\dot{\bar{I}}_b + \frac{L_b}{V_{dc}}\eta_b Sign\sigma_b\ . \tag{32}$$

The signal $\bar{I}_b$ is assumed to be slowly varying so its time derivative $\dot{\bar{I}}_b$ can be neglected in the control loop, or evaluated with an adequate differentiator filter.

Co-funded by the Erasmus+ Programme of the European Union

The European Commission support for the production of this publication does not constitute an endorsement of the contents which reflects the views only of the authors, and the Commission cannot be held responsible for any use which may be made of the information contained therein. Project number: 585796-EPP-1-2017-1-AT-EPPKA2-CBHE-JP

RESULTS

Simulations illustrate the performance of the proposed strategy. The simulation is run for one second to let the system to stabilize at an (almost) steady state condition. All that initial data is discarded, the timer is reset to zero and the figures show the evolution after that time up to 4 more seconds. Longer simulations were not possible to do at this stage due to memory limitations of the computer hardware.

The used SC dynamic model is a commonly used one, following (Oldham, 2008, Xu & Riley 2011). The battery dynamic model also is a standard one, following (Tremblay & Dessaint, 2009).

The converters are simulated by their averaged behaviour, discarding ripple effects and averaging discontinuous pulsating currents. The converter switches are simulated using their averaged effect on the circuits, depending on the duty cycles of the PWM drivers.

The simulated system parameters are listed in Table I, and correspond to model of a scaled laboratory prototype of an EMS which is under construction but still not operative due to COVID-19 lockout situations. The case study considers the system in steady state: The output current $I_0 = 0$, the SC loaded at its reference voltage and the battery SoC at 37.12%. So no recharge current is needed from the battery. From that condition, after one second a sudden request of $I_0 = 8A$ is imposed during a whole second and then changed to $-2A$ for 0.25 s. After that, a pulsed current demand of $+8A$, $-2A$, of period 0.5 s and 50% duty cycle is sustained.

Figure 2.a shows the averaged load current drained by the traction converter, and the dc link voltage V_{dc}, which is initially at $V_{dc} = 75V$ and later becomes barely affected by the current load. The voltage ripple is affected by the use of a simplified model for the SC and battery for the control design, where their internal resistances are neglected. It is worth to mention that the sliding regulator operates on the global energy error (8) as shown in Figure 3, instead of on the voltage error. During sliding mode, the energy error e evolves following the dynamics (18) given by $\dot{e} = -k\,.\,e$ where for the case it was selected $k = 5\ [1/s]$. It is also worth to mention that the voltage ripple does not affect the traction performance since the traction inverter controller is able to compensate it.

Parameter	Value	Unit
C_{sc}	160	[μF]
L_{sc}	800	[μHy]
L_b	800	[μHy]
C_{dc}	2400	[μF]
$\lvert I_b \rvert$	≤ 10	[A]
Battery capacity	10	[Ah]
Nominal battery voltage	48	[V]

Table 1: Main system parameters

Co-funded by the Erasmus+ Programme of the European Union

The European Commission support for the production of this publication does not constitute an endorsement of the contents which reflects the views only of the authors, and the Commission cannot be held responsible for any use which may be made of the information contained therein. Project number: 585796-EPP-1-2017-1-AT-EPPKA2-CBHE-JP

Figure 2.b shows the averaged output current at the SC terminals $I_{L_{sc}}$ which is equal to the current flowing through the respective SC converter inductor L_{sc}. Figure 2.c shows the averaged output current at the battery terminals I_{L_b} and flowing through the corresponding converter inductor L_b.

Figure 4 shows the sliding outputs σ_0 and σ_b. It is seen that σ_0 is barely affected by the sudden load changes, while σ_b remains practically around zero the whole time. The spikes on σ_b are mainly due to the finite time step of the simulation and the first-order derivative filters used to evaluate I_0, $\bar{I}_0$. The same effect is seen on σ_b, but with negligible amplitude. Note the fast reaching phases towards zero.

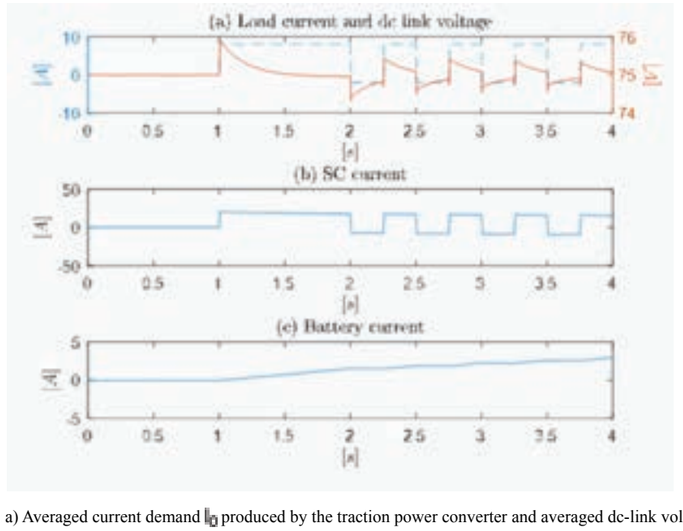

Figure 2: a) Averaged current demand I_0 produced by the traction power converter and averaged dc-link voltage V_{dc} b) Averaged output current at the SC terminals $I_{L_{sc}}$: c) Averaged output current at the battery terminals I_{L_b} .

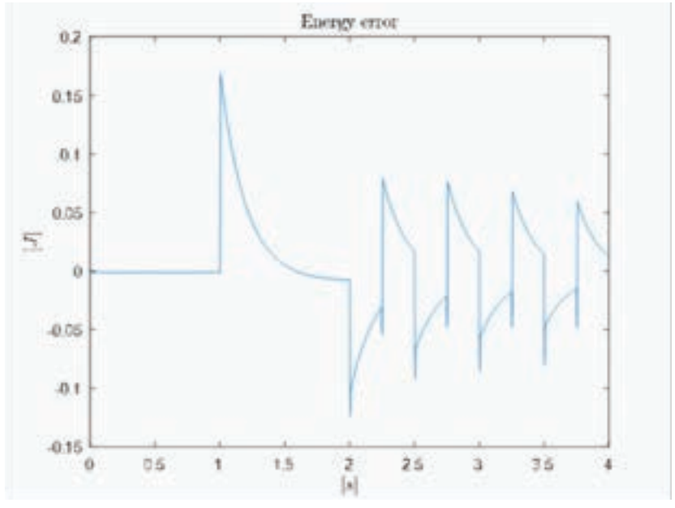

Figure 3: Difference between the total stored energy at the inductances and dc-link capacitor, and the reference energy value.

Co-funded by the Erasmus+ Programme of the European Union

Figure 5: a) shows the evolution of the SC voltage V_{sc} and its SoC, due to the effects of the drained current. Please note the effect of the internal SC output resistance on V_{sc} due to the current I_{sc} producing step changes on the voltage. Also fig 5.b shows the same for the battery. The voltage decreases continuously while the SoC decreases, but a much more noticeable effect is seen during the periods where the current increases, due to the combined effects of faradic and non faradic processes occurring within the battery.

The duty cycles u_b, u_{sc} and the reference current $\bar{I}_b$ are also presented in Figure 6. The discontinuous behaviour of the sliding controller is seen in the waveforms, where the discontinuous gains were selected as $\eta_b = 30$, $\eta_0 = 100$. Sudden reactions occur when the sliding variables σ_0, σ_b jump away from zero due to sudden changes in the current demand.

Finally, Figure 7 shows the reference signal created by the recharge controller for the battery current. It reacts slowly creating an extra current flow to the dc-link thus forcing the regulator to adjust the SC current accordingly. So, a net current flow appears from the battery to the SC when it needs recharging, and vice versa. The smooth variation of the reference current is copied into the real battery current, thus preserving it from the effects of high-frequency currents. For the case study, $\gamma = 100$ in (27).

The battery reference current in Figure 7 starts with a value different from zero since the numerical integrators were not exactly at the steady state condition at initial time. For the case, The signal $\bar{I}_b$, created from (27), is evaluated from the difference of the SC voltage, which is at 30.0062V at the initial time, and the reference voltage set to 30V. That produces an initial $\bar{I}_b = -0.031A$.

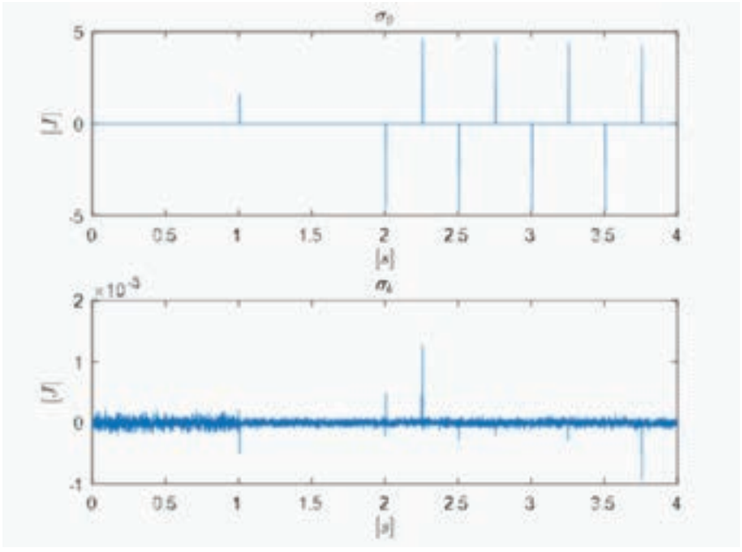

Figure 4: Sliding output σ_0 used by the sliding regulator (above). Sliding output σ_b used by the sliding recharge controller (below).

Co-funded by the Erasmus+ Programme of the European Union

The European Commission support for the production of this publication does not constitute an endorsement of the contents which reflects the views only of the authors, and the Commission cannot be held responsible for any use which may be made of the information contained therein. Project number: 585796-EPP-1-2017-1-AT-EPPKA2-CBHE-JP

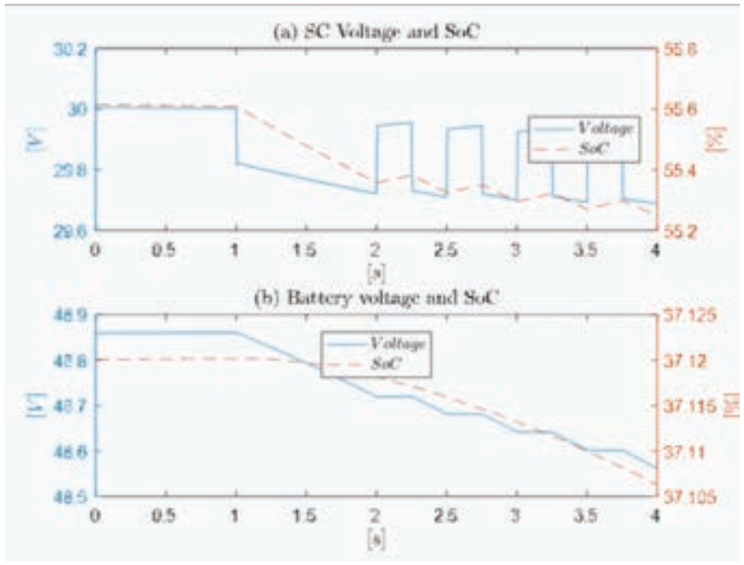

Figure 5: a) Evolution of the SC voltage V_{sc} and its State of Charge (SoC); b) Evolution of the battery voltage V_b and its State of Charge (SoC)

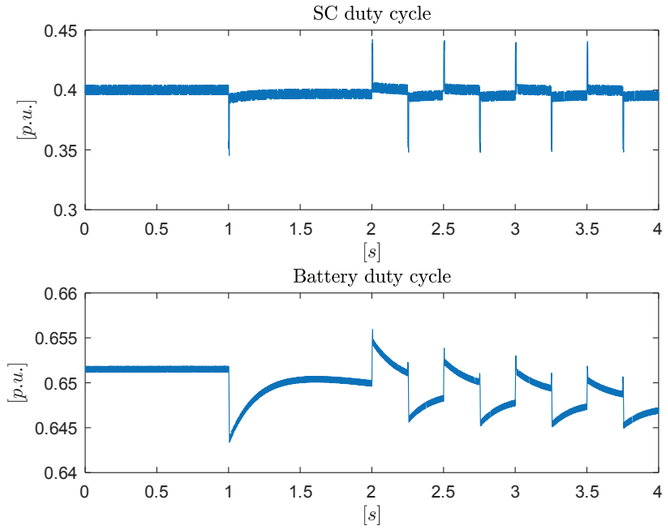

Figure 6: Duty cycle of the SC PWM driver (above). Duty cycle of the battery PWM driver (below)

Co-funded by the Erasmus+ Programme of the European Union

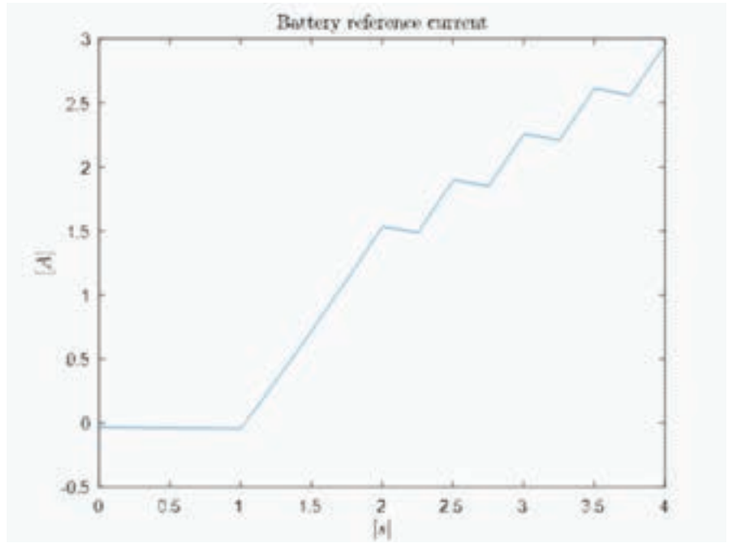

Figure 7: Battery reference current

CONCLUSIONS

A sliding mode control strategy was used to implement an EMS on a hybrid battery-supercapacitor HESS. The SC is commanded to provide the fast response while the battery is used to slowly adjust the SC charge. The performance can be tuned adjusting independently the desired time response of the charge restoring of the dc-link capacitor and charge restoring of the SC. The battery health is preserved by limiting high frequency components of the battery current. Other health preservation actions could also be considered, as for example: preventing extreme state of charge conditions, preventing extreme temperatures, and limiting the charge-discharge cycles. The proposed control strategy can be extended to include other restrictions according to the needs. For example, it is simple to add a charge-discharge oscillatory behaviour moving charge from the battery to the SC and back, to heat up the battery if necessary, as presented in Chiacchiarini et al., 2020.

The sliding mode strategy in general provides robustness to the control loop, and invariance against matched perturbations. Although some equations seem complex to evaluate, the control strategy follows rather simple ideas, being also possible to simplify some expressions at a cost of increasing the switching gains η_{0^*} η_b and preserving a satisfactory performance. The proposed strategy can also be extended to more complex HESS where the storage devices are connected through active converters like this case.

RECOMMENDATIONS

The design of expression (27) conditions the charge/discharge cycles of the battery during operation. Its design has to be done considering the SC capacity and the maximum load current, which together define the SC charge/discharge time. Naturally, the expected reaction speed of the recharge control loop must be high enough to guarantee proper regulation of the SC SoC, but an excessive reaction speed would increase the battery cycling thus degrading the lifespan.

As future work, it is planned to do laboratory experiments when the laboratories become accessible again, also comparing this strategy with other already-known strategies. Also, other different rules for SC recharging can be analysed and experimented.

Co-funded by the Erasmus+ Programme of the European Union

REFERENCES

Amaya, E. G., H. Chiacchiarini, C. De Angelo Manejo de energía en vehículos eléctricos: Una comparación de estrategias con monitores de estado y con lazos de tensión, 2016 IEEE Biennial Congress of Argentina (ARGENCON), 15-17 June 2016.

Amaya, E. G., H. Chiacchiarini, C. De Angelo, and M. Asensio, "The Energy Management Strategy of FC/Battery Vehicles Winner of the 2017 IEEE VTS Motor Vehicles Challenge," 2017 IEEE Vehicle Power and Propulsion Conference, VPPC 2017, pp. 1–6.

Amaya, E. G., H. Chiacchiarini, C. De Angelo, Energy Managment System Designed for Reducing Operational Costs of a Hybrid Fuel Cell-Battery-Ultracapacitor Vehicle IEEE Vehicular Power and Propulsion Conference (IEEE VPPC 2020), Guijon, Spain. Nov. 18 to Dec. 16, 2020.

Biswas, A., & A. Emadi, "Energy Management Systems for Electrified Powertrains: State-of-the-Art Review and Future Trends," IEEE Trans. on Vehicular Tech., vol. 68, pp. 6453-6467, 2019.

Cabrane Z., Batool D., Kim, J., Yoo K., Design and simulation studies of battery-supercapacitor hybrid energy storage system for improved performances of traction system of solar vehicle, Journal of Energy Storage, Volume 32, 2020, 101943, ISSN 2352-152X.

Chiacchiarini, H., C. De Angelo, G. Amaya, Health-conscious energy management of a hybrid battery-supercapacitor storage system, 27° Congreso Argentino de Control Automático, Buenos Aires, Arg. Oct. 2020.

Emadi, A., "Advanced Electric Drive Vehicles", CRC Press, Taylor & Francis Group, 2015.

Fu, Z., L. Zhu, F. Tao, P. Si, and L. Sun, "Optimization based energy management strategy for fuel cell/battery/ultracapacitor hybrid vehicle considering fuel economy and fuel cell lifespan," International Journal of Hydrogen Energy, vol. 45, pp. 8875-8886, 2020.

Hussain S, Ali MU, Park G-S, Nengroo SH, Khan MA, Kim H-J. A Real-Time Bi-Adaptive Controller-Based Energy Management System for Battery–Supercapacitor Hybrid Electric Vehicles. Energies. 2019; 12(24):4662.

Jafari, M., K. Khana, L. Gauchia, "Deterministic models of Li-ion battery aging: It is a matter of scale", Journal of Energy Storage 20 (2018) 67–77.

Kabir, M., D. Demirocak, "Degradation mechanisms in Li-ion batteries: a state-ofthe-art review", Int. J. Energy Res. 2017; 41:1963–1986.

Kouchachvili, W. Yaïci, E. Entchev, Hybrid battery/supercapacitor energy storage system for the electric vehicles, Journal of Power Sources, Volume 374, Pages 237-248, 2018.

Marino R., & Tomei P., Nonlinear Control Design: Geometric, Adaptive and Robust, Prentice Hall International (UK) Ltd., 1996.

Oldham, K. B. "A Gouy-Chapman-Stern model of the double layer at a (metal)/(ionic liquid) interface." J. Electroanalytical Chem. Vol. 613, No. 2, 2008, pp. 131–38.

Opitza, A., P. Badamia, L. Shena, K. Vignaroobana, A.M. Kannana, "Can Li-Ion batteries be the panacea for automotive applications?", Renewable Sustainable Energy Rev. 68 (2017) 685–692.

Song Z., Hou J., Hofmann H., Li J., Ouyang M., Sliding-mode and Lyapunov function-based control for battery/supercapacitor hybrid energy storage system used in electric vehicles, Energy, Vol. 122, 2017, Pages 601-612, ISSN 0360-5442, https://doi.org/10.1016/j.energy.2017.01.098.

Tremblay, O., L.-A. Dessaint, "Experimental Validation of a Battery Dynamic Model for EV Applications." World Electric Vehicle Journal. Vol. 3, May 13–16, 2009.

Utkin, V., Sliding Modes in Control and Optimization, Communication and Control Engineering. Berlin: Springer-Verlag, 1992.

Vukajlović, N., D. Milićević, B. Dumnić, B. Popadić, Comparative analysis of the supercapacitor influence on lithium battery cycle life in electric vehicle energy storage, J. Energy Storage, 31, 2020, 101603.

Waldmann, T., M. Wilka, M. Kasper, M. Fleischhammer, M. Wohlfahrt-Mehrens, "Temperature dependent ageing mechanisms in Lithium-ion batteries e A Post-Mortem study", Journal of Power Sources 262 (2014) 129-135.

Wang B., Xu J., Xu D., Yan Z., Implementation of an estimator-based adaptive sliding mode control strategy for a boost converter based battery/supercapacitor hybrid energy storage system in electric vehicles, Energy Conversion and Management, Volume 151, 2017, Pages 562-572, ISSN 0196-8904, https://doi.org/10.1016/j.enconman.2017.09.007.

Wang, X., Kerr, R., Chen, F., Goujon, N., Pringle, J.M., Mecerreyes, D., Forsyth, M., Howlett, P.C., Toward High-Energy-Density Lithium Metal Batteries: Opportunities and Challenges for Solid Organic Electrolytes, Advanced Materials, 32 (18), art. no. 1905219, 2020.

Xie, Y., J. Li, C. Yuan, "Multiphysics modeling of lithium ion battery capacity fading process with solid-electrolyte interphase growth by elementary reaction kinetics", Journal of Power Sources, Volume 248, 15 February 2014, pp. 172-179.

Xu, B., A. Oudalov, A. Ulbig, G. Andersson, and D. S. Kirschen, "Modeling of lithium-ion battery degradation for cell life assessment," IEEE Trans. on Smart Grid, vol. 9, no. 2, Mar. 2018 1131.

Xu, N., and J. Riley. "Nonlinear analysis of a classical system: The double-layer capacitor." Electrochemistry Communications. Vol. 13, No. 10, 2011, pp. 1077–81.

Yang B., Wang J., Zhang X., Wang J., Shu H. , Li S., He T., Lan C., Yu T., Applications of battery/supercapacitor hybrid energy storage systems for electric vehicles using perturbation observer based robust control, Journal of Power Sources, Vol. 448, 2020, 227444.

Yue, M., S. Jemei, R. Gouriveau, and N. Zerhouni, "Review on health-conscious energy management strategies for fuel cell hybrid electric vehicles: Degradation models and strategies," Int. Journal of Hydrogen Energy, vol. 44, pp. 6844-6861, 2019.

Zhai C., Luo F., and Liu Y., "A Novel Predictive Energy Management Strategy for Electric Vehicles Based on Velocity Prediction," in IEEE Trans. on Veh. Tech., vol. 69, no. 11, pp. 12559-12569, Nov. 2020.

Co-funded by the Erasmus+ Programme of the European Union

Co-funded by the Erasmus+ Programme of the European Union

The European Commission support for the production of this publication does not constitute an endorsement of the contents which reflects the views only of the authors, and the Commission cannot be held responsible for any use which may be made of the information contained therein. Project number: 585796-EPP-1-2017-1-AT-EPPKA2-CBHE-JP

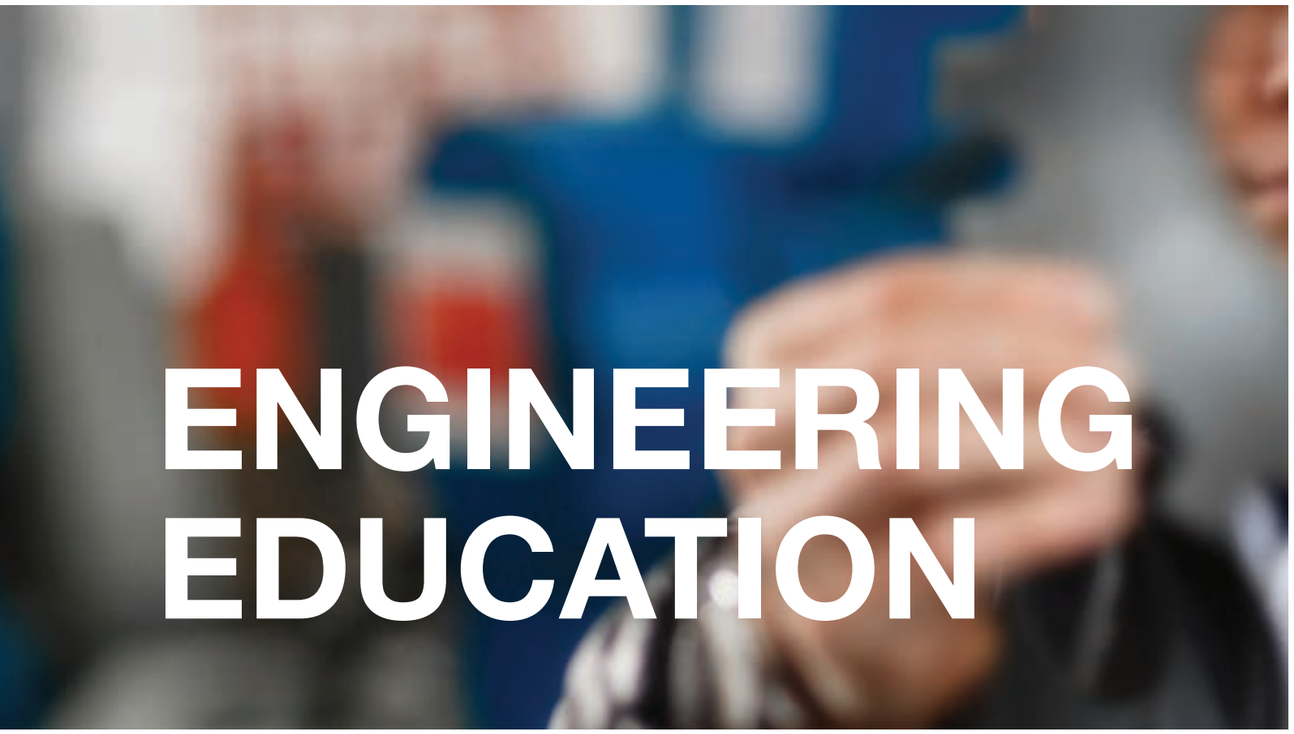

Co-funded by the Erasmus+ Programme of the European Union

The European Commission support for the production of this publication does not constitute an endorsement of the contents which reflects the views only of the authors, and the Commission cannot be held responsible for any use which may be made of the information contained therein. Project number: 585796-EPP-1-2017-1-AT-EPPKA2-CBHE-JP

EDUCATING FUTURE ENGINEERS-

CHALLENGES IN UNIVERSITY EDUCATION NOT ONLY DURING A GLOBAL PANDEMIC

Jörg Niemann[1], Claudia Fussenecker[2],
Martin Schlösser[3], Marius Schöning[4],
Alexander Paul[5]

Department of Mechanical Engineering, University of Applied Sciences Düsseldorf

[1] *joerg.niemann@hs-duesseldorf.de*
[2] *claudia.fussenecker@hs-duesseldorf.de*
[3] *martin.schloesser@hs-duesseldorf.de*
[4] *marius.schoening@hs-duesseldorf.de*
[5] *alexander.paul@hs-duesseldorf.de*

ABSTRACT

The Covid-19 pandemic has been influencing every aspect of the globalized world since its breakout. Not only the economic environment is changing rapidly, but also the education in universities all around the globe is facing challenges that have never been thought about before. But how are responsible decision makers dealing with these obstacles? And in addition to the challenges coming from a global pandemic, serious shortages of qualified professionals and technical job-specific skills are hampering Europe's sustainable growth. Even more so, relatively newer technologies, such as digitalization and Industry 4.0, require a new set of qualifications for future engineers. Deficiencies in these areas can have a negative impact on innovation and, therefore, also for the well-being of the industry and economy. New skills in education as well as new training methods are required in order to train successful engineers that meet the requirements set by industry and society. How does a future engineering education look like? And how does it fit in the new ways of teaching during these uncertain times? To get a qualified picture of the necessary requirements, as well as possible limitations, students of engineering studies have been questioned. This survey was combined with a literature review. Furthermore, a recently finished EU-research project regarding this subject has been taken into consideration and been evaluated in order to come up with future solutions.

Keywords: Engineering Education, Skills, Teaching Methods, Covid-19

1. INTRODUCTION

Engineering future engineers has not only been a challenge due to COVID-19 in 2020 but also due to the societal, industrial and engineering changes in recent years. The global pandemic as well as the changes in today's society cannot be viewed from an old-fashioned angle of scientific knowledge, soft skills and technology. Instead, they will have to be looked at from an interdisciplinary point of view that connects these branches and includes socio-economic capabilities. (Niemann et al., 2019) Bearing this in mind the teaching strategies of our educational system will have to be redesigned to match these new standards, especially with regard to topics such as digitalisation and Industry

Co-funded by the Erasmus+ Programme of the European Union

The European Commission support for the production of this publication does not constitute an endorsement of the contents which reflects the views only of the authors, and the Commission cannot be held responsible for any use which may be made of the information contained therein. Project number: 585796-EPP-1-2017-1-AT-EPPKA2-CBHE-JP

4.0, where interdisciplinary knowledge is crucial. The main content of Industry 4.0 are information and communication technologies, such as Cyber-Physical Systems, Internet of Things, Physical Internet and Internet of Services. Students need to be confronted with these topics quite early in their education so they can make a well thought out decision in which industrial branch they want to pursue a career, or if they want an industrial career at all. (Niemann et al., 2019), (Lee et al., 2014)

In this paper not only the engineering education at university level and the educational phase in school, which influences the choice of the study program will be taken into consideration, but also the forced changes in educating future engineers due to Covid-19 will be looked at. The paper will give a first insight into how students and teachers adopted to the changes on university level during the pandemic.

Several topics have emerged within the literature about higher education responses to these disasters and their transition to online or remote learning. Several papers regarding this subject have already been published in this short period of time. This includes the rapid adaptation of online learning including the set-up of suitable online tools such as moodle, TEAMS etc. and the importance of a clear and transparent communication from the university to students. (Gelles et al., 2020)

At the same time, faculty members are responsible for quickly redesigning and adjusting the curriculum and learning and adopting to new technologies and programs. The challenge is to learn how to best teach in the new virtual format where students do not react or respond in the same way as before. Here, constant feedback from student site has been considered to be extremely helpful. (Schwarz et al., 2018) Faculty members, not only at the Düsseldorf University of Applied Sciences, showed compassion and flexibility by adjusting the curriculum and assessment and effectively communicating with students in the past two semesters.

One finding was, that the different learning modalities such as online learning require a specific planning, to allow student autonomy and flexibility. Findings reported that flipped classroom for online teaching is executable. Furthermore, before-class activities, in-class activities, and after-class activities could promote learning performance. Furthermore, some students even had limited or inadequate access to resources such as computers, reliable internet and learning spaces free of distractions. Funding from the state or the university often tried to compensate this. (BMBF, 2020)

On the teachers site a digital literacy and netiquette carefully needed to be developed, managing student expectations as well as resolving technical difficulties beforehand. (Gelles et al., 2020) It showed that the resources to adapt to the technical aspects of the new reality were mainly possible to reach. However, universities could not completely be prepared for the pedagogical challenges that resulted from teaching remotely during a crisis. Showing compassion and care for students can be more difficult when there is physical and social distance. To show that they care, teachers have to be attentive and emphatic to the student by listening and reflecting on their needs and then responding in an understanding way. Moreover, a sense of humour while teaching and the atmosphere within the class were found to have positive benefits for online teaching. (Yen et al., 2020)

Looking at the more substantial problems of engineering education, the already mentioned point of interdisciplinary knowledge is one “of the main issues raised by industry […] that many university graduates lack skills which complement their technical knowledge, such as problem solving, teamwork and the ability to adapt to change”. (Solms et al., 2017) As one possible solution for this lack of skills, problem-based learning (PBL) in Science, Technology, Engineering and Mathematics (STEM) related subjects was introduced. PBL means that pupils will be given an understanding of

Co-funded by the Erasmus+ Programme of the European Union

the topics by solving “real-world, open-ended problems, mostly in groups”, to give them a feeling for later work experience in the industry. It is based on four modern insights into learning: constructive, self-directed, collaborative and contextual. (Solms et al., 2017), (Dolmans et al., 2005) Teaching methods like these are referred to as inductive, which is the “natural human learning style”, as every problem that needs to be solved comes with a real situation. The opposite of that is deductive, where students merely listen to what their professor has to say and try to memorize this information without having the ability to apply it to real world problems. (Felder & Silverman, 1988) To match industry’s requirements there needs to be a “relationship between academic institutions and industrial expectations” to improve students’ knowledge as well as their transition into the industry, which cannot be fulfilled by simply choosing the deductive learning style for students. (Littlefair, 2013), (Felder & Silverman, 1988)

In addition to the above-mentioned points of the industry’s expectations, Mahanija Md Kamal points out in the paper “Evaluation of an engineering program: A survey to assess fulfilment of industry requirements” from 2009 that “new engineering graduates are expected not only to be knowledgeable and technically competent but also good at communication, have leadership skills, able to work in teams and have lifelong learning attributes”. (Mahanija, 2009) Even though the evaluation is already 10 years old, the importance of the mentioned skills increased. These requirements mainly arise due to the changing industrial environment, such as digitalisation and Industry 4.0. (Richert et al., 2016) Another crucial factor is of course the teachers’ perspective on the different teaching approaches. When sticking to PBL as an example for practice-oriented teaching Madeleine Abrandt Dahlgren’s book “Higher Education”, published as long ago as 1998, provides us with valuable insights. Here she also refers to the teacher’s perspective on PBL and points out that “the teachers were in general positive to continue to work with the PBL program” and that they appreciated the closer and more effective contact with the students but that there are also difficulties, especially on how it is interpreted by the teachers. They looked at it either from their perspective as teaching staff or from the student’s perspective as the receiving part and not as a whole correlated concept. (Abrandt Dahlgren, 1998) This shows that teachers also need trainings to be able to apply inductive teaching methods and give their students an understanding of practice-oriented topics, whether it is through PBL or any other teaching style with practical relevance. (Capraro et al., 2009)

The challenge of today’s educational system is to give pupils a realistic view of what to expect by choosing studies in an engineering subject and from teacher’s point of view being able to adopt to changes by adjusting the pedagogical and technical settings to it.

2. SURVEY ON REQUIREMENTS ON THE ENGINEERING EDUCATION

To get an overview of the state of the art of engineering education, a survey was conducted. The aim of the survey was to get insights on the actual grade of preparation of pupils and students when starting an engineering education. Pupils as well as students were questioned to maybe see recent changes in the educational system.

4.2. SMC Strategy

As mentioned before students as well as pupils were questioned. Both groups had about 100 participants. Moreover, the same questions were questioned. To get deeper insights also the age, the gender and the semester they are in (students) were asked. The survey was conducted in German and was translated by the authors to fit to this subject. The pupil’s survey was conducted in several

Co-funded by the Erasmus+ Programme of the European Union

secondary schools in the state of North-Rhine Westfalia, Germany. In case of the student's survey, students from the Department of Mechanical- and Process-Engineering at the Düsseldorf University at Applied Sciences took part. The survey was conducted with an online tool and was evaluated by the authors.

For students already studying engineering or an engineering related subject, the survey touches upon the problem whether their expectation of the studied subject was fulfilled and whether they felt well prepared for their studied subject by their previous high school/secondary school education.
In order to achieve a representative result with the survey, the aim was to have an even number of female and male students take part. The survey took place at the Düsseldorf University of Applied Sciences in June 2019 and 109 students participated. However, due to the fact that only 16% of the students in the Department of Mechanical and Process Engineering are female, only 17% of the participants of the survey were women. (FB MV, 2019) But despite this uneven distribution of gender, it is still a representative survey, because it displays a normal gender distribution in an engineering study program in Germany. (Schneider, 2019)

- The age of the participating students reaches from 18 to 32.
- Nearly 60 % of the participants have got the general university entrance qualification. Only 40 % received their entrance qualification through other accepted paths. As you can see most of the students were educated at a Gymnasium (the highest general education in Germany).

The participants say that in order to receive a successful university degree in an engineering subject the three most important subjects in school are Mathematics, Physics and English. In these three subjects they did not feel well prepared for an engineering study program.
As you can see in Figure 1, 60.7 % of the participants did not feel well prepared for studying engineering when they first started to study. This is a huge lapse in educating future engineers, which should already be taken care of during school education.

Figure 1: Subjective preparation for studying engineering (students)

In Figure 2 you can see that approximately 41 % of the participants said that they do not know what the practical approach of the taught content of the STEM subjects could be. They know why the topics are relevant for their education, but they unfortunately do not know what to use them for. Only 31 % of all participants knew why the topics are important and what they could use them for in the future.

Co-funded by the Erasmus+ Programme of the European Union
The European Commission support for the production of this publication does not constitute an endorsement of the contents which reflects the views only of the authors, and the Commission cannot be held responsible for any use which may be made of the information contained therein. Project number: 585796-EPP-1-2017-1-AT-EPPKA2-CBHE-JP

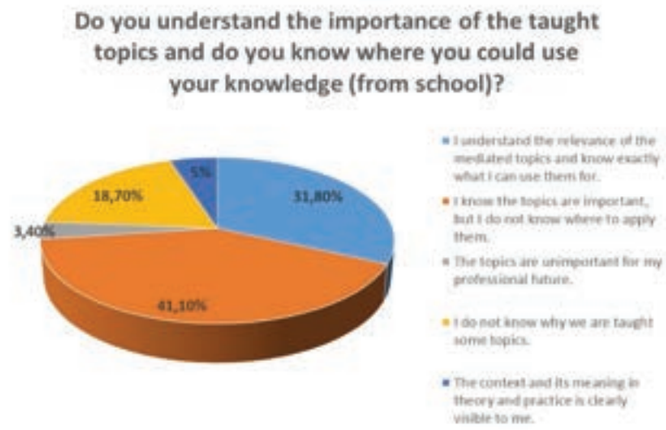

Figure 2: Connection between theory and practice (pupils)

In general, over 90 % of the participants asked for more classes focussed on practical issues in general education and at the university. They said that it would help to get a more detailed overview on their possible future job tasks. Moreover, you can see in Figure 3 that a great number of classes focussing on practical problems/issues would give the students a higher motivation to deal with the relevant topics.

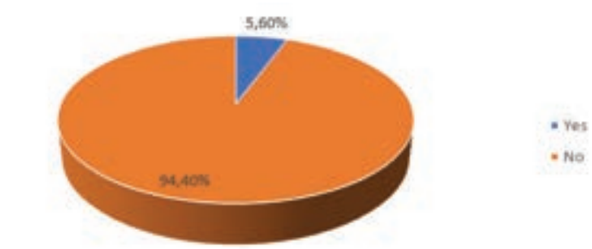

Figure 2: Connection between theory and practice (pupils)

At the beginning of the survey, pupils were explicitly asked, whether they were willing to pursue an engineering study program in the future.

- 39 % of the 73 participants answered this question with yes and consequently took part in the questionnaire.
- 86 % were from the German Gymnasium and 14 % from vocational training school.
- 46 % of the asked participants were 17 years old. All in all, the participants were between 16 and 19 years old. This is a normal distribution, because pupils in several school models were asked.
- 14 % of them did an apprenticeship prior to their advanced technical college entrance qualification (Fachhochschulreife). Because of that some of the pupils were a bit older than those that were enrolled at school at that moment. Similar to the survey for students 86 % were men. This is due to the most common distribution in German engineering classes.

Co-funded by the Erasmus+ Programme of the European Union
The European Commission support for the production of this publication does not constitute an endorsement of the contents which reflects the views only of the authors, and the Commission cannot be held responsible for any use which may be made of the information contained therein. Project number: 585796-EPP-1-2017-1-AT-EPPKA2-CBHE-JP

The survey was constructed in a way to create a comparability between both surveys. Similar to the student survey, the participants in the senior classes of the German educational system were asked whether they felt well prepared for an engineering study program by their general school education. Furthermore most of the pupils think that the same three subjects in school are important to reach a good engineering grade (Mathematics, Physics, English). In addition to that, nearly 70 % of the participants had the opinion that they were well prepared for studying engineering at a university (Figure 4). There is no correlation to the opinion of those students that are currently studying engineering.

Figure 4: Subjective preparation for studying engineering (pupils)

The next interesting aspect is that unlike to the student survey 50 % of the pupils said that they knew exactly why the mediated topics are important for an engineering class and what they could use them for (see Figure 5). Just 21 % said that they did not know what they could use their acquired knowledge for.

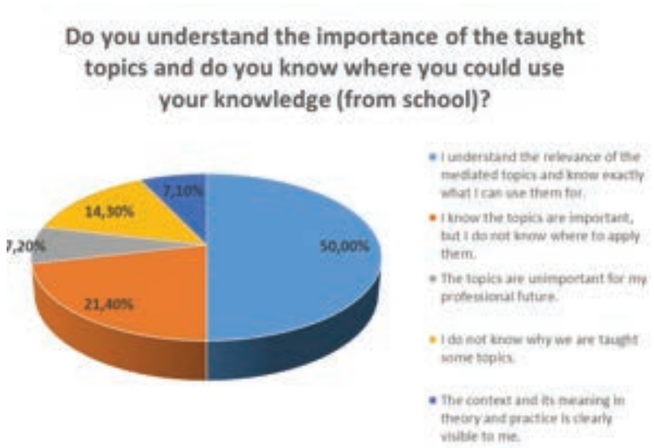

Figure 5: Connection between theory and practice (pupils)

As could already be seen in the students' survey, 100 % of the pupils said, that they wish for more practice-oriented classes in general school education. 96 % of them said that it would motivate them more to progress in the acquired topics (Figure 6).

Co-funded by the Erasmus+ Programme of the European Union

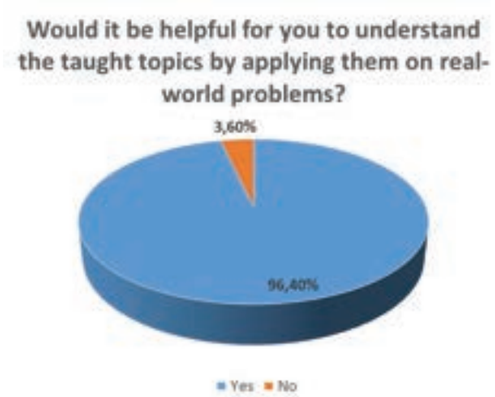

Figure 5: Keep themselves busy with acquired topics (pupils)

The results of the survey and the discussion with the stakeholders displayed interesting findings which will be detailed here. The pupils survey revealed that the majority of the participants would support more practice-oriented teaching methods because applying the taught topics to real-world problems would help them to understand them in more detail. Nevertheless, all in all they felt well prepared for starting their studies.
The student survey, on the other hand showed that most of the students did not feel very well prepared for an engineering study programme. They would also like to have a more practice-oriented teaching style as almost half of the participants were not sure how and where to use their gained knowledge.

Comparing both results it can be said that pupils seem to not have a specific expectation when they start their engineering study programme as they feel, opposed to the students, well prepared for their studies. As both groups wish for a more practice-oriented and real-world based teaching style these difficulties could be overcome by trying to give pupils a more detailed insight into the practical application of their theoretical knowledge. Based on this they could take a more informed and balanced decision on which studies are suitable for them.
The already finished EU-project ELIC (Engineering Literacy), which aims to increase engineering skills among secondary school pupils to increase their interest in technical occupations by installing a MOOC (massive open online course) for natural sciences teachers, as the several round tables with stakeholders, such as teachers, parents and members of STEM organisation, displayed a similar picture, namely every party involved welcomes the exchange of experience and bundled knowledge. Figure 7 shows how the different institutions are involved in the engineering education process and their relationship with each other. These three institutions influence each other on various levels and are in a constant exchange.

Co-funded by the Erasmus+ Programme of the European Union

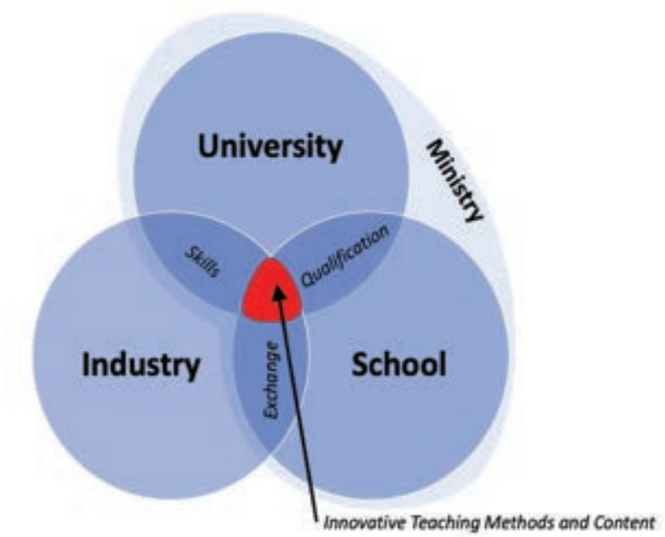

Figure 7: Stakeholder in engineering education

The figure shows clearly that schools need an exchange with the industry: experts from different industrial branches can share their experiences in schools in order to show the students what to expect when they choose a career in industry. The next step is the qualification that a pupil receives when graduating high school. With the industrial experts' expertise in mind, the pupils can choose which study field they want to pursue.

The key element of Figure 7, located at its heart, are the innovative teaching methods and contents, which are mutually influenced by industry, university, school and the ministry responsible. If this combination of techniques and contents is implemented in the schools in an adequate and flexible way, it can satisfy every stakeholder's requirements for future engineering graduates. The lack of a practical and interdisciplinary approach in STEM-subjects can be counteracted by these new inductive teaching methods.

The review of relevant literature and the results of the survey as well as the discussion lead to the following recommendations:

1. **Problem-based learning**

   Problem-based learning, as already mentioned and described in the introduction of this paper, is an inductive teaching methods, where pupils and student mostly work in groups to solve real-world and open-ended problems. (McQuade et al., 2017)

2. **Flipped classrooms**

   This teaching method relies on the pupil's/ student's independent learning behaviour. Here they have to learn the topics on a self-learning basis and will apply them during lessons with the support of a skilled teacher. (El-Senousy & Alquda, 2017)

3. **More experiments**

   For a better understanding more experiments can be helpful in order to visualise the taught topics.

Co-funded by the Erasmus+ Programme of the European Union
The European Commission support for the production of this publication does not constitute an endorsement of the contents which reflects the views only of the authors, and the Commission cannot be held responsible for any use which may be made of the information contained therein. Project number: 585796-EPP-1-2017-1-AT-EPPKA2-CBHE-JP

4. **Experts from industry/university**

   Experts from industrial branches or from universities can share their experiences in school/ university in order to prepare students and pupils on what to expect from their future work life. (ELIC, 2019)

5. **Curriculum update**

   By working together with the ministry, the current curriculum has to be updated in order to give it a more practical focus. Furthermore, an interdisciplinary nature and more space for new teaching methods should be implemented.

SURVEY ABOUT ONLINE TEACHING DURING PANDEMIC

To get the view of the students on online lectures a survey was conducted. Within the survey the students were able to give their opinion on different topics. In the following the methodology and the results of the survey are going to be displayed in detail.

3.1. Methodology

As already mentioned before a survey was conducted to get a good overview of the current situation at universities under the COVID-19 pandemic. Participants of the survey were solely students from engineering subjects at Düsseldorf University of Applied Sciences. The survey was conducted in German and for the purpose of this publication the results and graphs have been translated into English. To receive representative results 214 students were questioned. The main focus of the questionnaire dealt with the subject of online teaching and how students are dealing with it during these times. It was divided into three questions, which are going to be laid out in the following, of which the last two were designed to be answered in key words or full sentences.

3.2. Results

In Figure 8 the first question of the survey is shown. Here the students were asked whether or not the normal way of teaching could be fully replaced by online teaching.

Figure 8: Substitution of old teaching methods with online teaching

Co-funded by the Erasmus+ Programme of the European Union
The European Commission support for the production of this publication does not constitute an endorsement of the contents which reflects the views only of the authors, and the Commission cannot be held responsible for any use which may be made of the information contained therein. Project number: 585796-EPP-1-2017-1-AT-EPPKA2-CBHE-JP

As you can see, the results were not clear. Only 18% of the participants were fine with a fully remote way of teaching. On the other hand, 39% said that in no way they would want to have online lectures only and 43% were between these two viewpoints saying they could accept a partly remote teaching style where a few lectures taught online and the rest will be on site as usual.
In the second question of the survey the participants were asked what they would miss if on site teaching would be completely dropped out. Here the answers could be divided into four categories, namely the following:

- transferring knowledge by the teaching staff
- the intake of teaching contents by the students
- social aspects
- other topics that do not fall under any of the previous named categories

In the first category, the students had concerns regarding the communication between them and the teaching staff. Asking a question during lectures seems to be more difficult in an online environment and receiving an answer as well. Furthermore, for certain subjects, the practical aspect is missing. Another problem is the missing access to the universities and to the laboratories. Furthermore, sometimes a more powerful laptop than the ones students have at home is needed to work with certain programs. So, access to computer laboratories inside the university is often requested.
The second category is, as already mentioned, dealing with the student's intake of the taught material. Here, the students mostly criticized that their personal neatness and their will to study is not as high as during normal times with onsite lectures. Next to this point the motivation for participating in the lecture and reworking those is also not as high as normal.
The second to last category deals with the aspect, every person worldwide had to face during this pandemic, the social component. Here, of course, students lack social contacts, not only to the teaching staff but also to other students in their field of study. Especially for students starting off their study in these times, meeting new people while just having online classes is very difficult. In addition to that not knowing the teaching staff personally, can also be hindering when trying to contact them in the first place.
In the last category students mostly criticized the formalities of online teaching. Here they noted that it cannot be implied by the university that every student has the right equipment and internet connection at home to participate in online classes. Moreover, the possibility of field trips is not available due to restrictions following the pandemic. This upsets a lot of students because having an insight into different companies is a big benefit to their studies. The students also claimed that their orderly daily routine is missing with only online lectures.
On the other side, online lectures can be beneficial because some professors record their lectures as videos. This allows students to rewind and fast forward to new points and topics and listen to information again, where it was not clear right from the beginning.
In the following the last question of the survey will be discussed. It dealt with the online platforms in use and what kind of problems can occur using them. The answers to this topic can also be divided into sub-categories, namely the following:

- technical aspects
- lecturers
- transfer and intake of knowledge

In the first category the main problem is that different platforms of online teaching are used. Students can easily get confused by the number of different platforms and how the lecturer can be contacted.

Co-funded by the Erasmus+ Programme of the European Union

Also differences in the internet connection can lead to problems during the lecture and students can miss certain content.

Now, coming from the technical point of view, the teaching staff often has problem handling the online platforms. Here, the students claimed that some lecturers have very bad technical equipment, including their internet connection. As a result understanding of the taught topics is often more difficult. Furthermore, some lecturers seem not to be familiar with the platforms in use.
The last category, similar to the first ones in question two, deals with the transfer and intake of the taught material. Here, the students claimed as well that too many platforms are used for uploading the teaching material. One platform, where every lecturer uploads his material, would be way more convenient.

4. DISCUSSION & CONCLUSION

In the following a conclusion about the named topics as well as a discussion are drawn. The literature research showed that different approaches for the engineering education as well as online teaching are already available but need to be more specified and improved. In the nearer future subject related skills will not only be the main idea behind an engineering education anymore. Moreover, soft skills like the ability to teamwork and being a problem solver gain in relevance. In addition to that, an application of taught theories on real-world problems is needed to fulfil the requirements of future engineers. This could resume in new teaching methods like problem-based learning or flipped classrooms. Studies also show that such learning methods come with a huge increase of the output, which in this case is a deeper and well-founded knowledge of theories with the ability to adapt them to real-world problems.

The year 2020 has shown that nowadays online teaching should be provided for all educational purposes and that this way of teaching will play a major role in the future of education. To pursue this, a well thought out didactical concept is necessary to get the best learning results. This includes an implementation of the right software, meaning one that is the most useful and convenient for every party, as well as a different style of teaching. Mainly the lecturers must adapt their courses to reach the students and to transfer the knowledge in a way it is understandable and brings a plus in case of the outcomes.

Now having resumed the new teaching methods as well as the online teaching, the most difficult task is to combine both. Pure online teaching shows a lot of difficulties when trying to combine it with new methods of teaching. Problem-based learning, on the one hand, could be easily implemented in an online teaching environment. But, on the other hand, more practical lecture contents are difficult to fulfil when students are not onsite for most of the time during their studies.
So, a mixture of online and onsite teaching is probably the way to go in the near future. Although online teaching brings some advantages for students and lecturers, it should not be the only option. A balanced mix of online and offline teaching should be the approach of future education, leaving both parties the possibility to choose and implement the right teaching methods at the right time. To pursue this, the educational system must be improved and new methods and didactic concepts must be developed.

The need for a modern digital engineering education system was extremely urged by the COVID-19 pandemic, which showed that a digital way of teaching is possible but also that most educational institutions were not prepared for this kind of drastic change in their behaviour.

Co-funded by the Erasmus+ Programme of the European Union

REFERENCES

Abrandt Dahlgren, M.: Higher Education, 1998

Bundesministerium für Bildung und Forschung (BMBF): Überbrückungshilfen für Studierende, retrieved December 23rd 2020 from: https://www.bmbf.de/de/wissenswertes-zur-ueberbrueckungshilfe-fuer-studierende-11509.html

Capraro, R. M., Slough, S. W.: Why PBL? Why STEM? Why Now? An Introduction to STEM Project-Based Learning: An Integrated Science, Technology, Engineering, and Mathematics (STEM) Approach, 2009

Dolmans, D., De Grave, W., Wolfhagen, I., Van der Vleuten, C.: Problem-based learning: future challenges for educational practice and research, 2005

ELIC, Note Taking Form, Round Table Germany, 21.05.2019 Intercontinental Düsseldorf, Germany

El-Senousy, H. Alquda, J.: The Effect of Flipped Classroom strategy using Blackboard Mashup tools in enhancing achievement and Self– Regulated learning skills of university students. World Journal on Educational Technology: Current Issues. 6, 2017

Fachbereich Maschinenbau und Verfahrenstechnik - Hochschule Düsseldorf: Gender Diversity Action Plan, 2019

Felder, R. M., Silverman, L. K.: Learning and Teaching Styles in Engineering Education, 1988

Gelles, L.A.; Lord, S.M.; Hoople, G.D.; Chen, D.A.; Mejia, J.A. Compassionate Flexibility and Self-Discipline: Student Adaptation to Emergency Remote Teaching in an Integrated Engineering Energy Course during COVID-19. Educ. Sci. 2020, 10, 304

Lee, J., Bagheri, B., Kao, H.: A Cyber-Physical Systems architecture for Industry 4.0-based manufacturing systems, 2014

Littlefair, G.: Project-oriented design-based learning: aligning students' views with industry need, 2013

Mahanija, Md K.: Evaluation of an engineering program: A survey to assess fullfillment of industry requirements, 2009

McQuade, R., Wiggins, S., Ventura-Medina, E., Anderson, T.: Knowledge disagreement formulations in problem-based learning tutorials: balancing pedagogical demands with 'saving face'. Classroom Discourse. 1-17, 2018

Niemann, J., Fussenecker, C., Schlösser, M., Ahrens, T.: ELIC – Teachers as a Medium to Build a New Generation of Skilled Engineers, International Conference on Competitive Manufacturing (COMA) Conference 2019, Stellenbosch, South Africa

Richert, A., Shehade, M., Plumanns, L., Groß, K., Schuster, K., Jeschke, S.: Educating engineers for industry 4.0: Virtual worlds and human-robot-teams: Empirical studies towards a new educational age, 2016

Solms, von S., Nel, H.: STEM Project Based Learning: Towards improving secondary school performance in mathematics and science, 2017 IEEE AFRICON, 2017

Schneider, L.: Frauen erobern den Ingenieurberuf. Online: https://www.ingenieur.de/karriere/arbeitsleben/frauen-erobern-den-ingenieurberuf/
[Checked: 01.07.2019]

Swartz, B.C.; Gachago, D.; Belford, C. To care or not to care-reflections on the ethics of blended learning in times of disruption: The ethics of care & academic development. S. Afr. J. High. Educ. 2018, 32, 49–64

Yen, T.-F. (TF). (2020). The Performance of Online Teaching for Flipped Classroom Based on COVID-19 Aspect. Asian Journal of Education and Social Studies, 8(3), 57-64

Co-funded by the Erasmus+ Programme of the European Union

EDUCATION AND TRAINING OF SERVICE ENGINEERS – TOOLBOX OF METHODS

FOR THE DIGITAL BUSINESS TRANSFORMATION

Jörg Niemann[1],
Claudia Fussenecker[2]
and Martin Schlösser[3]

FLiX Research Centre, Duesseldorf University of Applied Sciences,
Münsterstrasse 156, 40476 Düsseldorf, Germany;
[1] joerg.niemann@hs-duesseldorf.de
[2] claudia.fussenecker@hs-duesseldorf.de
[3] martin.schloesser@hs-duesseldorf.de

ABSTRACT

Modern business models are increasingly seen as a source of outstanding organizational performance and competitive advantage that either synergizes with the previous business model or completely replaces the previous strategy. For enabling this transition the paper describes an advanced model to master the digital business transformation. Based on a large literature review the paper will identify useful methods and tools which are used in modern industrial companies. By this the findings serve as blueprint for the education and training of future service engineers and deliver the basis for the elaboration and design of according skill cards.

Keywords: Service, education, tools, digital business transformation

1. INTRODUCTION – BUSINESS MODELS AND TRENDS

1.1. A subsection Sample

Today's trends such as lean supply chain, smart manufacturing, cloud platforms, big data management, artificial intelligence, augmented and virtual reality, mobility, smart e2e transparency, additive manufacturing, customization, service-orientated business models and outsourcing etc. are all based on the changes of customer mentality and technological advancements. Through the faster means of communication caused by the introduction of worldwide accessible inter-net, trends form and can spread much faster than ever before in history. Figure 1 shows the different driving factors on business model trends.
Shorter product life cycles, continuous changes of business processes and higher customer expectations lead to a new kind of relationship between the customer and business partners within the value chain. Customers expect faster business transactions, one-stop-shop solutions and transparency in the supply chain. This is only possible, if companies can digitalise information and data about products, customers, processes and services and thereby digitally transform their business model. With this new working method, a high amount of data is collected about business procedures and production processes, customer demands, as well as data about internal and external communication, requiring a high amount of management and data analysis.

Co-funded by the Erasmus+ Programme of the European Union

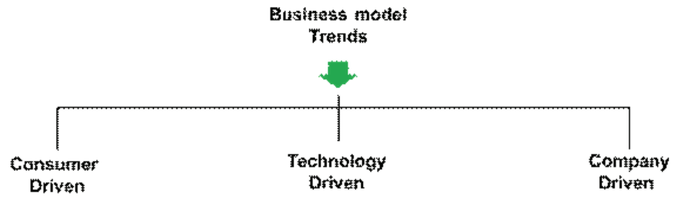

Figure 1: Business model trends

Digital transformation means a reorientation of products, services, processes and business models towards the continuously digitalised world and results in faster transactions and more reliability through quality and security and therefore leads to higher customer satisfaction (Kreutzer, 2017). The digital transformation of business models can be implemented in three general phases (see also Figure 2).

- Phase 1: Digitise the current business and build a platform for digital processes.
- Phase 2: Integrate Internet of Things (IoT) functionalities into the platform and develop digital services.
- Phase 3: Close e2e loop of the entire business operations and modularize platform services (Schallmo et al., 2017).

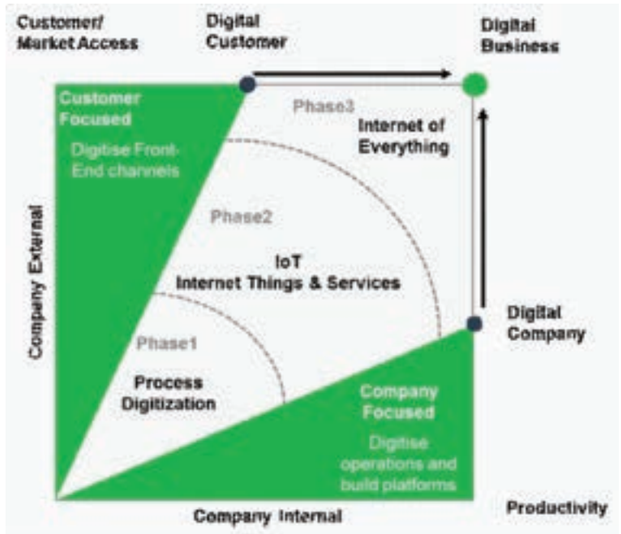

Figure 2: Digital transformation (modified and enhanced according to Schallmo et al., 2017)

Figure 2 depicts the journey from the traditional to the digital business. The model is divided into company internal and external elements, as the digitalisation of a business model can only work, if both the customer side and the own company can be “digitalised”. This begins through the digitalisation of the channels and processes used to create or provide value. Afterwards, the digitalisation of products, services and other objects included in the value chain. Finally, full digitalisation of all transactions and procedures with a high automation level leads to a fully digitalised business model. (Dehmer et al., 2017)

Co-funded by the Erasmus+ Programme of the European Union

2. TRANSITION FROM TRADITIONAL TO MODERN BUSINESS MODELS

Modern business models are increasingly seen as a source of outstanding organizational performance and competitive advantage that either synergizes with the previous business model or completely replaces the previous strategy.
New business models such as pay-per-use (usage-based payment e.g.: Car2go), peer-to-peer (trade between private individuals e.g.: Airbnb) or performance-based contracting (payment for the final performance e.g.: Rolls Royce) have revolutionised entire industries. Therefore, many companies have changed their model to move from pure product sales to the sale of problem solutions and services. When servitization moves a manufacturer all the way to becoming a solution provider there are major changes on the business model.
For enabling this transition, several frameworks are described in the literature (Niemann, 2016), (Niemann et al., 2009). Figure 3 shows a modified and advanced model based on Bucherer which is applied for the development of a new business model on the basis of an existing model. It consists of several phases in which different activities are proposed. After each phase there is a gate which requires a verification, if the planned solutions and the meaningfulness of the concepts are given. When this is fulfilled the next phase starts, otherwise there is a need to start from scratch with the previous phase. This model is to be understood as a cycle and should serve to question and optimize the business model during the entire life cycle.

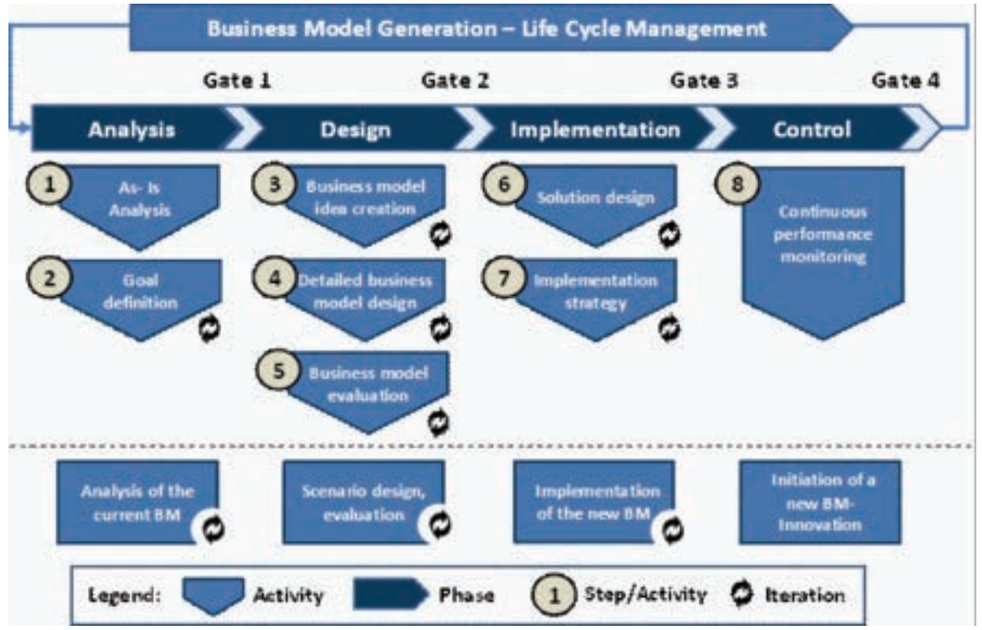

Figure 3: Process Model for Business Model Innovation (modified and enhanced according to Bucherer (2010)

Co-funded by the Erasmus+ Programme of the European Union

3. METHODOLOGY FOR TRANSFORMATION

To develop a new business model and to transform the current business model, numerous methods exist to support the process. To provide extensive applicability to any kind of business sector, the stepwise approach presented was based on a combination of methodologies from various authors. A methodology is defined as "a system of broad principles or rules from which specific methods or procedures may be derived to interpret or solve different problems within the scope of a particular discipline. Unlike an algorithm, a methodology is not a formula but a set of practices". (Business Dictionary, 2020) The following chapters will explain the created methodology and shows the recommended methods that can be used. The set of methods in use have been selected based on a literature research and interviews with practitioners from industrial companies. (Herrmann & Huber, 2020), (Staudter et al., 2013), (Schallmo, 2017), (Kohne, 2020), (Gerberich, 2005), (Osterwalder & Pigneur, 2005). However, this process and its tools must be followed and used by a competent team with a suitable set of skills. The selection of the team members is highly important, as the business model they will find could be crucial to success. The aim of the business model transformation is to improve the existing business or change it with the result of success and higher profitability. One of the keys to success is not only the team, but also the dedication of the top management to increase innovation and change. (Staudter et al., 2013)

3.1. Phase of business analysis

Companies are a complex of various elements and interdependencies. Three main parts of the company should be analysed: The own business model (customers, value proposition, value chain and profit model), the stakeholder (customer incentives, partners, competitors) and the external influences on the business (ecosystem). (Gassmann et al., 2020)

		Steps	Explanation	Proposed Methods
Analysis	1	As-Is-Analysis	The current state of the company is analysed to find out what issues exist and what the best practises are. The goal is to ensure common understanding on why a new business model is necessary and to find out what went wrong.	1. SWOT analysis 2. Benchmark 3. Ishikawa
	2	Goal Definition	Before developing ideas, the enterprise must decide which direction should be taken and what the goals are.	1. GAP analysis 2. Goal Pyramid 3. Scenario analysis

Figure 4: Analysis – steps and tools

Questions to be answered during the as-is-analysis of the business are:

- What can my company provide to be attractive and accepted in the future?
- What must change to ensure sustainable survival and competitiveness?
- What mechanisms must be implemented to recognise opportunities, risks and the need for change early on? (Nührich & Hauser, 2001).

Co-funded by the Erasmus+ Programme of the European Union

Step 1 - As- Is Analysis
The As-Is-analysis includes all functions and departments of a company, the product spectrum, technology, production depth, quantity framework, financial data, customer and supplier data, organization data, all methods and tools used, as well as the employees and their relationships toward each other and the company. During the As-Is-analysis deficits will be found, which are a result of various reasons. For example, wastage of resources or potential of the employees or not seizing opportunities by acting in a non-future orientated way. (Nührich & Hauser, 2001) A literature review shows that the methods have been listed to be the most suitable and applicable in operational business (see also Figure 4):

- SWOT (Niemann, 2016), (Niemann et al., 2009), (Hermann & Huber, 2020)
- Benchmarking (Staudter et al., 2013), (Nührich & Hauser, 2001)
- Ishikawa diagram (Niemann, 2016), (Niemann et al., 2009), (Munro, 2003).

Step 2 - Goal definition
The highest level of a company goal is the vision. The vision is the long-term goal of a company that describes the general purpose of the company (Hermann & Huber, 2020). An example for a vision from Procter & Gamble is the following:
"We will provide branded products and services of superior quality and value that improve the lives of the world's consumers, now and for generations to come. As a result, consumers will reward us with leadership sales, profit and value creation, allowing our people, our shareholders and the communities in which we live and work to prosper." (P&G, 2020)

When developing goals the company should decide what they want to achieve, where they want to stand in the future and in which amount of time the goal should be achieved. According to a literature review the following tools are essential in practical use (see also Figure 4):

- Goal pyramid (Niemann, 2016), (Hermann & Huber, 2020)
- Gap analysis (Niemann, 2016), (Hermann & Huber, 2020)
- Scenario analysis (Niemann, 2016), (Niemann et al., 2009), (Hermann & Huber, 2020).

3.2. Phase of design
In this phase ideas for the new business model will be systematically developed. This is mainly done by work groups applying creativity techniques.
The identified business models will then be designed and evaluated according to the company goals and capabilities. Figure 5 shows the single steps.

		Steps	Explanation	Proposed Methods
Design	3	Business model idea creation	Ideas are collected in groups and systematically developed. This phase lays the foundation for the further steps	1. Destroy your business 2. Empathy Map 3. St. Galler business model navigator
	4	Detailed business model design	The ideas are transformed into business models and described in detail.	1. Canvas 2. SIPOC
	5	Business model evaluation	The new-found business models are evaluated to enable a comparison and also to help decide on the most suitable one.	1. PESTEL Model 2. Porters Five Forces 3. Value Benefit

Figure 5: Design – steps and tools

Co-funded by the Erasmus+ Programme of the European Union

Step 3 - Business model idea creation
The idea finding phase marks the beginning of the business model development process. The goals have been defined and the development direction set. Either an existing product or service is to be improved or a completely new idea is to be developed. In either case a key aspect is to take the customers into account. It is crucial to understand what the customer needs and where his inconveniences lie, as well as what the customer expects from the company. Another question to be answered is, how the company can position itself in a way to satisfy the customers need in the best manner in comparison to the competition. All methods to develop creative ideas and to emphasise creativity underlie the same principles: understanding of the challenge, loosening of transfixed stereotypes and assumptions, recombining existing approaches and solutions and refining of ideas through criticism and improvement. (Hoffmann et al., 2016)
This phase helps to create new ideas through creative thinking, without being influenced by existing business models and ideas, as well as the current business model in place (Schallmo & Brecht, 2013). The following sections will explain some methods to develop creative, innovative ideas. The most commonly used idea generation methods are mind mapping and brainstorming. However, these will not be looked at further, as they are very simple and well known. For operational business applications the literature references the following tools (see also Figure 5):

- Destroy your business (Kohne, 2020)
- The empathy map (Osterwalder & Pigneur, 2011)
- St. Galler business model navigator (Gassmann et al., 2020)

Step 4 - Detailed business model design
After some ideas have been gathered, they should be thought through systematically. All aspects should be considered, to enable a holistic perspective of the business model and to ensure its functionality. For this the most proven tools used in practice are (see also Figure 5):

Step 5 - Business model evaluation
Having described the business models through the canvas and SIPOC method, the business models can now be evaluated. However, this can be a difficult task due to incomparability or through incomplete perspectives on the business models. Therefore, first of all an environmental analysis for each business model that is estimated to be promising should be made and then an objective evaluation with a systematic procedure and reasonable evaluation criteria should be followed. Literature reports to apply the following tools (see also Figure 5):

- PESTEL (Schallmo & Brecht, 2013)
- Porters five forces (Schallmo & Brecht, 2013)
- Value benefit analysis (Kühnapfel, 2014)

Co-funded by the Erasmus+ Programme of the European Union

3.3. Phase of implementation

In this phase the solution starts the design for the new found business model. All relevant aspects and details have to be considered and included into the new solution.

		Steps	Explanation	Proposed Methods
Implementation	6	Solution design	Considering all relevant details of the new-found business model on which the planning and implementation phase is based	1. Detailed Process design 2. Resource planning 3. Investment planning 4. Business Case
	7	Implementation strategy	Definition and development of the implementation strategy. Setup of a transformation plan regarding change management aspects	1. Project Charter 2. Action plan 3. RACI plan 4. Project Plan 5. Transformation Plan

Figure 6: Implementation – steps and tools

After the final approval of the solution design the business model has to be implemented into the daily operation and business routines. For this a detailed implementation strategy has to be elaborated to master this transition with regard to all kinds of management aspects.

Step 6 - Solution design
This step focuses on the business model that is planned to be used and helps to prepare and consider all aspects that are relevant for the implementation of the new business model. According to several authors this step is being performed by the application of the following tools (see also Figure 6):

- Detailed process design (Niemann, 2016), (Niemann et al., 2009), (Staudter et al., 2013)
- Resource & investment plan (Niemann, 2016), (Niemann et al., 2009), (Staudter et al., 2013), (Heesen, 2016)
- Business case (Staudter et al., 2013), (Heesen, 2016), (Brugger, 2009), (Wöltje, 2012), (Olfert, 2015)
- Performance management (Gerberich, 2005), (Gabler, n. d.), (Mühlencoert, 2015).

Step 7 - Implementation strategy
When all the framework has been set, the implementation strategy can be developed. The goal of the implementation strategy is, that the current processes can be transformed without major delays and downtimes. Furthermore, the resource availability is to be considered and the influence on the running operations or departments before setting up a project. It is recommended to start a pilot first, to stabilise the processes and find gaps and potentials for improvement. The old and the new process should be operated in parallel, so that the new process can gain maturity and stability (Staudter et al., 2013). The implementation of a new business model within a firm should be done through a project. Beforehand, some planning must be done to define the framework. Therefore, project management elements will be used to support the transformation (Schallmo & Brecht, 2013). Beginning with the project charter, that defines all important elements of the project a second important document will be presented, that is used throughout the entire transformation phase: the project plan. Furthermore, a RACI plan is put together, to define the roles and responsibilities during the transformation project. Finally, a budget plan for the project is set up. Applicable tools to finish this step are (see also Figure 6):

- Project charter (Staudter et al., 2013)

Co-funded by the Erasmus+ Programme of the European Union

- Action plan (Staudter et al., 2013)
- RACI matrix (Staudter et al., 2013), (Bergmann & Garrecht, 2015)
- Project plan (Staudter et al., 2013), (Bergmann & Garrecht, 2015)
- Transformation plan (Kohne, 2020), (Gerberich, 2005), (Mervelkemper & Paul, 2016), (Barsh et al., 2020), (Schein, 2010), (Gerberich et al., 2010)

3.4. Phase of control

The final phase aims at the continuous evaluation of the newly implemented business model. For this the operational performance figures have to continuously monitored and controlled in a structured manner.

		Steps	Explanation	Proposed Methods
Control	8	Continuous performance monitoring	Continuous evaluation of business model performance. In case of deviations activation of measures to keep business on track	1. Balanced scorecard 2. Break-even analysis 3. Rolling forecast

Figure 7: Control – steps and tools

Step 6 - Solution design

The objective of this final step is to ensure a durable and sustainable development of the new business model. Therefore, the current operational performance is permanently monitored and benchmarked against previously defined key performance figures. By this deviations and according counter measures can be taken at an early stage. Various authors recommend the following tools to master this step (see also Figure 7):

- Balance scorecard (Gerbreich, 2005), (Gassmann et al., 2020), (Gerberich et al., 2010), (Gassmann et al., 2014), (Glauner et al., 2014)
- Break even analysis (Gerbreich, 2005), (Gassmann et al., 2020), (Gerberich et al., 2010), (Gassmann et al., 2014), (Glauner et al., 2014)
- Rolling forecast (Gerbreich, 2005), (Gassmann et al., 2020), (Gerberich et al., 2010), (Gassmann et al., 2014), (Glauner et al., 2014).

4. SUMMARY AND OUTLOOK

The paper describes a process and a toolbox of methods for the digital business transformation. The single phases have been subdivided into smaller single steps. To master the steps a literature review has been performed to identify useful methods for the practical execution. This toolbox of methods can be used as a blueprint for the education and training of future service engineers. Therefore it is recommended to integrate the identified methods and tools into the curriculum and elaborate according skill cards for training and education.

Co-funded by the Erasmus+ Programme of the European Union

REFERENCES

Barsh, J.; Capozzi, M.; Davidson, J. (2020): Leadership in Innovation. In: McKinsey Quarterly. Online available: http://www.mckinsey.com/business-functions/strategy-and-corporate-finance/our-insights/leadership-and-innovation, last access 04.04.2020

Bergmann, R.; Garrecht, M. (2016): Organisation und Projektmanagement. 2. Aufl. 2016. Berlin, Heidelberg: Springer Gabler (BA KOMPAKT). online availbale: http://dx.doi.org/10.1007/978-3-642-32250-1, last access 04.04.2020

Brugger, R. (2020): Der IT Business Case. Kosten erfassen und analysieren, Nutzen erkennen und quantifizieren, Wirtschaftlichkeit nachweisen und realisieren. 2. Aufl. s.l.: Springer-Verlag, 2009 (Xpert.press). Online available: http://site.ebrary.com/lib/alltitles/docDetail.action?docID=10297037, last access 04.04.2020

Bucherer, E. (2010): Business model Innovation-Guidelines for a structured approach, Shaker Verlag, Aachen, 2010

Business Dictionary “Methodology” (2017): Methodology. Hg. v. Inc. WebFinance. businessdictionary.com. Online available http://www.businessdictionary.com/definition/methodology.html, last access 04.04.2020

Dehmer, J.; Kutzera, A. ; Niemann, J. (2017): Digitalisierung von Geschäftsmodellen durch platformbasiertes Value Chain Manage-ment. In: ZWF - Zeitschrift für wirtschaftlichen Fabrikbetrieb 112 (4), 2017, S. 253–256.

Gabler Kompakt-Lexikon Wirtschaft: 11., aktualisierte Aufl. Wiesbaden: Springer Gabler.

Gassmann, O.; Frankenberger, K.; Csik, M. (2020): Geschäftsmodelle entwickeln. 55 innovative Konzepte mit dem St. Galler Business Model Navigator. München: Hanser. Online available: http://www.hanser-elibrary.com/action/showBook?doi=10.3139/9783446437654, l last access 04.04.2020

Gassmann, O.; Frankenberger, K.; Csik, M. (2014): The business model navigator. 55 models that will revolutionise your business. Harlow: Pearson, 2014

Gerberich, C. (2005): Praxishandbuch Controlling. Trends, Konzepte, Instrumente. 1. Aufl. Wiesbaden: Gabler, 2005

Gerberich, C.; Teuber, J.; Schäfer, T. (2010): Integrierte Lean Balanced Scorecard. 1. Aufl. s.l.: Gabler Verlag, 2010. Online verfügbar unter http://gbv.eblib.com/patron/FullRecord.aspx?p=748707, last access 04.04.2020

Glauner, F. (2016): Zukunftsfähige Geschäftsmodelle und Werte. Strategieentwicklung und Unternehmensführung in disruptiven Märkten. Berlin, Heidelberg: Springer Gabler, 2016. Online available: http://dx.doi.org/10.1007/978-3-662-49242-0, last access 04.04.20

Heesen, B. (2016): Investitionsrechnung für Praktiker. Fallorientierte Darstellung der Verfahren und Berechnungen. 3. Auflage. Wiesbaden: Springer Gabler, 2016. Online available: http://search.ebscohost.com/login.aspx?direct=true&scope=site&db=nlebk&AN=1087143, last access 04.04.2020

Herrmann, A.; Huber, F. (2013): Produktmanagement. Grundlagen - Methoden - Beispiele. 3., vollst. überarb. u. erw. Aufl. Wiesbaden: Springer Gabler. Online available: http://dx.doi.org/10.1007/978-3-658-00004-2, last access 04.04.2020

Hoffmann, C.; Lennerts, S.; Schmitz, C.; Stölzle, W.; Uebernickel, F.(2016): Business Innovation: das St. Galler Modell. Wiesbaden: Springer Gabler, 2016. Online avaiblable: http://dx.doi.org/10.1007/978-3-658-07167-7, last access 04.04.2020

Kohne, A. (2020): Business Development. Kundenorientierte Geschäftsfeldentwicklung für erfolgreiche Unternehmen. Wiesbaden: Springer Vieweg. Online available: http://dx.doi.org/10.1007/978-3-658-13683-3, last access 04.04.2020

Kreutzer, R. (2017).: Konzeption und Grundlagen des Change- Managements. In: Wirtschaftswissenschaftliches Studium 1 (46), 2017, S. 10–17.

Kühnapfel, J. (2014): Nutzwertanalysen in Marketing und Vertrieb. Wiesbaden: Springer Fachmedien Wiesbaden, 2014

Melzer, A. (2015): Six Sigma-- Kompakt und praxisnah. Prozessverbesserung effizient und erfolgreich implementieren. Wiesbaden: Springer Gabler, 2015. Online available: http://search.ebscohost.com/login.aspx?direct=true&scope=site&db=nlebk&AN=1050548, last access 04.04.2020

Mervelskemper, L.; Paul, S. (2016): Unternehmenkultur als Innovationstreiber? Ein Einblick in die Praxis. In: Zeitschrift für das gesamte Kreditwesen 2016 (15), S. 746. Online available: https://www.wiso-net.de/document/ZFGK__081601014, last access 04.04.2020

Mühlencoert, T. (2012): Kontraktlogistik-Management. Grundlagen - Beispiele - Checklisten. Wiesbaden: Gabler Verlag, 2015. Online available: http://dx.doi.org/10.1007/978-3-8349-3733-9, last access 05.05.17.

Co-funded by the Erasmus+ Programme of the European Union
The European Commission support for the production of this publication does not constitute an endorsement of the contents which reflects the views only of the authors, and the Commission cannot be held responsible for any use which may be made of the information contained therein. Project number: 585796-EPP-1-2017-1-AT-EPPKA2-CBHE-JP

Munro, R. (2003): Six Sigma for the office. A pocket guide. Milwaukee, Wis.: ASQ Quality Press., 2003

Niemann, J.; Fussenecker, C.; Schlösser, M.; Ahrens, T. (2019): ELIC – Teacher as a medium to built a new generation of skilled engineers, In: Proceedings of the International Conference on Competitive Manufacturing (COMA´19), 30 January – 1 February 2019, Stellenbosch, South Africa, S. 234-238

Niemann, J. (2016): Die Services-Manufaktur, Industrielle Services planen –entwickeln – einführen. Ein Praxishandbuch Schritt für Schritt mit Übungen und Lösungen. Aachen, Shaker Verlag, 2016

Niemann, J. (2017): Life Cycle Management- das Paradigma der ganzheitlichen Produktlebenslaufbetrachtung. In: Spath, Dieter; Westkämper, Engelbert; Bullinger, Hans-Jörg; Warnecke, Hans-Jürgen (Hrsg.): Neue Entwicklungen in der Unternehmensorganisation. Berlin, Springer-Vieweg, VDI Buch, 2017

Niemann, J. (2017): Ökonomische Bewertung von Produktlebensläufen- Life Cycle Controlling. In: Spath, Dieter (Hrsg.) u.a.: Neue Organisationsformen im Unternehmen In: Spath, Dieter; Westkämper, Engelbert; Bullinger, Hans-Jörg; Warnecke, Hans-Jürgen (Hrsg.): Neue Entwicklungen in der Unternehmensorganisation. Berlin, Springer-Vieweg, VDI Buch, 2017

Niemann, J.; Tichkiewitch, S.; Westkämper E. (2009): Design of Sustainable Product Life Cycles, Springer Verlag, Heidelberg Berlin, 2009

Nührich, K.; Hauser, A. (2001): Unternehmensdiagnose. Ein Führungsinstrument zur Sicherung der nachhaltigen Existenzfähigkeit von Unternehmen. Berlin: Springer, 2001

Olfert, K. (2015): Investition. 13., aktualisierte Auflage. Herne: Kiehl (Kompendium der praktischen Betriebswirtschaft), 2015

Osterwalder, A.; Pigneur, Y. (2011): Business Model Generation. Ein Handbuch für Visionäre, Spielveränderer und Heraus-forderer. 1. Aufl. Frankfurt am Main: Campus Verl. (Business 2011). Online available: http://search.ebscohost.com/login.aspx?direct=true&scope=site&db=nlebk&db=nlabk&AN=832895, last access 04.04.2020

P&G (2020): Our Purpose. Online available: http://us.pg.com/who-we-are/our-approach/purpose-values-principles, last access 04.04.2020

Schallmo, D. (2017).: Design Thinking erfolgreich anwenden. So entwickeln Sie in 7 Phasen kundenorientierte Produkte und Dienstleistungen. Wiesbaden: Springer Fachmedien Wiesbaden, 2017

Schallmo, D.; Brecht, L. (2012): Geschäftsmodell-Innovation. Grundlagen, bestehende Ansätze, methodisches Vorge-hen und B2B-Geschäftsmodelle. Zugl.: Ulm, Univ., Diss., 2012. Wiesbaden: Springer Gabler, 2013

Schallmo, D.; Rusnjak, A.; Anzengruber, J.; Werani, T.; Jünger, M. (2017): Digitale Transformation von Geschäftsmodellen. Grundlagen, Instrumente und Best Practices. Wiesbaden: Springer Fachmedien Wiesbaden, 2017

Schein, E. (2010): Organizational culture and leadership. 4. ed. San Francisco, Calif.: Jossey-Bass (The Jossey-Bass business & management series), 2010. Online available: http://www.esmt.eblib.com/patron/FullRecord.aspx?p=588878, last access 04.04.2020

Staudter, C et al. (2013): Design for Six Sigma+Lean Toolset. Innovationen erfolgreich realisieren. 2., vollst. überarb. und erw. Aufl. Wiesbaden: Springer Gabler, 2013

Wöltje, J. (2012): Finanzkennzahlen und Unternehmensbewertung. 1. Aufl. s.l.: Haufe Verlag (Haufe TaschenGuide - Band 00381, v.381), 2012. Online available: http://www.wiso-net.de/document/HAUF,AHAU__9783648025130127, 12.05.17.

Co-funded by the Erasmus+ Programme of the European Union

INTRODUCTION TO THE KNOWLEDGE AND DESIGN OF CARS

MECHANIC PARTS IN EARLY STAGES OF MECHANICAL ENGINEERING DEGREE

Fuertes Laura[1], Gavino Sergio[2], Lopresti Laura[3], Speroni Lucas[4], Defranco Gabriel[5]

UIDET GIGA, Facultad de Ingeniería UNLP,

[1] *fuertes@ing.unlp.edu.ar*
[2] *sergio.gavino@ing.unlp.edu.ar*
[3] *laura.lopresti@ing.unlp.edu.ar*
[4] *lucas.speroni@ing.unlp.edu.ar*
[5] *ghdefran@ing.unlp.edu.ar*

ABSTRACT

Most of the students who arrive every year to study mechanical engineering at the National University of La Plata (UNLP), Argentina, do it so motivated by an innate passion for cars. Many of them dream of being part of competition teams like chassis designers or engine builders. Others aim to develop their careers in companies producers of cars or their parts. But none of them do find theoretical and practical content that satisfies their expectations during the first third part of the degree experiencing some grade of frustration and leading some of them even to the abandonment of the university. The reason is that the studies plan is organized around a strong starting block of basic sciences knowledge like mathematics and physics but no specific content of mechanics is developed in this period. One exception to that is given by the technical drawing which is the only one subject treating contents directly referred to engineering. Being technical drawing a discipline which needs real cases to be developed in a formal system of representation using real models like parts of machines, an intrinsic difficulty appears because of the lack of training about them by the students. In an attempt to overcome part of this situation the chair Gráfica para Ingeniería (GPI) at Facultad de Ingeniería, UNLP, has implemented a special practical work to be developed by teams of students into which they have to analyze a real mechanism belonging to a car or in general to a machine. The aim of this work is not only its representation through engineering drawings but make a detailed analysis of each part, their role in the whole, the materials present and the manufacturing processes. This proposal has shown being capable of giving meaningful learning (Ausubel, 1963) to the activity. Otherwise the models only have geometrical meaning but not an identified function. The work involves the representation of each part first as a sketch, then in CAD 3D and finally a technical report of the highlights of the mechanism. This work explains the complete experience and the results obtained after more than ten years of practice.

Keywords: technical drawing, engineering teaching, meaningful learning, mechanisms.

Co-funded by the Erasmus+ Programme of the European Union

The European Commission support for the production of this publication does not constitute an endorsement of the contents which reflects the views only of the authors, and the Commission cannot be held responsible for any use which may be made of the information contained therein. Project number: 585796-EPP-1-2017-1-AT-EPPKA2-CBHE-JP

OBJECTIVES

An Integrative activity is developed at UNLP, Faculty of Engineering by the chair GPI into the course given for several branches of Engineering training. From the point of view of the legal regulations the subject, which is technical drawing in fact, is included within the basic sciences block since the Ministry Resolution 1232/01 was released. But due to its technological characteristics, its role is that of the first subject including contents of Engineering. The didactic proposal of the experience here developed is to lead first-year students to initiate them in the study and representation of a mechanical system, analyzing the general characteristics of the assembly, the number of components, the materials employed, the physical principles involved in the operation, the linkage between the parts, whether mobile and / or fixed, technologies of manufacturing applied on each part, etc. Then the students have to write a report including sketches and CAD plans obtained from parametric modeling. Since this practice is being carried out from more than ten years and no repetition of themes are allowed, the spectrum of mechanical assemblies studied up to the present is very wide: from some developed for didactic purposes by the teachers to real ones such as gearboxes, small internal combustion engines, winches, brake systems, clutches, vehicle suspensions, small aircraft landing gears, etc.
Once each part of the selected mechanism is hand sketched, the second step is to model them in 3D parametric CAD. With the 3D model of the parts the students have to solve the virtual assembly of its components. If no conflict is found between the parts designed they are in conditions to give movement to the whole. This simulation for the real working of the joint is normally the most expected moment of the practice and from it they generate a video for the final presentation to their mates and the teachers.

Other output is an exploded view of the assembly following the IRAM standard for technical drawing. Arriving at this point, once the task is over, the students find the satisfaction of having worked with real things very close to those belonging to Mechanical Engineering. Also the teaching staff that guides the process gets high satisfaction regarding the performance of the future engineers challenged to develop a work very linked to the professional activity but in the first steps of Engineering studies. The final presentations have very high quality sometimes contrasting with the difficulties the same students find to afford the theoretical and normalized aspects of the technical drawing subject of the plan of studies.
The presentations include digital productions in virtual environments in addition to the sketches and drawings of each of the parts, an assembly drawing with an exploded isometric and the corresponding list of parts.

The activity has been consolidating year by year due to its didactic potential allowing the students to acquire and develop skills for reading, interpreting and carrying out technical graphic representations and writing technical reports.
Another important aspect is that as a team activity enables the understanding of key disciplinary principles of Engineering developing at the same time skills for independent learning and teamwork.

THEORETICAL FRAMEWORK

During the last decades in Argentina, the teaching of drawing of technical nature has been fed from different sources. On the one hand the successive changes in the study plans in Engineering as a response to the requirements of the changing technological scenario. In that sense the profile of the engineer in training is defined by agreements regarding the development of competencies ``to conceive, design and develop engineering projects (systems, components, products or processes) promoting the development of capacities" to "document and effectively communicate the selected solutions'' (Documentos de CONFEDI, 2014). On the other hand the recent resolution 1254/18 of the Ministerio de Educación modifying the 1232/01 one, published in the Official Bulletin on May 18th, regarding the establishment of the scope and definition of the professional activities reserved exclusively for the title of Engineer in their different branches. Also the contributions of specialists in education sciences in relation to the integration of Information and Communication Technologies (ICTs) with student-centered learning activities, collaborative work, etc. (Del Valle, 2005) challenge the teachers to review their teaching practices with a critical sense to promote the construction of technological knowledge.In a similar way the development of CAD systems, both those that only allow 2D drawing as others more evolved applications which follow the parametric paradigm with 3D modeling have integrated the drawing and the design of one component or several pieces as part of a process moving from the concept of drawing to the concept of computer aided design.

Several authors such as Anderson (2011), del Caño (2007) and Ramos dos Santos (2004) have put also into consideration the Computer Aided Engineering (CAE), which allows "the development of prototypes and laboratory tests to be replaced by virtual simulations, helping engineers to carry out a much greater number of analyzes in a short time and reducing project costs".
Drawing of a technical nature is included in the curricula of all the faculties of engineering in Argentina, taking different denominations such as technical drawing, technological language, technological drawing, representation systems, graphic expression, etc. Graphics for Engineering is the name adopted at La Plata University. Beyond the different names it is possible to detect thematic axes into its core independently of newest approaches to the discipline (Defranco 2015): the Monge system or system of orthogonal projections solved according to modern standards, enriched with the resources of sections, dimensioning and specific symbology. Computer aided design is considered as essential as one more way of learning design but not a knowledge itself.
Formative activities are promoted through these thematic units with the scope of helping the students to acquire skills that allow them to read and make graphic representations of a technical nature, elaborated according to national and international standards and made both by hand (sketching) as well as 2D and 3D modeling through computer aided design.

Some theoretical lines take for granted that it is no longer needed the hand sketching from the time the CAD systems became available in educative environments of HEIs. So if the value of sketches is to put under the magnifying glass the teaching and learning process of technical drawing the authors of this work share the criteria established by Martínez and Sentana "sketching exercises are a task that requires an individual process, although it is considered very useful to carry out a group-guided correction, allowing hand in the exercises once corrected individually. The freehand sketch is defended as a fundamental element in the professional work of the engineer" (Martínez 2002).

From the point of view of the teaching strategies the integrative activity, which is the axis of this work, was implemented for the first time around 2003 as a closing activity of GPI course which takes one semester of the curriculum and just sixteen lessons. Over the years this practice was changing and it was particularly enriched around 2007 when parametric CAD was introduced instead of metric CAD. Taking into account that different branches of the Engineering (such as mechanical, electromechanical, aerospace, materials, etc.) take the course, specific themes are selected according to that, trying always to give satisfaction to the student's expectations in concordance to the branch followed. So after one decade of successive experiences with different groups of students and reviewing year by year the results it is possible to affirm that the practice has been consolidated by its integrating nature: sketching of the parts, 3D modeling of them, assembly of the set, simulation of the movement, analysis of the operation and manufacturing methods, drafting of a technical report including drawings of the parts and the whole as an exploited isometrics with the respective list of parts.

Co-funded by the Erasmus+ Programme of the European Union

Co-funded by the Erasmus+ Programme of the European Union
The European Commission support for the production of this publication does not constitute an endorsement of the contents which reflects the views only of the authors, and the Commission cannot be held responsible for any use which may be made of the information contained therein. Project number: 585796-EPP-1-2017-1-AT-EPPKA2-CBHE-JP

METHODOLOGY

In the course of GPI the sketching is a practical activity normally developed from real models or virtual models. In the first case the students have available real parts like spare parts of machines or components of mechanical assemblies. They really have the models in their hands and can share their analysis and opinions with the rest of the team (of about five or six members) in order to make decisions of how to draw them. Those drawings are freehand and respecting the proportions of the dimensions but not in scale. In the second case interactive 3D models in pdf format are used. Those models are developed by the UIDET GIGA as part of an R&D project (Gavino 2013). This modality arises as a necessity of having available more quantity of models because of the raising of the number of students so, once the new set of models were produced it was possible to give them to a greater number of students through the website. Being the models purposely created for this activity it is possible to analyze and define variations in morphology specially selected to meet didactic requisites of increasing degree of difficulty. Both real and virtual models are aimed to improve graphical reading skills and get abstraction of real objects of variable complexity.

In this scenario the chair GPI with the support of its associated Unidad de Investigación y Desarrollo – Grupo de Ingeniería Gráfica Aplicada (UIDET-GIGA) has been testing the possibility of introducing students in the world of project and design from the early stages of Engineering training. The experiences carried out and their evolution and results have been progressively reported through various works of their production (Fuertes, 2008, Defranco 2010).
There is no doubt that all innovation requires feedback from the practices in order to continue contributing to the training of the future engineers while integrating new strategies that enhance drawing of technical nature as a communication language which is in constant evolution. Therefore, the teaching of graphic systems for Engineering requires to state:

- what to teach, which means to establish agreements on the selection of contents
- how to teach, which means to establish agreements on teaching strategies, activities and resources, etc.
- how to evaluate, which means to establish agreements on instruments and criteria of evaluation

As it was already said the starting point is a given mechanical system and the integration of the teams with a number of members from four up to six students. If it is possible each team must have their own system and it is not allowed to have more than two repeated systems into the same classroom. The students receive a written plan with detail of the tasks and the sequence into which it should be developed. The following is a synthesis of the plan:

1. Analysis of the mechanical assembly: the students must describe how the system operates and the function of each part, methods of linking between them, materials of each part, manufacturing process, etc. They also have to analyze, if there is any, the lubrication systems and other fluids for normal operation; describe the surfaces of the parts, especially those that are in mutual contact and degree of friction between them in a macroscopic scale.

2. Sketching the parts: the students must sketch each part under drawing standards on A3 graph paper. The sketch will be done with the usual techniques and with the piece in sight.

3. Three dimensional modeling: each part of the set must be solved in parametric 3D CAD from the sketch. Once the part is designed and the material of it is known the software calculates the weight of each component which must be specified in the list of parts which is included in the exploded isometric according to IRAM 4508 standard. Constructive plans can be obtained from the individual 3D designs.

4. Movement Simulation: once the assembly of each part is made the students will solve the cinematic. Two alternatives are allowed: the first, to simulate the cinematic of the mechanism in operation conditions; the second, to simulate the assembly process as it were in the mounting line following a logical order and closest to the true. In spite of being simplifications both cases are accepted as if they were the real processes since the students are in the initial stage of the Engineering training, just starting with Physics and they haven't still studied manufacturing processes. From both of the given alternatives they must produce a video using the educational license of the Autodesk Inventor® of free download from the official website: https://www.autodesk.com/education/free-software/featured
Regarding the evaluation, the process is progressively corrected by the assistants, some of them responsible for the sketches and others of the digital drawings. Within the mentioned process there are two correction times: a preliminary one or advance report and the deadline. The feedback of both presentations is complemented with a final meeting of discussion. The implementation of this work is supervised by the assistants of the chair, based on a work guide hosted on the website where the activities, the agenda and the presentation templates are available: hand sketches, printed plans and simulation videos (Figure 1).

Figure 1: Cover of the 2018 Guide for the Study and Representation of a Mechanism (only available in Spanish)

Co-funded by the Erasmus+ Programme of the European Union
The European Commission support for the production of this publication does not constitute an endorsement of the contents which reflects the views only of the authors, and the Commission cannot be held responsible for any use which may be made of the information contained therein. Project number: 585796-EPP-1-2017-1-AT-EPPKA2-CBHE-JP

Co-funded by the Erasmus+ Programme of the European Union
The European Commission support for the production of this publication does not constitute an endorsement of the contents which reflects the views only of the authors, and the Commission cannot be held responsible for any use which may be made of the information contained therein. Project number: 585796-EPP-1-2017-1-AT-EPPKA2-CBHE-JP

The mechanic assemblies are changed from year to year and have different levels of complexity both regarding the general characteristics, the number of parts that make it up, the physical principles of operation, the way of linking between the parts, whether mobile or fixed, etc.
In Table 1, some of the significant themes developed in recent years can be observed.


Crank and connecting rod mechanism (didactic system developed by the chair)


Improvement of crank and connecting rod mechanism (students' proposal)


Bicycle pedal box


Gearbox


Automotive clutch


Automotive differential


Plane rear wheel

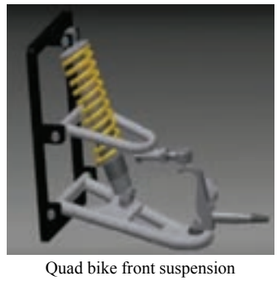
Quad bike front suspension


Stub axle quad bike


Automotive disc brake


Lift brake

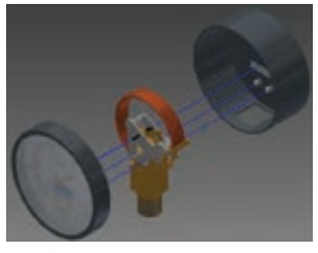
Bourdon tube pressure Gauge

Table 1: Samples of cases developed throughout different courses

Co-funded by the Erasmus+ Programme of the European Union

The European Commission support for the production of this publication does not constitute an endorsement of the contents which reflects the views only of the authors, and the Commission cannot be held responsible for any use which may be made of the information contained therein. Project number: 585796-EPP-1-2017-1-AT-EPPKA2-CBHE-JP

RESULTS

One sample taken from the large quantity of works developed during the last years by students of Mechanical Engineering is presented in this paper. The study was carried out on a small two strokes internal combustion engine of a scooter. In the abstract of the report the students describe how the engine works: "the engine under study is an internal combustion one; in other words within its combustion chamber combustion happens between the fuel (a mixture of gasoline and oil in fact) and air. The combustion starts when a spark is triggered and the result is an exothermic chemical reaction. A two-stroke engine is an alternative thermal machine where intake, compression, combustion and exhaust phases are generated with only two movements of the piston".

In the following pictures different phases of the work developed by students are presented: main parts of the analyzed engine (Figure 2), sketching of the parts (Figure 3), 3D modeling (Figure 4) and screenshots of the video of the cinematic (Figure 5)


Figure 2: Parts of the engine analyzed

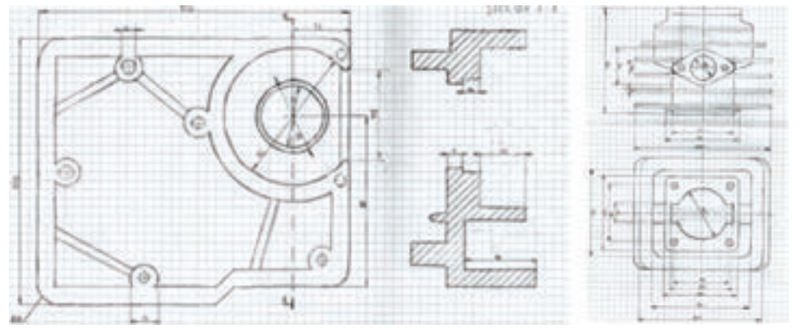
Figure 3: On the right, part of the sketch of the crankcase and on the left, sketch of the cylinder.

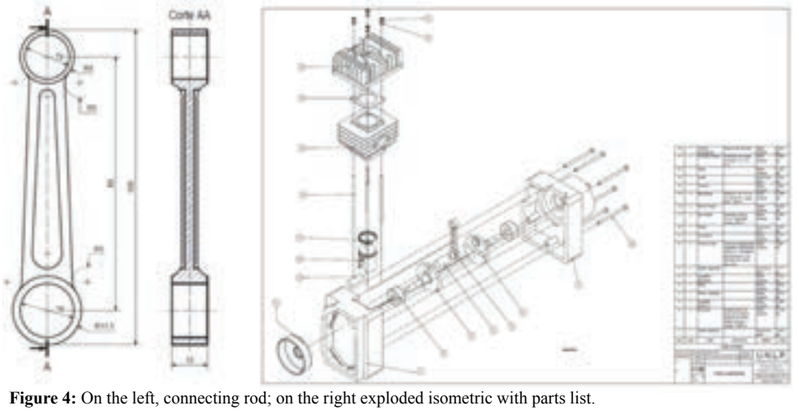
Figure 4: On the left, connecting rod; on the right exploded isometric with parts list.

Co-funded by the Erasmus+ Programme of the European Union

The European Commission support for the production of this publication does not constitute an endorsement of the contents which reflects the views only of the authors, and the Commission cannot be held responsible for any use which may be made of the information contained therein. Project number: 585796-EPP-1-2017-1-AT-EPPKA2-CBHE-JP

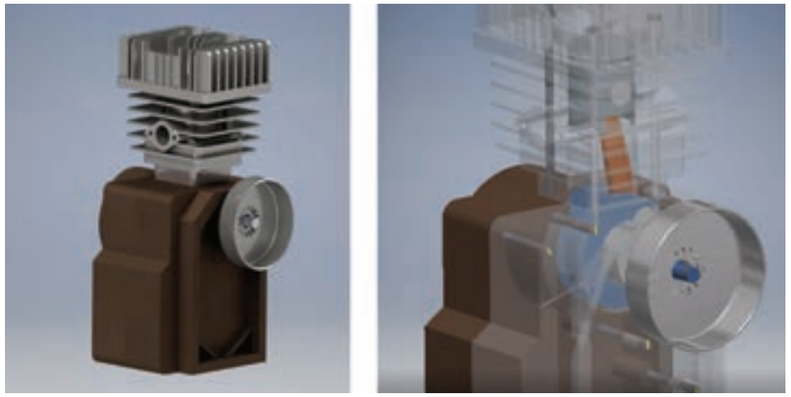

Figure 5: Screenshots of the video simulating the engine under operation. On the left, image of the assembled set. On the right, movement of the connecting rod and the piston shown through the resource of transparency for parts (Autodesk Inventor ®).

CONCLUSIONS

A didactic activity of analysis and representation of real mechanical systems guided to offer a preliminary contact with real assemblies in early stages of the Engineering training has demonstrated to be effective to catch the enthusiasm of students which otherwise don't find answers to their expectations up to the second third of the plan of studies. The motivation achieved is demonstrated by the results materialized in a technical report including the operation of the system, the linking between parts, the manufacturing and materials, sketches, solid 3D drawings and animations. Besides the hand sketching and digital 3D techniques during the development period the students learn soft skills as writing and team working. They also improve soft communication skills since each team has to get their own mechanical system which needs relationships with people who can lend it to them. It was verified that without any explicit requirement during the development of the work the students dedicate more time than usually during the course. Year after year the practice was consolidated given its didactic potential since it allows the stimulation of the students on reading of plans and spatial comprehension of the objects represented, analyzing functional and constructive aspects and the materials used in addition to the development of skills for independent learning and teamwork.

The division of the task between the members of each team is clearly promoted by the teachers involved in the activity highlighting the respect for the opinion of the others, especially in decision-making in order to achieve the objectives and results. It is also observed how this integrative work promotes "research skills and its development also involve the promotion and management of spatial capacity and creativity" (Urruza 2006).

Finally it is observed that parametric CAD enlarges the possibilities of exploring the morphology of the parts since this paradigm of CAD allows obtaining a wide range of results just by changing some few parameters. At the same time while designing the students are getting started in some manufacturing concepts. For example to generate a hole in the project it is needed to mark a center and set the diameter just like when making a real hole. This means a qualitative leap in the conception of the morphology of objects. The student "no longer draws the plane", but models the part in three dimensions, and then solves the plane with very simple tools for creating main and auxiliary views. It is a great difference to the 2D CAD design and introduces the students in a way of thinking which necessarily requires thinking in 3D, to imagine or make a mental abstraction of the part to be modeled.

Co-funded by the Erasmus+ Programme of the European Union

ACKNOWLEDGMENTS

The authors want to thank the students members of the team responsible of the work presented in this paper Martín Allende, Joaquín Antonini, Ulises Grande, Bernardino Capra, Agustín Lausada and Ignacio Dada. The latter is currently working as assistant of the chair of Gráfica para Ingeniería.
The authors also want to thank to the members and former members of the staff of Gráfica para Ingeniería at La Plata University: Jorge Miró, Néstor Basilotta, Ángel Fabris, Marianela Lara, Alberto Ristevich, Esteban Curcio, Sebastián Seghini, Andrés Raggio, Gustavo Lanciotti, Guillermo Lembo and Javier Torres.

REFERENCES

Anderson, J. & Tang, M. (2011). *La forma sigue los parámetros: Modelado paramétrico para los procesos de fabricación y manufactura*. The University of Newcastle. Australia

Ausubel, D. (1963). *The psychology of meaningful verbal learning.* New York. Grune & Stratton

Defranco, G., Fuertes, L., Gavino, S., Lopresti L. & Ristevich, A. (2010) *Diseño Paramétrico en la Enseñanza de la Gráfica para Ingeniería.* II Congreso Argentino de Ingeniería Mecánica San Juan. Instituto de Mecánica Aplicada. Universidad Nacional de San Juan. San Juan. Argentina

Defranco, G., Fuertes, L., Gavino, S., Lopresti L. & Lara, M. (2015) *De la forma a la dimensión: una propuesta metodológica para la enseñanza del dibujo para ingenieros*. EGRAFIA 2015 Río Cuarto, Córdoba, Argentina 8 y 9 de octubre de 2015.

Del Caño, A., De La Cruz, M. & Solano, L. (2007). *Diseño, ingeniería, fabricación y ejecución asistidos por ordenador en la construcción: evolución y desafíos a futuro*. Informes de la Construcción Vol. 59, 505, 53-71.

Del Valle López, G. & López, M. (2005) *Las TIC y el trabajo colaborativo en el proceso de enseñanza-aprendizaje en el nivel universitario.* Centro de Investigaciones Físico-Químicas, Teóricas y Aplicadas (CIFTA). Facultad de Tecnología y Ciencias Aplicadas. Catamarca. Argentina.

Documentos de CONFEDI. *Competencias en ingeniería.* (2014). Universidad FASTA Ediciones.

Fuertes, L., Lopresti, L., Gavino, S., Ristevich, A & Defranco, G. (2008) *De los sistemas CAD al modelado paramétrico: una experiencia de innovación en la enseñanza de dibujo tecnológico en Ingeniería.* VI Congreso Nacional de Profesores de Expresión Gráfica - EGRAFIA 2008. San Juan. Argentina.

Gavino, S., Fuertes, L., Lopresti, L., Lara, M. & Defranco, G. (2013). *Learning resources for technical drawing: 3d models from photographic register of mechanical parts.* GRAPHICA'13 - XXI Simpósio Nacional de Geometria Descritiva e Desenho Técnico e X International Conference on Graphics for Arts and Design. Florianópolis. Editora do CCE - Universidade Federal de Santa Catarina. Brasil.

IRAM Instituto Argentino de Normalización y Certificación, (2017). *Manual de normas de Dibujo Tecnológico 2017*

Ministerio de Educación (2018) *Alcances y definición de las actividades profesionales reservadas exclusivamente al título.* Resolución Ministerial 1.254/18. Boletín oficial, 18 de Mayo de 2018. Id SAIJ: NV19867

Martínez, A.; Sentana, I. (2002). *Evolución en la enseñanza del dibujo técnico mecánico en las enseñanzas técnicas* Actas del X CUIEET, Congreso Universitario de Innovación Educativa en las Enseñanzas Técnicas. Valencia.

Ramos Dos Santos, F.; Da Costa Ferreira, S.; Piaia J. (2004). *Computer aided engineering – CAE* - Universidade do Estado de Santa Catarina Centro de Ciências Tecnológicas.

Urruza, G.; Ortega, J.; Sierra, E. (2006). *Diseño de conjuntos mecánicos con un enfoque de aprendizaje constructivista.* Actas del XVIII INGEGRAF 2006 - Asociación Española de Ingeniería Gráfica. Departament d'Expressió Gràfica a l'Enginyeria. Universidad Politècnica de Catalunya.

Co-funded by the Erasmus+ Programme of the European Union

STUDENTS MOTIVATION USING EXTRACURRICULAR ACTIVITIES

Marcelo Augusto Leal Alves

Escola Politécnica da USP,
malalves@usp.br

ABSTRACT

Extracurricular activities such as the Formula SAE and the Mini-Baja projects are recognized as essential activities to engage engineering students. However, we observe that sometimes such activities can deviate students' attention to their academic progress. Mentoring such activities is a way to make them significant to student progress. The author presents his experience in mentoring such activities and how his methodology has helped students balance the normal curricular activities and extracurricular projects.

Keywords: Experimental Engineering, Vehicle design

INTRODUCTION

SAE Mini-Baja and Formula Student are among the several extracurricular activities available to engineering students in which they can put to the test what they learn in the classroom, their skills for teamwork and organization, to name a few. In a short survey conducted by the author with students (50 undergraduates, 25 members of a team, and 25 non-members), the results were as shown on table 1

Question	Participants	Non-Participants
Why do you take part in an e/c activity?		
To better use my time	5	N/A
To apply what I have learned	2	N/A
To learn more	15	N/A
Other	3	N/A
Why do you NOT take part in an e/c activity?		
I do not have time	N/A	5
Fear of negative impact on grades	N/A	12
I am nor interested at all	N/A	6
Other	N/A	2
Do you think E/C activities may enhance your employability?		
Yes	20	2
No	1	17
No effect at all	0	3
Do not know	5	3

Co-funded by the Erasmus+ Programme of the European Union

Do you think the university recognizes the E/C activities?		
Yes	5	5
No	19	2
I do not know	1	20
Do you feel motivated in your studies?		
Yes	5	3
No	20	18
I do not know	0	2

Table 1: Initial survey on student views on Extracurricular activities (E/C)

Although the number of participants in the survey is not high, it can be seen some differences between the two group of students regarding their motivation to be part of an extracurricular group. However, the similarity on the lack of general motivation towards their studies, in general, is a very negative point of agreement between the two groups. A more in-depth survey has to be conducted to identify if this trend is significant among a larger group of students and the origins of this lack of motivation.

The student engagement is normally very strong and normally the participants dedicate a considerable amount of time. The next two images show some of the work developed by the students. The F-SAE team uses a manual of good practices for assembly activities that helped to save time and reducer errors in this kind of activities shown on figure 1. The Mini-Baja team developed a reconfigurable welding frame for roll-cage manufacturing, as shown on figure 2. Both were results of projects developed in class.

Figure 1: Suspension assembly F-SAE

Figure 2: Reconfigurable welding frame for the SAE Mini-Baja

Co-funded by the Erasmus+ Programme of the European Union

This paper focuses on how mentoring can help the students better integrate extracurricular activities into their regular courses and use such activities academically.

INTEGRATING THE EXTRACURRICULAR ACTIVITIES

After some research in other contexts such as presented by (Dalrymple, O.; Evangelou, D., 2006), (Kholiavko, N.; Detsiuk, T.; Tarasenko, O., 2020), (Jungert, T., 2008), (Silva de Freitas, C. C., Figueiredo, D. A., Iano, Y., 2013), (Poh-Sun S.; Pan, G., 2014), and (Khorbotly, S.; Al-Olimat, K., 2010) a decision was made to create a class in which one instructor, ideally the team faculty mentor, would closely follow the development of the proposed activity by a group of students, and they would be graded according to how the task was performed. The idea was to recognize with academic credits the hours spent on the project and recognize the time devoted by the mentor to the project and the teams.
This new class was introduced in 2014 for the SAE Mini-Baja, Formula SAE, and Aero design teams. Two instructors were assigned to the class, and on average, about 10 to 15 students enrolled each semester. Some of the main challenges that surfaced were

1. Not to curb the students initiative
2. Not to lecture the student on the projects
3. To include content that could help the whole team, not just the students enrolled

The first two points are related to the "ownership" of the project. With more than ten years of mentoring, the two instructors identified that project ownership is vital. Ownership entails full responsibility for the project decisions, which is very important for student development as an engineer. Students will not mature if they are told to follow a design or roadmap drawn by their instructors. The function of the instructors and mentors are:

- Act as a mediator when conflicts can not be sorted out by the team members.
- Guarantee ethical conduct and that the team keeps acceptable practices.
- Instruct and provide information when the team is having difficulties with any technical matter.
- Work to help the students interact with the administration to help the team benefit from the institutional resources (facilities, laboratories, other faculty, and specialists).

The third point is related to other content that can benefit the team. For instance, all projects have scrutineering events where students have to present and answer technical questions from the competition judging team. The evaluation of this class is based on presentation and written reports, basically following each competitions' guidelines. During the presentation events, the full teams are invited, and instructors limit their questions to technical matters, but there is an emphasis on the format, posture, and handling of stern questioning and criticism. The sessions are to be debated later with the teams to remind them of the lessons learned.

CLASS FORMAT AND EVALUATION

The class format is made of sessions that last one hour and forty minutes, every week, for 17 weeks. During the sessions, students present the instructors question the development of their projects. Other guest speakers are invited; for instance, one can invite a specialist in the projects' subjects under development. For instance, the two instructors are mechanical engineers, and some project demands an additional knowledge of electronics, then, to better evaluate the technical aspects of the developed hardware a faculty of electronics is invited to discuss with the students.
Non-technical subjects are also presented; for instance, one seminar that is always repeated deals with techniques to better present content in short periods, a challenge to many students.

Co-funded by the Erasmus+ Programme of the European Union

The project developed during the semester usually is not the main project developed by the teams. The focus is on the development of procedures and equipment that will be used by the team in several design cycles and will have to be passed to new team members every year. The reason for this is to improve project documentation and usability. One of the requirements is that new members may use what was developed in less time than they initially would have taken to learn the task without the project results available to the team. For instance, the SAE mini-Baja team developed a procedure to measure the resistance forces to movement based on a "coast down test" (Yasin, Y., 1978). The new members now have a document and procedure textbook on how to perform the test, calibrate the instrumentation, and format the results to obtain data useful for the vehicle design and performance evaluation. This procedure is done without the new team members having to "re-invent" the procedure.

Another example is the adjustable welding frame developed by the Formula Student team. This equipment is used to position the vehicle body tubular parts and held them in place during the chassis manufacturing. The frame can be configured according to the team's designs every year and is now in use for more than four years. Its designers have left the team after graduation, and the new team members can be trained quickly on how to use it and why it is crucial to have this frame for the correct manufacture of the tubular chassis.

The main evaluation events are the mid-term and final presentation events, and which students have twenty minutes to present their results. They must also have to write a report that is the primary document to detail what was done during the semester. Usually, other faculty or industry specialists can be invited to attend the presentation and provide feedback. However, due to academic rules, the final grade is done by the class instructors only.

RESULTS AND CONCLUSIONS

Compared to other experiences described in the literature, such as (Kholiavko, N.; Detsiuk, T.; Tarasenko, O., 2020) and (Poh-Sun S.; Pan, G., 2014), the author believes that the presented approach effectively provides the students with a recognition of their engagement to the teams. As identified in the initial survey, some students do not think the institution fully supports their project. This class was proposed to provide some institutional and academic recognition to their efforts without taking the project ownership from the students. Ownership is a crucial point for both students and mentors. This activity loses its meaning if the students only do what they are told by the instructors and have no responsibility for their project decisions. It may lead to some failures at the competitions, but the students must learn to balance risks and rewards. Learning how to make project decisions is perhaps one of the primary skills the students will learn as members of such teams. If they are directed to obey their teachers and faculty members, then the project will lose the allure that attracts most students. Feedback from the students is overall positive. They like the recognition, and another point raised is that they report that the class helps them to better know their mentors. This is a point that is raised mostly by new team members who choose to do the class to integrate on the team under closer supervision of the faculty mentor.

Co-funded by the Erasmus+ Programme of the European Union

REFERENCES

Dalrymple, O.; Evangelou, D. (2006) “The Role of Extracurricular activities in Education of Engineers”, Proceedings of the 9 th International Conference on Engineering Education, July 23 – 28, 2006, San Juan, PR

Kholiavko, N.; Detsiuk, T.; Tarasenko, O. (2020); “Extracurricular activity of engineering: Trends and Motives”, Journal of Educational Sciences & Psychology . 2020, Vol. 10 Issue 1, p62-72. 11p

Jungert, T. (2008) Opportunities of student influence as a context for the development of engineering students’ study motivation. Soc Psychol Educ 11, p. 79–94 (2008). https://doi.org/10.1007/s11218-007-9037-8

Silva de Freitas, C. C., Figueiredo, D. A., Iano, Y., (2013) “Inclusion of extracurricular activities and student competitions in the curriculum structure for engineering education: Experience based on the Brazilian reality,” *2013 International Conference on Interactive Collaborative Learning (ICL)*, Kazan, Russia, 2013, pp. 793-800, doi: 10.1109/ICL.2013.6644710.

Poh-Sun S.; Pan, G. (2014) “A Literature Review of the Impact of Extracurricular Activities Participation on Students Academic Performance”, Journal of Education for Business, 89:7, p.361-366, DOI: 10.1080/08832323.2014.912195

Khorbotly, S.; Al-Olimat, K. (2010) “Engineering student-design competition teams: Capstone or extracurricular?,” *2010 IEEE Frontiers in Education Conference (FIE)*, Washington, DC, 2010, pp. F1C-1-F1C-5, doi: 10.1109/FIE.2010.5673644.

Yasin, Y. (1978) “The Analytical Basis of Automovile Coastdown Testing”, SAE Technical Paper 780334, 1978

Co-funded by the Erasmus+ Programme of the European Union

The European Commission support for the production of this publication does not constitute an endorsement of the contents which reflects the views only of the authors, and the Commission cannot be held responsible for any use which may be made of the information contained therein. Project number: 585796-EPP-1-2017-1-AT-EPPKA2-CBHE-JP

Co-funded by the Erasmus+ Programme of the European Union

The European Commission support for the production of this publication does not constitute an endorsement of the contents which reflects the views only of the authors, and the Commission cannot be held responsible for any use which may be made of the information contained therein. Project number: 585796-EPP-1-2017-1-AT-EPPKA2-CBHE-JP

CALCULATION OF SPLASHING LOSSES IN AN SPUR GEARBOX WITH SPH-METHOD

Ermin Hujdur

University of Applied Sciences Graz,
ermin.hujdur@me.com

ABSTRACT

Most CFD simulation programs are based on a grid-based method. My bachelor's thesis, supervised by Dr. Karl Reisinger, aimed to investigate how accurate splashing losses with the grid-free SPH-Method can be predicted. The total losses are made up of power-dependent (bearing and gearing losses) and power-independent losses (bearing, seal and splashing losses). This paper will show the results of an oil flow simulation with a fully functional Renault Twizy spur gearbox and with the differential as standalone part at different speeds, temperatures and oil levels. The occurring splashing losses, caused by these three different factors were compared. The Simulations were done with the Software PreonLab by AVL, and the Smoothed-Particles-Hydrodynamics-Method. Transmission and the individual parts were designed in CATIA V5 and embedded in PreonLab. To verify and compare the simulation results, testbed measurements were done on a transmission testbed at the University of Applied Sciences.

Keywords: SPH-Method, Gearbox, PreonLab, CFD, Losses

INTRODUCTION

The reduction of losses in any part of a vehicle is the key to reduce emissions and to meet legal requirements. In the case of electric vehicles, every percentage of efficiency found through optimization is equivalent to an increase in range. This is the reason why the occurring splashing losses inside the gearbox have to be reduced. Two principal approaches to computational simulations have evolved to enable these numerical simulations. The classical Computational Fluid Dynamics (CFD) simulation methods are using an Euler approach, where the fluid and surface need to be computationally meshed to discretize the domain of interest using a grid. This approach leads often to issues in dealing with free surfaces, moving interface, deformable boundaries (Domski & Katzer 2013). Compared to a Smoothed Particle Hydrodynamics (SPH) simulation method, where a meshfree Lagrangian particle-based approach is used. This method has a greater range of use, and time expenditure is reduced significantly. Each particle carries field variables such as mass, density, velocity, acceleration, stress tensor, etc. and can move independently of each other (Zirui, et al 2017). This method was developed in the seventies and initially formulated in the field of astrophysics to simulate nonaxisymmetric phenomena (Monaghan 1992). The collective movement of these particles is similar to the movement of a fluid, so SPH was rapidly extended and applied to a vast range of applications (Zirui, et al 2017).

The aim of my work was to investigate the simulation quality and the fields of applications for PreonLab and the used SPH-Method. With the gained knowledge information should be provided about the advantages and disadvantages for future fluid simulations. The work of AVL incorporation with Schaeffler (AVL & Schaeffler, 2019) provided useful orientation.
The work was accomplished within an undergraduate research project in their third year of study (Hujdur, 2020).

Co-funded by the Erasmus+ Programme of the European Union

OBJECTIVES

In the first step, the gearbox should be disassembled, analyzed and remodeled to create a 3D-Model, which could be implemented in PreonLab. With the Model a first ProenLab simulation should be performed, to check the functionality and to preset the correct the settings, like particle size, viscosity, etc.

Next, stationary measurement points had to be defined and measurements on the transmission testbed should be performed, for validation and verification process of the simulations. A software or calculation had to be found for the bearing and sealing losses, which occur during transmission operation. At the beginning simulations and testbed trials were only done for the differential, and then for the complete gearbox.

In the last step, simulations for the gearbox were added, bearing and sealing losses were calculated, difference between testbed trials and simulations were calculated.

LITERATURE REVIEW

SPH simulation methods and PreonLab

Simulation methodologies changed product development and research tremendous. SPH simulation methods were developed in the 1970s and initially described by Gingold and Monaghan in an article for the Royal Astronomical Society in 1977 (Gingold & Monaghan 1977). Since the beginning of the development of simulation methods based on Lagrange a huge amount of time and research money went into development and improvement of SPH simulation software. PreonLab was mainly developed by Markus Ihmsen at the University of Freiburg in 2007. Since the first version Markus Ihmsen and the University of Freiburg worked until 2015 on the software and it was launched in the same year (AVL, Schaeffer 2019 & Fifty2 Technologies 2020). AVL became sales partner for the automotive sector in 2017 and developed PreonLab further (AVL, Schaeffer 2019 & Fifty2 Technologies 2020). CFD-Schuck made a comparison between a classical CFD and an SPH simulation. The accuracy and outcome of the SPH simulation was identical to a standard CFD software, but the simulation and preparation time was considerably less (CFD Schuck 2016). AVL made in cooperation with Schaeffler an oil distribution and volume flow simulation of an electrical gearbox for the ABT Audi Formula-E Team. The aim of this investigation was to increase the volume flow through the gearbox and reduce pressure loss. The PreonLab simulations showed that with an optimised inlay the volume flow can be increased by the factor six. To verify simulation results testbed measurements were made and showed similar results (AVL, Schaeffer 2019). J. Idoffson compared classical CFD and SPH simulations. The aim of the thesis was to investigate the forces that act on the vehicle during a deep-water passage and water distribution inside the air intake. Simulation results correlated well with real world water drive throughs (Idoffson 2019).

Spur gearboxes

Motor vehicles usually have an installed gear transmission, which consists of one or more gear speeds. The installed transmission transfers input speed and drive torque depending on tooth numbers and gear stages. An idealized transmission has a constant system performance, despite the changeable input speed and drive torque ratings, which means that input and output power stays identical. A real

Co-funded by the Erasmus+ Programme of the European Union

transmission is a mechanical system with gear mashes and mechanical losses. The total losses are made up of performance-independent (bearing and gearing losses) and performance-dependent losses (bearing, seal and splashing losses).

M. Hoppert dealt with gear drives and their efficiency behavior. The optimization of the axles and the improvement of the efficiency of drive trains with inline engines or all-wheel drives was his major topic (Hoppert 2015).
B. Höhn, K. Michaelis, M. Hinterstoisser investigated spur gearboxes and their efficiency at different temperatures and viscosities. They dealt with different methods to reduce power loss within a gearbox. Especially they investigated the occurring losses at low temperatures, by variation of oil immersion depth of the teeth and part load conditions. As well they dealed with the occurring cooling issues by using oil with low viscosity (Höhn, Miachelis, Hinterstoisser 2009).

J. Broušek and T. Zvolsky investigated in their paper the overall efficiency of an electric vehicle gearbox at different input torques and input speeds with different oil levels. The result of their study is that the overall efficiency at 500 g oil level is over 99 % at some input speeds but at high speeds and low input torques the efficiency drops down to 60 % to 70 %. Compared to the measurements with over 800 g of oil in the gearbox housing the efficiency drops by 3 %.

METHODOLOGY

In this chapter the used methods, required steps for a simulation with PreonLab and the basics for the calculation of the equivalent power losses will be covered.

Modelling of gearbox

The specified gearbox has to be generated as a CAD model for implementation in the PreonLab simulation software. The Renault Twizy gearbox from Figure 1 is manufactured by Comex S.P.A. and has a gear ratio of 8,470:1. Despite the fact that we have so scale the gears a good CAD-Design reduces the workload to implement it into PreonLab. It consists of an input shaft, intermediate shaft and a differential, like shown in Figure 2 and Figure 3. The gearbox was disassembled, and each part was measured to ensure the most accurate possible modeling of the individual components, except the upper and lower cover which was 3D-scanned.

Figure 1: Renault Twizy Gearbox, Manufacturer Comex (Comex 2020)

Co-funded by the Erasmus+ Programme of the European Union

Figure 2: Renault Twizy Gearbox without upper cover

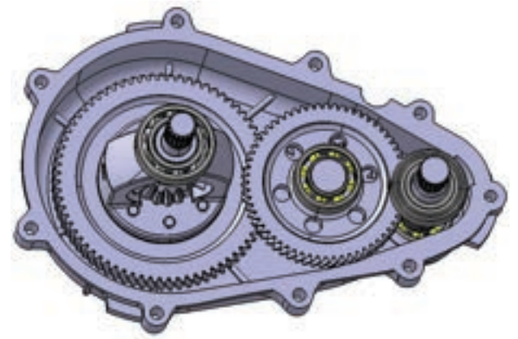

Figure 3: Renault Twizy Gearbox without upper cover as CAD-Model

SPH-Method and Fluid simulation in PreonLab

SPH was initially formulated in the field of astrophysics to simulate nonaxisymmetric phenomena. Due to its stability and predictability, it was later extended to model fluid flows. It is a purely Lagrangian method where the fluid volume is represented by a set of particles.
In order to derive the governing equations of the SPH formulation the Navier-Stokes equations are written on Lagrangian form. The equations are written here on incompressible form and can be expressed as

$$\rho\frac{\mathrm{d}\vec{u}}{\mathrm{d}t} = -\vec{\nabla}p + \eta\vec{\nabla}^2\vec{v} + \rho\vec{g}.$$

On the left hand side the time derivative of the particle velocity is given. On the right hand side the pressure gradient, viscous diffusion and a body force are given.

Simulation algorithm in PreonLab
The purpose of the PreonLab-Solver is the time dependent calculation of liquid. At first PreonLab calculates the intermediate velocity field according to the Navier-Stokes equation, apart from the pressure term. Calculation of the velocity term with

$$\vec{v_i^*} = \vec{v_i} + \Delta t(\frac{\nabla \cdot \tau_i}{\rho_i}) + \nabla\phi_i + \vec{f_i^b}.$$

In this equation, the left hand side indicates the new velocity of the particle, based on the right hand side consisting of the previous velocity, viscosity term, surface tension and external forces.

Co-funded by the Erasmus+ Programme of the European Union

The pressure field is defined by

$$\nabla^2 p_i = \frac{\rho_{i,0} - \rho_i^*}{\Delta t^2},$$

The pressure field is then determined to meet the incompressibility condition. ρi,0 is the density of particle i at rest, ρ*i is the predicted density based on the momentary density ρi.
The predicted density is calculated as follows

$$\rho_i^* = \rho_i - \Delta t \rho_i \nabla \cdot (\vec{v_i^*}).$$

Once the speed and pressure fields have been determined, the speed and position of each particle can be determined

$$\vec{v}_{i,t+\Delta t} = \vec{v_i^*} - \Delta t(\frac{\nabla p_i}{\rho_i}),$$

$$\vec{x}_{i,t+\Delta t} = \vec{x_i} + \Delta t \vec{v}_{i,t+\Delta t}.$$

In Figure 4 and Figure 5 an fluid at rest and at movement is visualized. During halt the calculations of the velocity and position are done fast, but once the fluid and the particles move the calculation time increases rapidly.

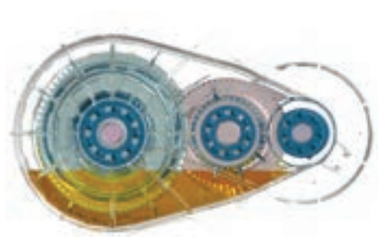

Figure 4: Fluid at halt

Figure 5: Fluid at movement

Testbed setup

The test item was put on the testbed, as in Figure 12, and measured at different speeds, levels and temperatures. Since the differential has a low locking effect, the differential was locked 100 %, this means that there is no speed difference between the left and right gear output

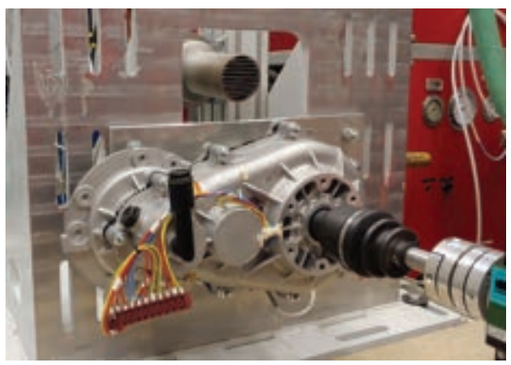

Figure 6: Testbed setup

Co-funded by the Erasmus+ Programme of the European Union

The European Commission support for the production of this publication does not constitute an endorsement of the contents which reflects the views only of the authors, and the Commission cannot be held responsible for any use which may be made of the information contained therein. Project number: 585796-EPP-1-2017-1-AT-EPPKA2-CBHE-JP

The gearbox output on the right is used to initiate the speed, which means that the required output speed can be specified and measured at the same time without converting it using the gear ratio. The filling level can be varied using the oil drain plug below. The oil bath was brought to the required temperature level by passive heating.

Calculation of bearing and sealing losses

The bearing losses were calculated using the SKF online bearing calculator and the forces and moments obtained from the simulation. The bearing lubrication for the SKF online bearing calculator was based on the simulation model, which means that the bearings are only lubricated using the oil that is swirled up in the housing.

The gearbox has one radial shaft seal on the input shaft and one radial shaft seal on each of the two differential outputs. The losses in the radial shaft seals were calculated using Engelke's method and based on Hofer's 2017 bachelor thesis (Hofer 2017). A more precise analysis was not possible due to lack of time. Therefore, the respective parameters were accepted based on experience. The parameters to be varied are summarized in Table 1

Radial force F_N in N/m	Sealing width *b* in mm	Lubrication height *h* in mm	Coefficient of Friction μ	Temperature-coefficient λ in K/(W/mm2)
11,2	0,2	0,00146	0,3	16,5

Table 1: Influencing parameters for sealings

Due to the temperature dependency of the oil viscosity the sealing losses vary. The speed and viscosity dependent power losses at the sealing rings are summarized in Table 2 and Table 3.

Temperature in °C	Shaft losses at 30 km/h in W	Shaft losses at 50 km/h in W	Shaft losses at 80 km/h in W	Shaft losses at 140 km/h in W
30	1,621	2,790	4,515	7,711
50	1,476	2,549	4,155	7,257
80	1,385	2,366	3,870	6,861

Table 2: Power loss of radial shaft seal of the input shaft

Temperature in °C	Shaft losses at 30 km/h in W	Shaft losses at 50 km/h in W	Shaft losses at 80 km/h in W	Shaft losses at 140 km/h in W
30	1,071	1,816	2,974	5,395
50	1,052	1,769	2,873	5,131
80	1,046	1,748	2,814	4,969

Table 3: Power loss of radial shaft seal of the output shafts

Co-funded by the Erasmus+ Programme of the European Union

The European Commission support for the production of this publication does not constitute an endorsement of the contents which reflects the views only of the authors, and the Commission cannot be held responsible for any use which may be made of the information contained therein. Project number: 585796-EPP-1-2017-1-AT-EPPKA2-CBHE-JP

RESULTS

The calculated, simulated and measured gearbox and differential overall losses are shown in the figures and tables below. The results in this chapter are shown for one temperature or at one output speed. For the differential as standalone 24 different testcases were simulated and measured at the testbed. The gearbox was only simulated for 3 different temperature at one speed but measured also at 24 testcases. Output speeds and oil temperatures are based on real driving conditions. The gearbox and differential were simulated with two different oil levels, the manufacturer's oil level of 600 ml and 300 ml for comparison purposes. The testcases in Table 1 were simulated for the gearbox and differential as standalone.

Velocity in km/h	Temperature in °C	Oil level in ml
50	30	300
50	50	300
50	80	300
50	30	600
50	50	600
50	80	600

Table 4: Testcases for constant speed

Losses for differential at constant temperature

First, a comparison between test bench and the simulation at constant temperature and then at constant speed is made. The composition of the respective power loss is also described. The differential at an oil temperature of 30 ° C is used as an illustration for the composition of the total power loss. The power losses of the simulation, including bearing and seal losses, reflect reality well regardless of the filling volume, which is shown in Figure 1. The power loss on the testbed and the total power loss calculated with the simulation results increases approximately linearly over the speed range.

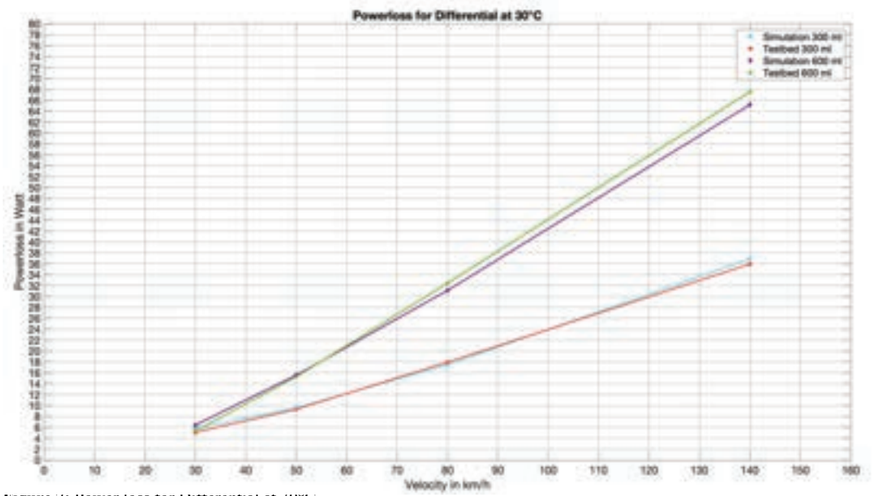

Figure 7: Power loss for Differential at 30°C

Co-funded by the Erasmus+ Programme of the European Union
The European Commission support for the production of this publication does not constitute an endorsement of the contents which reflects the views only of the authors, and the Commission cannot be held responsible for any use which may be made of the information contained therein. Project number: 585796-EPP-1-2017-1-AT-EPPKA2-CBHE-JP

The main cause for the total power loss is primarily the bearings, followed by the splashing losses and the losses in radial shaft sealing rings, as summarized in Table 2. The simulation quality is independent of speed. The relatively large difference, which is shown in Table 3, at 140 km/h and 600 ml filling level could be remedied with a smaller particle diameter. Due to the smaller diameter, more particles can intervene in the tooth flanks and apply a higher force or higher torque to the gear wheel. The causes and power distributions mentioned above are also valid at 50°C and 80°C.

Velocity in km/h	Oil level in ml	Losses Bearings in W	Losses Sealing in W	Losses Splashing in W
30	300	5,847	5,089	+0,758
50	300	9,584	9,320	+0,264
80	300	17,478	17,953	-0,475
140	300	36,875	35,943	+0,932
30	600	6,423	5,369	+1,054
50	600	15,563	15,281	+0,282
80	600	31,099	32,434	-1,335
140	600	65,167	67,542	-2,375

Table 6: Power loss comparison between simulation and testbed, differential at 30°C

Losses for differential at constant temperature

The simulation and test bench results can be seen in Figure 2. The differential at a speed of 50 km/h is used to illustrate the composition of the total power loss. By displaying the power loss as a function of the temperature and its viscosity, the choice of oil has less of an influence on the losses than the speed.

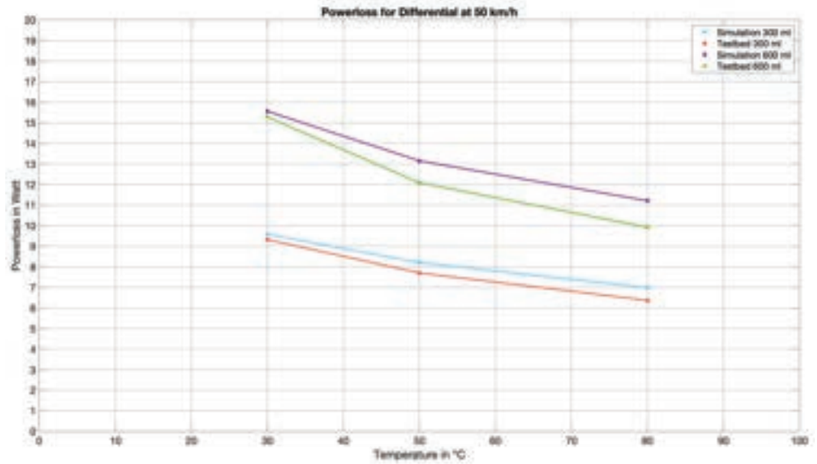

Figure 8: Power loss for Differential at 50 km/h

The main reason for the losses are the bearing losses, which are shown in Table 4. The simulated and calculated losses are in the middle 0,750 W higher than the measured power losses, like shown in Table 5.

Co-funded by the Erasmus+ Programme of the European Union
The European Commission support for the production of this publication does not constitute an endorsement of the contents which reflects the views only of the authors, and the Commission cannot be held responsible for any use which may be made of the information contained therein. Project number: 585796-EPP-1-2017-1-AT-EPPKA2-CBHE-JP

Temperature in °C	Oil level in ml	Losses Bearings in W	Losses Sealing in W	Losses Splashing in W
30	300	6,000	1,817	1,767
50	300	5,000	1,770	1,434
80	300	4,000	1,749	1,235
30	600	3,000	1,817	3,814
50	600	6,000	1,770	3,519
80	600	35,000	1,749	2,967

Table 7: Power losses caused by bearings, seals and splashing, differential at 50 km/h

Temperature in °C	Oil level in ml	Losses Simulation in W	Losses Testbed in W	Losses Difference in W
30	300	9,584	9,320	+0,264
50	300	8,204	7,704	+0,500
80	300	6,984	6,368	+0,615
30	600	4,990	3,923	+1,067
50	600	11,211	9,992	+1,218
80	600	55,442	54,597	+0,845

Table 8: Power loss comparison between simulation and testbed, differential at 50 km/h

Losses for differential at constant temperature

Due to the limited computing capacity, simulations for the complete gearbox could only be carried out at 50 km/h, which is why a direct comparison of the power losses at constant temperature is not possible. The measured power loss of the complete gearbox at 30°C in Figure 3 is used as an illustration. In case of a complete transmission, it can be seen that at 30°C, 50°C and 80°C the power loss increases more sharply in the range from 80 km/h to 140 km/h. This could be related to the basic design of the transmission, because according to Comex, the manufacturer of the transmission, the transmission is designed for a maximum input speed of 7000 revolutions per minute. With the known gear ratio and an output speed of 1400 revolutions per minute, 140 km/h, this results in an input speed of approximately 11000 revolutions per minute. The increase, in the range from 80 km/h to 140 km/h, at a level of 300 ml is also present there, but less pronounced than at a 600 ml oil level, which can be seen in Table 6.

Co-funded by the Erasmus+ Programme of the European Union

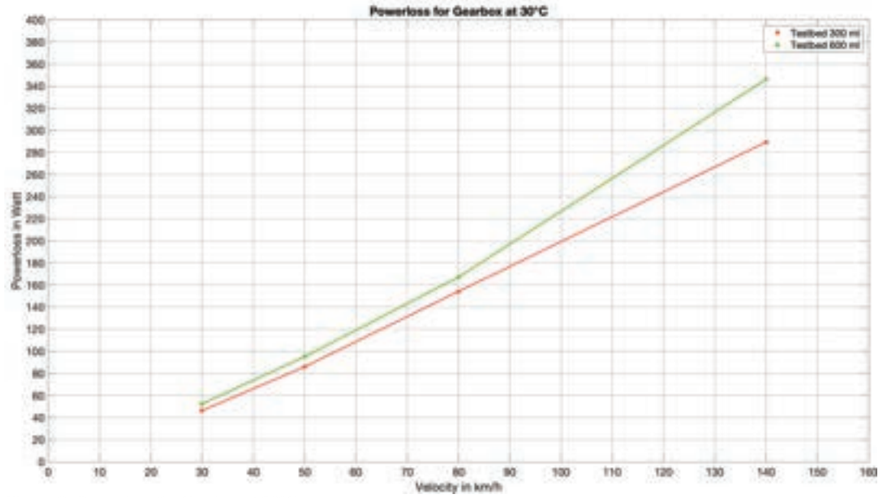

Figure 9: Power loss for Gearbox at 30°C

Velocity in km/h	Oil level in ml	Losses Testbed in W
30	300	46,315
50	300	85,891
80	300	154,122
140	300	289,278
30	600	52,391
50	600	95,047
80	600	167,071
140	600	346,199

Table 9: Power loss on testbed, gearbox at 30°C

Losses for differential at constant temperature

Like mentioned due to the limited calculation capacity a comparison between simulation and measured results can only be made for 50 km/h. Figure 4 shows the power loss from the entire transmission. In both the diagram and in Table 8 that there is a large discrepancy between the testbed and the simulation. This relatively large difference has two primary causes, partly the particle shrinkage is over 0,1 % and PreonLab cannot measure external forces and moments (Fifty2 Technologies 2020). This point is not addressed in the publications of AVL and Schuck, as their tasks primarily focus on optimizing the flow course (AVL & Schaffler 2019). The simulation would have to be repeated with a smaller particle diameter in order to achieve a better simulation quality. Due to the increased particle shrinkage, the calculated bearing losses from Table 7 must also be questioned, as they were determined using the forces and moments exported from PreonLab. The complete transmission was measured on the testbed without transmission oil, which results in the pure bearing and toothing losses in the transmission.

Co-funded by the Erasmus+ Programme of the European Union

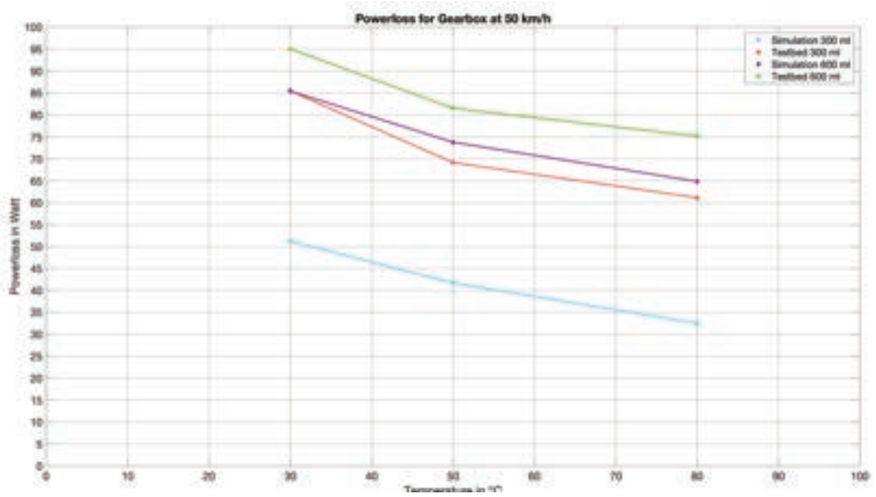

Figure 10: Power loss for Gearbox at 50 km/h

Temperature in °C	Oil level in ml	Losses Bearings in W	Losses Sealing in W	Losses Splashing in W
30	300	45,000	4,608	1,612
50	300	4,320	1,374	1,374
80	300	27,000	4,115	1,358
30	600	73,000	4,608	7,826
50	600	61,000	4,320	8,482
80	600	48,000	4,115	12,735

Table 10: Power losses caused by bearings, seals and splashing, gearbox at 50 km/h

Temperature in °C	Oil level in ml	Losses Simulation in W	Losses Testbed in W	Losses Difference in W
30	300	51,220	85,891	−34,250
50	300	40,693	69,162	−28,469
80	300	32,474	60,579	−28,669
30	600	85,434	95,047	−9,613
50	600	73,801	81,535	−7,733
80	600	64,851	75,171	−10,321

Table 11: Power loss comparison between simulation and testbed, gearbox at 50 km/h

Co-funded by the Erasmus+ Programme of the European Union

CONCLUSION

In this paper the use of SPH and more specifically PreonLab is investigated in order to determine its usefulness as a simulation tool for oil flow distribution and as base for calculation of splashing losses. The main advantage of the SPH is that the computational domain is discretized with particles without a fixed connectivity and discretization. The refinement of the particles is also much easier to perform than the mesh refinement.
The paper sums the oil flow distribution and occurring forces based on a Renault Twizy gearbox and its differential as standalone part up and compares them with testbed measurements at different speeds, temperatures and oil levels. Simulation quality for the differential as standalone part is promising, but quality of the spur gearbox in assembly is not satisfying.

The discrepancy between simulation and measurements for the spur gearbox have to be investigated further with smaller particles. Furthermore, the performance and reliability of the simulations can be also improved with more CPU kernels and an optimized simulation setup. Especially the gear intersection between the gears and rotation of bearings can help to improve simulation quality and reduce discrepancy between testbed trials and simulations. Finally, the received simulation data can be used to make an easier decision, which simulation method should be used for future projects.

RECOMMENDATIONS

When simulating the complete transmission, there is a large discrepancy due to the particle diameter being too large and the lack of possibility to measure the gear losses. The influence of the particle diameter and the particle shrinkage have to be investigated further. In conclusion, it can be said that PreonLab is not completely suitable for simulating a complete gear unit or gearbox and their occurring losses. Nevertheless, it should be considered for simulating individual gears and differentials, displaying flow curves and optimizing housings and shielding plates.

Co-funded by the Erasmus+ Programme of the European Union

REFERENCES

Domski, J. & Katzer, J. (2013). *Load-deflection characteristic of fibre concrete based on waste ceramic aggregate*

Zirui, M., et al. (2017). *A Comprehensive study on the parameters setting in smoothed particle hydrodynamics (SPH) method applied to hydrodynamics problems*

Hujdur, E. (2020). *Berechnung der Planschverluste in einem Stirnradgetriebe mittels SPH-Methode.* Bachelor's thesis. Institute of Automotive Engineering, Joanneum University of Applied Sciences, Graz

Monaghan, J. (1992). *Smoothed Particle Hydrodynamics.* Annu. Rev. Anstron. Anstrophys 30

Dashtimanesh, A. & Ghadami, P. (2013). *Simulation of Free Surface Flow by Using SPH Method and a Comparison Study on Two Different Smoothing Functions*

Gingold, R. & Monaghan, J. (1977). *Smoothed particle hydrodynamics: theory and application to non-spherical stars.* Monthly Notices Royal Astronomical Society.

AVL & Schaeffler. (2019). *Simulationsbasierte Entwicklung der funktionsgerechten Ölverteilung in elektrischen Achssystemen.* Technical Report

Fifty2Technologies. (2020). Retrieved February 10, 2020, from https://www.fifty2.eu/about-us/ (2020).

Schuck. (2016). *Aktuelles Über CFD-Schuck*. In Infobrief 4/2016. Retrieved May 15, 2020, from https://www.cfd-schuck.de/fileadmin/user_upload/ Downloads/CFD-Schuck_infobrief_4_2016.pdf

Idoffson, J. (2019). *Wading – Evaluation of SPH-based simulations versus traditional Finite Volume CFD.* Master's thesis. Chalmers University of Technology. Goteborg

Hoppert, M. (2015). *Analytische und experimentelle Untersuchungen zum Wirkungsgradverhalten von Achsgetrieben.* PhD-Thesis. Technical University Ilmenau

Höhn, B., Michaelis, K., Hinterstoisser M. (2009). *Optimization of Gearbox Efficiency.* Research Paper. ISSN: 0350-350X.

Broušek, J. & Zvolsky, T. (2018). *Experimental study of electric vehicle gearbox efficiency.* Research paper. Technical University of Liberec.

Comex S.p.A. *Differential Gearboxes*. Retrieved June 13, 2020, from https://www.comexspa.com/index.php/en/products/item/38-differential-gearboxes&catid=23:differential-gearboxes

Hofer, S. (2017) *Reibmoment von Radialwellendichtringen*. Technical Calculation. Joanneum University of Applied Sciences, Graz

Co-funded by the Erasmus+ Programme of the European Union

DESIGN, FABRICATION AND PROJECT WORKFLOW OF LOW-COST IMPACT ATTENUATOR FOR FORMULA SAE CAR

Dr.Ing. Fernando Augusto de Noronha Castro Pinto[1],
João Victor da Cruz Almeida[2], Clara Roussenq Daibert[3],
Matheus Belo de Lima[4], Marcus Vinicius Filgueiras Silva[5]

[1] Dr. Ing. Professor, Mechanical Engineering, Escola Politécnica, UFRJ, fcpinto@poli.ufrj.br
[2]Student, Mechanical Engineering, Escola Politécnica, UFRJ, j.victoralmeida@poli.ufrj.br
[3]Student, Mechanical Engineering, Escola Politécnica, UFRJ, claradaibert@poli.ufrj.br
[4]Student, Mechanical Engineering, Escola Politécnica, UFRJ, mbelo18@poli.ufrj.br
[5]Student, Metallurgical Engineering, Escola Politécnica, UFRJ, marcusfilgueiras@poli.ufrj.br

ABSTRACT

The automotive industry is constantly investing in research and development of safety devices capable of actively or passively protecting the driver and passengers of crash related injuries. The impact attenuator is a key device of the safety pack items in production and race cars. This component is purposely designed to absorb the impact energy by progressive plastic deformation, diminishing the deceleration relative to a direct impact. Research and design have advanced in the passive and active safety items to reinforce and secure safety for humans interacting with the vehicle, causing costs for high end carbon fiber or foam impact attenuator to be common in FSAE use globally. But the financial and logistical cost of impact attenuators made of off these materials remains a problem for the majority of FSAE teams in countries like Brazil or India. This paper aims to design and manufacture a cost-effective, lightweight, easy to manufacture FSAE type impact attenuator made of widely available materials (low-cost aluminum alloys). The design was made on Solidworks 2020, and the dynamic explicit crash test simulations were performed on Abaqus v.14. The project workflow and optimization relied on a series of factors: comparative study of aluminum alloy crash test performance, plastic and elastic energy absorption, safety factor, front bulkhead deformation, peak deceleration and mass. The experimental drop test was delayed due to the pandemic and will be performed in the following months in the laboratory. The project requirements used were set accordingly with the 2020 Formula SAE rules. Thus, creating a device and project workflow that tackles logistical, performance and cost issues for the majority of Brazilian FSAE teams.

Keywords: Drop Test Analysis, Low-Cost Impact attenuator, Formula SAE, Project Workflow, Crash Test Analysis.

Co-funded by the Erasmus+ Programme of the European Union

1. INTRODUCTION

The development of impact attenuators for Formula SAE has encompassed different types of geometry and materials throughout the recent years, promoting technological advancements relating to the knowledge surrounding the device, how to design, simulate, and validate the attenuator in different configurations. The main kinds of attenuators are based, generally speaking, on carbon fiber nosecones, polymeric foam, or aluminum (usually in a honeycomb structure). Teams all around the world make use of these kinds of attenuators. However, teams that haven't established themselves in the competitive sphere or that haven't gotten financial support from sponsoring organizations have difficulty in adopting the solutions previously mentioned. This is especially true in countries like Brazil and India, where high importation costs and device logistics elevate project costs.

To address these challenges, the aspects that guided the development of the project were: cost, material availability, manufacturing complexity, and safety margins required by FSAE.

The impact attenuators are built according to the following considerations: it must reduce the initial impacts force, redistributing it through its deformation and gradual energy transfer to the structure; it must bring down the deceleration of the vehicle to acceptable levels, minimizing damages to the passenger and to the vehicle itself; in constructing aspects, it must be built with the development of the impact and the deformation of the device and adjacent structural items in mind; as well as the consideration of the mass of the attenuator and its dimensions, which affect other areas of the car, as in the aerodynamic set.

The structural part of the chassis where the impact attenuator is mounted is the front bulkhead, where the anti-intrusion plate is also mounted. According to the competition rules (Formula SAE, 2020), the front bulkhead and anti-intrusion plate set can't permanently deform more than 25mm into the cockpit along the length of the car, besides the functional, dimensional, and building rules that the attenuator must follow.

The computer simulation models of the attenuator are usually made with one of these two methods: explicit dynamic or static. Since other components involved in a Formula SAE car project are usually simulated using the static method, students prefer to submit the impact attenuator prototype to this kind of simulation. However, this component suffers impact forces, in other words, dynamic forces, as opposed to the other parts of the vehicle. Consequently, the most fitting type of simulation to observe the behavior of the attenuator in an impact situation is the explicit dynamic, which allows the student to understand the crushing mechanisms and prototype deformation, and optimize it according to their objectives and observations.

The validation can be made in two different ways: dynamic or quasi-static. The quasi-static test is the most chosen among Brazilian team, due to its high availability and low cost, although this test is not representative of an impact scenario. For this reason, a dynamic test was chosen for the validation.

Co-funded by the Erasmus+ Programme of the European Union

2. OBJETIVES

Based on observations made of the Brazilian teams, it is notable that few have developed a process for the construction and optimization of the impact attenuator, this causes them to utilize commercially available devices, which perpetuates this internal cycle of inexperience in constructing this device that is present in these teams. This cycle encompasses problems in many other parts of the project, such as: initial definitions and evaluations of a project; important factors for prototype optimization; data and observations made in computer simulations for project decision making and analysis; material definition; definition of security margins for the device, etc. Taking these factors into account, this project's main objectives are:

To present a low-cost impact attenuator that follows the current FSAE rules, made with widely available materials, that positively impacts the items adjacent to the impact attenuator regarding simplicity, manufacture time, and mass and performance.

To establish methods and organize a work logic for the design and construction of the device, serving as a guide for teams that seek an impact attenuator that follows the rules, is safe, easy to build, cheap, and with high efficiency in absorbing impact.

3. LITERATURE REVIEW

The FSAE rulebook (Formula SAE, 2020), establishes the rules that this project must meet, being it dimensional rules, material specification rules, functional requirements and assembly rules.

The dimensional requirements state that the impact attenuator must have at least 200 mm width and 100 mm height at the 200 mm mark orthogonally to the front bulkhead. The assembly requirements state that the attenuator must be mounted on a anti intrusion plate made of SAE 1020 steel with a minimum thickness of 1,5 mm.

According to the functional requirements of the impact attenuator and anti-intrusion plate, experimental testing must be performed to prove that: the impact attenuator absorbs at least 7350 J; the peak deceleration value is below 40 g; the average deceleration value is below 20 g; the anti-intrusion plate does not permanently deflect more than 25 mm inwards to the cockpit.

In his work, Pereira (2013) developed a method to perform the validation of an impact attenuator made of PVC Divinycell H60 foam via a scaled-down drop test, that served as a method to validate the FE simulations of real size prototypes, describing the processes of preparation, execution and data processing regarding the drop test. The drop test is triggered by a quick release mechanism, controlled manually with the use of tubes and steel cables.

According to Belingardi and Obradovic (2010), holes positioned along the attenuator act in ways to optimize the crush patterns, energy absorption and deceleration. These optimizations are due to changes based on the observation of the FE dynamic simulations and its generated data. The impact evolution was observed and comparatively analyzed between non-modified models and modified models, as well as the kinetic energy, velocity and acceleration diagrams.

It was observed that the preferential crush pattern of a hollow impact attenuator under an impact situation is to buckle in ways of generating folds, according to Boria (2010). To optimize the crush

Co-funded by the Erasmus+ Programme of the European Union

behavior of the component, it must have elements to trigger localized buckling and folding. In her work, the FE simulation modelling consists of a crash mass of 300 kg, the impact attenuator is fixed to a barrier which is retrained in all degrees of freedom. The experimental validation was performed using a drop test with a drop mass of 300 kg, released from a height of 2,5 m by a hydraulic actuator and guided to the attenuator by guides, elevating the safety measures of the experiment.

An aluminum shell and grid type of impact attenuator tested under a drop-test was proposed by D. Kumar, S. Kumar, Singh, Khanna. (2012) using commercially available and highly weldable material.

4. METHODOLOGY

4.1. Project Workflow

The development of the project encountered many problems as it unfolded. These challenges were mainly logistics or cost-related and consumed a precious amount of time, which is a rare resource for FSAE teams. The aim of this project workflow is to illustrate each and every major step of the development of the impact attenuator.

At the beginning of the project (Figure1), the available information surrounding the previous impact attenuator project of the Minerva ERacing team was gathered. This served as a benchmark in performance, design, cost, and feedback from previous team members and competition judges.
The “Model Concept” was composed of a “minimum viable product” (MVP) for the attenuator, which strictly followed the FSAE Rulebook. Later in this stage, a series of desirable features were described for further optimization processing of CAD and CAE setups. This “MVP” model was then designed using Solidworks and then simulated using Abaqus for material selection and model optimization (Figure1).

The optimization process is led by a specific set of problems surrounding the following issues: logistics, dimensions and mass, overall cost, difficulties in manufacturing, and performance. Performance, in terms of an impact attenuator, is comprised of a safety margin of operation, permanent deformation of structural items, average and peak deceleration, and total absorbed energy. The optimization was effectively achieved through a series of cycles of these steps.
Once the issues are identified, objectives and goals were set for the cycle, and a new model was designed, having all of the past models’ mistakes, issues, and failures on the many aspects regarding it (CAD, CAE, dimensions, mounting, etc) taken into account. The CAD is then checked accordingly to the FSAE Rulebook, team chassis, and aerodynamics projects. FE simulation is performed in the CAE model following a series of setups, designed for time efficiency, performance optimization, data collection, and defect or failure prediction.
After the model development is done, the observations and results of the data collected during the previous stage of different models are put in comparison through a decision matrix and the final model is chosen.

Then, a down-sized attenuator is designed and simulated using the same FE simulation modelling used in the true-to-size sample. After the simulation results, the down-sized impact attenuator is manufactured and the drop test is performed. As the results of deceleration and absorbed energy from the drop test and FE simulation are obtained, they are then compared to validate the simulation model. The validation of the simulation model of the scaled-down version means that the simulation model is validated, thus the impact attenuator is validated. Then, the true-to-size impact attenuator is manufactured and the project is completed.

Co-funded by the Erasmus+ Programme of the European Union

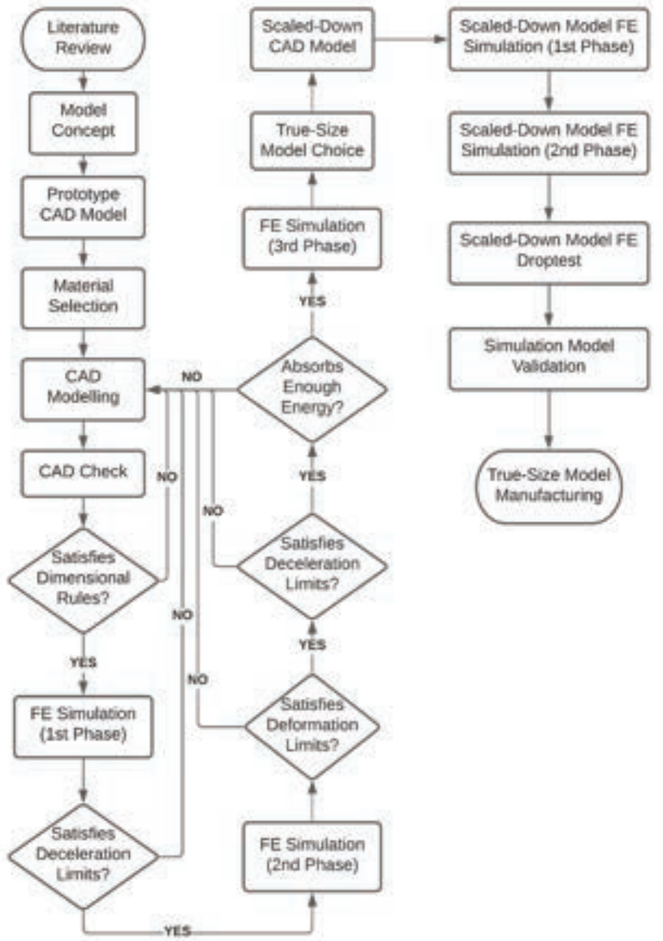

Figure 1: Project Flowchart

4.2. Design

The impact attenuator design is based of five features: FSAE rules attendance; reduced costs of manufacture; simple manufacturing; mass reduction; and performance. The aluminum is the main material for the device and, due to its availability in the university laboratory, another material which is considered for the project is the PVC DivinyCell H60 foam.

For CAD assembly checks and FE simulations reasons, the anti-intrusion plate and a simplified version of the Minerva ERacing car’s front bulkhead are designed, as seen in the Figure 2 and Figure 3, respectively. Despite the energy absorption and the gradual impact deceleration capabilities of the impact attenuator, it is crucial to note that even when the attenuator is in attendance of the functional requirements of energy absorption and deceleration, it may fail under impact loading, provoking an excessive deformation on the anti-intrusion plate and front bulkhead, as seen in Figure 4, putting the integrity of the car and its passengers at risk.

Co-funded by the Erasmus+ Programme of the European Union

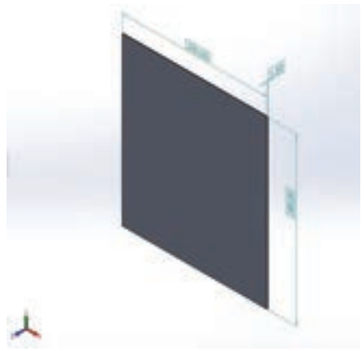

Figure 2: Anti-Intrusion Plate

Figure 3: Front Bulkhead

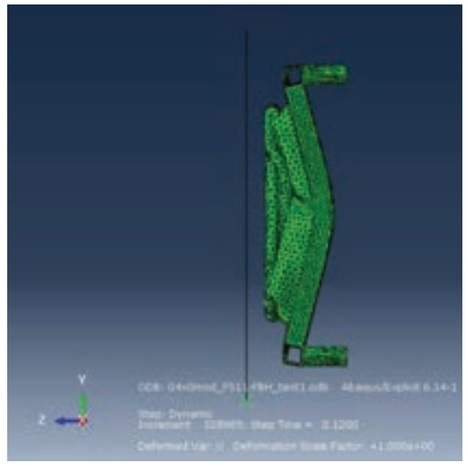

Figure 4: Excessive Deformation of Anti-intrusion Plate and Front Bulkhead

Parting from issues observed in the UFRJ FSAE teams impact attenuators, four concepts of impact attenuators are modeled. The G1 (Fig.5) and G2 (Fig.6) concepts are based on past years' Minerva ERacing and Icarus impact attenuators, utilizing aluminum and PVC foam. The G3 (Fig.7) and G4 (Fig.8) concepts are based on models made of aluminum sheets, like the ones presented in the works of Kumar et al (2012) and Belingardi and Obradovic (2010).

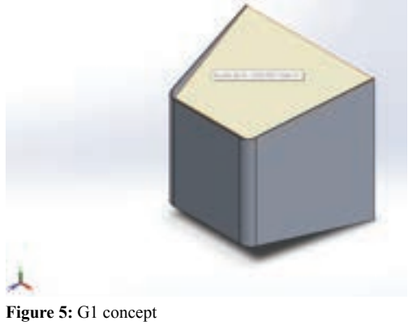

Figure 5: G1 concept

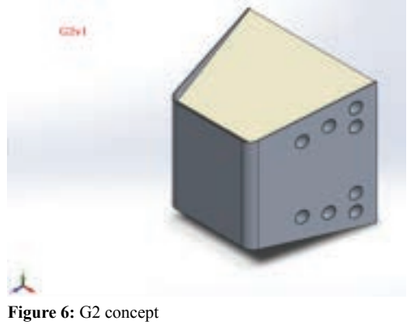

Figure 6: G2 concept

Co-funded by the Erasmus+ Programme of the European Union

The European Commission support for the production of this publication does not constitute an endorsement of the contents which reflects the views only of the authors, and the Commission cannot be held responsible for any use which may be made of the information contained therein. Project number: 585796-EPP-1-2017-1-AT-EPPKA2-CBHE-JP

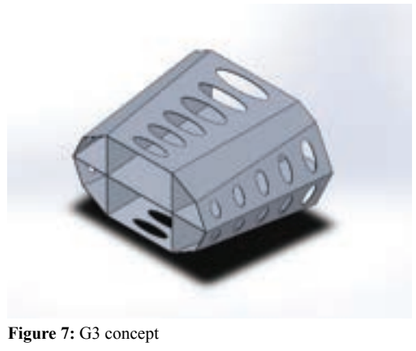

Figure 7: G3 concept

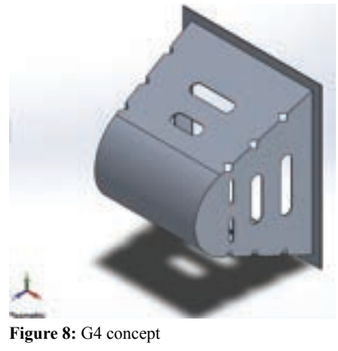

Figure 8: G4 concept

Using a feedback loop between the stages of design and FE simulation, optimizations are made that consist in changes of dimensions, addition of holes or details to trigger a crush pattern that does not build highly rigid topology as it crumbles, as this causes peaks in deceleration and anti-intrusion plate deformation, as seen in Figure 9.

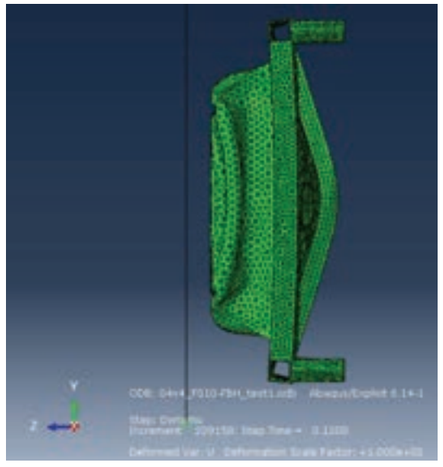

Figure 9: Rigid topology related deformation

After dozens of iterations submitted to the design and FE simulation optimizations, the thirteenth version of the G4 concept (Fig.10) is chosen. This impact attenuator consists of 2 mm thick 5052-H34 aluminum welded plates, with holes to trigger desirable crush behavior during the impact.

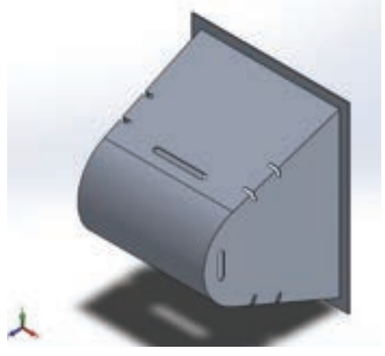

Figure 10: G4v13 model

Co-funded by the Erasmus+ Programme of the European Union

The European Commission support for the production of this publication does not constitute an endorsement of the contents which reflects the views only of the authors, and the Commission cannot be held responsible for any use which may be made of the information contained therein. Project number: 585796-EPP-1-2017-1-AT-EPPKA2-CBHE-JP

4.3. Material Selection Criteria

There are some materials that are commonly used for the construction of the Formula SAE impact attenuators, carbon fiber nosecones and polymeric foams are some of them. But the one that stands out is aluminum, due to its mechanical characteristics, reduced cost, easy manipulation, lightness in weight and availability.

Some aluminum alloys are tested comparatively in the first phase of the FE simulations to check for compatibility with the rules established by SAE. After some simulations and study of their application, there are three materials being considered, which are 6063-T4, 5052-O, and 5052-H34. However, due to the availability of sheet-shaped alloys, the list of some materials has been reduced to just one aluminum alloy that would be the 5052-H34, popularly known as naval aluminum, commercially and openly available and consequently cheaper than the other options.

COMPARATIVE TABLE OF MATERIALS		
Material	**Average Deceleration G)**	**Peak Deceleration (G)**
6063-T4	10,71	36,03
5052-O	9,31	32,71
5052-H34	11,75	23,33

Table 1: Comparative Table of Materials

Among the initially chosen alloys, the most important properties are the ability to deform elastically and plastically, in this particular case, the elastic regime being smaller, and the plastic regime being larger. An analysis of the simulations shows that higher yield limits tend to generate a higher maximum deceleration, which goes against the rules.

The material cost is of great importance to the project, as the reduction of the total cost of the project is the main motivation for the development of this project. As was said at the beginning of this section, the availability of this material is high, making the material have a cost of approximately US$122 for a plate of 2000 x 1000 x 2 mm. With a plate of these dimensions, it is possible to produce up to 4 impact attenuators. For reference, the cost of a standard SAE attenuator is €360 (Formula Seven, n.d.), approximately US$430 (not including the cost of shipping and taxes related to importation).

4.4 Simulation Setup

The prototype simulation methods are designed in specific ways in order to save time and obtain conclusive data. These data are not restricted to the impact attenuator characteristics and behavior in an isolated manner, but also how it behaves when it is assembled on the anti-intrusion plate and front bulkhead and what kind of damages are made in these components during the impact. To explore these features the FE simulations are divided in three phases, all of them are dynamic explicit.

In the first phase (Fig. 11) the attenuator base is restricted in all degrees of freedom, and an analytic rigid wall with an inertial mass of 300 kg is restricted in five degrees of freedom, being free to dislocate only in the direction of the collision. The wall has a constant initial speed of 7 m/s. In this

Co-funded by the Erasmus+ Programme of the European Union

The European Commission support for the production of this publication does not constitute an endorsement of the contents which reflects the views only of the authors, and the Commission cannot be held responsible for any use which may be made of the information contained therein. Project number: 585796-EPP-1-2017-1-AT-EPPKA2-CBHE-JP

phase the prototypes that don't fit the parameters of peak and average deceleration are discarded. Those that have values of deceleration below the limits established by the rules are taken to the next phase.

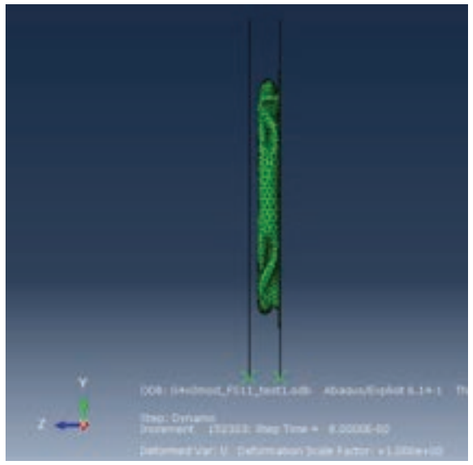

Figure 11: Prototype undergoing the first phase of FE simulation

The second phase (Fig.12) has as an objective to understand how the evolution of the crash will develop in the attenuator and the extent of the deformation caused in the structure of the front bulkhead and anti-intrusion plate. And, to model and analyze this behavior, the shearing effects between the components are ignored, as it would increase the complexity of the model and thus increase the processing time unnecessarily. The simulation setup of this phase consists in the fixation of the attenuator onto the anti-intrusion plate, which is fixated onto the front bulkhead. The bases of the front bulkhead are restrained in all degrees of freedom and the analytical rigid wall has a velocity of 7 m/s and inertial mass of 300 kg. In the second phase are eliminated all the prototypes that cause a permanent deformation in the front bulkhead or anti-intrusion plate of 25 mm or above, generate peak deceleration values over 40G or average deceleration values over 20G. The other models are submitted to the third phase

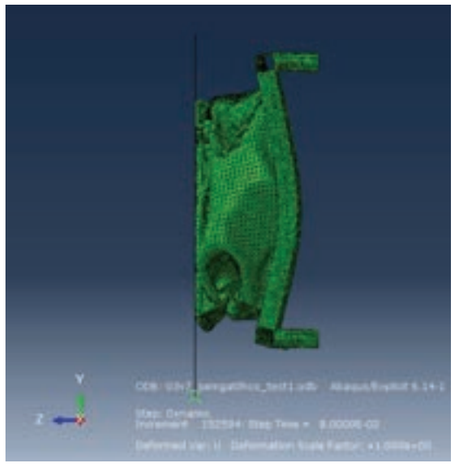

Figure 12: Prototype undergoing the second phase of FE simulation

Co-funded by the Erasmus+ Programme of the European Union

The European Commission support for the production of this publication does not constitute an endorsement of the contents which reflects the views only of the authors, and the Commission cannot be held responsible for any use which may be made of the information contained therein. Project number: 585796-EPP-1-2017-1-AT-EPPKA2-CBHE-JP

The third phase of FE simulations' main objective is to estimate the margin of safety that the impact attenuator withstands. This is done considering that the main safety indicator is the energy absorbed during the impact, which its reference value is 7350 J. For the margin of safety to be considered the device must present acceptable values for the peak and average deceleration, absorbed energy and permanent deformation for the anti-intrusion plate and front bulkhead. The setup of the simulation is the same as in the second phase, with an exception for the speed of the analytical rigid wall, that is modified to generate a specific amount of energy. The models simulated in the third phase are submitted to the model selection.

To exemplify, when a model is being simulated with a safety factor of 1,1 it means that the system's total energy is 8035 J (110% of 7350 J). And to generate this amount of energy the velocity of the analytical rigid wall must be of 7,34 m/s.

The deceleration, kinetic energy, absorbed energy and plastically dissipated energy data are collected in every phase of the FE simulation process. In the second and third phase also are collected the front bulkhead and anti-intrusion plate deformation data.

4.5 Manufacture

4.5.1 Front Bulk Head

To verify if the deformation suffered by the front bulkhead fits the maximum deformation allowed by FSAE rules, it is necessary to manufacture this component for the validation of the impact attenuator, acting as a support for the device. This component has a rectangular geometry, composed of square tubes that have been welded to one another. The material used is SAE 1020 steel.

To minimize potential errors and to obtain a more precise final product, cutting templates are made for the front bulkhead tubes, these will be glued to the extremities of the tubes. The software Solidworks is used to model a prototype for each part.

After cutting the tubes using the templates as guides, the tubes welded together using the MAG (metal active gas) process. The cost of this process is very low, due to the resources already available at the Federal University of Rio de Janeiro (UFRJ), where the team is based.

4.5.2 Impact Attenuator

As with the selection of the material and the definition of the geometry, the manufacturing of the impact attenuator is influenced by the cost and quality of the project. For this process, the resources available at UFRJ will be heavily used.

The chosen material is 5052 H34 aluminum. The plate is cut using a water jet, guaranteeing better precision and quality of the cut. The processes of folding and calendaring are done to make the attenuator's fixation holes on the front bulkhead and to make the beak, respectively. Lastly, the plates will be welded using the TIG (tungsten inert gas) process.

Co-funded by the Erasmus+ Programme of the European Union

4.5 Manufacture

A drop test is a method of validation in which a suspended mass is released from a determined height in order to generate the amount of energy necessary to emulate the desired conditions. To validate the impact attenuator, a weight of 300 kg is required to be lifted to a height of 2.5 meters. However, due to obstacles imposed by the pandemic and the cost of a test at this scale, it is necessary to re-dimension this test to fit our reality.

This will be done by reducing the weight suspended and the height at which it is dropped. These new conditions will have been previously simulated in Abaqus, following the same simulation model used on the real scale version of the attenuator. By using this reduced version, it will be possible to compare the simulation model to the validation by drop test model and calculate the deviations between both models. The results will then be scaled to real size so that the real size simulations can be validated as well. Consequently, the original impact attenuator will be validated, seeing as the simulations will be considered reliable, as per the rules' set criteria.

5. RESULTS

5.1. Real Size Simulation Results

The criteria taken in consideration to select the geometry of the impact attenuator are such as: Formula SAE rules attendance, cost, performance, simple manufacturing, mass and innovation.

The chosen model has a mass of 1427 grams and a margin of safety of 1,05. Absorbing 7712,56 J (Fig. 13) with an energy absorption efficiency of 99,94% when assembled onto the anti-intrusion plate and front bulkhead. The peak deceleration value is 23,33 G (Fig. 14), and the average deceleration value is 11,75 G (Fig. 14), with a permanent deformation of the front bulkhead of 7,78 mm (Fig. 15).

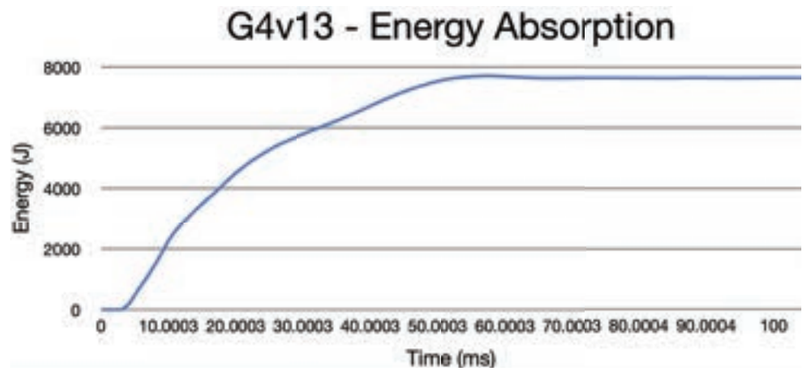

Figure 13: G4v13 Energy Absorption

Co-funded by the Erasmus+ Programme of the European Union

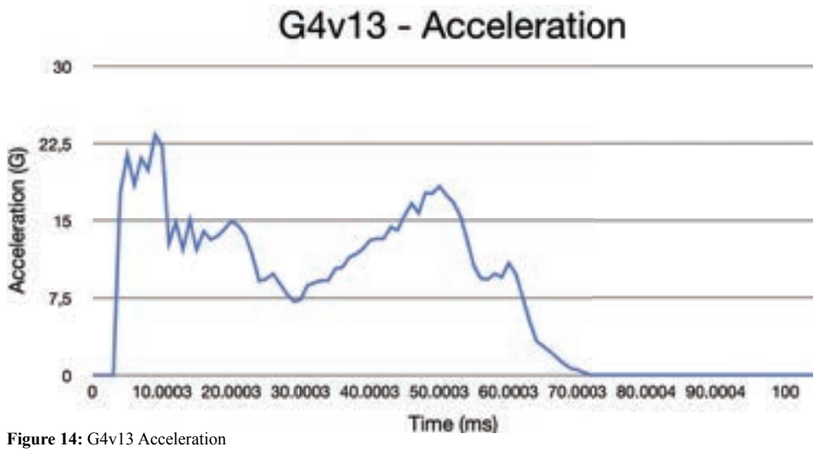

Figure 14: G4v13 Acceleration

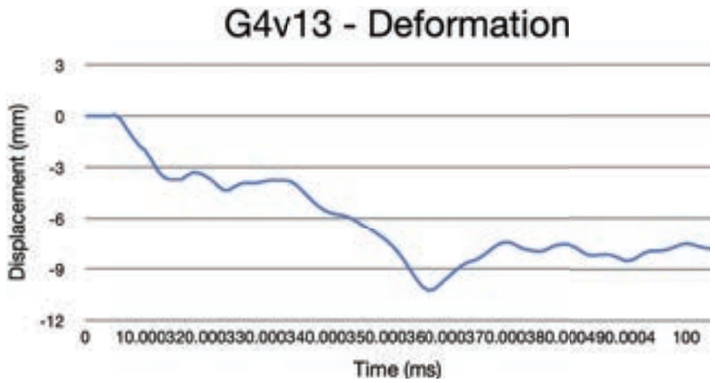

Figure 15: G4v13 Deformation

6. CONCLUSION

6.1. Comparative Examination vs. Standard Foam Attenuator - Cost, Availability, Mass, Efficiency

A comparative examination to access the cost effectiveness of the aluminum impact attenuator versus the standard component is key to comprehend how optimal the project is, taking its costs, availability, mass, efficiency and overall behavior in an impact situation.

The Standard Foam Attenuator is made out of Dow Impaxx 770 Foam (Fig.16), and weighs 700g. Data surrounding its efficiency, average and peak deceleration or energy absorption was not found. The average price for the Standard Impact Attenuator is €360 (Formula Seven, n.d.), approximately US$430 in current exchange (not including the cost of shipping and taxes related to importation). This impact attenuator is only available via online stores based on Europe, United States of America or India.

Co-funded by the Erasmus+ Programme of the European Union

The European Commission support for the production of this publication does not constitute an endorsement of the contents which reflects the views only of the authors, and the Commission cannot be held responsible for any use which may be made of the information contained therein. Project number: 585796-EPP-1-2017-1-AT-EPPKA2-CBHE-JP

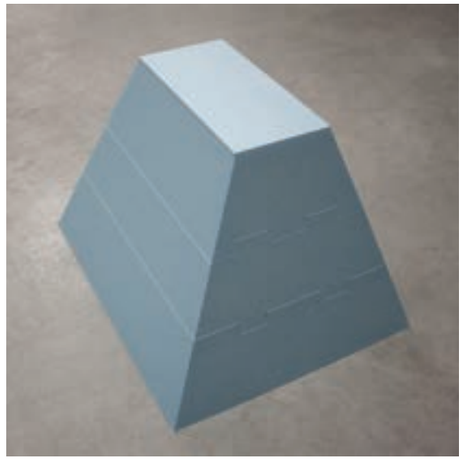

Figure 16: Standard Impact Attenuator

The aluminum impact attenuator (Fig.17) is made out of a 2 mm thick 5052-H34 Aluminum sheet and weighs 1427 grams. It has a safety margin of 1,05, absorbing 7712,56 J at a peak deceleration value of 23,33 G and average deceleration value of 10,75 G. The total cost for one attenuator is US$30,50. The material is widely accessible and available, facilitating the purchase, manufacturing and logistics procedures.

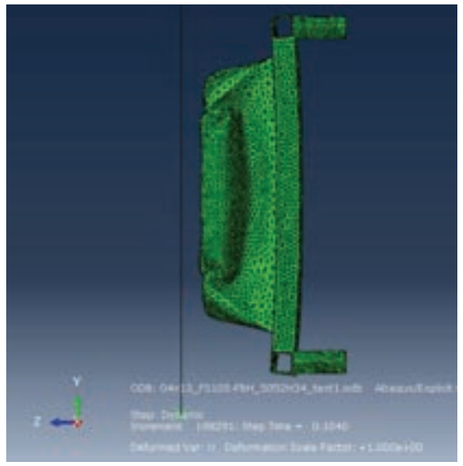

Figure 17: G4v13 post-crash test simulation

The aluminum attenuator is designed and optimized accordingly to the Minerva ERacing car's front bulkhead and the aerodynamics of the car, and because of its cost and customization it can be easily adapted or discarded if any major component needs to be changed. In contrast, the standard foam attenuator does not allow for modifications and its cost does not allow for it to be discarded as easily as the aluminum attenuator in case of any changes in adjacent car parts. It also requires a stiffer front bulkhead to prevent front bulkhead and anti-intrusion plate buckling and, according to simulations (Fig.19), it would need additional diagonal brace tubing or "x-brace" tubing, depending on the size of the front bulkhead it is mounted to. This reduces the weight advantage that the standard foam attenuator has over the aluminum impact attenuator and requires the manufacturing of chassis tubing.

Co-funded by the Erasmus+ Programme of the European Union

The European Commission support for the production of this publication does not constitute an endorsement of the contents which reflects the views only of the authors, and the Commission cannot be held responsible for any use which may be made of the information contained therein. Project number: 585796-EPP-1-2017-1-AT-EPPKA2-CBHE-JP

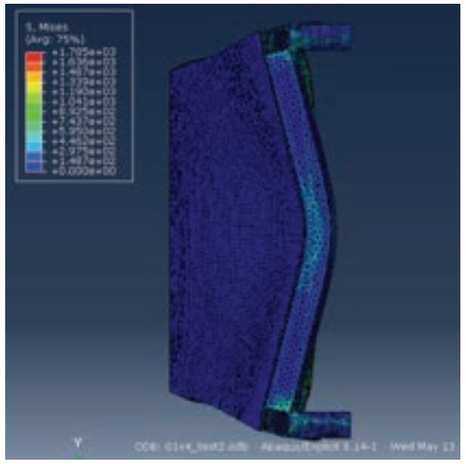

Figure 19: Excessive deformation caused by foam attenuator

6.2 Pandemic Impact on the Project

The impact attenuator project, as well as any other projects related to the 2021 Minerva ERacing car, had a schedule and deadlines for its execution. However, with the pandemic, the deadlines had to be delayed and the schedule changed completely.

One of the major factors regarding the development of this project was the cost, as the logistics became more complicated due to lockdown, quarantine and other factors like closing businesses or the American dollar, the project was further delayed and much more costly. Facing this scenario, a new market search was needed with the objective to lower all of the manufacturing costs.

Another difficulty was the execution of the drop test validation, as all university laboratories that could be used to perform the test are functioning with fewer people and a high demand of activities. This resulted in the delay of the deadline of the drop test execution.

6.3 Overall Conclusion

The project for the impact attenuator was motivated by a need for cheap and simple manufacturing and, also, to design something that would absorb as much energy as possible in case of a collision. How could this be achieved?

By choosing a geometry and a material that can assure that the impact attenuator will deform and transmit the least possible damage to other elements and the passenger in case of a collision, we can be sure that the device is fulfilling its purpose of absorbing the maximum amount of energy from the impact stipulated by Formula SAE regulations. The use of simulation software along with the validations are fundamental to the construction of the attenuator and was decisive in the material optimization, geometry, and collision analysis presented throughout the project.

The effects of the first and second wave of the COVID-19 pandemic cases were greatly felt in the project, resulting in the delay of the drop test execution, which will be held in the months to come, seeking to validate the simulation modelling using a down-sized impact attenuator.

Co-funded by the Erasmus+ Programme of the European Union

The European Commission support for the production of this publication does not constitute an endorsement of the contents which reflects the views only of the authors, and the Commission cannot be held responsible for any use which may be made of the information contained therein. Project number: 585796-EPP-1-2017-1-AT-EPPKA2-CBHE-JP

This project symbolizes a step forward in relation to Formula SAE oriented impact attenuator projects, having had all its aspects considered and analyzed for their optimization. The project also represents a significant stepping stone for future modifications and enhancements of the impact attenuator, being a comprehensive guide of the paths to be taken for the elaboration of impact attenuators that are progressively more accessible and engineeringly elevated.

7. RECOMENDATIONS

The key points in the development of the impact attenuator project were adherence to the rules and the use of correct methods of analysis. These points must be prioritized in the development of future projects, especially impact attenuator projects.

Firstly, an impact attenuator must fit the front bulkhead's dimensions. The front bulkhead is an important element to keep in mind throughout the project, as when the impact attenuator is crushed, the deformation of the bulkhead must be minimal in order to adhere to the rules while also protecting other structures and the pilot. There are two main ways to avoid front bulkhead excessive deformation. The first is to direct the energy to the structural nodes of the bulkhead. This can be achieved by increasing the width and height of a shell impact attenuator or by adding diagonal tubes to the frame, as known as diagonal braces or "x-braces". The second way to avoid excessive deformation of the front bulkhead is to design an impact attenuator that does not build up highly rigid topology, as seen in the Figure. Because these areas will not absorb much energy and will transfer the force of impact to the anti-intrusion plate and front bulkhead.

To be sure that the impact attenuator will absorb energy properly, while also ensuring minimal deformation of the front bulkhead, the correct form of analysis must be made. The attenuator suffers forces from high velocity impact; therefore, it must be analyzed in the dynamic explicit method. The static method analyses bodies that suffer constant or slowly applied forces, which is not representative of the collision situation that the attenuator is subject to. An attenuator that has been analyzed using only the static method will be flawed and potentially dangerous, seeing as it's real deformation and crush evolution in an impact situation will be unknown.

This logic can be extended to the validation method for the attenuator. The quasi-static test, in which the attenuator is slowly compressed by a machine, while being very commonly used among Brazilian teams, is a uncomplete validation method for this device, as with the static simulation analysis, because it does not reflect the complete true behavior of the attenuator under an impact situation. Therefore, a drop test or a crash test validation is recommended, as it is a dynamic test that truly emulates the impact conditions set by FSAE rules.

Co-funded by the Erasmus+ Programme of the European Union

The European Commission support for the production of this publication does not constitute an endorsement of the contents which reflects the views only of the authors, and the Commission cannot be held responsible for any use which may be made of the information contained therein. Project number: 585796-EPP-1-2017-1-AT-EPPKA2-CBHE-JP

REFERENCES

Pereira, L. O. (2013). Projeto de um atenuador de impacto para o protótipo da equipe de Fórmula SAE da UFRJ. Escola Politécnica.

Belingardi, G., & Obradovic, J. (2010). Design of the impact attenuator for a Formula Student racing car: Numerical simulation of the impact crash test. Journal of the Serbian Society for Computational Mechanics.

Kumar, D., Kumar, S., Singh, G., Khanna, N. (2012). Drop test analysis of impact attenuator for Formula SAE car. International Journal of Scientific and Research Publications, Volume 2, Issue 10.

Boria, S. (2010). Behaviour of an impact attenuator for Formula SAE under dynamic loading. International Journal of Vehicle Structures & Systems.

Belingardi, G., Boria, S., Obradovic, J. (2013). Energy absorbing sacrificial structures made of composite materials for vehicle crash design. Dynamic Failure of Composite and Sandwich Structures, Solid Mechanics and Its Applications. Ed. S. Abrate et al., Springer, 192, 577-609.

Formula SAE. (2020). Formula SAE Rules 2020 Version 2.1.

DIAB Group. (n.d.). Datasheet DivinyCell H Barracuda.
Formula Seven. (n.d.). Standard Impact Attenuator Type 12. Retrieved from http://www.formula-seven.com/shop-products/impact-attenuator-t-12/

Department of defense of The U.S.A. (2003). Metallic Materials and Elements for Aerospace Vehicle Structures.

Orduña, J.M.C. (2017). Diseño, fabricación y validación del atenuador de impacto para um vehículo de Formula Student. Escola Técnica Superior de Ingeniería del Diseño, Universitat Politècnica de Valencia.

Vardhan, H.T., Mishra, M.K., Singh, R., Pandey, U.K., Kumar, D. (2018). Design and fabrication of impact attenuator for Formula SAE car. International Journal of Engineering Research & Technology, Vol. 7, Issue 05.

Santos, D.J., (2016). Atenuador de impacto para Fórmula SAE: Análise dinâmica não linear pelo método dos elementos finitos. Departamento de Engenharia de Materiais, Centro Federal de Educação Tecnológica de Minas Gerais.

Co-funded by the Erasmus+ Programme of the European Union

ANALYTICAL SIZING OF A HEAT EXCHANGER FOR A FSEE COMBUSTION CAR

João Gabriel Barcelos dos Santos[1],
Prof. Dr. -Ing. Fernando Augusto de Noronha Castro Pinto[2]

[1]Student, Mechanical Engineering, Escola Politécnica, UFRJ, jgbarceloss@poli.ufrj.br
[2]Dr. Ing. Professor, Mechanical Engineering, Escola Politécnica, UFRJ, fcpinto@poli.ufrj.br

ABSTRACT

First, the ideal engine operating temperature was defined through studies by Prado (2007), which related the thermodynamics involved in the internal combustion process of an engine with its volumetric efficiency. Afterwards, the necessary thermal rejection at different engine speeds was defined, using the empirical method developed by Heywood (1988), this method relates the engine power to the required thermal rejection performance of the cooling system for certain speed ranges. The analytical method chosen to dimension the heat exchanger was the NUT-effectiveness, developed by Keys and London in 1984. For this purpose, a dimensioning tool developed in Excel software was developed in order to obtain the amount of heat dissipated by the system cooling in a range of engine operating regimes. This dimensioning tool had as main objective to be able to simulate the heat exchange of radiators with different dimensions, but only with brazed hives. It also considers the conditions of the air and water flow contour of the system. Besides that, simulations were developed in Ansys Fluent and Optimum Lap to predict the behavior of air flow through the radiator, as well as validations in specific operating regimes of the engine itself to obtain the mass flow of water flow in the cooling system. Among all the possibilities of heat exchangers analyzed, the cross-flow radiator with a brazed core of 260x263x62mm was chosen as it fits within our size restrictions imposed by the rules of the Formula SAE International competition, and also proved to be the best heat exchanger, according to our analytical method.

Keywords: Sizing, Formula SAE, Radiator, Cooling system, ideal temperature.

INTRODUCTION

This project aims to analytically dimension a heat exchanger and, consequently, the cooling system for the Icarus UFRJ FSAE prototype. Thus, the study of literature such as heat transfer books and thermal machines, articles, course completion projects and projects by other FSAE teams is necessary for the complete execution of the project. In addition, it is consistent that the reader understands that the project was developed based on a radiator with a brazed core (Figure 3) and that all geometric formulas were for that specific model of radiator, however the applicability of the analytical model to others types of radiators is possible by adapting the geometric formulas and some factors inherent to the composition of the heat exchanger.

Co-funded by the Erasmus+ Programme of the European Union

The European Commission support for the production of this publication does not constitute an endorsement of the contents which reflects the views only of the authors, and the Commission cannot be held responsible for any use which may be made of the information contained therein. Project number: 585796-EPP-1-2017-1-AT-EPPKA2-CBHE-JP

As Prado (2007) point out, from the thermodynamic point of view, engine cooling is undesirable. However, conventional engine materials cannot withstand excessively high temperatures and oils lose their lubrication characteristics when the temperature exceeds a certain value, resulting in excessive wear and other problems. On the other hand, excessively cooled engines present a series of problems, including increased fuel consumption, increased oil dilution, a tendency for sediment formation and oxidation, in addition to accelerated wear of the piston and cylinder rings. Therefore, a good dimensioning of the cooling system, and consequently of the heat exchanger, works by balancing these two critical operating situations of an engine and consequently keeps it with the best performance and durability.

There are basically three reasons that justify the existence of a cooling system in the engine:

1. Promote high volumetric efficiency by minimizing the heat flow from the engine structure to the intake air.
2. Prevent detonation due to high temperatures in the combustion chamber.
3. Avoid mechanical failures in materials due to high thermal loads that come from excessive thermal gradients.

There are many factors that make a cooling system work well to the objectives set for the performance and durability of the engine, and most of the main factors will be present in this article, however, it is important to note that all the characteristics of a project like this, they are guided by the objectives and working conditions of the designer and the team. Therefore, for the reapplication of a dimension like this in other FSAE teams, the conditions for such a project to be executed and checked must be studied primarily.

It should be noted that until the end of the writing of this paper, the experimental validation of the project proposed by the team will not be carried out, but there is concern about the real performance of the radiator and the conditions of its contour operation. This phase of the project can be published later.

OBJECTIVES

Project adapted to a 40 °C environment

Due to the climatic conditions of the countries hosting the competitions, favorable to having a “hot” environment at the time of the event, this system’s working temperature is the one that best adapts to different situations.

Designed to keep water at a critical temperature below 110 °C

Above 110 °C the pressure in the cooling line increases a lot due to the evaporation of water, so it is important that this temperature is controlled, thus avoiding bursts in the cooling line and always keeping the volume of water in the system as constant as possible.

Co-funded by the Erasmus+ Programme of the European Union

LITERATURE REVIEW

1. Distribution of fuel energy and definition of the thermal load repelled by the system

For the design of the cooling system, it is essential to determine the thermal load to be dissipated. According to Willard W. Pulkrabek, the energy lost to the refrigerant at high load is about half the axle power (Brake Power), rising to about double at low load. (PULKRABEK, 2003) Figure 1 illustrates the energy distribution of the fuel. Heywood presents very close values, stating that between 25% and 28% of the fuel energy is transformed into axle power, while 17% to 26% of the fuel energy must be removed from the engine by the cooling system. Heywood also presents the graph shown in figure 2, relating the engine’s thermal load to its shaft power.

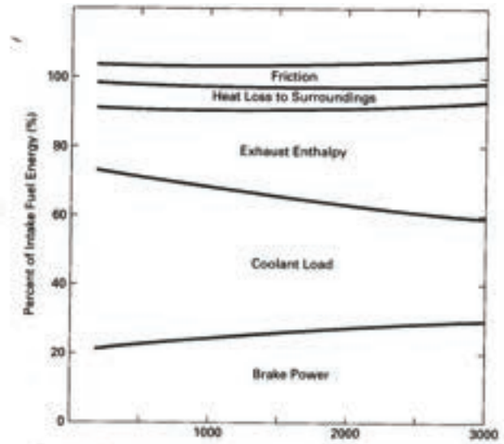

Figure 1: Fuel energy distribution (PULKRABEK, 2003)

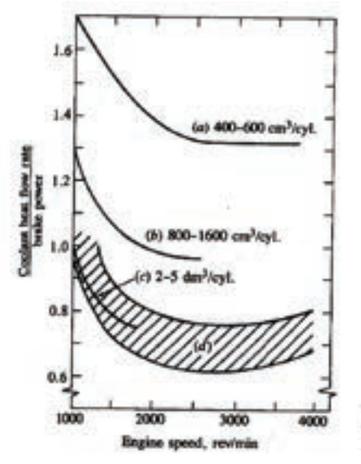

Figure 2: Ratio between the heat flow rate of the coolant and the engine power as a function of its rotation. (HEYWOOD, 1988)

The thermal load effectively removed by the cooling system is affected by the heat dissipated by the engine block, usually resulting in lower loads than those presented. (HEYWOOD, 1988).

Co-funded by the Erasmus+ Programme of the European Union

2. Heat exchangers (or radiator)

It is the main component of the conventional car cooling system, as it is responsible for conducting the heat of the water to the environment. In order to dimension it correctly, its core and the type of fluid flow present in it are taken into account.

The selection of the radiator core is a compromise between cost, space, and core characteristics. Schmidt (1965) presents graphics that allow to optimize the choice of the radiator core according to the resistance to air flow, rejected heat and air velocity through the core. He points out that by doubling the area of the radiator core, there will be a reduction in engine power, it will take much more than twice the power of the fan for equal cooling.

Schmidt (1965) also presents graphs that show the influence of the number of rows of tubes and fins of the radiator on the losses with the use of the fan. By increasing the number of rows of tubes and fins per unit of length, the power used by the use of the fan decreases, until a value that the increase becomes ineffective.

There are 3 basic types of radiator matrix design used today. They are:

Type 1:
The radiator's cellular matrix has the highest thermal efficiency relative to weight compared to the other two types, and the inherent flexibility of the cellular construction of this design is likely to have less danger of damaging with impact and vibration. These radiators are easier to repair than those with a tubular core. Consequently, the flexibility of cell construction can make you more prone to failure and subject to a large and rapid change in internal pressure.

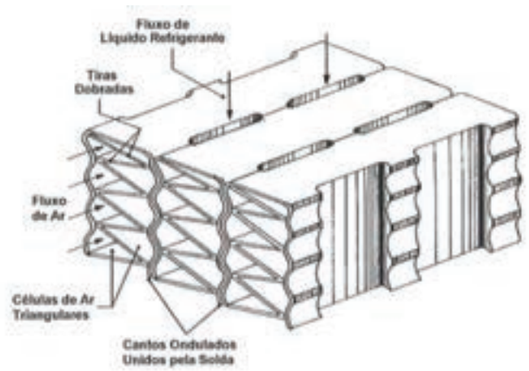

Figure 3: Radiator diagram. (PRADO, W.B. Simulação do Sistema de Arrefecimento de Motores Diesel em Matlab)

Type 2:
The structure composed of tubes and corrugated sheets combines the strength of the tube and the accordion type (resistance to high internal pressures) with the high thermal efficiency of the cell construction.

Co-funded by the Erasmus+ Programme of the European Union
The European Commission support for the production of this publication does not constitute an endorsement of the contents which reflects the views only of the authors, and the Commission cannot be held responsible for any use which may be made of the information contained therein. Project number: 585796-EPP-1-2017-1-AT-EPPKA2-CBHE-JP

With the increase in space between tubes and accordion plates, the construction process becomes less expensive when compared to the flat fin type and, for this reason, it is currently the most common form of radiator construction.

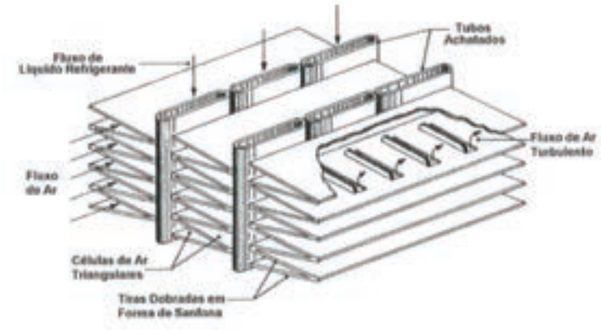

Figure 4: Radiator diagram. (PRADO, W.B. Simulação do Sistema de Arrefecimento de Motores Diesel em Matlab)

Type 3:
The tube and flat plate radiator has superior structural strength and can withstand high internal pressures. These radiators are used in heavy vehicles. However, the efficiency for this construction is less than for the others presented above and is more costly for the builders than the others.

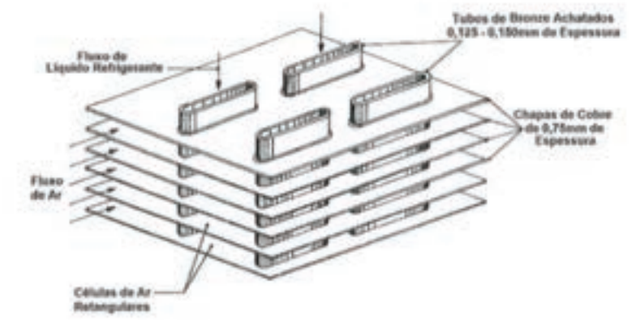

Figure 5: Radiator diagram. (PRADO, W.B. Simulação do Sistema de Arrefecimento de Motores Diesel em Matlab)

METHODOLOGY

1. Setting the optimum engine operating temperature

On a FSAE's project, temperatures above 100 °C cause the water in the system to boil, increasing the pressure in the cooling line, which can generate leaks. Although there are cooling fluids with higher boiling points and interesting additives to the engine, they are not allowed by competition regulations.

All this context and bibliographic studies lead us to believe that temperatures between 90°C and 100°C are ideal for the project, and this is confirmed when observing the opening temperature of

Co-funded by the Erasmus+ Programme of the European Union
The European Commission support for the production of this publication does not constitute an endorsement of the contents which reflects the views only of the authors, and the Commission cannot be held responsible for any use which may be made of the information contained therein. Project number: 585796-EPP-1-2017-1-AT-EPPKA2-CBHE-JP

the original engine thermostat used by the team (CB600f, Honda hornet) seen in the motorcycle manual, which is 95°C. Therefore, 95°C will be the ideal working temperature for the engine, but values between 90°C and 100°C are allowed.

2. Objective thermal rejection of the system

For the design of the cooling system, it is essential to determine the thermal load to be dissipated. However, there is no information about the thermal dissipation necessary to dimension the engine cooling system. Thus, the empirical study of Heywood is used, which relates the power of the team's engine, obtained in the roller dynamometer, to thermal rejection by the cooling system (Figure 2).

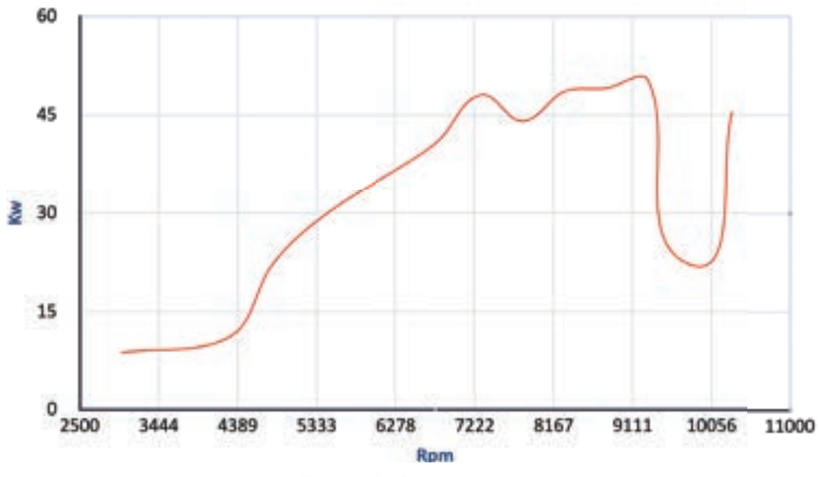

Figure 6: Engine power curve per rpm.

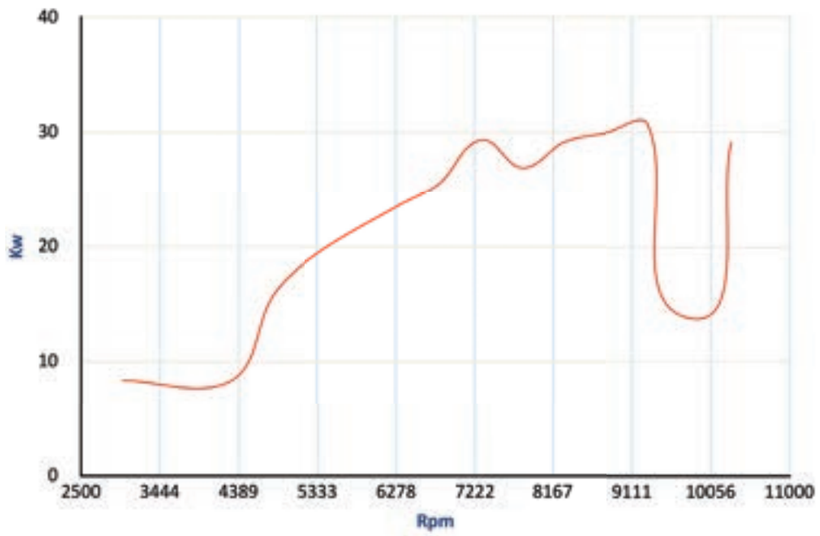

Figure 7: Thermal rejection curve as a function of engine power at different speeds.

Co-funded by the Erasmus+ Programme of the European Union

The European Commission support for the production of this publication does not constitute an endorsement of the contents which reflects the views only of the authors, and the Commission cannot be held responsible for any use which may be made of the information contained therein. Project number: 585796-EPP-1-2017-1-AT-EPPKA2-CBHE-JP

3. System boundary conditions

3.1. Frequency of engine operating conditions

With the aid of Optimum Lap, it is simulated what the prototype's performance would be on an enduro. The endurance track of the 2017 FSAE Brasil competition is used as a parameter because many car abandonments of FSAE in enduros are due to overheating of the engine, so the goal is the system to perform better in this test, which contributes a lot to the reliability of our prototype. From these simulations, the most frequent operating regime of the engine is defined and studies on it are focused.

3.1.1. Speed estimation on an enduro

As can be seen in the graph below, during approximately 90% of the track the car is at speeds between 18 km/h and 67 km/h (5 m/s and 18.6 m/s).

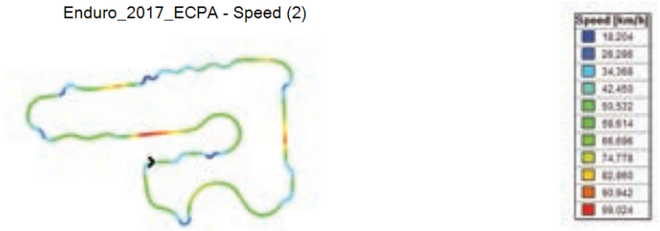

Figure 8: Simulation of car speeds at enduro.

3.1.2. Estimated engine rpm

During the entire race, the engine goes from 4200 rpm to 10000 rpm, with a modal range of 7600 rpm to 9500 rpm.

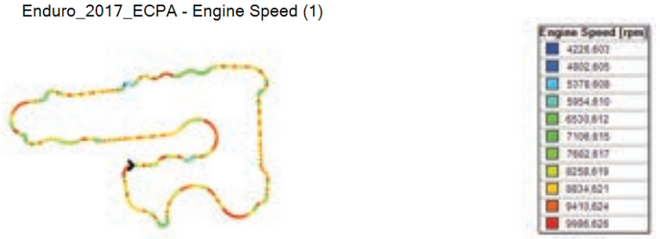

Figure 9: Simulation of engine speeds (rpm) at enduro

3.1.3. Gears frequently used

During the course, essentially, the car is most frequently in 2nd, 1st and 3rd gears, in that order.

Figure 10: Simulation of gears in each part of the enduro.

Co-funded by the Erasmus+ Programme of the European Union

The European Commission support for the production of this publication does not constitute an endorsement of the contents which reflects the views only of the authors, and the Commission cannot be held responsible for any use which may be made of the information contained therein. Project number: 585796-EPP-1-2017-1-AT-EPPKA2-CBHE-JP

3.2. Air flow

With the aid of Optimum Lap, it is simulated what the prototype's performance would be on an enduro. The endurance track of the 2017 FSAE Brasil competition is used as a parameter because many car abandonments of FSAE in enduros are due to overheating of the engine, so the goal is the system to perform better in this test, which contributes a lot to the reliability of our prototype. From these simulations, the most frequent operating regime of the engine is defined and studies on it are focused.

3.2.1. CFD Simulation in Ansys Fluid

For the CFD simulation, the estimated car speed data is used for each rotation, these were acquired through a roller dynamometer test done by the team. From there, we consider that as the speed is relative between two or more bodies, it was necessary to define the speed of the car as the speed of the air. Therefore, these velocities are used to study the flow in each specific regime.
It is simulated only from a speed of 5 m/s up to a speed of 30.5 m/s since they are very acceptable speed ranges for FSAE cars.

3.2.1.1.Simulation method

Images of one of the simulation variations that were made, with an air speed of 5 m/s could be seen below. A simplified model of air flow is developed considering the dynamics of the wheels. Also, the radiator is analyzed as a plane in space referring to its actual positioning in the car, therefore, only the speed of the air just before the radiator.

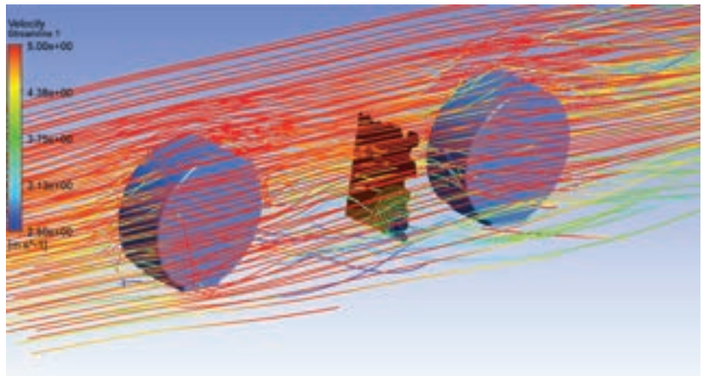

Figure 11: Streamline rendering

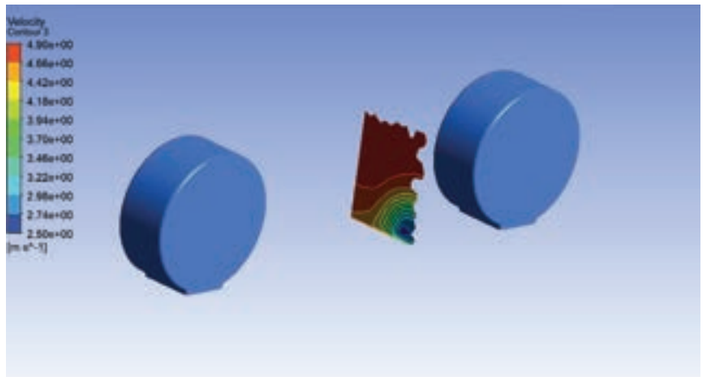

Figure 12: Rendering without streamline

Co-funded by the Erasmus+ Programme of the European Union

The European Commission support for the production of this publication does not constitute an endorsement of the contents which reflects the views only of the authors, and the Commission cannot be held responsible for any use which may be made of the information contained therein. Project number: 585796-EPP-1-2017-1-AT-EPPKA2-CBHE-JP

3.2.1.2.Simulation analysis

As in the method chosen for sizing the radiator, only one air speed that reaches the radiator must be chosen to obtain the weighted average between the speeds that reached the plane of the heat exchanger. Then, speeds are defined as:

Air speed before wheels (m/s)	Air speed after wheels (m/s)	Reduction
30,5	28,1	8%
28,6	26,5	8%
26,8	24,9	7%
25,0	23,1	8%
23,1	21,4	7%
21,3	19,8	7%
19,5	18,0	8%
17,6	16,3	7%
15,8	14,6	8%
11,4	10,5	8%
8,8	8,1	8%
5,0	4,6	8%

Table 1: Reduction of air speed towards the radiator

It is observed, then, a reduction in the air speed of the environment outside the car and the air speed that reaches the radiator from 7% to 8%. Therefore, the greatest reduction is applied in all the speed regimes defined for dimensioning the heat exchanger.

3.2.2. Air speed and rpm ratio

Considering that the relationship between engine rpm and air speed is not constant due to the gear ratios that exist in the engine's gearbox system, the car's performance in a straight line start is estimated through Optimum Lap simulations. Below, the graph obtained:

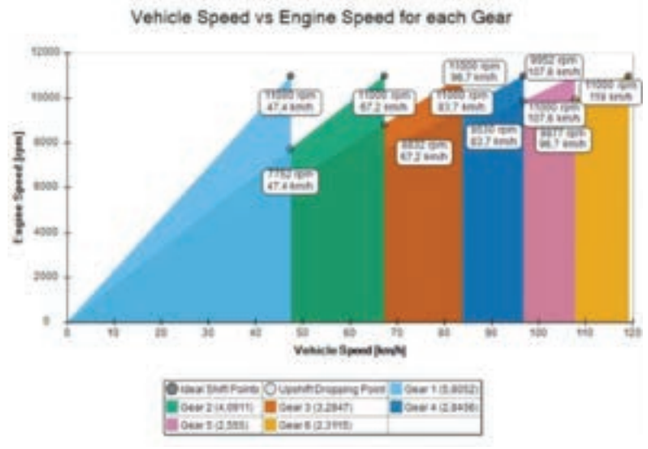

Figure 13: Car speed and engine speed (rpm) in different gears (Optimum Lap).

Co-funded by the Erasmus+ Programme of the European Union

The European Commission support for the production of this publication does not constitute an endorsement of the contents which reflects the views only of the authors, and the Commission cannot be held responsible for any use which may be made of the information contained therein. Project number: 585796-EPP-1-2017-1-AT-EPPKA2-CBHE-JP

Therefore, taking into account that the speed of the car is the speed of the air and applying the reduction of that speed in the radiator obtained by simulations in CFD, it is possible to estimate the air flow at each engine rotation and most recurring gear. Below is the air speed table for each gear.

RPM	Air velocity in 1st gear (m/s)	Air velocity in 2nd gear (m/s)	Air velocity in 3rd gear (m/s)
10300	12,1	16,6	19,9
9800	11,4	16,1	19,2
9300	10,2	14,8	18,7
8800	9,7	14,1	x
8300	8,9	13,5	x
7800	8,4	12,1	x
7300	7,7	x	x
6800	7,2	x	x
6300	6,4	x	x
5800	5,9	x	x
5300	5,1	x	x
4800	4,6	x	x
4300	3,8	x	x

Table 2: Air speed in each gear.

3.3. Water flow

The exchange of heat between moving fluids is directly related to their mass flow. And as the mechanical water pump present in the engine of the CB600F Honda Hornet is connected to the crankshaft and this connection follows a constant proportionality, the engine speeds are connected linearly with the water flow that the pump provides.

3.3.1. Mass flow of water at all engine speeds

An experiment is carried out to measure the mass flow of the water at idle (0.23 kg/s) and at the peak engine power (1.02 kg/s) 3000 rpm and 9200 rpm, respectively. As this connection is linear, using a simple linear equation, the mass flow rate of the water is obtained at each rotation. This data is explained in the table below:

RPM	Mass flow of water (kg/s)
10300	1,15
9800	1,08
9300	1,02
8800	0,96
8300	0,90
7800	0,83
7300	0,77
6800	0,70
6300	0,64
5800	0,58
5300	0,52
4800	0,45
4300	0,39
3000	0,23

Table 3: Mass flow of water as a function of engine RPM

3.4. System boundary conditions

Below, we conclude the relationship between air flow and water flow present in the cooling system with the car moving and with the car idling. This relationship is of paramount importance, since it is possible to calculate and estimate precisely the dimensions that the radiator must have in order for the thermal rejection curve to be satisfied, prioritizing the areas of greatest work on the enduro and prioritizing the slow idle of the car. With this in mind, the system's reliability tends to increase as well as efficiency.

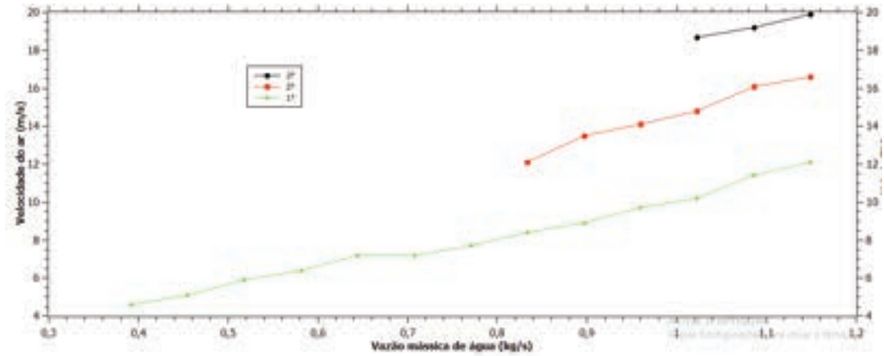

Figure 14: Air speed in each gear as a function of the mass flow of water (Qtiplot)

MARCHA LENTA			
RPM	**Mass flow of water (kg/s)**	**Velocity air (m/s)**	**Rejection (Kw)**
3000	0,23	4,1	8,4

Table 4: Relation between water speed and air speed at idle.

Co-funded by the Erasmus+ Programme of the European Union
The European Commission support for the production of this publication does not constitute an endorsement of the contents which reflects the views only of the authors, and the Commission cannot be held responsible for any use which may be made of the information contained therein. Project number: 585796-EPP-1-2017-1-AT-EPPKA2-CBHE-JP

Co-funded by the Erasmus+ Programme of the European Union
The European Commission support for the production of this publication does not constitute an endorsement of the contents which reflects the views only of the authors, and the Commission cannot be held responsible for any use which may be made of the information contained therein. Project number: 585796-EPP-1-2017-1-AT-EPPKA2-CBHE-JP

4. Analytical sizing of the NTU method

Initially, the thermal transfer coefficient or heat transfer coefficient is obtained from the air and water side so that later these data can be used in the calculation of the global heat transfer. Thus, the heat transfer coefficient on the air side can be obtained from:

$$har = \frac{j\ Gar\ Cpar}{Pr^{\frac{2}{3}}} \quad (1)$$

Being:

har = Air heat exchange coefficient (W/m² °C)
j = Colburn Factor
Gar = Mass air flow per minimum area (kg/m² s)
Cpar = Specific heat at constant air pressure (Kj/kg K)
Pr = Prandtl number

However, in order to obtain the mass air flow per minimum area (Gar), it should be noted that, through Bernoulli, one point is chosen after and another before the radiator. Then, the speed after the radiator is calculated using:

$$V_2^2 = V_1^2 + \frac{2\Delta P}{\rho ar} \quad (2)$$

Being:

V1 = Air speed before radiator (m/s)
V2 = Air speed after radiator (m/s)
ΔP = Variation of air pressure (Pascal)
ρar = Air density (kg/m³)

As the data on the loss of static pressure of the air passing through the radiator is not obtained, the constant pressure is thus considered V1 = V2. The idea is that in the validation of the project it is estimated which was the error imposed by this decision.
Then from there, the mass flow of air (**mar**) is considered:

$$mar = V1\ par\ Ama \quad (3)$$

Being:

mar = Mass air flow (kg/s)
Ama = Area of air passage through the radiator core (m)

Co-funded by the Erasmus+ Programme of the European Union

Thus, it is possible to obtain the Mass air flow per minimum area through the equation:

$$Gar = \frac{mar}{Ama} \quad (4)$$

To obtain the Colburn factor j, the Reynolds number of the air flow must first be obtained.
To do so, use:

$$Re = \frac{Gar\ Dha}{\mu ar} \quad (5)$$

Being:

Dha = Hydraulic diameter for air (m)
μar = Dynamic air viscosity (kg/m s)

Subsequently, the Reynolds number obtained with the Colburn factor j is related, this relationship is acquired through, figure 15. This was obtained empirically for this configuration, different from the configuration of the studied heat exchanger, so there is an error when using it. But in the absence of the appropriate graph, one that is as close as possible should be used.

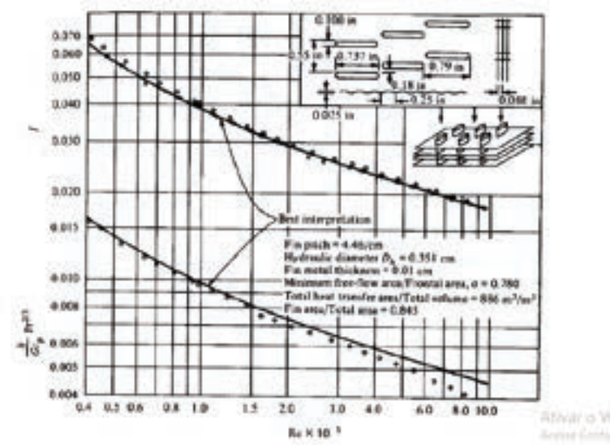

Figure 15: Reynolds number x Colburn J factor (Figure 11-24, Heat Transfer, OZISIK, 1985)

The last data necessary to acquire the heat exchange coefficient of air is the Prandtl number, it is a dimensionless number that shows the relationship between the moment diffusion and the thermal diffusion. To obtain the Prandtl number, use the graph in Appendix B of the reference (OZISIK,1985).

Co-funded by the Erasmus+ Programme of the European Union

After obtaining the heat transfer coefficient from the air, the heat transfer coefficient from water must be obtained using the formula below:

$$hw = \frac{Nu\ Kw}{Dhw} \tag{6}$$

Being:

hw = Water heat exchange coefficient (W/m² °C)
Kw = Thermal conductivity of water (W/m °C)
Nu = Nusselt number for water
Dhw = Hydraulic diameter for water (m)

To perform this calculation, it is necessary to find the Nusselt number for the water. This number is a dimensionless dimension that represents the ratio between heat exchange by convection and conduction and must be obtained by the formula:

$$Nu = 0{,}023\ Re^{0,8}\ Pr^{0,4} \tag{7}$$

Being:

Nu = Nusselt number for water
Re = Water Reynolds Number
Pr = Water Prandtl Number

To calculate the number of Prandtl, the temperature of 100 °C was used as a fixed parameter, as it is the working temperature of the prototype engine. The table below taken from Appendix B (Table B-2) of the reference (OZISIK,1985) is used.

Subsequently, the Reynolds number of the water must be calculated using the formula below:

$$Re = \frac{mw\ Dhw}{vw} \tag{8}$$

Being:

mw = Mass flow of water (kg/s)
Dhw = Hydraulic diameter for water (m)
vw = Kinematic viscosity of water (m²/s)

Co-funded by the Erasmus+ Programme of the European Union

$$Vw = \frac{mw}{\rho w\ Amw} \tag{9}$$

Being:

Vw = Speed of water flow in the radiator (m/s)
ρw = Water density (kg/m³)
Amw = Minimum water drainage area. (m)

Having acquired the heat transfer coefficient of water and air, one must acquire the global heat transfer coefficient from these data. This coefficient represents the system's ability to conduct a series of conductive and convective barriers to transfer heat. This can be represented by the internal fluid (water) or the external (air) side. External fluid is generally used. Therefore, the formula below is applied to obtain the global coefficient. This considers the tube wall negligible, as well as the fouling factor and the efficiency of the fins.

$$\frac{1}{Ua} = \frac{1}{har} + \frac{Aar}{Aw\ hw} \tag{10}$$

Being:

Ua = Universal heat exchange coefficient (W/m² °C)
har = Air heat exchange coefficient (W/m² °C)
hw = Water heat exchange coefficient (W/m² °C)
Aar = Air-side heat transfer area (m²)
Aw = Water side heat transfer area (m²)

Looking at the equation below, it can be seen that the heat transfer area on the water side is equal to the sum of the cross-sectional areas of the radiator tubes.

$$Aw = Pt\ -2ep\ 2l + Ct\ -2ep\ 2l\ Nt \tag{11}$$

Being:

Ua = Universal heat exchange coefficient (W/m² °C)
Pt = Tube depth (m)
ep = Tube wall thickness (m)
l = Radiator core width (m)
Ct = Tube length (m)
Nt = Number of tubes

It should be noted again in the formula below that the heat transfer area on the air side is the sum of the external area of the tubes (except for the rear part that due to the separation of the flow is not in contact with the tube) with the sum of the fins area (front, top, bottom and side).

Co-funded by the Erasmus+ Programme of the European Union

$$Aar = ha^2 + \frac{Pa^2}{2}\ 2naf\ nfa\ 2Pro + 2Aft + 2Afa + Pa\ Pt\ 2naf\ nfa \quad (12)$$

Being:

Ua = Universal heat exchange coefficient (W/m² °C)

Aar = Air-side heat transfer area (m²)

ha = Fins height (m)

Pa = Fin pitch (m)

naf = Number of fins per row. Equivalent to the number of fins per inch.

nfa = Row number of fins

Pro = Radiator core depth (m)

Aft = Considered the frontal area of the tubes. (m²)

Afa = Considered the frontal area of the fins. (m²)

Pt = Tube depth (m)

Obtaining the global heat transfer coefficient, the NTU (number of transfer units) of the problem must be calculated and thus the effectiveness of the radiator is obtained. The system NTU is acquired by the formula below:

$$NTU = \frac{A` Ua}{Cmin} \quad (13)$$

Being:

A` = Aar Aw

Ua = Universal heat exchange coefficient (W/m² °C)

Cmin = Lower thermal capacity between the two fluids.

Subsequently, from **Cmin**/**Cmax** and NTU we can evaluate ε in the graph:

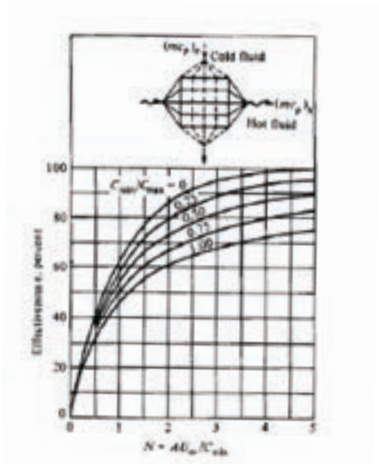

Figure 16: Effectiveness of a radiator using the NTU method (Figure 11-19, heat transfer, OZISIK, 1985)

Co-funded by the Erasmus+ Programme of the European Union

The European Commission support for the production of this publication does not constitute an endorsement of the contents which reflects the views only of the authors, and the Commission cannot be held responsible for any use which may be made of the information contained therein. Project number: 585796-EPP-1-2017-1-AT-EPPKA2-CBHE-JP

The original formula of effectiveness of a cross-flow heat exchanger with different fluids that do not mix is used.

$$\varepsilon = 1 - \exp\left(\frac{NTU^{0,22}\ (\exp(-C\ NTU^{0,78}) - 1)}{C}\right) \quad (14)$$

Being:

ε = Heat exchanger effectiveness

C = **Cmin/Cmáx**

Cmáx = Higher thermal capacity between the two fluids

Cmin = Lower thermal capacity between the two fluids

Finally, after obtaining the radiator's effectiveness, the thermal rejection provided by the radiator and the outlet temperature of the fluids are calculated using the equation below:

$$Q = \varepsilon\ Cmin(Tain - Twin) \quad (15)$$

Being:

Q = Thermal rejection (KW)

Tain = Air inlet temperature (°C)

Twin = Inlet water temperature (°C)

Cmin = Lower thermal capacity between the two fluids

$$Taot = Tain + \frac{Q}{Car} \quad (16)$$

Being:

Taot = Air outlet temperature (C°)

Car = Thermal air capacity (W/°C)

Tain = Air inlet temperature (°C)

Q = Thermal rejection (KW)

$$Twot = Twin - \frac{Q}{Cw} \quad (17)$$

Being:

Twot = Leaving water temperature (C°)

Cw = Thermal water capacity (W/°C)

Twin = Inlet water temperature (°C)

Q = Thermal rejection (KW)

Co-funded by the Erasmus+ Programme of the European Union

The European Commission support for the production of this publication does not constitute an endorsement of the contents which reflects the views only of the authors, and the Commission cannot be held responsible for any use which may be made of the information contained therein. Project number: 585796-EPP-1-2017-1-AT-EPPKA2-CBHE-JP

RESULTS

From the tests, considering all the boundary conditions and particularities of the system, we obtained the following result:

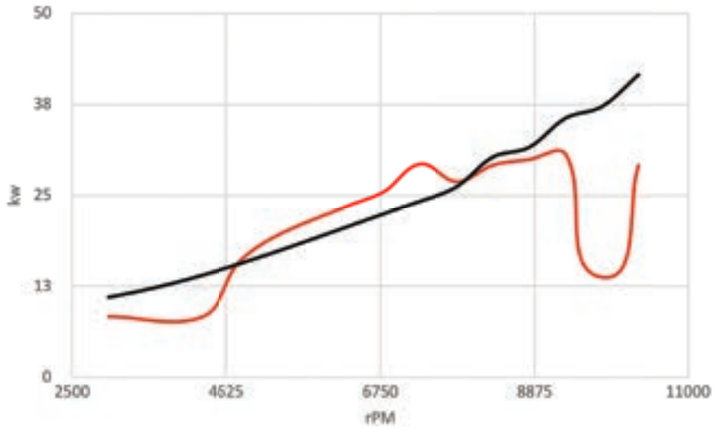

Figure 17: Comparison between the objective thermal rejection curve (red) and the thermal rejection curve (black) obtained by the chosen radiator.

The data is obtained from the commercial radiator most optimized for the prototype and also with the air inlet air boundary conditions of 40 °C and water inlet boundary conditions as being 100 °C, considering the ideal temperature engine work. Thus, the table below shows the temperature of the water leaving after the heat exchange with the air.

Water leaving temperature in 1st gear (ºC)	Water leaving temperature in 2nd gear (ºC)	Water leaving temperature in 3rd gear (ºC)
92,7	92,0	89,5
92,7	91,8	91,1
92,9	91,8	90,6
92,7	91,6	x
92,7	91,3	x
92,5	x	x
92,5	x	x
92,3	x	x
92,4	x	x
92,1	x	x
92,2	x	x
91,9	x	x
92,0	x	x

Table 5: Relationship of water speed and air speed at idle.

Co-funded by the Erasmus+ Programme of the European Union

CONCLUSION

It is then determined that the new radiator is manufactured in a brazed aluminum core. Thus, from the analysis and results, the commercial radiator that proved to be the most efficient for our prototype is the one described in the table below:

Parameters	2021 Radiator
Core height	260 mm
Core width	260 mm
Core depth	60 mm
Free-flowing area	52.360 mm²
Front core area	67.600 mm²

Table 6: Icarus team's 2021 prototype radiator structural data (Master Cooler)

RECOMMENDATIONS

An approximate simulation model of what would be the flow of air to the radiator is used. However, this model disregards the influence of the radiator itself in this air flow, that is, we consider the radiator as a plane. In this way, the best CFD simulation would be to model the radiator as realistic as possible and to be able to discretize the simulation mesh as much as possible.

REFERENCES

[1] HONDA (2012). *Manual do proprietário.* Honda. Disponível em: <https://www.honda.com.br/pos-venda/motos/sites/customer_ service_motos/files/manuais/CB%20600F%20Hornet%202012.pdf>.

[2] HEYWOOD, J. B. (1988). *Internal Combustion Engine Fundamentals*. London, McGraw Hill.

[3] KAYS, W.M; LONDON, A.L. (1984). *Compact heat exchangers.* 3°edition. Krieger Pub.Co.

[4] WILLARD W. PULKRABEK. (2003). *Engineering Fundamentals of the Internal Combustion Engine.* 2°edition. Prentice Hall.

[5] PRADO, W.B. (2007). *Simulação do Sistema de Arrefecimento de Motores Diesel em Matlab.* Escola de Engenharia de São Carlos (Universidade de São Paulo).

[6] OZISIK, M.N. (1985). *Heat transfer: A Basic Approach*. North Carolina State University, McGraw-Hill.

[7] SCHMIDT, R.C. (1965). *Optimum Core Vital to Best Cooling System Design*. SAE Journal, v.73, n.1, p.78-79, jan.

Co-funded by the Erasmus+ Programme of the European Union

A PROOF OF CONCEPT SYSTEM FOR THE IMPLEMENTATION OF OPTIMIZATION PATH PLANNING STRATEGIES IN ADDITIVE MANUFACTURING.

Sergio Salinas, Pedro Orta-Castañón & Horacio Ahuett-Garza

Escuela de Ingeniería y Ciencias, Tecnologico de Monterrey,
Ave. Eugenio Garza Sada 2501, Monterrey 64849, Mexico
A01280509@itesm.mx, porta@tec.mx, horacio.ahuett@tec.mx

ABSTRACT

Additive manufacturing (AM) technologies have gained acceptance in industrial implementation. Unfortunately, in AM processes like FDM (Fused Deposition Modeling), which can produce complex shapes created layer by layer, the end-product presents anisotropic mechanical properties that depend mostly on the deposition trajectory. The limitations of the deposition trajectory control of current commercial systems; result in reduced end-product mechanical properties. Current machines offer limited options for toolpath strategies to help solve this issue.
This work presents a proof of concept system integrated by an adapted machine system and a software framework that allows the designer to implement and test the path planning strategies for the deposition trajectory control. An overview of the hardware conditioning is explained. A machine and control were developed to test the concept system for implementing a proposed strategy for increasing the deposition trajectory continuity, as an example of additive manufacturing. The path planning strategy was integrated and evaluated, resulting in an improved trajectory continuity, overall better performance, and an increased path continuity. Optimization of path trajectories improves mechanical properties and reduces defects, creating better products.

Keywords: Additive manufacturing, path planning, Fused Deposition Modeling, trajectory continuity.

1. INTRODUCTION

Although the idea of 3D printing has been known for decades (Inc, 1989), in the 1980s, rapid prototyping was introduced, focusing on the creation of physical models to verify design test concepts, visual aids, form-fitting checks, and get manufacturing validation. Since then, many additive manufacturing (AM) processes have been developed and commercially distributed. One of the most commonly known and documented is the Fused Deposition Modeling (FDM), also known as Fused Filament Fabrication (FFF). By using AM, three-dimensional (3D) workpieces are fabricated directly from computer-aided design (CAD) models, built layer by layer, allowing a flexible manufacturing process capable of producing complex geometries with relative simplicity (Guo & Leu, 2013).

FFF technology has several advantages. It is flexible enough to be used on a wide range of machine systems, in this case, set on a 3-axis Gantry system. Overall, it has low input energy and a relatively low material cost, which gives a cost-effective process (Ning et al., 2015). Several groups of materials are compatible depending on the hardware working temperature.

Co-funded by the Erasmus+ Programme of the European Union

Co-funded by the Erasmus+ Programme of the European Union

The layer upon layer deposition has inherent disadvantages, such as having limited mechanical performance. To overcome these limitations, 3D printed continuous fiber reinforcement composites (CFR) (Mark & Gozdz, 2014) have been integrated into AM processes, and different techniques have been developed where a reinforced fiber is combined with a polymer that serves as a matrix. These techniques have shown improved mechanical properties, similar to aluminum, raising the interest for the potential application (Naranjo-Lozada et al., 2019), and expanding the growing necessity in controlling process parameters for improving the CFR mechanical properties or reducing the fabrication cost and time (Baumann et al., 2017; Dickson et al., 2017).

According to Shafighfard et al. (2019), fiber discontinuities are inevitable in many composite material applications, depending on the used algorithm. The fiber discontinuities reduce the strength capacity of a workpiece due to the lack of material between segments, which leads to a decrease of the stiffness and a stress concentration in the vicinity of these discontinuities (Anitha Priyadharshani et al. , 2017; Hao et al., 2018). The algorithm, which must be carefully selected by the designer depending on the application, is used by the slicer software, which slices the CAD model in polygons layer by layer and then generates the trajectories in the form of G-Code instructions for the machine system to follow.

Tensile properties and failure behavior analysis of probes with chopped and continuous carbon fiber composites produced by AM have been the subject of studies (Naranjo-Lozada et al., 2019). The study was done by selecting different infill density and infill pattern geometry and found that AM fiber-reinforced composites are characterized by their closely related tensile properties with the amount of reinforcement fiber and defined internal geometry.

Although Naranjo's findings (2019) linked better tensile properties when the fiber reinforcement was increased and the triangular infill pattern was selected, the available user-changeable process parameters were restricted to the 3D printer limitations, a common problem on commercial systems. Hence, features such as the continuity of the reinforcement fiber or the toolpath generation could not be controlled for research of relevant case studies, creating a bottleneck on improving workpiece properties. This work focused on improving the quality of FFF products.

With these considerations, this document details the integration of a proof of concept system that allows the user to control the deposition trajectory to increase the capacity to explore different strategies that could benefit the workpiece production. Further, a strategy to improve the deposition trajectory continuity is proposed and implemented on the adapted system.

This article is organized as follows. Section 2 describes de objectives of this work. Section 3 presents a literature review for strategies to improve different AM process related issues. Section 4 details the methodology followed to solve the technical challenges of this project. Section 5 presents the results from a case study to improve the trajectory continuity from a post-processed Gcode file. Section 6 summarizes the conclusions. Finally, in Section 7 several recommendations are given for improving the obtained results and future work to follow is proposed.

Co-funded by the Erasmus+ Programme of the European Union

2. OBJECTIVES

The objective of this work is to develop a system that allows the user to control the deposition trajectory for increasing the capacity to explore different strategies that could benefit the workpiece production. In particular:

- Development of a positioning AM system to:
  - Identify areas of opportunity from slicer's generated GCode.
  - Implementing the proof of concept strategy.

- The path planning strategy must aim to:
  - Reduce the number of segments.
  - Increasing the fiber continuity.
  - Evaluate and compare differences in performance.

3. LITERATURE REVIEW

Extensive research has been done to attend issues linked to the toolpath generation.
Xiaomao et al. (2011) identified that the start point and endpoints from the contour trajectory generate filling artifacts that decrease the surface quality and may cause severe problems in appearance and quality applied to processes such as plasma welding and FDM. They aimed to reduce the filling defect by proposing a path planning algorithm that moves the start point and endpoint of the contour trajectory into the infill region, diminishing the filling defects.

To reduce the number of sharp corners, which are linked to low quality and high printing time, Jin et al. (2015) approached a parallel-filling path generation based on adaptive gaps between the contour and the internal toolpath, depending on the space in-between.

For improving the deposition quality and surface finish of printed parts, in another article written by some of the same authors, Jin et al. (2017), attempted to solve the sharp corners and non-uniform spacing between adjacent path elements, by using an algorithm derived from the level set of the input contours, as these problems cause irregularities on the deposited surface.

Another common problem in surface quality is the stair-step artifact that causes a rough printing finish, especially when the slope of the contour is close to horizontal. Ahlers (2019) proposes the combination of nonplanar and planar layers for obtaining smoother surfaces. The toolpath is then generated by the same open-source slicer used in this project, Slic3r, and printed with a commercial 3D printer.

Similarly, Jin et al. (2016) aimed to solve the stair-step artifact by implementing an adaptive slicing strategy that adjusted the thickness distribution of each layer based on the inclination of the curve of the model at a certain height using an Insight software (Stratasys Inc.). The purpose of their research was to not only address the surface quality, but also aimed to increase the structural strength of their product, which is an ankle-foot-orthosis. They sought this, by generating for layers with narrow and long cross-sectional shapes a wavy toolpath, as an infill and substitute to a direction-parallel toolpath.

Liu et al. (2018) propose a purely theoretical methodology that integrates optimal hybrid deposition paths. They use contour path planning to support the zigzag and contour-offset deposition path

Co-funded by the Erasmus+ Programme of the European Union

patterns, to improve the structural performance with shape and topology optimization in a level set framework.

From the path planning perspective and on relatively large-volume solid parts, Jiang et al. (2019) try to reduce the material consumption and save time, by proposing an algorithm for reducing the cases of overfilling on the layers' toolpaths. For this, they follow two steps: Generate initial contour parallel paths based on the desired space between these parallel contours and the input polygon, and analyze and identify the possible overfilling and underfilling cases to optimize the paths. Giberti et al. (2017) also treat the process time optimization by proposing Bezier curves in the path planning algorithm to assure a regulated velocity.

When the nozzle is traveling between deposition points, also called idle trajectories, a lot of time inefficiencies arise, thus, Weidong (2009) proposes an optimal path planning based on a Genetic Algorithm for linking points with shorter distances between different objects on the printing bed. Fok et al. (2017) propose a refinement process for the undirected rural postman problem (URPP) algorithm applied for 3D printing, tackling the same problem. As well, Wah et al. (2002) sought to reduce the time wasted in straight-line motion by proposing a new strategy that combines the Asymmetric Traveling Salesman Problem and the Integer Programming to solve it.

Jin et al. (2014) developed a strategy for enhancing the milling efficiency and fabrication precision by optimizing the parallel-paths' inclination from the interior infill. The optimized path was found by iterating with different inclinations and selecting the best candidate according to the build time and the overfill and underfill area from a specific layer.

All the research papers previously presented different address issues that, once solved, the algorithm satisfies with the intended application. However, none of these algorithms addresses the issue presented in this document, which is to develop strategies to improve deposition continuity and part strength. Nevertheless, several authors addressed the issue of avoiding tool's retraction, which is beneficial for the enhancement of the deposition quality and the process efficiency. Jin et al. (2017) presented a path planning strategy called "go and back" that generates continuous paths for simple areas by connecting the start point to the endpoint to decrease the number of startups and shutdowns of the extruder. Park et al. (2003) developed a contour parallel offset toolpath linking algorithm to avoid the same issue.

Zhao et al. (2016) proposed a new fill pattern called 'Fermat spirals' which could connect a 2D region with a continuous path. Tang et al. (1998) pointed out that the tool retraction was an important problem in zigzag pocket milling; thus, they proposed optimizing the local and global minimization of the number of retractions in the toolpath. Elber et al. (2006) presented a strategy to construct a C1 continuous toolpath for a 5-axis machine by using circular and linear segments to generate the continuous toolpath.

Dwivedi and Kovacevic (2004) proposed a method to generate a continuous toolpath, applied in FDM. They do this by subdividing the 2D polygonal section into a set of monotone polygons, making a zigzag path for each sub-polygon, and then joining the sub-paths to each other to have the final toolpath. Ding et al. (2014), applied a strategy for wire and arc manufacturing, where 2D geometry is decomposed into a group of polygons to generate a continuous toolpath for each polygon, after the optimal direction is identified, then all the closed sub-paths are connected to form a closed curve.

Co-funded by the Erasmus+ Programme of the European Union

4. METHODOLOGY

To give a deeper insight into the technical challenges of this project, first, we present the overall AM process workflow (Figure 2). The AM sequence starts with the CAD model generation; this is exported as an STL file. The software slicer uses the STL file to generate the GCode file. This file is read by the control that drives the machine's motion and builds the part or product.

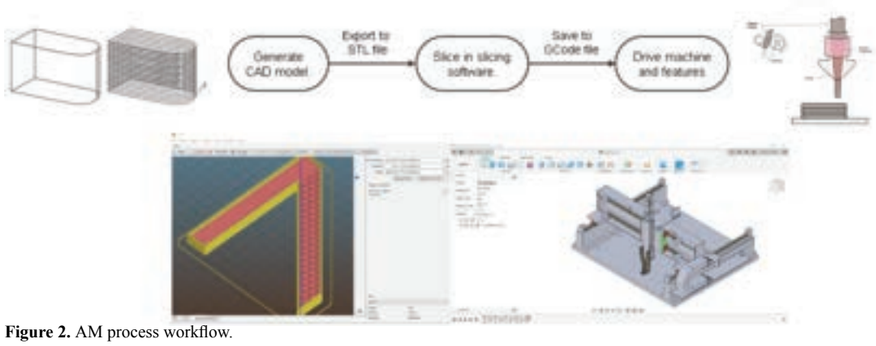

Figure 2. AM process workflow.

The technical challenges of this project lie in the final section of the AM workflow (Figure 3), on the post-processing of the slicer-generated GCode file, and driving the machine and the features for doing the test.

The challenge of driving the machine and its features, was due to the system's attribute of being customed to our necessities and integrated by several external components. Several modifications were made to the core files of the Machinekit distribution used on the controller, a Beaglebone Black Industrial, in order to be able to actuate the motors' drivers.

From the challenges on the post-processing of the Gcode file, before proposing an approach to improve the deposition algorithm, it was of most importance to analyze and identify the areas of opportunity of the generated trajectory. Once it was identified, a proof of concept strategy was formulated to improve the deposition continuity, due to its relation to the improvement of the workpiece mechanical properties (Naranjo-Lozada et al., 2019), choosing a specific approach to fill the deposition intermittence.

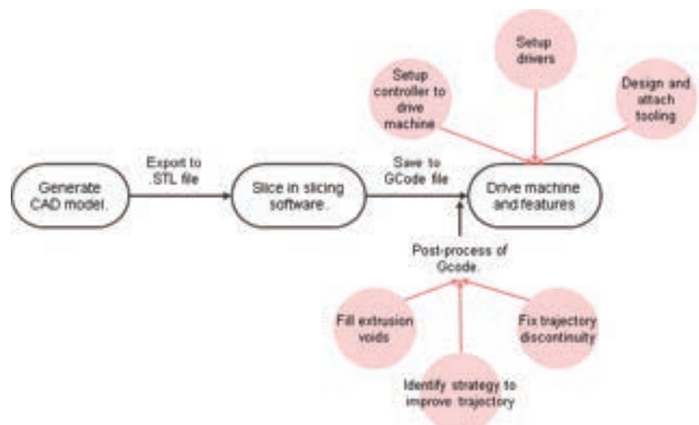

Figure 2: AM process workflow.

Co-funded by the Erasmus+ Programme of the European Union

Several distinctive characteristics of the proof of concept system overcome the commercial system limitations. Most of these systems have a closed-source platform and the performance parameters displayed to the user are limited and can not be changed. It is difficult to adapt new sensors or actuators to these systems. The variety of options to change the deposition trajectory is very low, and for this same reason, there is almost no insight into the trajectory algorithm strategy used. One last aspect is that the commercial system does not consider the mechanical properties of the workpiece.

With the open-source platform implemented in the proposed system, it is easier to integrate external user's code routines mostly in Python or C, and the GUI panel can be customized to display performance variables and process indicators. The proposed system is flexible to integrate more hardware elements into the system, and the GCode post-processing later explained allows modifying the toolpath to implement the desired strategy.

4.1. System Integration on the Case Solution

Although the slicing software used is open-source, and the source code can be modified and compiled to a new version, due to the available time, a post-processing of the GCode file was implemented in order to focus the efforts on the proof of concept testing of the machine system, the software framework, and the toolpath strategy.

For the post-processing, to identify the areas of opportunity of the slicer-generated toolpath, several GCode simulators were explored, and the produced simulation was not enough to give an insight into the path planning algorithm sequence. A common deficit was in describing the direction and sequence of the trajectory. Thus, a GCode simulator was coded in Matlab to help identify strategies to improve the trajectory performance.

The Matlab simulator was coded in three different files

Test.m to:

- Initialize parameters
- Call for another method or function.

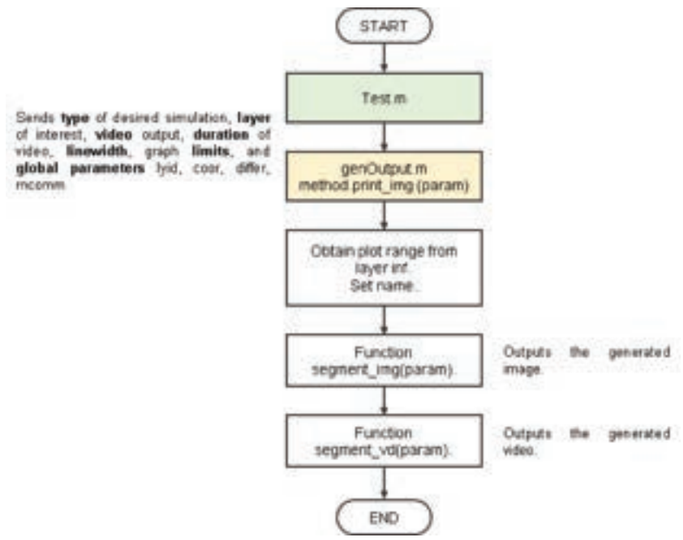

Figure 4: Flow diagram of the main code file for generating the image and video assets.

Co-funded by the Erasmus+ Programme of the European Union

The European Commission support for the production of this publication does not constitute an endorsement of the contents which reflects the views only of the authors, and the Commission cannot be held responsible for any use which may be made of the information contained therein. Project number: 585796-EPP-1-2017-1-AT-EPPKA2-CBHE-JP

GCodeProcessing.m to:

- Identify G commands (G1, G92) from GCode text file.
- Create a variable and file with coordinates, rate speed, and extrusion (X, Y, Z, F, A).
- Identify the different layers, and isolate a layer or section of interest.

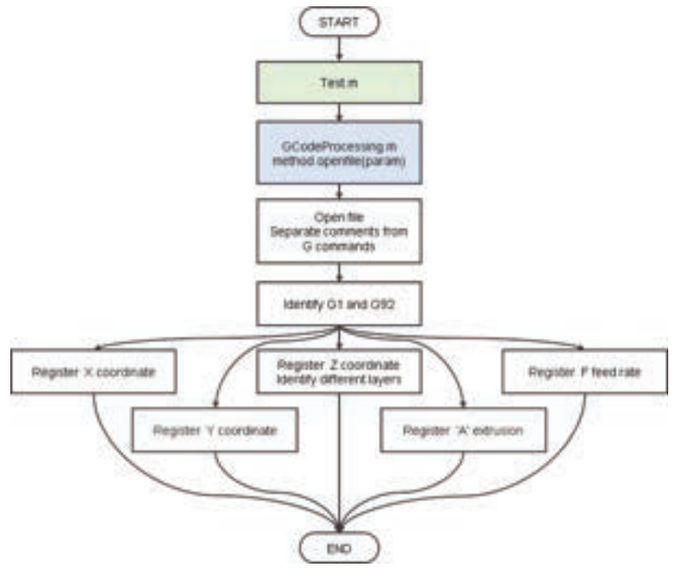

Figure 5: Simplified diagram of how the data is collected from the text file.

genOutput.m to:

- Identify the difference between depositing trajectories and 'idle' trajectories.
- Calculate process parameters (distance traveled, process time, and deposition discontinuities.
- Indicate trajectory direction.
- Create
  - An image.
  - A video.
- Fill the extrusion voids.
- Join two segments with an arc

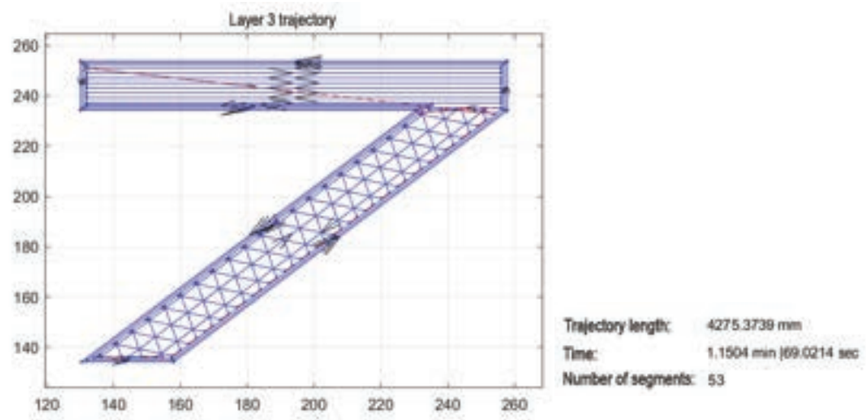

Figure 6. Image output of the selected layer from the case of study. The video output can be found in the next link: shorturl.at/jvNRU

Co-funded by the Erasmus+ Programme of the European Union

The European Commission support for the production of this publication does not constitute an endorsement of the contents which reflects the views only of the authors, and the Commission cannot be held responsible for any use which may be made of the information contained therein. Project number: 585796-EPP-1-2017-1-AT-EPPKA2-CBHE-JP

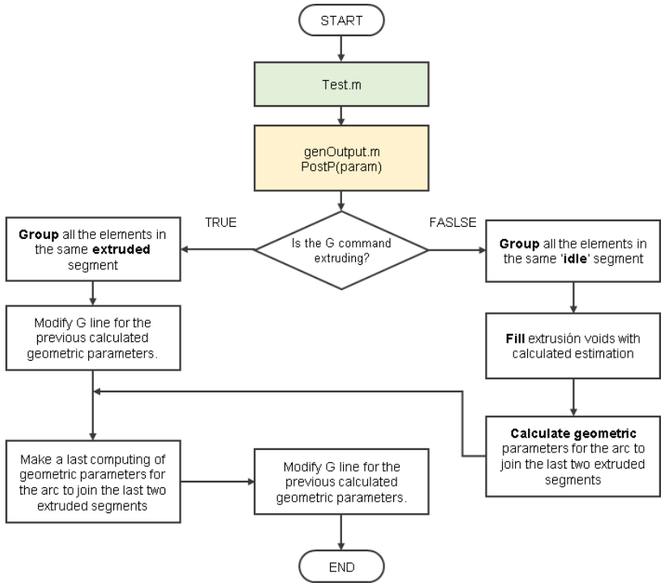

Figure 7: Simplification of the sequence of modifying the GCode file to comply with the proposed strategies.

From observing the generated toolpath, two main issues are identified and will be addressed: the filling of extrusion voids and the joining of trajectory discontinuities.

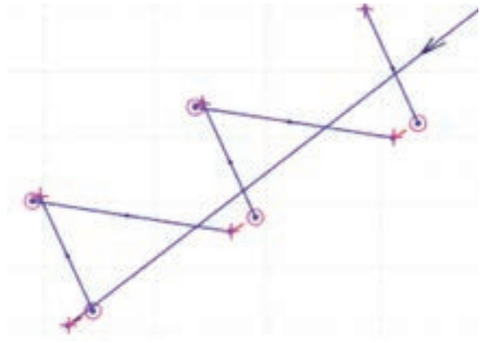

Figure 8: Section of the infill trajectory. Several discontinuous segments are shown.

4.2 Filling of Extrusion Gaps

The issue is that when joining two toolpaths previously linked by an ‘idle’ segment with no material deposition, there is no information about the extrusion values that must exist between paths. When the discontinuity is fixed with an arc, the G2/G3 command must have the extrusion value ‘A’ to work.

Thus, the strategy used to solve this is by adding to the last segment’s last deposition, the difference of the first deposition of the new segment, and the last deposition of the last segment divided by the number of elements that are ‘idle’. This gives a value that increases from the last value to the first value. The procedure is shown in Figure 9

Co-funded by the Erasmus+ Programme of the European Union

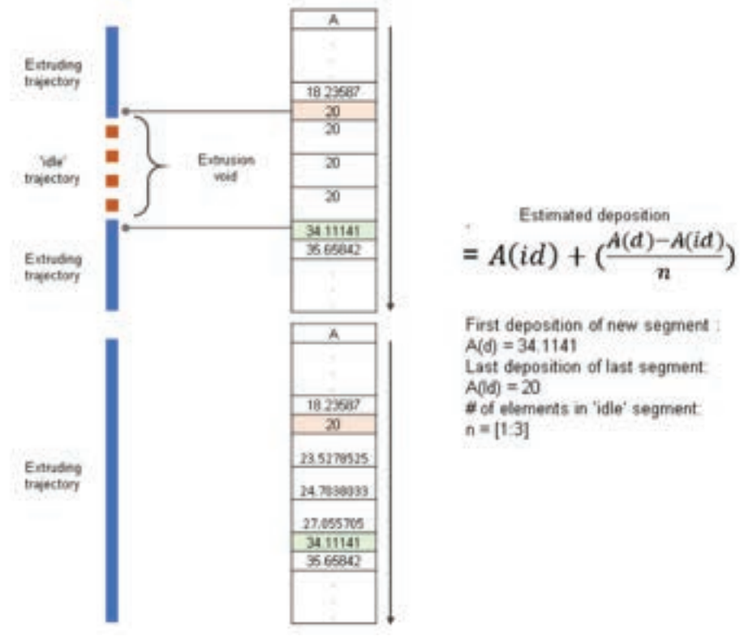

Figure 9: Example of the strategy for filling the extrusion void.

4.3 Joining two Neighbour Segments with an Arc

The deposition discontinuities appeared when going from the contour to the infill, changing the infill pattern (from rectangular to triangular), and in the sub-paths elements of the triangular infill.

When having a trajectory formed by two deposition trajectories joined by an ‘idle’ segment, which causes the discontinuity on the trajectory, the strategy proposed is to substitute the ‘idle’ segment with an arc tangent to both deposition trajectories and to the ‘idle’ segment too.

To do this, using the geometry shown in Figure 10. the slopes from the deposition segments are calculated, and the intersection Pc is computed. With that coordinate, and using the triangle bisector, a procedure, shown in Figure 11, with the angles and trigonometric properties is calculated for computing the points A1 and A2 and the circle radius. A1 and A2 are needed, for setting the new coordinate in the G command instead of using P1 and P2.

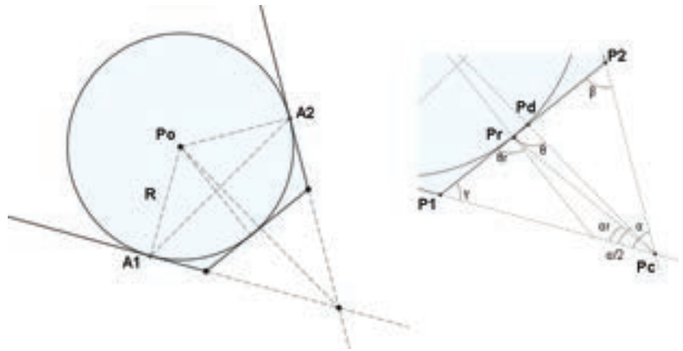

Figure 10. Geometric analysis for calculating necessary parameters.

Co-funded by the Erasmus+ Programme of the European Union

Since for creating the arc using G2 or G3, one of the formats is to use the start (A1) and end (A2) points, and the radius of the circle, all the necessary data is already known.

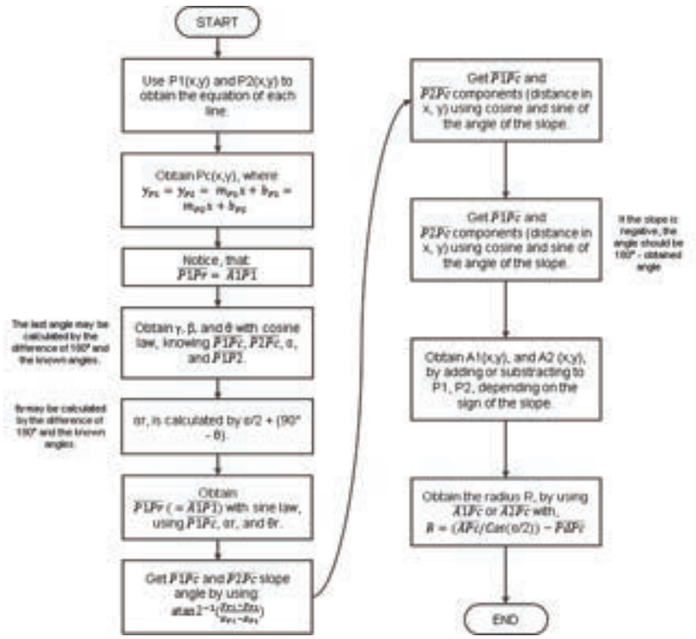

Figure 11: Parameter calculation diagram for joining segments.

5. RESULTS

For testing concepts, an end tool fixture was built and used to draw the commanded trajectories on paper, which was mounted on the 'Z' axis block, traveling along the ballscrew. To reach the base of the system and displace the workspace, a fixture was designed, simulated, printed, and attached to the 'Z' axis (Figure 12).

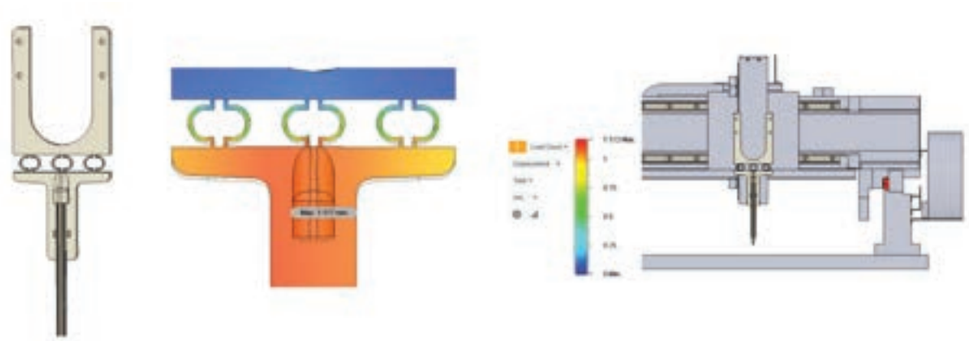

Figure 11: Parameter calculation diagram for joining segments.

The fixture was printed by the commercial printer Markforged Mark 2 in a nylon composite (Onyx). It was integrated with a complaint mechanism (Figure 12) that damps the tool impact when touching the machine's base, and assures a constant force to draw on the sheet.

Co-funded by the Erasmus+ Programme of the European Union

The European Commission support for the production of this publication does not constitute an endorsement of the contents which reflects the views only of the authors, and the Commission cannot be held responsible for any use which may be made of the information contained therein. Project number: 585796-EPP-1-2017-1-AT-EPPKA2-CBHE-JP

A section of the infill from the slicer-generated GCode file was used to test the strategy to increase the deposition trajectory's continuity. The original file and the modified were processed by two different simulators. The trajectory is shown in Figure 13, after the strategy was applied, the discontinuities were eliminated.

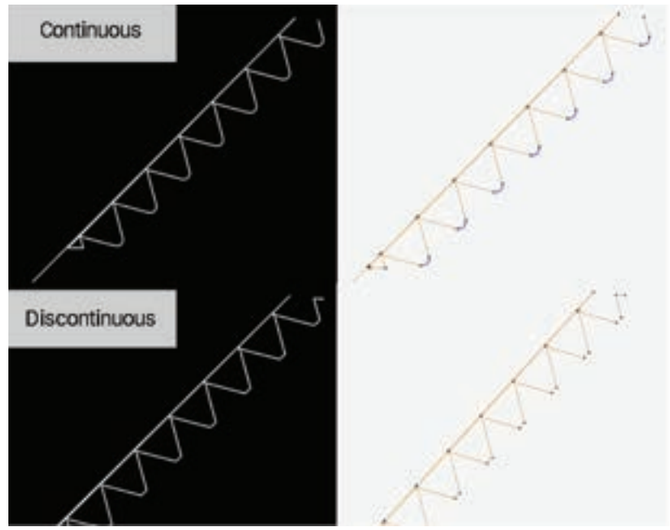

Figure 13. Simulated trajectories. Done on the simulator Webgcode (left), ncviewer.com (right)

Using an online GCode-simulator (https://www.gcodeanalyser.com/) several parameters were computed. The results are shown in Table 1, and graphed in bar plots.

Parameter	*Original*	*Modified*
Print time (ms)	146	140
Distance accelerating / desaccelerating (m)	0.46	0.45
Distance at target speed (m)	0.65	0.67
Average speed (mm/s)	74.9	75.8
Move commands reached target speed (%)	45.9	46.6
# Segments	8	3

Table 1: Resulting parameters computed.

The number of segments was reduced to less than half the original value.
Most of the improvements were marginal to the original values, but demonstrated that by having a system with the capabilities to allow the user to control and change the path planning strategies, process and workpiece parameters could be improved.

The distance accelerating or decelerating was improved by a 2.2%, and the average speed was improved by 1.2%, meaning that the tool traveled more distance at its maximum speed than the original file. The print time was reduced a 4.1%.

Co-funded by the Erasmus+ Programme of the European Union

The European Commission support for the production of this publication does not constitute an endorsement of the contents which reflects the views only of the authors, and the Commission cannot be held responsible for any use which may be made of the information contained therein. Project number: 585796-EPP-1-2017-1-AT-EPPKA2-CBHE-JP

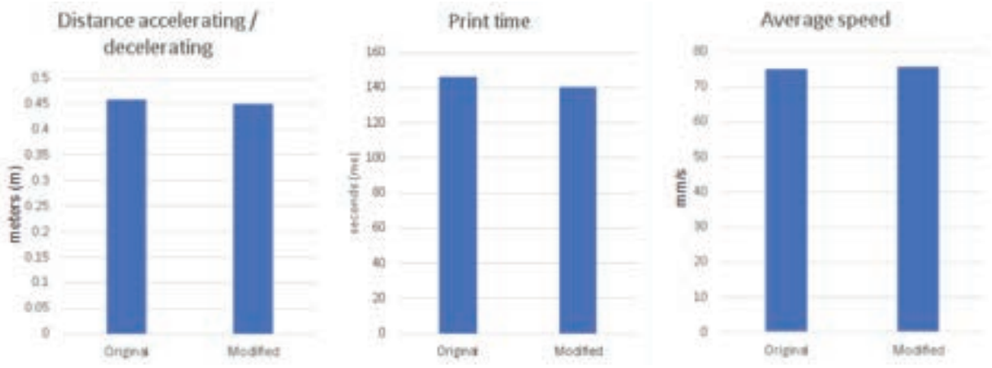

Figure 14: Distance accelerating/decelerating improved by 2.2%. Average speed improved by 1.2%. Print time was improved by 4.1%.

The number of discontinuous segments in the selected infill section was reduced from 8 segments to 1 segment, an improvement of 87.5%. When selecting the whole infill sequence instead of just this section, the improvement was from 51 segments to 3 segments, a 94.1% improvement. The distance at target speed was improved a 3.1%, and the move commands that reached this target speed improved by 1.5%, meaning that there was less intermittence in the extrusion sequence.

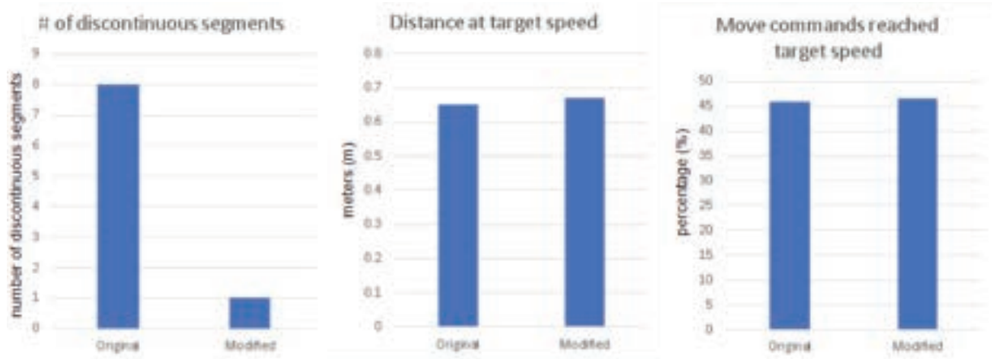

Figure 15: The number of segments was improved by 87.5%. The distance at the target speed improved by 3.1%. The move commands that reached the target speed improved by 1.5%.

The results showed a relevant improvement in trajectory continuity and a marginal improvement in the rest of the parameters.

The test of the working system consisted of drawing the trajectory on paper. The modified toolpath strategy worked well in the novel system. In Figure 16, the drawn path is shown. The evidence video can be checked at this link: https://youtu.be/2VBkKiphaFQ

Co-funded by the Erasmus+ Programme of the European Union

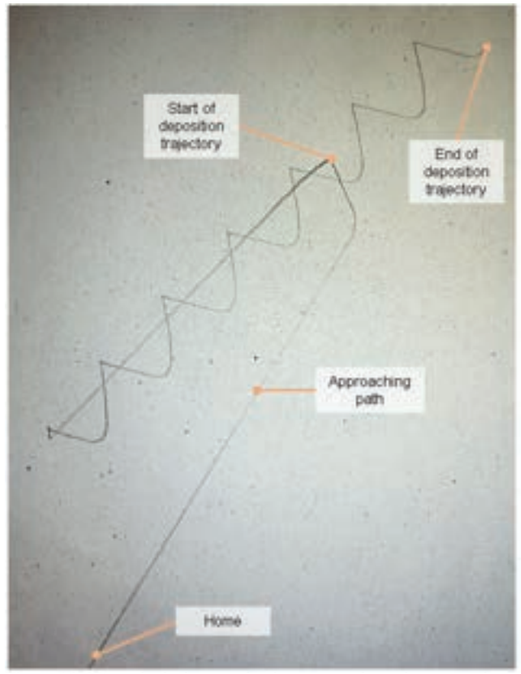

Figure 16: 2D result, the improved trajectory was drawn in a paper sheet.

Radius	Value
R1	3,4 mm
R2	3,2 mm
GCode	2.7 mm

Figure 16: 2D result, the improved trajectory was drawn in a paper sheet.

The findings to enhance the performance of the toolpath strategy is to make a better estimation of the extrusion parameter ‘A’, as the computed value does not take into consideration the material flux needed. The proposed technique for filling the deposition gaps between trajectories was just to have an increasing ‘A’ value until the original value is reached, in an actual deposition sequence, the speed and material flow must be considered for computing this parameter.

Since the proposed strategy uses the intersection of the two slopes to find the parameters, the case of joining parallel paths must be considered due to a non-existent intersection Pc.

Co-funded by the Erasmus+ Programme of the European Union

6. CONCLUSIONS

As proof of concept, the adapted system could control the deposition trajectory and flexible to adapt to new components. With the system, the designer must now be able to test different path planning strategies and choose process parameters that in commercial systems are not accessible.
The GCode simulator developed in matlab, aided on the identification of areas of opportunity for the generated slicer's GCode file. The trajectory insight given by this tool could not be obtained from other explored simulators, and the possibility to add new features of interest increases its importance.
The path planning strategy was integrated and evaluated, resulting in an improvement on the trajectory continuity, having an overall better performance. However, the differences are marginal with the exception of the number of segments, which were significantly reduced, increasing the path continuity.

7. RECOMMENDATIONS

The Matlab-GCode simulator could be implemented in an open-source platform (Python) to not depend on the Matlab license. As well, the path planning strategy could be coded directly to the slicer's source code. In Slic3r, by using the variables generated from the .STL file, a deeper Insight to the used algorithm could help for having more data from the slicing process to improve the GCode before is generated than depending on the post-processing results.

Other path planning techniques can be explored, instead of joining the segments with arcs, the same infill could be used, but with a different path strategy, working with the deposition direction and sequence to measure the effect on the mechanical properties.

While trying to simulate the trajectory, it was found a pattern that most of the simulators, including the GCode generated by Slic3r does not use G2 or G3, only a G1 approximation. Then, an implementation of G1 move command is easier to implement from the coding perspective and more accepted on simulators.

For getting closer to the implementation of the toolpath strategies on AM workpieces, the system must be able to produce the trajectory with actual composite material. For this, the fixture and tool for drawing in the paper sheet must be substituted by the extruder and hot-end. By making composite workpieces, strength tests can be done, and more knowledge about how to improve the mechanical properties for AM can be obtained.

One possible improvement to the positioning system is to tune the gains and filter parameters, avoiding using the auto-tune and auto-phase center on the driver's software. The designer can have more control in the control-loop and machine response.

Additionally, using the system's characteristic of being flexible for implementing external components in hardware and software, the system could be adapted for an IoT network and Implement cloud communication for adapting the system further to Industry 4.0.

Co-funded by the Erasmus+ Programme of the European Union

REFERENCES

Ahlers, D., Wasserfall, F., Hendrich, N., & Zhang, J. (2019). 3D printing of nonplanar layers for smooth surface generation. *IEEE International Conference on Automation Science and Engineering,* 2019-Augus(October 2018), 1737–1743. https://doi.org/10.1109/COASE.2019.8843116

Anitha Priyadharshani, S., Meher Prasad, A., & Sundaravadivelu, R. (2017). Analysis of GFRP stiffened composite plates with rectangular cutout. *Composite Structures,* 169, 42–51. https://doi.org/10.1016/j.compstruct.2016.10.054

Baumann, F., Scholz, J., & Fleischer, J. (2017). Investigation of a New Approach for Additively Manufactured Continuous Fiber-reinforced Polymers. In Procedia CIRP (Vol. 66, pp. 323–328). Elsevier B.V. https://doi.org/10.1016/j.procir.2017.03.276

Dickson, A. N., Barry, J. N., McDonnell, K. A., & Dowling, D. P. (2017). Fabrication of continuous carbon, glass and Kevlar fibre reinforced polymer composites using additive manufacturing. *Additive Manufacturing,* 16, 146–152. https://doi.org/10.1016/j.addma.2017.06.004

Ding, D., Pan, Z., Cuiuri, D., & Li, H. (2014). A tool-path generation strategy for wire and arc additive manufacturing. *International Journal of Advanced Manufacturing Technology,* 73(1–4), 173–183. https://doi.org/10.1007/s00170-014-5808-5

Dwivedi, R., & Kovacevic, R. (2004). Automated torch path planning using polygon subdivision for solid freeform fabrication based on welding. *Journal of Manufacturing Systems,* 23(4), 278–291. https://doi.org/10.1016/S0278-6125(04)80040-2

Elber, G., Cohen, E., & Drake, S. (2006). C1 Continuous Toolpath Generation Toward 5-axis High Speed Machining. *Computer-Aided Design and Applications,* 3(6), 803–810. https://doi.org/10.1080/16864360.2006.10738433

Fok, K. Y., Cheng, C. T., & Tse, C. K. (2017). A refinement process for nozzle path planning in 3D printing. Proceedings - *IEEE International Symposium on Circuits and Systems,* 0–3. https://doi.org/10.1109/ISCAS.2017.8050471

Giberti, H., Sbaglia, L., & Urgo, M. (2017). A path planning algorithm for industrial processes under velocity constraints with an application to additive manufacturing. *Journal of Manufacturing Systems*, 43, 160–167. https://doi.org/10.1016/j.jmsy.2017.03.003

Guo, N., & Leu, M. C. (2013). Additive manufacturing: Technology, applications and research needs. *Frontiers of Mechanical Engineering,* 8(3), 215–243. https://doi.org/10.1007/s11465-013-0248-8

Hao, P., Liu, C., Liu, X., Yuan, X., Wang, B., Li, G., … Chen, L. (2018). Isogeometric analysis and design of variable-stiffness aircraft panels with multiple cutouts by level set method. *Composite Structures,* 206, 888–902. https://doi.org/10.1016/j.compstruct.2018.08.086

Inc, S. (1989). United States Patent (19) Crump (54) APPARATUS AND METHOD FOR CREATING THREE-DIMENSIONAL OBJECTS.

Jiang, J., Xu, X., & Stringer, J. (2019). Optimization of process planning for reducing material waste in extrusion based additive manufacturing. *Robotics and Computer-Integrated Manufacturing,* 59, 317–325. https://doi.org/10.1016/j.rcim.2019.05.007

Jin, Y., He, Y., Xue, G. H., & Fu, J. Z. (2015). A parallel-based path generation method for fused deposition modeling. *International Journaal of Advanced Manufacturing Technology,* 77(5–8), 927–937. https://doi.org/10.1007/s00170-014-6530-z

Jin, Y., He, Y., Fu, J. zhong, Gan, W. feng, & Lin, Z. wei. (2014). Optimization of tool-path generation for material extrusion-based additive manufacturing technology. *Additive Manufacturing,* 1, 32–47. https://doi.org/10.1016/j.addma.2014.08.004

Jin, Y., Du, J., Ma, Z., Liu, A., & He, Y. (2017). An optimization approach for path planning of high-quality and uniform additive manufacturing. *International Journal of Advanced Manufacturing Technology,* 92(1–4), 651–662. https://doi.org/10.1007/s00170-017-0207-3

Jin, Y., He, Y., Fu, G., Zhang, A., & Du, J. (2017). A non-retraction path planning approach for extrusion-based additive manufacturing. *Robotics and Computer-Integrated Manufacturing, 48*(December 2016), 132–144. https://doi.org/10.1016/j.rcim.2017.03.008

Jin, Y., He, Y., & Shih, A. (2016). Process Planning for the Fuse Deposition Modeling of Ankle-Foot-Othoses. *Procedia CIRP, 42*(Isem Xviii), 760–765. https://doi.org/10.1016/j.procir.2016.02.315

Liu, J., Ma, Y., Qureshi, A. J., & Ahmad, R. (2018). Light-weight shape and topology optimization with hybrid deposition

Co-funded by the Erasmus+ Programme of the European Union
The European Commission support for the production of this publication does not constitute an endorsement of the contents which reflects the views only of the authors, and the Commission cannot be held responsible for any use which may be made of the information contained therein. Project number: 585796-EPP-1-2017-1-AT-EPPKA2-CBHE-JP

path planning for FDM parts. *International Journal of Advanced Manufacturing Technology,* 97(1–4), 1123–1135. https://doi.org/10.1007/s00170-018-1955-4

Mark, G. T., & Gozdz, A. S. (2014). Apparatus for fiber reinforced additive manufacturing. *Markforged Inc.*

Naranjo-Lozada, J., Ahuett-Garza, H., Orta-Castañón, P., Verbeeten, W. M. H., & Sáiz-González, D. (2019). Tensile properties and failure behavior of chopped and continuous carbon fiber composites produced by additive manufacturing. *Additive Manufacturing, 26*(December 2018), 227–241. https://doi.org/10.1016/j.addma.2018.12.020

Ning, F., Cong, W., Qiu, J., Wei, J., & Wang, S. (2015). Additive manufacturing of carbon fiber reinforced thermoplastic composites using fused deposition modeling. *Composites Part B: Engineering, 80*, 369–378. https://doi.org/10.1016/j.compositesb.2015.06.013

Park, S. C., Chung, Y. C., & Choi, B. K. (2003). Contour-parallel offset machining without tool-retractions. *CAD Computer Aided Design, 35*(9), 841–849. https://doi.org/10.1016/S0010-4485(02)00111-2

Shafighfard, T., Demir, E., & Yildiz, M. (2019). Design of fiber-reinforced variable-stiffness composites for different open-hole geometries with fiber continuity and curvature constraints. Composite Structures, 226(May), 1–14. https://doi.org/10.1016/j.compstruct.2019.111280

Tang, K., Chou, S. Y., & Chen, L. L. (1998). An algorithm for reducing tool retractions in zigzag pocket machining. *CAD Computer Aided Design, 30*(2), 123–129. https://doi.org/10.1016/S0010-4485(97)00064-X

Wah, P. K., Murty, K. G., Joneja, A., & Chiu, L. C. (2002). Tool path optimization in layered manufacturing. *IIE Transactions (Institute of Industrial Engineers), 34*(4), 335–347. https://doi.org/10.1080/07408170208928874

Weidong, Y. (2009). Optimal path planning in rapid prototyping based on genetic algorithm. *2009 Chinese Control and Decision Conference, CCDC 2009*, 5068–5072. https://doi.org/10.1109/CCDC.2009.5194966

Xiaomao, H., Chunsheng, Y., & Yongjun, H. (2011). Tool path planning based on endpoint build-in optimization in rapid prototyping. *Proceedings of the Institution of Mechanical Engineers, Part C: Journal of Mechanical Engineering Science, 225*(12), 2919–2926. https://doi.org/10.1177/0954406211411643

Zhao, H., Gu, F., Huang, Q. X., Garcia, J., Chen, Y., Tu, C., … Chen, B. (2016). Connected fermat spirals for layered fabrication. *ACM Transactions on Graphics, 35*(4), 1–10. https://doi.org/10.1145/2897824.2925958

Co-funded by the Erasmus+ Programme of the European Union

The European Commission support for the production of this publication does not constitute an endorsement of the contents which reflects the views only of the authors, and the Commission cannot be held responsible for any use which may be made of the information contained therein. Project number: 585796-EPP-1-2017-1-AT-EPPKA2-CBHE-JP

CHULA ENGINEERING
Foundation toward Innovation

INTRODUCTION OF CONNECTED AND AUTONOMOUS VEHICLE R&D IN THAILAND

AssOC.Prof. Witaya Wannasuphoprasit[1]
Asst. PRof. Nuksit noomwongs[2]

[1]International School of Engineering
[2]Department of Mechanical Engineering,
Chulalongkorn University Bangkok, THAILAND

CHULALONGKORN UNIVERSITY Department of Mechanical Engineering
ISE: International School of Engineering
Faculty of Engineering
Phayathai Road
Pathumwan, Bangkok 10330
https://www.eng.chula.ac.th/en/

Dr. Witaya and Dr. Nuksit are both employed at the most prestige university in Thailand, Chulalongkorn University since 2000.

Their research interest includes: Vehicle Dynamics and Control, Robotics, Collaborative Robots, Hardware-in-the-Loop Simulator (HILS), Driving Simulator, Automotive Engineering, Student formula car development, Eco and Safety Driving, ITS and Vehicle Active Safety, EV and Hybrid vehicle, Rolling Stock Engineering

Thailand is an important manufacturer of motor vehicles, ranking 11th in the world in terms of vehicles produced (2020). It is also one of the largest producers of motorcycles and scooters. It is a matter of national proud the automotive and vehicle industry.
However, Thailand also ranks number 1 in Southeast Asia and number 9 globally for road deaths, with motorbikes being the largest cause of accidents, mainly because of reckless driving. Therefore, a lot of work is being done to increase safety and reduce accidents.
Traffic congestion is another big problem, particularly in the cities, where it contributes significantly to dangerous air pollution.

The Easter Economic Corridor (EEC) that has been developed in recent years, is becoming an important hub for technological development and innovation. In this context Chulalongkorn University has an important role working in topics such as 5G networks, robotics and smart mobility. Regarding mobility there are important projects and initiatives within the university´s campus.

Co-funded by the Erasmus+ Programme of the European Union

The European Commission support for the production of this publication does not constitute an endorsement of the contents which reflects the views only of the authors, and the Commission cannot be held responsible for any use which may be made of the information contained therein. Project number: 585796-EPP-1-2017-1-AT-EPPKA2-CBHE-JP

Extensive work in connected and autonomous vehicles (CAVs) is also being developed in several institutions and companies across Thailand, for different purposes and environments. For example, forklifts to be used within industrial facilities, or AVs used for drug delivery within medical facilities, in contrast to vehicles intended to move people in less controlled environments. A recently developed Automotive and Tyre Testing, Research and Innovation Centre (ATTRIC) offers new opportunities for autonomous driving testing.

Several projects in CAVs are being developed at Chulalongkorn University. For example, a micro EV low cost autonomous driving vehicle, smart parking with a Toyota Hamo, and a teleoperated golf cart using 5G. It is important to remark the prominent role of software in this kind of vehicles.

The deployment of CAVs will require more extensive preparation than what is needed for purely electric vehicles because of the communication capabilities required through fast 5G networks, and also the regulatory framework necessary for using CAVS in real life situations.

Co-funded by the Erasmus+ Programme of the European Union

EVOLUTION & FUTURE HUMAN MOBILITY

Dr. Hermann Knoflacher

Vienna University of Technology, Austria
Institute of Transportation
Research Unit of Transport Planning and Traffic Engineering

Prof. DI Dr. techn. Hermann Knoflacher
Vienna University of Technology
Institute of Transportation
Research Unit of Transport Planning
and Traffic Engineering

Gußhausstraße 30/230
A-1040 Wien
Tel.: +43 1 58 801/231 23
https://www.fvv.tuwien.ac.at/home

Dr. Knoflacher completed degrees in civil engineering, geodesy and mathematics. Since 1985 he is head of the Institute for Transport Planning and is the current global pedestrian representative at the United Nations.

Dr. Knoflacher is well known for his criticism of excessive automobile usage and invented the “walkmobile”. According to Knoflacher, the walkmobile allows people to visualize the irrationality of urban motor traffic and its excessive land consumption.

Publications:
https://publik.tuwien.ac.at/publist.php?pers=122635&sort=3&inv=1

For most of their history, human beings have relied on themselves for mobility (walking and running). Later on came horse riding and, with the invention of the wheel, carts in different forms were possible. Mostly horse drawn, these vehicles allowed for moving greater amounts of people and goods over longer distances. It was only in the last couple of centuries that engines, first steam and later internal combustion ones, revolutionized human and goods mobility on the ground, with faster speeds and greater hauling capacity.

Through time, progress in technology led to individual motorized mobility using cars and, as income increased, the availability and ownership of cars incremented swiftly. Nowadays there is a large amount of cars in the world and that has caused a series of problems, particularly in the cities, where space tend to be limited.

Co-funded by the Erasmus+ Programme of the European Union

It could be extrapolated that more cars mean increased mobility and more opportunities. Also, that being able to move at more speed would mean more travel time savings. However, through time it has been evident that this is no necessarily the case. Too much cars within a city usually leads to congestion, thus reducing or even annulling some of the initial advantages of personal motorized mobility,

Different studies had evidenced several paradoxical effects of individual mobility using cars. For example, one person can certainly move faster in a car than walking, but that does not reflect in effective time saving for, saying, go shopping. The reason is that with more speed, people tend to go farther away, increasing the distance required to get the desired goods. So, in effect, travel time tends to remain constant.

In the last decades, an excess of cars has created big congestion problems in the cities, reducing speeds, and incrementing travel times and pollution. Even the handling of idle cars has become a big problem, requiring large amounts of space for public parking and for storage in residential buildings, for example. This situation is becoming unsustainable, so there is the need to rethink urban mobility, moving away from the car and favoring public transportation and alternative individual mobility, like bicycles.

It is also important to analyze with care new technologies for cars and transportation in general, in order to devise integral solutions. For example, switching from combustion engine cars to electric cars help with pollution, but does not help with the problem of congestion and many of the other problems of current cars.

As science has demonstrated, throughout evolution all species that used more space, resources and energy for the same purpose became extinct, often causing severe damage to other fellow creatures, sometimes irreversible. Human beings are still in a position to think and take actions that lead to a more sustainable future, particularly in urban environments, without losing sight of the need for a truly integral approach.

Co-funded by the Erasmus+ Programme of the European Union

CLIMATE-FRIENDLY LIFESTYLES & MOBILITY

Dr. Gerfried Jungmaier

JOANNEUM RESEARCH
LIFE - Institute for Climate, Energy and Society
Graz, AUSTRIA

JOANNEUM RESEARCH LIFE – Institute for Climate, Energy and Society
Science Tower, Waagner-Biro-Str. 100,
A-8020 Graz, Austria
www.joanneum.at

DI Dr. Gerfried Jungmeier studied mechanical engineering at the University of Technology in Graz, Austria. As part of his dissertation, he dealt with the greenhouse gas balance of bioenergy (1999).

Dr. Jungmeier is scientific employee at the Institute for Energy Research of the Joanneum Research Forschungsgesellschaft mbH since 1993. Since 2002 Dr. Jungmeier Chairperson of Cost Action E31 “Management of Recovered Wood”.
His main research areas are: life cycle analyzes, energy from biomass, emissions and energy balances, sustainable energy systems. Dr. Jungmeier works on current national and international projects on topics: biofuels in the transport sector, hydrogen as a future energy carrier, waste wood and scenarios for sustainable energy systems.

Co-funded by the Erasmus+ Programme of the European Union

VIRTUAL AND AUGMENTED REALITY IN ENGINEERING

Javier Posselt, PhD

Specialist in VR and AR applications & interactions
Groupe Renault
Paris, FRANCE

Javier Posselt, PhD
1 avenue du Golf - 78084 GUYANCOURT Cedex
FRANCE

Javier Posselt studied mechanical engineering in Mexico and robotics in France.
As part of his dissertation, he dealt with robotics design.

His career path is exciting and today Mr. Posselt is responsible for the development and deployment of new digital platforms based on virtual and augmented reality technologies to prototyping and simulate the results of engineering design. He is member of "Autonomous Driving and Virtual Reality Center" team at RENAULT Technical Center.

The activity is divided into four estates:

1. R&D: technology watch, research new technologies and methods associated to immersive simulators and developing new use cases with costumers.
2. Validation, Industrialization, Deployment of solutions: integration of new technologies in the current standards of the company and create associated methods.
3. Evolution of platforms: push the limits of the technology and explore new uses cases.
4. Protocols of use: develop and validate standards in the engineering process and publish protocols of use and health rules of use for the users.

In an interesting way, some virtual, mixed and augmented reality techniques were shown, including the experience of the Renault company using these techniques, such as the CAVE IRIS project. Likewise, the reasons for the use of simulators in the industry were presented, among which the observation of the car in the real context, the subjective evaluations on a 1: 1 scale and finally the cost reduction stand out.

Co-funded by the Erasmus+ Programme of the European Union

URBAN LIVING LABS – NEW MOBILITY CONCEPTS

Dr. Oliver Lah

Wuppertal Institute
Head of Mobility and International Cooperation Research Unit

Dr. Oliver Lah
Wuppertal Institut für Klima, Umwelt, Energie gGmbH
Döppersberg 19
42103 Wuppertal
Germany
https://wupperinst.org/en/

Oliver has worked with international organisations, such as the OECD/ITF, UN-Habitat, UN Environment, UNDP and GIZ on urban mobility and climate change issues.
He was a lead author for the fifth IPCC Assessment Report and was a member of the Habitat III Policy Unit on Urban Services and Technology.

He teaches at the Erasmus University of Rotterdam and at the Technical University Berlin. Prior to that Oliver worked for the New Zealand government, the University of Munich and the Minister of State to the German Federal Chancellor. He holds a Bachelor of Arts with Honours in Political Science, a Master of Environmental Studies from Victoria University of Wellington and a PhD in Urban Ecology from Technical University. Further he coordinates the Urban Electric Mobility Initiative and the EU-funded SOLUTIONSplus flagship project on sustainable urban mobility in Europe, Asia, Africa and Latin America.

Co-funded by the Erasmus+ Programme of the European Union

STATUS OF AUTOMOTIVE INDUSTRY IN MEXICO AND ITS RELATIONSHIP WITH INDUSTRY 4.0

José Zozaya

President of the Mexican Association of the Automotive Industry

Mexican Association of the Automotive Industry
Ensenada 90, Hipódromo, Cuauhtémoc, 06100 Ciudad de México, CDMX
Tel.: +52 55 5272 1144
http://amia.com.mx

Clelia Hernández

Director of Initiative Nuevo León 4.0

Clelia Hernández
Initiative Nuevo León 4.0
Av. Parque Fundidora #501, 95A
Col. Obrera, Monterrey, NL 64010
https://www.nuevoleon40.org/

Dr. Zozaya was recently named President of the Mexican Association of the Automotive Industry; where he aims to direct the industry in a post-COVID world.

He has more than 40 years of experience in public, legal and international affairs. He has assumed directive roles in Kansas City Southern of Mexico and the Mexican Railways Association, and currently is the Vice-president of the Conference of Industrial Chambers of Mexico.

Eng. Clelia Hernández is currently the director of the Initiative "Nuevo León 4.0". Here, she coordinates numerous projects that aim to make the Mexican state the leading smart economy in America by 2025.

She completed her degree in computational engineering, and postgraduate studies in administration, informatics and economy.

The current state of the automotive industry in Mexico and the vision of the future were presented, considering the proximity to the United States market and that Mexico is the 6th producer of cars in the world. Also, the importance of Industry 4.0 was highlighted to maintain the competitiveness of the country's automotive plants and the need for specialized human resources in Industry 4.0.

Co-funded by the Erasmus+ Programme of the European Union